



# **Investigating the therapeutic potential of targeting NF- $\kappa$ B p52 in pre-clinical models of breast cancer**

**Syn Kok Yeo**

Thesis submitted for the award of PhD,  
9<sup>th</sup> January 2012

Under the supervision of:

Dr. Richard Clarkson

Co-supervised by:

Prof. Trevor Dale

School of Biosciences, Cardiff University, Museum Avenue,  
Cardiff CF10 3US

# Table of Contents

Table of Contents .....	ii
Abstract .....	vi
Acknowledgements .....	viii
Declaration .....	ix
List of abbreviations .....	x
Table of Figures .....	xiv
Table of Tables .....	xvii
<b>CHAPTER 1</b> .....	<b>1</b>
<b>1 Introduction</b> .....	<b>2</b>
<b>1.1 The mammary gland</b> .....	<b>2</b>
1.1.1 <i>Embryonic and fetal development of the mammary gland</i> .....	2
1.1.2 <i>Postnatal mammary gland morphogenesis</i> .....	3
1.1.3 <i>Role of apoptosis during postnatal mammary gland</i> <i>development</i> .....	5
1.1.3.1 <i>Extrinsic and intrinsic apoptotic pathways</i> .....	5
1.1.3.2 <i>The caspase cascade and regulators of apoptosis</i> .....	7
1.1.3.3 <i>Apoptosis during mammary ductal morphogenesis</i> .....	7
1.1.3.4 <i>Apoptosis during mammary gland involution</i> .....	8
1.1.4 <i>Mammary gland architecture</i> .....	10
1.1.5 <i>Key differences between human and murine mammary glands</i> .....	10
<b>1.2 Breast cancer</b> .....	<b>11</b>
1.2.1 <i>Breast carcinogenesis</i> .....	11
1.2.2 <i>Breast cancer progression</i> .....	13
1.2.3 <i>The metastatic cascade</i> .....	13
1.2.4 <i>Evading apoptosis: A hallmark of cancer cells</i> .....	15
1.2.5 <i>Apoptosis as a multistep barrier to metastasis</i> .....	15
1.2.6 <i>Epithelial to mesenchymal transition (EMT) and the</i> <i>acquisition of malignant traits</i> .....	16
1.2.7 <i>Clonal evolution of tumours and breast cancer stem cells</i> .....	18
1.2.8 <i>Breast cancer epidemiology</i> .....	19
1.2.9 <i>Breast cancer incidence and survival rates</i> .....	20
1.2.10 <i>Heterogeneity of breast cancers and intrinsic subtypes</i> .....	21
1.2.11 <i>Targeted therapeutics in breast cancer</i> .....	22
1.2.12 <i>Targeting breast cancer stem cells</i> .....	23
1.2.13 <i>Mouse models of breast cancer</i> .....	24
1.2.14 <i>The tetracycline conditional expression system</i> .....	25
1.2.15 <i>Transplantation models of breast cancer</i> .....	27
<b>1.3 NF-<math>\kappa</math>B signaling</b> .....	<b>27</b>
1.3.1 <i>NF-<math>\kappa</math>B and I<math>\kappa</math>B superfamily of proteins</i> .....	27
1.3.2 <i>Activation of NF-<math>\kappa</math>B pathways</i> .....	29
1.3.3 <i>Gene targets of NF-<math>\kappa</math>B</i> .....	31
1.3.4 <i>Modulation of NF-<math>\kappa</math>B subunit activity</i> .....	31
1.3.5 <i>Role of NF-<math>\kappa</math>B in development</i> .....	32
1.3.6 <i>NF-<math>\kappa</math>B signalling during post-natal mammary gland</i> <i>development</i> .....	33
1.3.7 <i>Aberrant NF-<math>\kappa</math>B activity in breast cancer</i> .....	34

1.3.8	<i>The NFkB2 gene and its relevance to breast cancer</i> .....	36
1.4	<b>Aims &amp; Objectives</b> .....	38
<b>CHAPTER 2</b>	.....	40
<b>2</b>	<b>Materials and methods</b> .....	41
<b>2.1</b>	<b>Animal experiments</b> .....	41
2.1.1	<i>Animals</i> .....	41
2.1.2	<i>Genotyping</i> .....	41
2.1.3	<i>Experimental procedures involving animals</i> .....	45
<b>2.2</b>	<b>Tissue sampling and processing</b> .....	46
2.2.1	<i>Removal and fixation of tissues</i> .....	46
2.2.2	<i>Tissue processing and sectioning for histology</i> .....	47
<b>2.3</b>	<b>Histological analysis of tissue sections</b> .....	47
2.3.1	<i>Dewaxing and rehydration</i> .....	47
2.3.2	<i>Haematoxylin and eosin (H&amp;E) staining</i> .....	47
2.3.3	<i>Immuno-histochemistry (IHC)</i> .....	48
2.3.4	<i>Terminal deoxy-nucleotidyl transferase dUTP nick end labeling (TUNEL)</i> .....	50
2.3.5	<i>Visualization and quantification of stained sections</i> .....	51
<b>2.4</b>	<b>DNA sub-cloning and vectors</b> .....	52
2.4.1	<i>Amplification of DNA constructs and general cloning procedures</i> .....	52
2.4.2	<i>Packaged Nfkb2 shRNA lentiviral vectors</i> .....	53
2.4.3	<i>Sub-cloning of p52 constructs into lentiviral vectors</i> .....	54
2.4.4	<i>NF-<math>\kappa</math>B Luciferase reporter plasmid</i> .....	54
<b>2.5</b>	<b>Maintenance and culture of cells</b> .....	54
2.5.1	<i>Experimental cell lines</i> .....	54
2.5.2	<i>Maintenance of cell lines</i> .....	57
2.5.3	<i>Long term cell storage</i> .....	57
2.5.4	<i>Cell counting</i> .....	58
2.5.5	<i>Lentiviral transduction of cell lines</i> .....	58
2.5.6	<i>NF-<math>\kappa</math>B luciferase reporter assays</i> .....	61
2.5.7	<i>Cell Titer Blue viability assays</i> .....	62
2.5.8	<i>Trypan blue exclusion cell viability counts</i> .....	62
2.5.9	<i>Colony formation assays</i> .....	63
2.5.10	<i>Boyden chamber (Transwell) migration and invasion assays</i> .....	63
2.5.11	<i>Anoikis and mammosphere formation assays</i> .....	64
2.5.12	<i>Treatment of cells with NF-<math>\kappa</math>B inhibitor, BAY 11-7082</i> .....	65
<b>2.6</b>	<b>Protein analysis by immuno-blotting</b> .....	66
2.6.1	<i>Protein extraction from cells</i> .....	66
2.6.2	<i>Determination of protein concentrations</i> .....	67
2.6.3	<i>Analysis of proteins by Western blotting</i> .....	67
<b>2.7</b>	<b>RNA analysis</b> .....	72
2.7.1	<i>RNA isolation</i> .....	72
2.7.2	<i>Reverse transcriptase (RT) cDNA synthesis</i> .....	73
2.7.3	<i>Quantitative real-time polymerase chain reaction (qRT-PCR)</i> .....	74
<b>2.8</b>	<b>Statistical analysis</b> .....	77
2.8.1	<i>Student's t-test</i> .....	77
2.8.2	<i>Spearman's ranked correlation test</i> .....	77

2.8.3	<i>Analysis of variance (ANOVA) test and Tukey's post-hoc analysis test</i>	78
2.8.4	<i>Analysis of co-variance (ANCOVA) test</i>	78
<b>CHAPTER 3</b>		<b>79</b>
<b>3</b>	<b>Elucidating the effects of caspase inhibition during mammary tumour growth and metastasis</b>	<b>80</b>
3.1	<b>Introduction</b>	80
	<b>Characterization of rtTA/p35 transgenic mice</b>	81
3.2		81
3.2.1	<i>Induction of p35 transcript levels in rtTA/p35 double transgenic mice is dependent on doxycycline administration</i>	81
3.2.2	<i>Caspase inhibition during mammary gland involution results in the accumulation of atypical luminal bodies</i>	81
3.2.3	<i>Inhibition of caspases by p35 does not delay the first phase of mammary gland involution</i>	83
3.3	<b>Effects of caspase inhibition during primary tumour growth and breast cancer progression</b>	88
3.3.1	<i>Inhibition of caspases by p35 does not affect the growth rate of MMTV-Neu driven tumours</i>	88
3.3.2	<i>Inhibition of caspases in MMTV-Neu tumours increases their metastatic potential</i>	90
3.4	<b>Discussion</b>	95
3.5	<b>Summary</b>	98
<b>CHAPTER 4</b>		<b>99</b>
<b>4</b>	<b>Elucidating the effects of silencing <i>Nfkb2</i> in mammary cancer cell lines</b>	<b>100</b>
4.1	<b>Introduction</b>	100
4.2	<b>Effects of silencing <i>Nfkb2</i> in mammary cancer cell lines</b>	101
4.2.1	<i>Silencing of <i>Nfkb2</i> leads to elevated basal NF-<math>\kappa</math>B activity in ErbB2<sup>-ve</sup> 4T1 and EPH4 cell lines but decreases the basal NF-<math>\kappa</math>B activity of ErbB2<sup>+ve</sup> N202.1a cells</i>	101
4.2.2	<i>Loss of <i>Nfkb2</i> in 4T1 cells is associated with an increase in nuclear and cytoplasmic p50 levels</i>	103
4.2.3	<i>Loss of <i>Nfkb2</i> sensitizes N202.1a cells to anoikis under non-adherent culture conditions in vitro</i>	103
4.2.4	<i>Silencing of <i>Nfkb2</i> does not affect the proliferation of mouse mammary cancer cell lines</i>	106
4.2.5	<i>Silencing of <i>Nfkb2</i> does not affect the colony forming potential of mouse mammary cancer cell lines</i>	106
4.2.6	<i>Silencing of <i>Nfkb2</i> increases the motility of 4T1 cells</i>	106
4.2.7	<i>Loss of <i>Nfkb2</i> leads to EMT in 4T1 cells</i>	109
4.2.8	<i>The motility of 4T1 cells is dependent on NF-<math>\kappa</math>B activity</i>	109
4.2.9	<i>The mammosphere forming potential of mammary cancer cell lines correlates with the changes in NF-<math>\kappa</math>B activity after <i>Nfkb2</i> silencing</i>	112
4.2.10	<i>The mammosphere forming potential of mammary cancer cell lines are dependent on NF-<math>\kappa</math>B activity</i>	118

4.2.11	<i>Over-expression of p52 rescues the decrease in mammosphere forming potential of N202.1a cells but not the increase in motility and mammosphere forming potential of 4T1 cells after Nfkb2 silencing</i>	118
4.2.12	<i>Loss of Nfkb2 enhances 4T1 tumour growth in vivo</i>	121
4.2.13	<i>Loss of Nfkb2 diminishes N202.1A tumour growth in vivo</i>	124
4.4	<b>Summary</b>	130
<b>CHAPTER 5</b>		132
Elucidating the effects of Ser-222 phosphorylation of p52 on the phenotypes of mammary cancer cells		132
<b>5 Elucidating the effects of Ser-222 phosphorylation of p52 on the phenotypes of mammary cancer cells</b>		133
5.1	<b>Introduction</b>	133
5.2	<b>Over-expression of phospho-mimetic p52 mutant in 4T1 cells</b>	134
5.2.1	<i>Effects of over-expressing phospho-mimetic p52 mutant on basal NF-κB activity</i>	134
5.2.2	<i>Effects of over-expressing phospho-mimetic p52 mutants on the sensitivity of 4T1 cells to anoikis</i>	134
5.2.3	<i>Effects of over-expressing phospho-mimetic p52 mutant on the proliferative, colony forming potential and mammosphere forming potential of 4T1 cells</i>	136
5.2.4	<i>Effects of over-expressing phospho-mimetic p52 mutant on the motility of 4T1 cells</i>	140
5.3	<b>Discussion</b>	142
5.4	<b>Summary</b>	144
<b>CHAPTER 6</b>		145
Identifying a correlation between levels of nuclear p52 and subtypes of breast cancer		145
<b>6 Identifying a correlation between levels of nuclear p52 and subtypes of breast cancer</b>		146
6.1	<b>Introduction</b>	146
6.2	<b>Identifying possible correlations between the levels of nuclear p52 and ErbB2, vimentin or p63 in BRCA2<sup>-/-</sup> p53<sup>-/-</sup> tumours by immuno-histochemistry</b>	147
6.2.1	<i>Nuclear p52 levels correlate with p63 expression in a cohort of BRCA2<sup>-/-</sup> p53<sup>-/-</sup> tumours</i>	147
6.3	<b>Discussion</b>	147
6.4	<b>Summary</b>	154
<b>CHAPTER 7</b>		155
<b>7 General Discussion</b>		156
7.1	<b>Apoptosis and mammary gland involution</b>	156
7.2	<b>Regulators of apoptosis as therapeutic targets in the prevention of breast cancer metastasis</b>	156
7.3	<b>The NF-κB p52 subunit and its potential as a therapeutic target in breast cancer metastasis</b>	157
7.4	<b>Strategies for targeting p52</b>	160
<b>Bibliography</b>		161

## Abstract

Apoptosis is an important process in normal mammary gland physiology and has been implicated in mammary gland involution. In breast cancer cells, apoptotic resistance is an acquired feature that can promote tumour growth and progression. In order to assess the importance of apoptosis in these processes, caspases were directly inhibited by conditional expression of baculovirus p35 protein, a pan-caspase inhibitor, in the mammary glands of mice (rtTA/p35 mouse model). Inhibition of caspases during the first phase of involution in rtTA/p35 mice increased the number of sloughed luminal bodies which stained negatively for cleaved caspase-3. However, the total number of sloughed luminal bodies between mice with and without p35 expression was not changed. This suggests that caspase activation is not essential for the sloughing of mammary epithelial cells into lumen of alveoli and the initiation of involution may be a caspase-independent event. The importance of apoptotic resistance in breast cancer progression was also addressed by crossing rtTA/p35 mice with mice over-expressing the ErbB2 oncogene (Neu). Expression of p35 in established Neu mammary tumours did not affect the growth rates of tumours relative to un-induced controls. However, an increased number of mice with lung and liver metastases were observed when p35 was induced. This result substantiates the importance of apoptotic resistance in promoting metastasis and warrants the targeting of apoptosis regulators as an anti-metastatic therapy.

The NF- $\kappa$ B signalling pathway regulates a range of anti-apoptotic genes and can also induce the expression of a variety of metastatic promoting genes. Accordingly, the role and potential of the NF- $\kappa$ B p52 subunit as a therapeutic target was investigated. Firstly, this was addressed by silencing the *Nfkb2* gene, which encodes p100/p52, in mammary cancer cell lines. Interestingly, assessment of these cells in *in vitro* assays measuring motility and tumour initiating potential revealed opposing effects in differing cell lines upon *Nfkb2* knockdown. In N202.1A cells (ER<sup>+</sup>/ErbB2<sup>+ve</sup>), therapeutically beneficial effects were seen whereas in the 4T1 cell line (ER<sup>+ve</sup>/ErbB2<sup>-ve</sup>), malignancy was exacerbated. One explanation for the differential effects observed is that the negative regulatory subunit p100 and the transcriptional subunit p52 alternately have dominant roles in the respective cell lines. Although these results demonstrate a role for p52 in regulating tumour initiating potential in particular cell lines, the contextual outcomes indicate that targeting p52 at the gene

level may be detrimental in cases where the loss of p100 outweighs the loss of p52. This indicates that strategies aimed at disrupting p52 activity should circumvent the loss of p100. Therefore, we addressed the possibility of diminishing p52 transcriptional activity via promotion of repressive transcriptional complexes. As the formation of repressive complexes is favoured by phosphorylation of Ser-222 in p52, we addressed the effects of over-expressing the S222D p52 mutant in 4T1 cells. In *in vitro* assays assessing proliferation, colony forming potential, tumour initiating potential and motility, we did not observe any differences upon expression of S222D p52. However, over-expression of S222A p52 did increase the motility of 4T1 cells and this demonstrates that the lack of Ser-222 phosphorylation (promoting transcriptionally active complexes) can contribute to the malignancy of breast cancer cells.

Due to the context dependent effects of *Nfkb2* silencing, it was important to identify the particular subtypes of breast cancer which are dependent on p52 activity. We assessed a cohort of BRCA2<sup>-/-</sup> p53<sup>-/-</sup> tumours for nuclear p52 staining along with markers for respective breast cancer subtypes by immuno-histochemistry and found a positive correlation between p52 and p63. This suggests that aberrant p52 activity may be common in basal-like breast cancers which typically express p63 and could benefit most from p52 targeted therapies. In summary, our results indicate that targeting p52 in breast cancer cells can be therapeutically beneficial but only in particular subtypes of breast cancer and by certain therapeutic strategies.

## Acknowledgements

It is without uncertainty that the work carried out throughout my PhD project and the writing of this thesis would not have been possible if valuable assistance and support had not been generously bestowed by those around and affiliated. Accordingly, it is most appropriate that my gratitude be extended to the below-mentioned persons.

I would like to thank my supervisor, Dr. Richard Clarkson, who has been instrumental in the conception, guidance and direction of this project. Challenging times were made manageable and aspirations rekindled after each long, thoughtful meeting. I also appreciate the many lessons that will prove to be useful in this ‘Musical chairs of academia’, the passage of postdoc-ing around the globe with the aim of eventually finding a ‘chair’. I am also grateful to Breast Cancer Campaign for sponsoring this PhD studentship. Much of the cutting edge work had been made possible with reagents from collaborators. I’m really grateful for the p52 mutant constructs and phospho-p52 antibodies from Professor Neil Perkins (Newcastle University), p305 vector and packaging of lentiviral vectors by Dr. Riccardo Brambilla (Cardiff University) and BRCA2<sup>-/-</sup> p53<sup>-/-</sup> tumour sections from Dr. Trevor Hay and Professor Alan Clarke (Cardiff University). I would also like to thank Derek Scarborough from the Histology Unit for assistance with histology and processing of tissues and all the hard-working people from the animal facility at Cardiff University.

To the people whom which I have spent most of my time with for the past three years, I could not thank you enough for the help and company. This includes the past and present members of RWEC lab; Alison Wakefield, Luke Piggott, Nader Omidvar, Nuria Marquez-Almuina, , James Knight, Jitka Soukupova and Rhiannon French. Also, thanks to my former students Tamar Avades and Filomena Spada (IHCs), and Joe Farmer (Cell culture) for their assistance. I am also grateful to everyone from 4<sup>th</sup> and 5<sup>th</sup> floors of Biosi 3, for technical advice that is readily available, communal use of equipment and being wonderful people to work with.

Much gratitude is also owed to family and friends whom have added purpose to the work carried out throughout my project. As I may not be able to acknowledge the contributions of all dear persons by name due to the injustices of space, it is only fair that I should state that my thoughtfulness stays affixed with all those who have been exceedingly kind upon me.

# Declaration

## DECLARATION

This work has not been submitted in substance for any other degree or award at this or any other university or place of learning, nor is being submitted concurrently in candidature for any degree or other award.

Signed ..... (candidate) Date .....

## STATEMENT 1

This thesis is being submitted in partial fulfillment of the requirements for the degree of .....(insert MCh, MD, MPhil, PhD etc, as appropriate)

Signed ..... (candidate) Date .....

## STATEMENT 2

This thesis is the result of my own independent work/investigation, except where otherwise stated.

Other sources are acknowledged by explicit references. The views expressed are my own.

Signed ..... (candidate) Date .....

## STATEMENT 3

I hereby give consent for my thesis, if accepted, to be available for photocopying and for inter-library loan, and for the title and summary to be made available to outside organisations.

Signed ..... (candidate) Date .....

## STATEMENT 4: PREVIOUSLY APPROVED BAR ON ACCESS

I hereby give consent for my thesis, if accepted, to be available for photocopying and for inter-library loans **after expiry of a bar on access previously approved by the Academic Standards & Quality Committee.**

Signed ..... (candidate) Date .....

## List of abbreviations

ALDH1	- aldehyde dehydrogenase 1
ANOVA	- analysis of variance
ANCOVA	- analysis of co-variance
Apaf-1	- apoptosis protease-activating factor 1
BAFF	- B-cell activating factor of the TNF family
Bcl-2	- B-cell lymphoma 2
Bcl-3	- B-cell lymphoma 3
BLG	- $\beta$ -lactoglobulin
BSA	- bovine serum albumin
CAD	- caspase activated DNase
CaSC	- cancer stem cell
CC3	- cleaved caspase-3
cDNA	- complementary DNA
c-FLIP	- cellular Flice-like inhibitory protein
CK	- cyto-keratin.
CK2	- casein-kinase-II
CXCL12	- C-X-C motif ligand 12
CXCR4	- C-X-C motif receptor 4
DAB	- 3,3'-diaminobenzidine
DBM	- DNA binding mutant
DISC	- death inducing signalling complex
Dox+	- doxycycline positive
Dox-	- doxycycline negative
DMBA	- 7,12-dimethylbenz(a)anthracene
DMEM	- Dulbecco's modified Eagle's medium
DNA	- deoxyribonucleic acid
dNTP	- deoxynucleotide triphosphate
Dox	- doxycycline
DPP IV	- dipeptidyl peptidase IV
DR	- death receptor
DTT	- 1,4 dithiothreitol
ECM	- extracellular matrix

EDTA	- ethylenediaminetetraacetic acid
EGFR	- epidermal growth factor receptor
EMT	- epithelial-mesenchymal transition
ER	- oestrogen receptor
FACS	- fluorescence assisted cell sorting
FBS	- foetal bovine serum
GFP	- green fluorescent protein
GLM	- general linear model
H&E	- haematoxylin and eosin
HCl	- hydrochloric
HDAC1	- histone deacetylase 1
HGF	- hepatocyte growth factor
HIF-1 $\alpha$	- hypoxia inducible factor 1alpha
HRP	- horseradish-peroxidase
IAP	- inhibitor of apoptosis protein
I $\kappa$ B	- inhibitor of NF- $\kappa$ B
I $\kappa$ K	- I kappa B kinase
IHC	- immuno-histochemistry
IL	-Interleukin
IP	- intra-peritoneal
I $\times$ P	- product of intensity and percentage of cover
LIF	- leukemia inhibitory factor
LPS	- lipo-polysaccharide
LT $\beta$ R	- lymphotoxin- $\beta$ receptor
LTR	- long terminal repeat
MEBM	- mammary epithelial basal media
MEC	- mammary epithelial cell
MEK	- mitogen-activated protein kinase kinase
MerTK	- c-mer proto-oncogene tyrosine kinase
MET	- mesenchymal to epithelial transition
MFG-E8	- milk fat globule-EGF factor 8
MFU	- mammosphere forming units
MMP	- matrix metallo-proteinases
MMTV	- mouse mammary tumour virus

MoAb	- monoclonal antibody
mRNA	- messenger ribonucleic acid
NF-KB	- nuclear factor kappa B
NIK	- NF- $\kappa$ B inducing kinase
NK	- natural killer
NLS	- nuclear localization signal
NOD	- non obese diabetic
NT	- non target
PARP	- poly ADP ribose polymerase
PBS	- phosphate buffered saline
Pcmv	- cytomegalovirus promoter IE
PCR	- polymerase chain reaction
PET	- polyethylene terephthalate
PKAc	- protein kinase A
PLL	- poly-L-lysine
PR	- progesterone receptor
PVDF	- polyvinylidene difluoride
PyVT	- Polyoma middle T oncogene
qRT-PCR	- quantitative real time PCR
RANK	- receptor activator of NF- $\kappa$ B
RANKL	- receptor activator of NF- $\kappa$ B ligand
RHD	- Rel homology domain
R.L.U.	- relative light units
rpm	- rotations per minute
rtTA	- reverse tetracycline controlled trans-activator
S222A	- Serine-222 to alanine mutation
S222D	- Serine-222 to aspartate mutation
SCID	- severe combined immunodeficiency
SDS	- sodium dodecyl sulphate
SEM	- standard error of the mean
Ser	- serine
SHH	- Sonic Hedgehog
shRNA	- short hairpin ribonucleic acid
SR	- super repressor

STAT	- signal transducer and activator of transcription
TAE	- Tris-Acetic Acid-EDTA
TAK1	- TGF-beta associated kinase
TDLU	- terminal ductal lobular unit
TdT	- deoxynucleotidyl transferase
TEB	- terminal end bud
tetO	- <i>E. coli</i> tet operator
tetR	- tetracycline repressor
TGF- $\beta$	- transforming growth factor beta
TNF- $\alpha$	- tumour necrosis factor $\alpha$
TRAIL	- tumour necrosis factor $\alpha$ associated apoptosis inducing ligand
TRE	-tetracycline responsive element
tTA	- tetracycline controlled trans-activator
TUNEL	- terminal deoxy-nucleotidyl transferase dUTP nick end labeling
VEGF	- vascular endothelial growth factor
VP16	- virion protein 16
WAP	- whey acidic protein
WT	- wild-type
XIAP	- X-linked inhibitor of apoptosis protein

## Table of Figures

Figure 1.1: Post-natal mammary gland development in mice. ....	4
Figure 1.2: The intrinsic and extrinsic pathways of apoptosis. ....	6
Figure 1.3: Apoptosis during mammary gland morphogenesis and involution. ...	9
Figure 1.4: Architecture of the mammary gland. ....	12
Figure 1.5: Breast cancer progression. ....	14
Figure 1.6: Features of epithelial to mesenchymal transition. ....	17
Figure 1.7: The tetracycline inducible system. ....	26
Figure 1.8: NF- $\kappa$ B and I $\kappa$ B super-family of proteins. ....	28
Figure 1.9: Canonical and alternative NF- $\kappa$ B pathways. ....	30
Figure 1.10: The NFKB2 gene and its gene products p100/p52. ....	37
Figure 2.1: Cloning details for p52 into p305 vector. ....	55
Figure 2.2: Establishing stable 4T1 cell lines with <i>Nfkb2</i> knocked down. ....	60
Figure 3.1: Expression of p35 mRNA in rtTA/p35 mice is dependent on doxycycline administration. ....	82
Figure 3.2: Caspase inhibition during mammary gland involution leads to the formation of atypical luminal bodies. ....	84
Figure 3.3: Cleaved caspase-3 staining of involuting mammary glands from rtTA/p35 mice. ....	85
Figure 3.4: TUNEL staining of involuting mammary glands from rtTA/p35 mice. ....	86
Figure 3.5: Gross morphology of involuting mammary glands from rtTA/p35 mice. ....	87
Figure 3.6: Caspase inhibition during early phase mammary gland involution does not affect the number of luminal bodies. ....	89
Figure 3.7: Inhibition of caspases does not affect the growth rate of MMTV-Neu driven primary tumours. ....	91
Figure 3.8: Inhibition of caspases does not alter the proportion of cleaved caspase-3 positive cells in MMTV-Neu driven primary tumours. ....	92
Figure 3.9: Caspase inhibition increases the metastatic potential of MMTV-Neu driven tumours. ....	93
Figure 3.10: Inhibition of caspases does not alter the proportion of cleaved Caspase-3 positive cells in lung metastases from MMTV-Neu tumours. ....	94

Figure 4.1: Silencing of <i>Nfkb2</i> alters the basal NF-κB activity of mammary cell lines. ....	102
Figure 4.2: Silencing of <i>Nfkb2</i> in 4T1 cells is associated with an increase in nuclear and cytoplasmic p50 levels. ....	104
Figure 4.3: Silencing of <i>Nfkb2</i> sensitizes N202.1A cells to anoikis in vitro. ....	105
Figure 4.4: Silencing of <i>Nfkb2</i> does not affect proliferation of 4T1, N202.1A and EPH4 cells. ....	107
Figure 4.5: Silencing of <i>Nfkb2</i> does not affect the colony forming potential of mammary cell lines.....	108
Figure 4.6: Silencing of <i>Nfkb2</i> increases the motility of 4T1 cells. ....	110
Figure 4.7: Silencing of <i>Nfkb2</i> induces EMT in 4T1 cells. ....	111
Figure 4.8: The increase in motility in 4T1 cells upon <i>Nfkb2</i> silencing is dependent on NF-κB activity. ....	113
Figure 4.9: Effects of silencing <i>Nfkb2</i> on mammosphere forming potential of mammary cell lines. ....	116
Figure 4.10: The mammosphere forming potential of 4T1 and N202.1A cells are dependent on NF-κB activity. ....	119
Figure 4.11: Rescue experiments by over-expression of p52. ....	120
Figure 4.12: Loss of <i>Nfkb2</i> enhances 4T1 tumour growth in vivo. ....	122
Figure 4.13: The increased 4T1 tumour growth in vivo is not associated with a change in the proliferation to apoptosis ratio. ....	123
Figure 4.14: Metastatic burden of mice transplanted with 4T1 NT and <i>Nfkb2</i> kd cells. ....	125
Figure 4.15: Loss of <i>Nfkb2</i> diminishes N202.1A tumour growth in vivo. ....	126
Figure 4.16: Summary of changes due to silencing of <i>Nfkb2</i> in Eph4, N202.1A... and 4T1 cells. ....	131
Figure 5.1: Effects of over-expressing p52 and corresponding mutants on the basal NF-κB activity of 4T1 cells. ....	135
Figure 5.2: Effects of over-expressing p52 and corresponding mutants on the ability of 4T1 cells to survive under anoikis conditions. ....	137
Figure 5.3: Effects of over-expressing p52 and corresponding mutants on the proliferative and colony forming potential of 4T1 cells. ....	138
Figure 5.4: Effects of over-expressing p52 and corresponding mutants on the mammosphere forming potential of 4T1 cells. ....	139

Figure 5.5: Effects of over-expressing p52 and corresponding mutants on the motility of 4T1 cells. ....141

Figure 6.1: Immuno-histochemical staining of p52, p63, ErbB2 and vimentin in BRCA2<sup>-/-</sup> p53<sup>-/-</sup> tumours. ....148

## Table of Tables

Table 2.1: Cycling conditions for PCR reactions. ....	43
Table 2.2: Sequence of primers used for genotyping. ....	44
Table 2.3: Composition of PCR reactions. ....	44
Table 2.4: Details of antibodies and conditions used for immune-histochemistry..	48
Table 2.5: Reaction volumes and components for restriction enzyme digests. ....	53
Table 2.6: List of primers used for sequencing p305:HA-p52 plasmids. ....	56
Table 2.7: List of shRNA sequences targeting the Nfkb2 gene. ....	59
Table 2.8: Composition of gels for SDS-PAGE. ....	68
Table 2.9: Buffers for Western blot analysis. ....	70
Table 2.10: Details of antibodies used for Western blot analysis. ....	71
Table 2.11: Components of reverse-transcriptase reactions. ....	74
Table 2.12: List of primers used for qRT-PCR. ....	76
Table 2.13: Reagents and components for qRT-PCR. ....	77
Table 3.1: Caspase inhibition increases the metastatic potential of MMTV-Neu Driven tumours. ....	93
Table 6.1: Table of scores for respective antigens in BRCA2-/- p53-/- tumours. ...	152

# **CHAPTER 1**

An introduction to  
the mammary gland, breast cancer and  
NF- $\kappa$ B signalling

## 1 Introduction

In this thesis, our initial aim was to investigate and substantiate the importance of apoptotic resistance in the formation of breast cancer metastases. For that purpose, a triple transgenic mouse model (rtTA/p35/Neu) was utilized. With this model, inducible expression of baculovirus p35 protein allows the effects of caspase inhibition on mammary tumour growth and metastasis formation to be addressed. The baculovirus p35 protein is an anti-apoptotic protein which helps the propagation of the virus (Clem et al., 1991) and is capable of inhibiting cell death in a variety of organisms including *C. elegans*, *Drosophila melanogaster* and mammalian cells (Beidler et al., 1995, Hay et al., 1994, Sugimoto et al., 1994). Baculovirus p35 protein is a pan-caspase inhibitor and prevents apoptosis through direct interaction with caspases.

Based on the findings of our initial aim and that of published data (Pinkas et al., 2004), apoptotic resistance promotes the formation of breast cancer metastases. Hence, the consequent aim of the thesis was to address whether targeting of anti-apoptotic signals in breast cancer cells would retard the formation of metastases. As the NF- $\kappa$ B pathway has been shown to be able to induce pro-survival signals in mammary epithelial cells (MECs) (Clarkson et al., 2000b) and regulate the tumorigenicity of breast cancer cells (Liu et al., 2010, Pratt et al., 2009), the potential of targeting this pathway, in particular the NF- $\kappa$ B p52 subunit was addressed. The effects of diminishing the activity of NF- $\kappa$ B p52 on breast cancer cell lines were investigated by silencing the gene which encodes p52 and through over-expression of an inhibitory form of p52.

Since breast cancer is a heterogenous disease, it was also important to identify the specific subtypes which would most likely benefit from manipulation of p52 activity. This was addressed by correlating levels of p52 with markers of particular subtypes of breast cancer in immuno-histochemical sections.

### 1.1 The mammary gland

#### 1.1.1 Embryonic and fetal development of the mammary gland

Mammals have a distinct ability to produce and secrete milk to nourish their progeny. Although the mammary gland is only required to fulfill that role after gestation, the first signs of mammary gland morphogenesis can be traced in embryonic development. The mammary gland originates from a layer of epidermis

that bulges and forms a line on both sides of the embryonic mid-ventral line. This lateral line is located between the fore and hind limbs and has been described as the ‘milk line’ (Kon and Cowie, 1961). The ‘milk line’ consists of epidermal cells which are columnar and multilayered. Placode formation at specific points of the milk line ensues and these placodes form invaginations into the mesenchymal layer beneath. This would lead to the formation of mammary buds which progressively extend into the mammary fat pad. Within this environment, ductal branching is stimulated and this gives rise to a rudimentary mammary tree by the time of birth (Figure 1.1) (Hens and Wysolmerski, 2005).

### ***1.1.2 Postnatal mammary gland morphogenesis***

The period between birth and puberty is when the mammary gland undergoes isometric growth in proportion to overall development of the organism. It is only during puberty when rapid allometric growth occurs. During this phase, various hormones influence branching and growth of the ductal tree by inducing the formation of terminal end buds (TEBs) at the tips of ducts (Silberstein, 2001). The TEBs progressively penetrate to the edges of the mammary fat pad and at the same time, side-branches are formed giving rise to a mature ductal tree. Tertiary branching and formation of lobulo-alveolar structures then occur and is governed by cycling ovarian hormones (Hovey et al., 2002). Within each estrous cycle, a transient increase of alveoli illustrates the mammary gland’s preparation for pregnancy. These alveoli would develop into the milk secreting units but regress in the absence of pregnancy associated hormones. The extent of alveolar budding varies between species and strains, largely because of variation in estrous hormone levels and cycle lengths.

During pregnancy, increased levels of prolactin and progesterone induce extensive proliferation of ductal and alveolar epithelial cells. This is followed by differentiation of alveolar epithelial cells into milk secreting cells (Oakes et al., 2008). Lactation commences after progesterone withdrawal and involves the secretion of milk and lipids into the alveoli. The process of mammary gland involution commences upon cessation of lactation and can be induced experimentally in mice by forced weaning. As the milk producing alveoli are no longer required after lactation, involution is responsible for the removal of these structures and returning the gland to a state that is similar to pre-pregnancy (Figure 1.1) without invoking excessive inflammation.

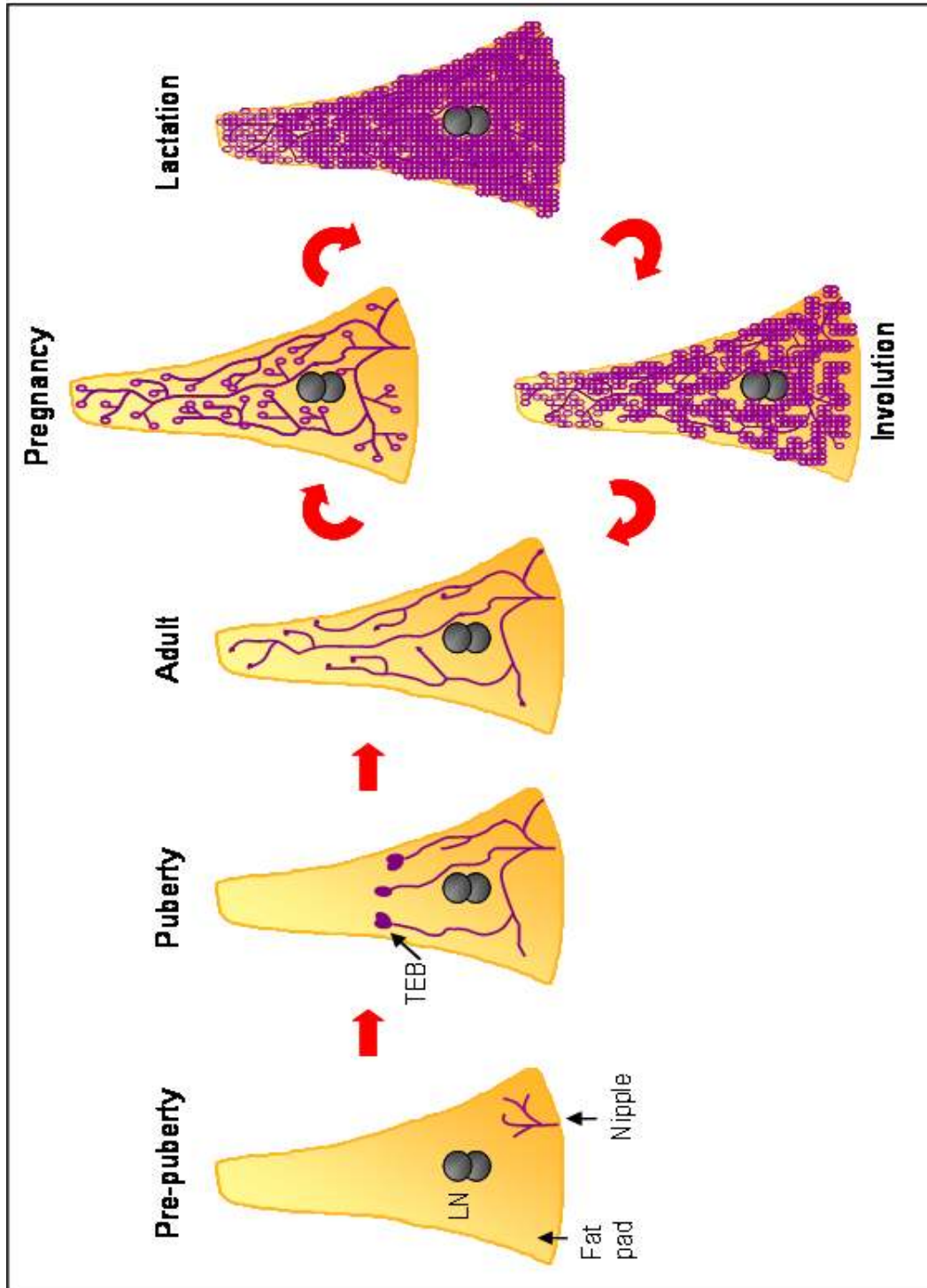


**Figure 1.1: Post-natal mammary gland development in mice.** Illustration of mammary ductal morphogenesis in pre-pubertal, pubertal, adult nulliparous, pregnant, lactating and involuting mammary glands in mice. Epithelial structures illustrated in purple. LN: lymph nodes, TEB: terminal end buds,

### 1.1.3 Role of apoptosis during postnatal mammary gland development

Apoptosis is a form of programmed cell death characterised by morphological changes which include chromatin condensation, nuclear fragmentation, cell shrinkage and membrane blebbing. A cell that has undergone apoptosis will then be engulfed by phagocytes to avoid inflammatory responses in the surrounding tissue, an important feature of this neat form of cell death (Savill and Fadok, 2000). Apoptosis is an essential process in multicellular organisms not only during development where excess cells are removed to form well defined tissue ‘sculptures’, but also for tissue homeostasis in a mature organism (Meier et al., 2000, Prindull, 1995).

#### 1.1.3.1 Extrinsic and intrinsic apoptotic pathways

There are two major pathways of apoptosis in mammals, namely, the extrinsic pathway which can be triggered through death receptors and the intrinsic pathway which is mitochondrial dependent (figure 1.2). The extrinsic pathway involves stimulation of death receptors such as CD95, DR4 or TNF- $\alpha$  receptor by their respective ligands, which then induces receptor oligomerization and recruitment of adaptor proteins with death domains. Caspase-8, the initiator caspase of the extrinsic pathway associates with the activated receptor and adaptor proteins forming a death-inducing signalling complex (DISC). This is followed by autoactivation of caspase-8 which subsequently activates the effector caspases (caspase-3, -6 and -7) (Ashkenazi and Dixit, 1998). Alternatively, the intrinsic pathway is mediated by release of cytochrome c from the mitochondrion into the cytoplasm, which associates with apoptosis protease-activating factor 1 (Apaf-1) and caspase-9 to form the ‘apoptosome’. Consequently, the apoptosome induces activation of caspase-9 in the intrinsic pathway and this leads to cleavage of effector caspases, the point where both pathways converge (Shi, 2002). Consequently, other nucleases (e.g. CAD) and proteases which are responsible for the terminal stages of apoptosis are activated by the caspase cascade. Over-activation of caspase-8 via death receptor signalling can also lead to truncation of bid and mitochondrial membrane permeation. This can result in crosstalk from death receptor signalling through to the intrinsic pathway in certain cell types (Miller, 1997).

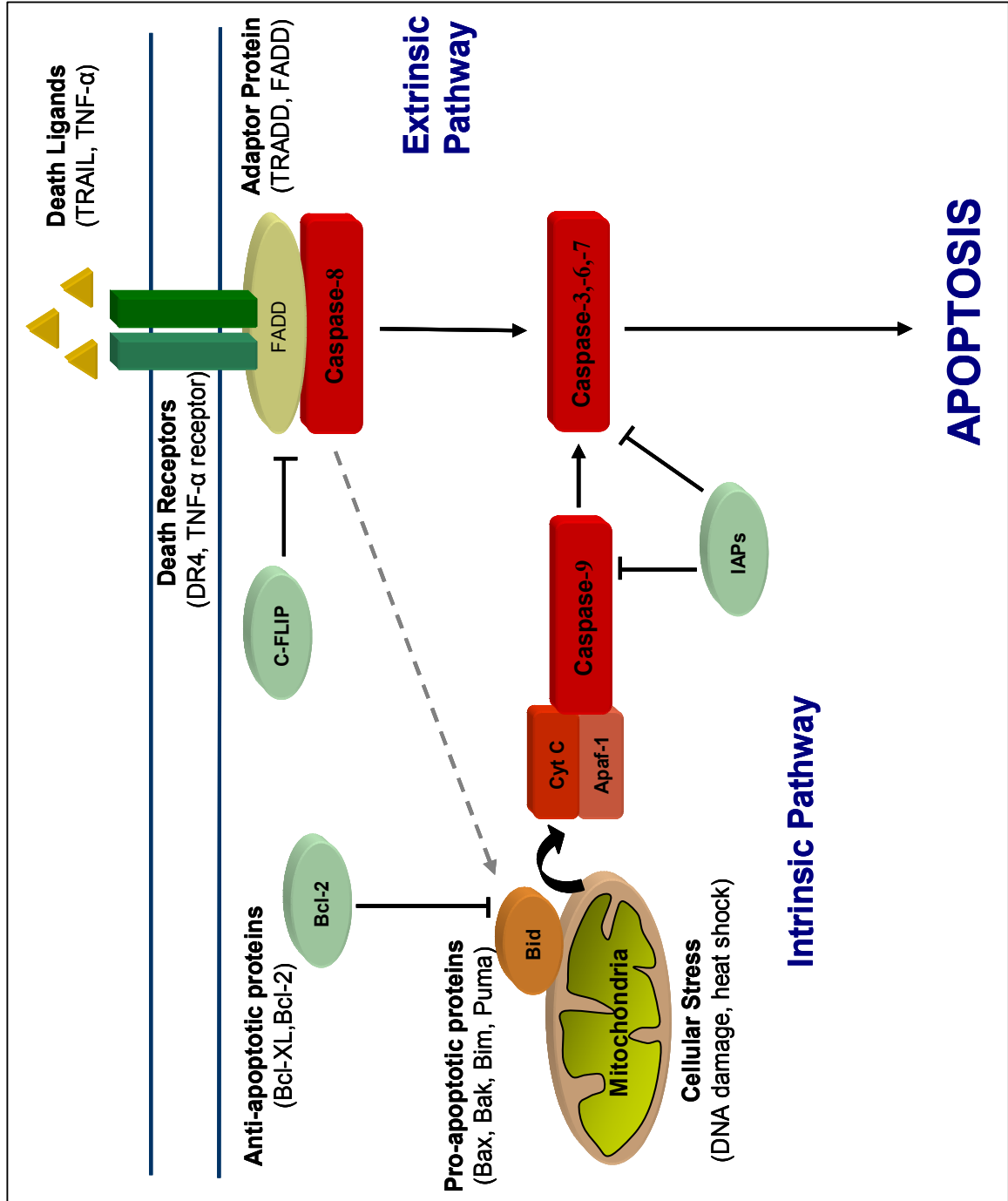


Figure 1.2: The intrinsic and extrinsic pathways of apoptosis. Illustration of the extrinsic apoptotic pathway mediated by death receptors and the intrinsic pathway that is dependent on mitochondrial permeability. Caspases, the key players of this process are illustrated in red boxes. Dotted lines show possible crosstalk between extrinsic and intrinsic pathways.

### 1.1.3.2 *The caspase cascade and regulators of apoptosis*

On the whole, a series of proteolytic cascades involving caspases are integral to the apoptotic process (Figure 1.2). Caspases are cysteine proteases which cleave their respective substrates at aspartate residues (Vaux and Strasser, 1996). For that reason, they are synthesized as zymogens and their activation is regulated by various apoptosis regulators because over-activation of caspases will lead to degenerative diseases whereas over-inhibition would promote tumorigenesis (Degterev et al., 2003). It is the balance of pro-apoptotic and anti-apoptotic regulators in a cell which determines the sensitivity of cells to a particular death stimulus. At the death receptor level, pro-survival proteins such as cellular FLICE inhibitory protein (c-FLIP) antagonize the activation of caspase-8. Similarly, pro- and anti-apoptotic proteins of the B-cell lymphoma 2 (Bcl-2) family govern mitochondrial permeation. In addition, inhibitor of apoptosis proteins (IAPs) can inhibit the effector caspases and caspase-9 through direct binding.

### 1.1.3.3 *Apoptosis during mammary ductal morphogenesis*

As described, the extensive ductal network of the mammary gland is only formed during puberty. This involves the invasion of TEBs into the mammary fat pad and is driven by proliferation in these structures. Another important aspect of ductal morphogenesis is the formation of intact and hollow lumen as the TEB structures progress towards the edges of the mammary fat pad. Apoptosis has an important role in lumen formation and can be detected in a proportion of body cells in the TEB (Figure 1.3a). Inhibition of apoptosis by specific overexpression of Bcl-2 under the whey acidic protein (WAP) promoter reduces the percentage and disrupts the localization of apoptotic cells within TEBs. Moreover, convoluted layers of cells can be observed in these TEB structures implicating a role for apoptosis in maintaining the integrity of TEBs as they progress (Humphreys et al., 1996). More specifically, the pro-apoptotic factor, Bim has been shown to be important for luminal clearance by inducing anoikis and the lack of it results in a delay in clearance but this can be compensated by alternative cell death mechanisms (Mailleux et al., 2007). Similarly, insights from *in vitro* experiments utilising MCF-10A cells show that lumen formation in acini can be delayed but not prevented by inhibiting apoptosis (Debnath et al., 2002). These studies demonstrate a role for apoptosis in the formation of the ductal network and acinar structures of the mammary gland.

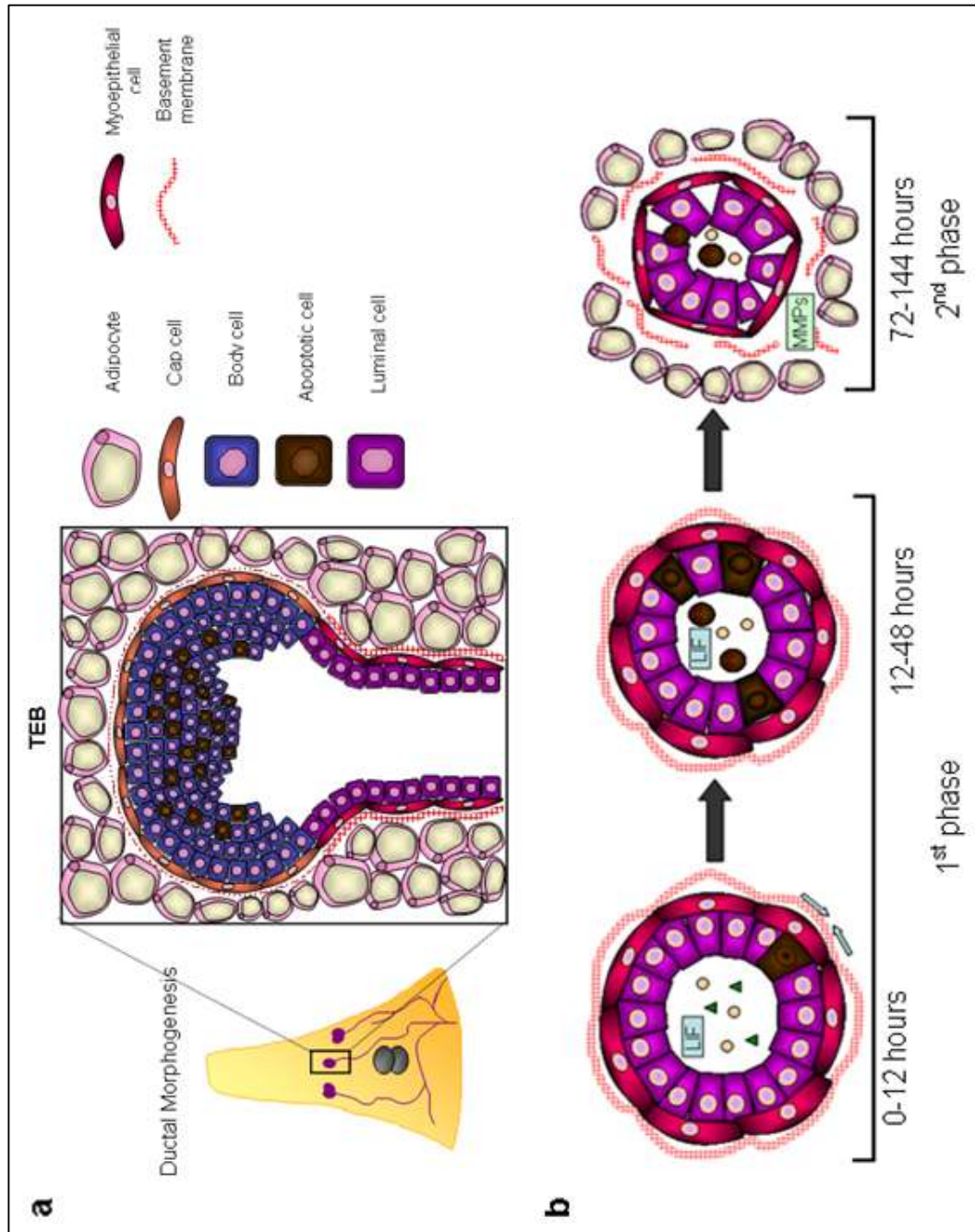
#### **1.1.3.4 Apoptosis during mammary gland involution**

There are two phases of involution in mice, a first reversible phase that occurs within 0-2 days post weaning and a second phase which involves remodeling of the mammary gland by matrix metallo-proteinases (MMPs). In the first phase, alveolar cells that are undergoing programmed cell death are shed into the lumen, giving rise to luminal bodies that stain positive for activated caspase-3 (Watson, 2006). In the second phase, substantial remodelling of the gland occurs. Matrix metalloproteases (MMPs) regulate the collapse of alveoli structures and induces tissue remodelling which is accompanied by apoptosis (Green and Streuli, 2004). The loss of extracellular matrix support contributes to cell death by induction of anoikis in the second phase (Figure 1.3b).

As weaning occurs, milk stasis in the secretory structures of the gland leads to production of leukemia inhibitory factor (LIF) and transforming growth factor (TGF)  $\beta$ 3. Both these factors are activators of signal transducer and activator of transcription (STAT) 3, (Kritikou et al., 2003, Nguyen and Pollard, 2000, Schere-Levy et al., 2003) which plays an important role in the initiation of involution. This is in line with the gene expression profile of mammary glands during the initial phase of involution, where acute phase response genes which are known targets of STAT 3 and NF- $\kappa$ B are expressed (Clarkson et al., 2004, Stein et al., 2004). In fact, conditional deletion of STAT 3 in the mammary gland reduces cell death, extends the reversible first phase and delays the onset of the second phase of involution (Chapman et al., 1999). The role of STAT 3 in the second phase is sustained by oncostatin M receptor (OSMR), which transduces signals from a cytokine, oncostatin M, capable of potently activating STAT3 in the mammary gland. Deletion of OSMR led to a reduction in the expression of MMPs and consequently, a reduction in MMP-dependent apoptosis (Tiffen et al., 2008).

The large number of luminal bodies is then cleared in the initial phase by non-professional macrophages. These are epithelial cells capable of efferocytosis to internalize milk globules and cellular debris. The phagocytic process is dependent on phosphatidyl-serine exposure on the outer leaflet of the membrane, a characteristic feature of apoptotic cells (Monks and Henson, 2009). It is only by day 4 post-weaning that professional macrophages can be detected in the mammary gland and contribute to the clearance of apoptotic bodies. The importance of the clearing process is highlighted by knockout of c-mer proto-oncogene tyrosine kinase (MerTK) or milk fat

**Figure 1.3: Apoptosis during mammary gland morphogenesis and involution.** (a) Illustration of cell populations within TEB structures during ductal morphogenesis. Apoptotic cells (dark brown) are present behind leading cap cells. (b) Illustration of mammary acini structures during first and second phases of mammary gland involution. Dying cells (dark brown) are sloughed into the lumens of acini and appear as luminal bodies (rounded dark brown). LIF: leukemia inhibitory factor, MMPs: matrix metalloproteinases. Meshed lines represent basement membrane.



globule-EGF factor 8 (MFG-E8), molecules shown to have a role in cell uptake by macrophages. The deletion of these molecules respectively led to delayed clearance of apoptotic bodies which may result in secondary necrosis and increased inflammation. As a result, increased matrix deposition and fibrosis were observed in knockout glands and this led to the inability for the gland to regrow in a subsequent pregnancy (Atabai et al., 2005, Hanayama and Nagata, 2005, Sandah et al., 2010). Taken together, this demonstrates the importance of apoptosis in mammary tissue homeostasis and indicates that aberrant regulation of apoptosis in the mammary gland would be pathological.

#### 1.1.4 Mammary gland architecture

The basic structure of the mammary gland is similar to other epithelial gland structures. Numerous alveoli or acini, the milk producing units, are connected to a network of ducts which supply the nipple. It can be illustrated as a ‘mammary tree’ where the nipple is the root from where ducts branch outwards (Figures 1.4 a-c), forming secondary and tertiary branches with multiple acini. This epithelial ‘tree’ structure is bounded within stroma which comprise mainly of fibroblasts and adipocytes (Hovey et al., 2002).

At the cellular level, mammary ducts and acini are structures made up of two layers of polarized epithelium (Figure 1.4d). These structures are hollow and the inner layer of cells are termed the luminal cells because their apical surface is in contact with the lumen. The outer layer of ductal cells are termed basal cells, whereas in acini they are termed myoepithelial cells (Howard and Gusterson, 2000). However, the basal and myoepithelial cells do not differ functionally and are located between the luminal cells and a layer of basement membrane consisting of laminin (Adams and Watt, 1993).

#### 1.1.5 Key differences between human and murine mammary glands

Although the murine mammary gland has provided many insights into mammary gland morphogenesis, it does not represent all the features of the human breast. Some key differences are present even in embryonic development. While the sexual dimorphism of the mammary gland occurs *in utero* for mice, the mammary glands of men and women are indistinguishable until puberty. More evidently, mice have five pairs of mammary glands compared to a pair in humans. This is a result of

the milk line segregating into multiple placodes before mammary bud formation in mice (Kon and Cowie, 1961).

Rigorous assessment of mammary gland architecture will also reveal that the milk secreting units between the two species differ. Alveolar buds feature along primary ducts in mice, while in humans, acini are within terminal ductal lobular units (TDLU) (*Figures 1.4 a-c*). TDLUs are encapsulated by intralobular stroma made up mostly of fibroblasts along with some adipocytes. An additional layer of interlobular stroma borders the intralobular stroma. The interlobular stroma is more densely packed and is discernable from intralobular stroma by the expression of cell surface dipeptidyl peptidase IV (DPP IV). Contrastingly, the stroma of mice is populated mainly by adipocytes. (Richert et al., 2000, Howard and Gusterson, 2000).

## **1.2 Breast cancer**

### *1.2.1 Breast carcinogenesis*

Uncontrolled cell growth gives rise to tumours which could either be benign or malignant. Benign tumours remain encapsulated whereas malignant ones have the ability to invade and form metastases. Such malignancies are described as cancers but they include various forms, each with different characteristics depending on their origin. Cancers derived from connective tissue such as muscle are termed sarcomas while those of epithelial lineage are carcinomas (Pecorino, 2008, Alison, 2001). Accordingly, cancers of glandular epithelia are adenocarcinomas and these are the most prevalent cancers in the breast. Owing to the different glandular structures in the breast, adenocarcinomas of the breast can be further divided into ductal carcinomas and lobular carcinomas, with the former being the more common form. Despite the heterogeneity of cancers, there are unifying traits which are acquired by most cancer cells and these have been described as the ‘hallmarks of cancer’. Essentially, a cancer cell would attain the ability to circumvent apoptosis, acquire independent growth stimuli, resist growth inhibitory signals, have inexhaustible replicative potential, induce angiogenesis and metastasize in its progress towards malignancy (Hanahan and Weinberg, 2000b). It is acknowledged that genetic and epigenetic aberrations in cancer cells lead to the accumulation of these hallmark features.

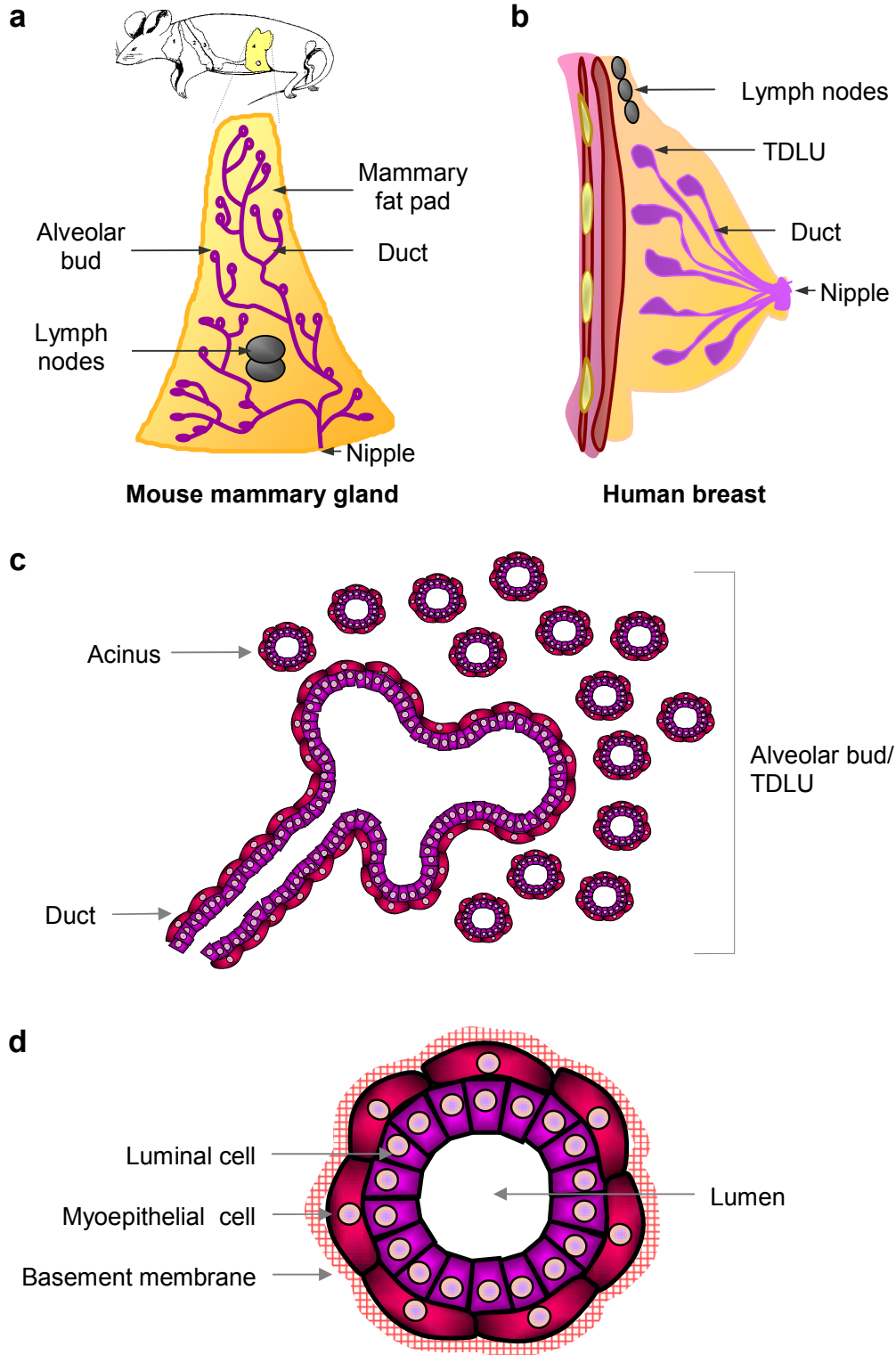


**Figure 1.4:** Basic architecture of **(a)** mouse mammary gland and **(b)** human breast. **(c)** Structure of the ductal secreting unit; alveolar bud in mouse and TDLU in humans. **(d)** Arrangement of epithelial cells within an acinus.

### 1.2.2 Breast cancer progression

In breast cancer, the conventional view of disease progression can be described based on histology of breast lesions (Figure 1.5a). The initial signs of carcinogenesis manifest in the form of hyperplasia, then atypical hyperplasia or an increase in cell number with abnormal nuclear morphology. This would progress into carcinoma in situ where cell numbers have increased to an extent where the lumen of a duct or acini is hardly visible but the basement membrane is still intact. Consequently, lesions would culminate with invasive carcinoma where tumour cells are no longer bound by a basement membrane and invade into the surrounding tissue (Bonadonna et al., 2006, Bombonati and Sgroi, 2011).

### 1.2.3 The metastatic cascade

Following that, scores of tumour cells will partake in the metastasis cascade but only a small portion of these cells successfully colonize secondary sites such as the lung and brain. This is mainly because it is an elaborate process (Figure 1.5b) where adequate angiogenesis needs to take place first, to provide a route by which tumour cells can reach a distant organ. Basically, angiogenesis is the process where either blood or lymph vessel sprouting is induced. Vascular endothelial growth factor (VEGF) proteins play an important part in the angiogenic process where VEGFA and VEGFC induce hemangiogenesis and lymphangiogenesis respectively. It is also noteworthy that angiogenesis, a hallmark of cancer cells, enables adequate supply of nutrients and oxygen needed for a tumour to maintain its rapid growth. However, the importance of lymphangiogenesis is not fully understood and could be a consequent effect of hemangiogenesis (Cao, 2005). With networks of vasculature within close proximity, the migration of tumour cells towards blood or lymphatic vessels is stimulated by chemokine gradients and leads to intravasation, circulation and extravasation of cells out of the respective vessels. This is not a new concept and conforms to Paget's 'seed and soil' hypothesis that metastases arise from cancer cells or 'seeds' and would only grow in suitable microenvironments, i.e. the 'soil' (Paget, 1889). True enough, breast cancer cells with the ability to metastasize to lung, liver, lymph node or bone marrow express the C-X-C motif receptor 4 (CXCR4) receptor and are attracted towards C-X-C motif ligand 12 (CXCL12), its ligand which is expressed in the tissues mentioned (Muller et al., 2001). At the secondary site, these cells would then require the ability to adapt and colonize the new micro-environment

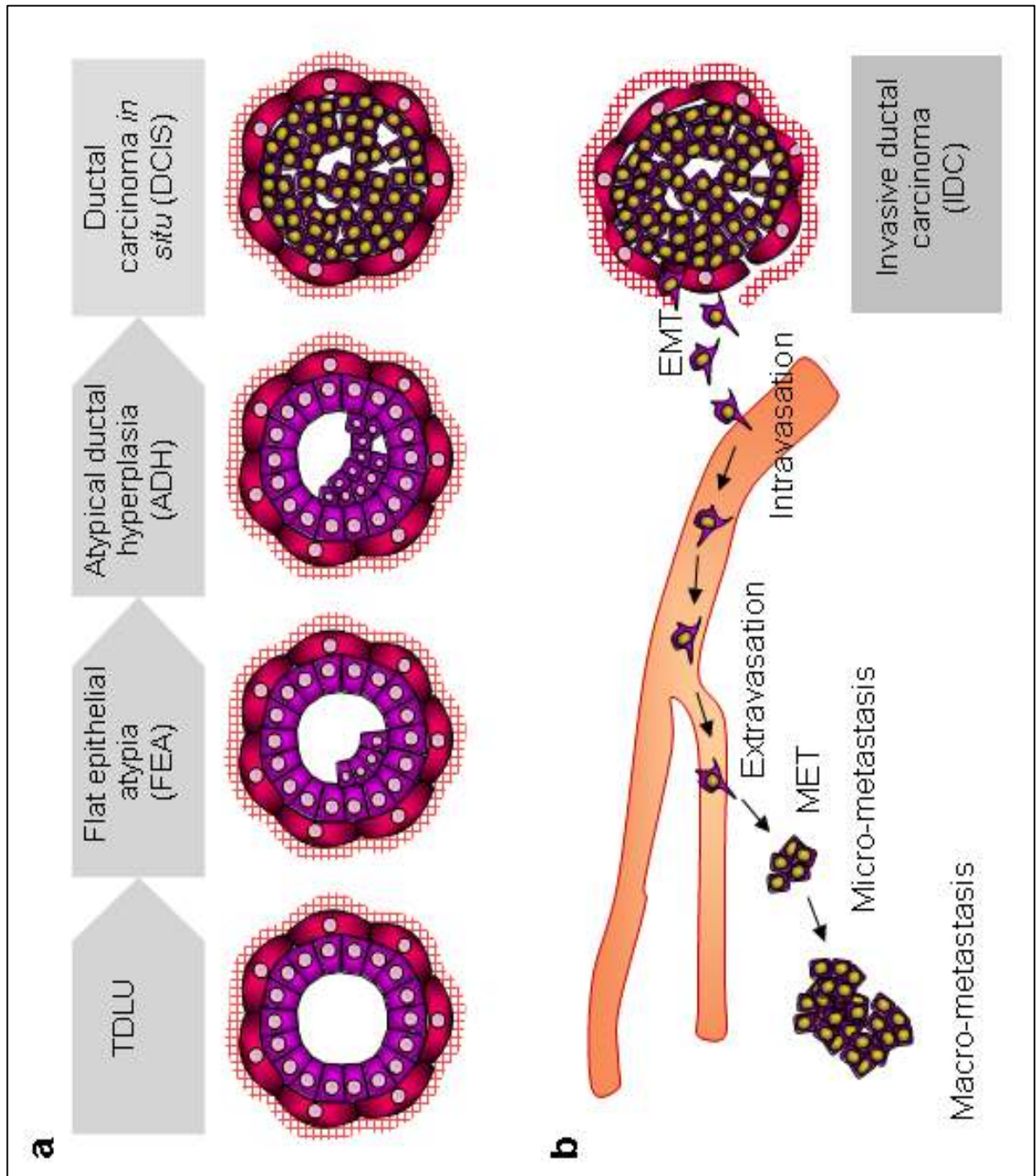


**Figure 1.5: Breast cancer progression.** (a) Illustration of histologically defined stages of breast cancer progression. Meshed line represents basal membrane. (b) Illustration of the metastatic cascade and some of the key stages involved.

(Geiger and Peeper, 2009). Furthermore, only a select number of micro-metastases are capable of developing macro-metastases.

#### ***1.2.4 Evading apoptosis: A hallmark of cancer cells***

Since the initial conception that decreased apoptosis in cancer cells can contribute to aberrant tissue turnover in tumours (Kerr et al., 1972), it is now well accepted that the ability to evade apoptosis is a hallmark of cancer cells (Hanahan and Weinberg, 2000a). Evidence for a role of anti-apoptotic proteins in tumourigenesis was provided through expression of Bcl-2 in haematopoietic cells, where it can cooperate with c-Myc to promote neoplastic progression (Vaux et al., 1988). This led to the notion that apoptosis regulators which are pro-survival can be potential oncogenes.

#### ***1.2.5 Apoptosis as a multistep barrier to metastasis***

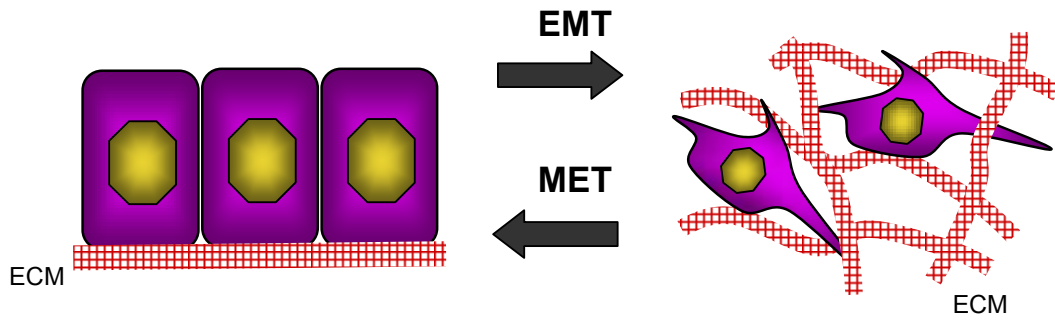
In the elaborate metastatic process, there are various stages where cancer cells are exposed to death inducing stimuli. One of the early steps where apoptosis limits the efficiency of cancer cells to metastasize is when cells detach from surrounding cells and/or the extra-cellular matrix (ECM). In normal mammary epithelial cells, this would induce anoikis or cell death due to loss of adhesion (Martin and Leder, 2001, Streuli and Gilmore, 1999). Furthermore, it has been shown that tumour cells die when they come into contact with endothelial cells of blood vessels during intravasion (Wyckoff et al., 2000). Tumour cells that manage to circulate in vessels are further subjected to mechanical stress due to shear forces and also surveillance by immune cells such as natural killer (NK) cells (Kim et al., 2000, Weiss et al., 1993). Upon reaching secondary sites, tumour cells will then need to adapt to a foreign microenvironment and only a small percentage will give rise to micro-metastases (Wong et al., 2001). All these factors suggest that metastasis is an inefficient process and the ability to suppress apoptosis would be necessary for the formation of metastasis. In fact, over-expression of anti-apoptotic Bcl-2 family proteins in tumourigenic mammary epithelial cells have been shown to increase the metastatic potential of these cells, highlighting apoptosis as a limiting factor towards metastases formation (Bufalo et al., 1997, Martin et al., 2004, Pinkas et al., 2004). However, there are limitations with these studies as they involve transplants of cell lines into immuno-compromised mice. This means that the early steps of metastasis where

anoikis takes place and immune surveillance could be neglected. Hence, the development of more adequate models could provide additional insights into the role of apoptosis as a safeguard from metastasis and ways of reactivating apoptotic pathways in cancer cells (Mehlen and Puisieux, 2006).

### ***1.2.6 Epithelial to mesenchymal transition (EMT) and the acquisition of malignant traits***

The process of epithelial to mesenchymal transition (EMT) is important throughout embryonic development for organogenesis (Baum et al., 2008). Similarly during postnatal mammary gland development, EMT has been implicated during ductal morphogenesis in the TEBs where a motile phenotype is necessary for cells to invade through the mammary fat pad (Kouros-Mehr and Werb, 2006). Mammary epithelial cells at ductal branch points and the leading edge of the mammary ductal tree also exhibit mesenchymal features during morphogenesis (Fata et al., 2004, Nelson et al., 2006). Since the mammary gland develops extensively only after birth, it is not surprising that EMT can be induced in mammary epithelial cells postnatally.

Some of the key features of EMT include the loss of E-cadherin expression along with cell-cell adhesion proteins (Figure 1.6). In line with this, a cell undergoing EMT would express mesenchymal markers such as N-cadherin, fibronectin and vimentin. A morphological change from cuboidal epithelial cells with apical-basal polarity to a more motile appearance with leading and trailing edge asymmetry is evident in this process (Christiansen and Rajasekaran, 2006). A large range of stimuli such as hypoxia, cell-stroma interactions and activation of signalling pathways, namely transforming growth factor  $\beta$  (TGF- $\beta$ ), NF- $\kappa$ B, hepatocyte growth factor (HGF), Wnt, Notch and Sonic Hedgehog (SHH) are able to induce EMT. These diverse stimuli converge in the expression of a group of EMT-inducers which are capable of orchestrating the EMT process. The EMT-inducers are a group of transcription factors which include Twist, Snail, Slug, Zeb1, Zeb2 and FoxC2 (Polyak and Weinberg, 2009).



Epithelial	Mesenchymal
Apical / basolateral polarity	Leading / trailing edge asymmetry
Cell adhesion & contact inhibition	Cell motility & invasiveness
Adherens, tight and gap junctions	Focal adhesions & transient gap junctions
E-cadherin & cytokeratins	N-cadherin, vimentin, SMA & MMPs

**Figure 1.6: Features of epithelial to mesenchymal transition (EMT).** Illustration of epithelial and mesenchymal cells and the processes EMT and MET that govern the switch between the different cell states. (Meshed lines represent extracellular matrix ECM, SMA denotes smooth muscle actin, MMP denotes matrix metallo-proteases ).Table listing the main characteristics of epithelial and mesenchymal cell states. Adapted from Christiansen & Rajasekaran 2006.

In the context of cancer cells, the EMT program is similar to that in embryonic development but its activation is due to aberrant stimuli. EMT has been associated with tumour progression and metastasis because it confers cancer cells with more motile and invasive phenotypes (Hugo et al., 2007, Yang and Weinberg, 2008). These would be important in the early stages of the metastatic cascade when cancer cells invade through the basement membrane into surrounding tissue and intravasate. Moreover, there is also evidence to indicate that trans-differentiation of breast cancer cells via EMT confers them with stem-cell like phenotypes (Mani et al., 2008, Morel et al., 2008). Apart from EMT, mesenchymal to epithelial transition (MET), the reverse process has also been shown to be important for the colonization of cancer cells at secondary sites (Dykxhoorn et al., 2009). This correlates with observations where metastases maintain an epithelial phenotype similar to its primary tumour. It would also suggest that the mesenchymal state is transient in cancer cells and its maintenance can be influenced by the tumour micro-environment (May et al., 2011).

### *1.2.7 Clonal evolution of tumours and breast cancer stem cells*

It has been a longstanding observation that heterogeneity exists within breast tumours. An obvious illustration of this phenomenon is in oestrogen receptor (ER) positive breast cancers where the levels of ER expression between cells in a tumour can vary considerably (Aubele et al., 1999). Accordingly, there is also evidence to support the fact that cells within a tumour acquire varying levels of genetic alterations (Fujii et al., 1996, Glockner et al., 2002). In the model of clonal selection, where it is proposed that cancers originate from a single cell, such heterogeneity can arise due to the acquisition of genetic changes that confers cells with a survival advantage. As a tumour progresses, sequential selection of cancer cells with increasing genetic alterations can give rise to progressively malignant clones (Nowell, 1976). Consequently, a tumour would comprise of cells with diverse genetic alterations and corresponding tumorigenic properties.

Alternatively, the heterogeneity of tumour cells could also arise due to hierarchical differences between cancer cell populations. The ‘cancer stem cell’ (CaSC) concept states that cells within a tumour are not equal in their proliferative potential. Within this hierarchy, it is the CaSCs that fuel the growth of a tumour and have the ability to self-renew whereas the bulk of differentiated or post-mitotic cells lack tumour initiating potential. Hence, CaSCs have also been implicated in the

seeding and progression of metastases. Importantly, both clonal evolution and CaSC models need not be mutually exclusive and could coherently depict the progression of tumours. The existence of CaSCs were first shown in hematopoietic malignancies (Furth and Kahn, 1937, Lapidot et al., 1994) and more recently, the presence of CaSCs in breast tumours represented the first indication of CaSCs in solid tumours (Al-Hajj et al., 2003). However, the CaSC concept does not stipulate the cell of origin of cancers and it is possible for CaSCs to arise from transformed mature, progenitor or normal stem cells. The characterization of breast CaSCs have been assisted by the use of putative CaSC markers such as CD24<sup>-</sup>/CD44<sup>+</sup>, aldehyde dehydrogenase 1 (ALDH1) and CD61<sup>+</sup> for different tumour subtypes. Even so, there is currently not a consensus for markers that are able to enrich for CaSCs from differing tumour subtypes. This may be a result of CaSCs arising from different cells of origin and/or their dependence on diverse oncogenic pathways.

Phenotypically, CaSCs have also been shown to be more resistant to chemotherapy (Li et al., 2008) and radiotherapy (Diehn et al., 2009). This has important implications with regards to therapeutics because targeting the bulk of the tumour will leave residual CaSCs which can remain dormant and lead to relapse of disease. In addition, it has been shown that plasticity can exist within a tumour cell population where non CaSCs can be induced to acquire CaSC phenotypes (Meyer et al., 2009). This is further supported by the fact that EMT can induce the acquisition of CaSC phenotypes in cancer cells (Mani et al., 2008, Polyak and Weinberg, 2009). As such, the EMT process could also contribute to intratumour heterogeneity. Taken together, this would imply that the elimination of CaSCs by itself is not sufficient for preventing the recurrence of disease and pathways which enable plasticity in cancer cells need to be targeted simultaneously.

### **1.2.8 Breast cancer epidemiology**

Breast cancer is the main cause of cancer related deaths in women worldwide (Murray and Lope, 1997). In general breast cancer incidence is much higher in developed countries relative to developing countries. The hormone oestradiol accounts for most of the epidemiology of breast cancer (Key et al., 2001). When women are within their reproductive age, incidence of breast cancer increases rapidly with age and this increase occurs at a slower rate once women reach the average age of menopause (about 50 years) (cancer., 1997). Risk factors for breast cancer include

the age for menarche, where an early menarche is associated with increased risk of breast cancer (Kelsey et al., 1993) Childbearing has a protective effect against breast cancer where women who have gone through more full term pregnancies have a lower risk relative to nulliparous women (Layde et al., 1989). In addition, the age during first full term pregnancy also determines breast cancer risk and this effect is independent of the total number of pregnancies. Women with an early age (younger than 20 years) of first term pregnancy have been shown to have a lower risk of breast cancer relative to women with a first term pregnancy after 35 (Kelsey et al., 1993). Apart from that, breastfeeding also has significant protective effects against breast cancer (Lipworth et al., 2000). The onset of menopause also affects breast cancer risk, with an increased risk observed for later onset (cancer., 1997).

Oral contraceptives (cancer., 1996) and hormone replacement therapy for menopause (Magnusson et al., 1999) have both been associated with increased risk for breast cancer and this illustrates the effects of hormones (oestrogen and progesterone) on the epidemiology of breast cancer . Other lifestyle factors which increase the risk of breast cancer include high fat diets (Hunter et al., 1996) and consumption of alcohol (Smith-Warner et al., 1998), whereas exercise appears to have a protective effect (Friedenreich et al., 1998).

A large number of environmental and lifestyle risk factors determine the incidence of breast cancers. Genetic determinants, particularly high risk mutations such as p53, PTEN, BRCA1 and BRCA2 account for only about 5% of breast cancer cases (Easton, 1999, Ford et al., 1998, Peto et al., 1999).

### ***1.2.9 Breast cancer incidence and survival rates***

Even though breast cancer predominantly affects women, it is the most common form of cancer in the United Kingdom (UK) with about 46,000 people diagnosed within 2007 (Northern Ireland Cancer Registry, 2010, Office for National Statistics, 2010, Welsh Cancer Intelligence and Surveillance Unit, 2010). On the global scale, figures from 2008 indicate that 1.38 million women were diagnosed and that accounts for about 11% of all cancer cases (Ferlay et al., 2010). This highlights the extent of this disease and stresses the need to understand the risks of developing breast cancer and finding ways of managing the disease to improve the lifestyles of people affected. Fittingly, much progress has been made and this is reflected by the increase in five year relative survival rates of patients in the UK, from 52% in the

early 1970s to 82% at present (Rachet et al., 2009). This is also illustrated by the decrease in mortality rates where breast cancer is no longer the leading cause of cancer related deaths. Even so, the reality is that breast cancer is a heterogeneous disease which comprises many subtypes. While prognoses have improved for certain subtypes, some remain less adequate. This is mainly due to therapeutic resistance, metastasis and tumour relapse.

#### *1.2.10 Heterogeneity of breast cancers and intrinsic subtypes*

The advent of gene expression microarrays has led to the classification of breast cancers into intrinsic subtypes based on their molecular profiles. At the outset, the classification was based on gene clusters correlating to proliferation, hormone receptor signalling, Her2 signalling and a basal cluster which is associated with basal epithelial cells of the breast (Perou et al., 2000). As a result, the different gene profiles can now be used to segregate breast cancers into six groups designated luminal A, luminal B, Her2-enriched, basal-like, normal-like and claudin-low (Carey, 2010).

Both the luminal subtypes as their names suggest, have expression profiles reminiscent of the luminal epithelial cells. In exact, they usually express luminal cytokeratins (CKs) 8 and 18, oestrogen receptor (ER), progesterone receptor (PgR) or ER associated genes such as GATA3. Both luminal A and luminal B are very common subtypes which make up around 40% and 20% of breast cancers respectively. These subtypes can be distinguished based on the fact that luminal A subtypes have higher expression of ER associated genes but lower expression of proliferation and Her2 related genes.

The Her2-enriched is one of the hormone receptor negative subtypes and comprise about 10% of breast cancers. These have high expression of genes in the Her2 cluster which include genes which are in proximity to the Her2 locus in the genome. These neighboring genes are expressed in tandem because aberrant expression of Her2 in breast cancers is usually a result of gene amplification events (Couturier et al., 2008). The tumours are usually high-grade based on histological analysis and have relatively poor prognoses.

In the basal-like group, these tumours do not express ER, PgR or Her2 and are closely associated to 'triple negative' (ER<sup>-</sup> PgR<sup>-</sup> Her2<sup>-</sup>) breast cancers. Although these two subsets overlap to a large degree, they are not synonymous. As this subtype is

categorized based on expression of basal epithelial genes, the tumours typically express CK 5, CK14, CK17, vimentin and epidermal growth factor receptor (EGFR) (Lerma et al., 2007a). Moreover, the basal-like tumours also over-express genes of the proliferation cluster. Up to 20% of breast cancers are of this subtype and most of them show high-grade histologies. Interestingly, BRCA1 germline mutations have been identified as risk factors for basal-like breast cancer and give rise to tumours with identical features (Turner et al., 2004).

One of the other subtypes that were initially characterized was the normal-like group but its attributes remain elusive and it could be an artifact of stromal tissue contamination. The claudin-low subtype has also emerged after larger scale gene expression analyses were carried out. It is another 'triple negative' subtype with low expression in all gene clusters and especially cell adhesion and interaction genes such as claudin and E-cadherin. Until now, not much is known about the clinical aspects of the claudin-low subtype but it is associated with metaplastic carcinoma and is enriched with tumour initiating phenotypes (Carey, 2010).

#### *1.2.11 Targeted therapeutics in breast cancer*

Targeted therapeutics are drugs which specifically target a signalling pathway and due to its specific mode of action, reduce the level of systemic toxicity. This is in contrast to conventional chemotherapy which target highly proliferative cells. The concept of targeted therapy has been employed in breast cancer since the early 1970s with the use of tamoxifen, an antagonist for ER. The rationale behind tamoxifen was that a proportion of breast cancers depend on estrogen signaling for growth. By interrupting this signalling between ligand and receptor, it is possible to restrict the growth of breast cancers. Tamoxifen had a great impact on survival rates of hormone dependent breast cancers and was a gold standard of targeted therapies for decades. This provided proof of principle and paved the way for the development of targeted therapeutics in breast cancer (Jordan, 2007). Following tamoxifen's success in estrogen responsive breast cancers, aromatase inhibitors and improved ER antagonists such as fulvestrant have been successful in targeting the estrogen signalling pathway, albeit with different mechanisms (Hiscox et al., 2009). Luminal subtypes of breast cancer have benefited greatly from these advances but some challenges such as endocrine resistance remain, especially in the luminal B subtypes.

Another fundamental breakthrough for target based approaches was trastuzumab, a monoclonal antibody (MoAb) which interfered with Her2 receptor signalling. Prognoses for the Her2-enriched subtype improved markedly and relapse rates for endocrine resistant breast cancers can be decreased significantly when trastuzumab is administered with conventional treatment regimens (Normanno et al., 2009).

Unfortunately, effective treatments specifically targeting the basal-like subtype are still lacking at present. The fact that basal-like tumours are mostly ‘triple negative’ (i.e. lack expression of ER, HER2 and PgR) means that they do not respond to endocrine therapy or trastuzumab. One of the prospective targets for this subtype was EGFR because its expression correlates with the basal-like intrinsic profile. As with trastuzumab, cetuximab is a MoAb designed to abolish EGFR mediated signalling. However, only modest results were seen for patients treated with cetuximab. This highlights some of the challenges faced by targeted therapies. The specific nature of such drugs could be ineffective because of redundant pathways, multiple patterns of resistance or the adaptive capacity of tumours. This has not halted the search for ‘magic bullets’ for this disease subtype and instead have stimulated the need for understanding its mechanisms further. There are many targeted therapies in development at present and the poly ADP ribose polymerase (PARP) inhibitors carry much promise for treatment of basal-like cancers. PARP inhibitors function by impairing the DNA damage repair mechanism, leaving cancer cells more susceptible to DNA damaging agents such as cisplatin. The clinical efficacy of this class of drugs will be apparent in the near future but until then, the search for potential targets continues (Carey, 2010).

### ***1.2.12 Targeting breast cancer stem cells***

As it is becoming more apparent that CaSCs are the cause of therapeutic resistance, disease relapse and the seeding of metastases in a range of breast cancer subtypes, it is only sensible that CaSCs are accounted for when designing targeted therapeutics. However, due to the plasticity that exists in tumours, the bulk of tumour cells should also be eliminated to prevent reemergence of CaSCs. Ideally, treatments would target CaSCs and bulk tumour cells with minimal adverse effects to patients (McDermott and Wicha, 2010).

A number of pathways pertinent to normal stem cells have been shown to be important in breast CaSCs. These include Hedgehog (Liu et al., 2006), PTEN/AKT/WNT signalling axis (Korkaya et al., 2009) and Notch (Harrison et al., 2010). Inhibition of these particular pathways either decreased mammosphere formation and/or tumour initiation, indicating the loss of CaSCs. In addition, a number of cytokines such as IL-6 (Sansone et al., 2007) and IL-8 can also regulate breast CaSCs. By targeting CXCR1, the cognate receptor for IL-8, CaSCs can be sensitized to a bystander killing effect mediated by FAS ligand (Charafe-Jauffret et al., 2009). Another pathway that has been increasingly associated with breast CaSCs is the NF- $\kappa$ B pathway, where its inactivation led to the decrease of CaSCs in Neu-driven tumours (Liu et al., 2010). All these pathways represent possible avenues where CaSCs can be selectively targeted.

### ***1.2.13 Mouse models of breast cancer***

Mouse models have provided an important understanding into the development of breast cancer. Moreover, these models also serve as important pre-clinical platforms to verify efficacy of potential drugs. In some of the early models, mammary lesions were induced by external factors such as the mouse mammary tumour virus (MMTV) and chemical carcinogens. Progress in transgenic technology then led to the development of a new generation of models where tumour suppressors can be knocked out or oncogenes over-expressed. Apart from providing an understanding for the role of a gene in breast carcinogenesis or progression, these models have also been useful in elucidating molecular pathways. Moreover, the use of mammary gland specific promoters such as MMTV-long terminal repeat (MMTV-LTR),  $\beta$ -lactoglobulin (BLG) and whey acidic protein (WAP) promoters have allowed spatial control of transgene expression in the mammary compartment. Even so, there are limitations with using constitutively active promoters especially when the transgene of interest has unwanted effects throughout development. This problem can be resolved with the use of inducible transgenic systems. Added to that, conditional expression systems such as the tetracycline-controlled system have also proved useful in revealing mechanisms such as oncogene addiction. This is possible with conditional systems because expression of a gene can be switched on or off in the presence or absence of its inducer (Allred and Medina, 2008).

#### 1.2.14 The tetracycline conditional expression system

The basic components required in conditional inducible systems are an inducing agent, a regulatory unit and a responsive element linked to the promoter of a gene of interest (Figure 1.7a). The tetracycline-controlled transcriptional regulator is one of the most widely used conditional systems. Two variants of the system exist, namely, the tTA (tet-off system) and the rtTA (tet-on system). In each system, there are two features required. First, either the tTA or rtTA will be driven by a constitutive promoter. Second, the gene of interest will be under the control of a tetracycline responsive element (TRE) which is made up of promoter sequences from human cytomegalovirus promoter IE (Pcmv) and *E. coli* tet operator (tetO) sequences (Gossen and Bujard, 1992). The tTA unit consists of the tetracycline repressor (tetR) fused with the transcription activation domain of virion protein 16 (VP16) of herpes simplex virus. When doxycycline (dox), an analogue of tetracycline is present, it induces a conformational change in tTA, causing it to dissociate from the TRE. As a result, the gene of interest will not be transcribed in the presence of dox, hence the tet-off system (Figure 1.7b). The rtTA system works in a similar fashion except that the rtTA is a mutant derivative of tTA which only binds TRE in the presence of dox. With the rtTA, presence of dox will then switch on expression of a gene of interest (Figure 1.7c).

The main advantages of the rtTA system are that gene expression can be reversibly switched on rapidly in the presence of dox and off by removing dox. In contrast to the tTA system, there is less delay and no need to administer dox for long periods to keep a gene off, especially while growth and development is taking place. However, the setback of the rtTA system is leaky expression due to undesired interactions between rtTA and the TRE when dox is not present. Despite its leaky expression, the rtTA system has been used successfully to discern phenotypes as a consequence of transgene induction (Ray et al., 1997, Zheng et al., 2000).

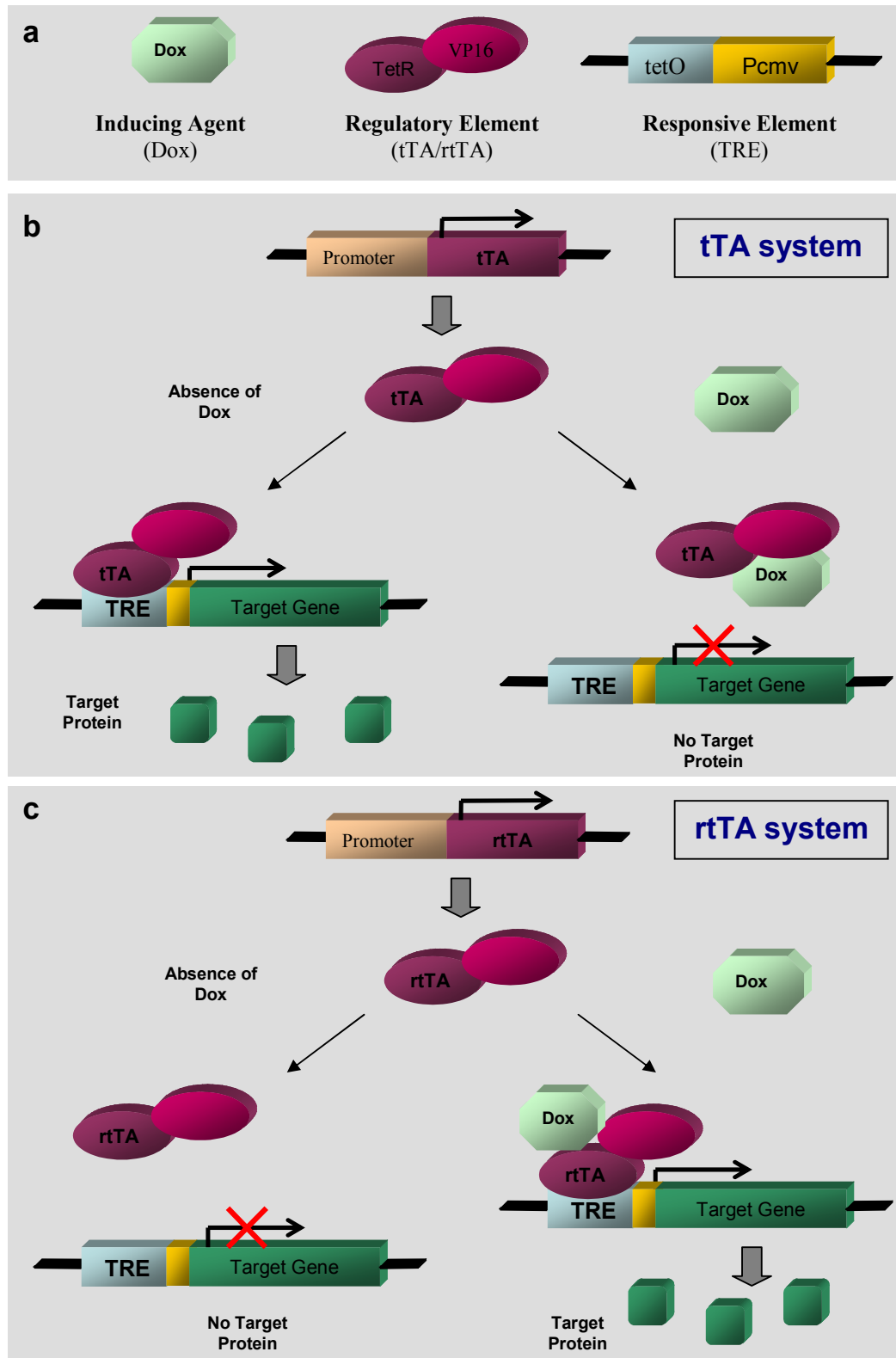


**Figure 1.7 The tetracycline inducible system.** (a) Basic components of the system; doxycycline as inducing agent, TetR fused with VP16 as the regulatory element, tetO and Pcmv as the responsive element. (b) The tTA system: In the presence of dox, tTA is unable to bind the TRE element and transgene expression is switched off. (c) The rtTA system: Presence of dox allows rtTA to bind to TRE element inducing expression of transgene.

### 1.2.15 Transplantation models of breast cancer

An alternative approach to modelling breast cancer has been the use of cell lines for transplantation into the mouse. This could either be syngeneic transplants of murine cells into an appropriate host, giving rise to allografts or the transplant of cells into immuno-compromised mice, resulting in xenografts. All of these approaches have their limitations and advantages. Xenografts could produce tumours which are more closely related to breast cancers in human, since human cancer cell lines can be transplanted. However, the use of immuno-compromised mice to establish xenografts neglects the contribution of certain components of the immune system to tumour progression. In general, the use of established cancer cell lines in transplantation means that aspects related to tumour initiation are omitted. On the other hand, transplantation could be a way of rapidly elucidating questions pertaining to the latter steps of breast cancer progression. Hence the selection of a particular model depends largely on the questions to be addressed because as of now, none of the available models fully encompass all the features of breast cancer (Vargo-Gogola and Rosen, 2007).

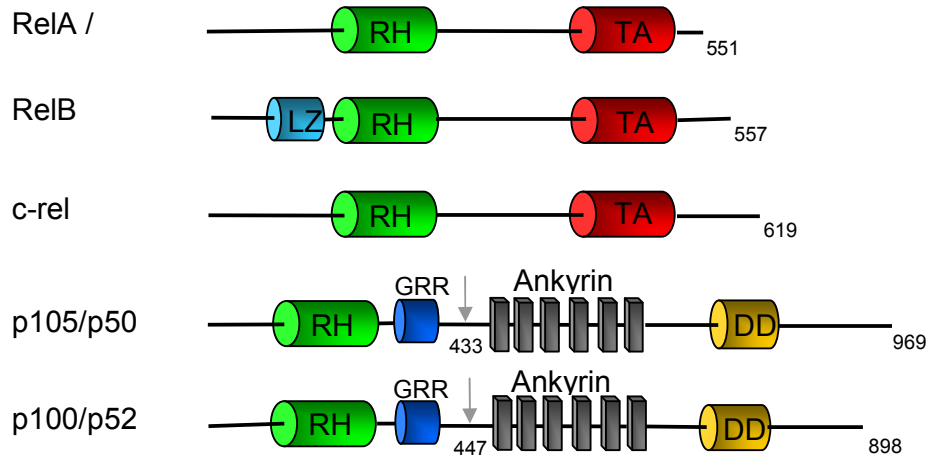
## 1.3 NF- $\kappa$ B signaling

### 1.3.1 NF- $\kappa$ B and I $\kappa$ B superfamily of proteins

The NF- $\kappa$ B proteins are transcription factors which were initially identified as regulators of the immune system. There are five different subunits which can form homo- or heterodimers to regulate the expression of genes. Namely, these are RelA (p65), RelB, c-rel, p50 and p52 (Figure 1.8a). All of these subunits have a conserved Rel homology domain (RHD) which facilitates DNA binding and dimerization. However, the Rel proteins differ from p50 and p52 in two ways. Firstly, they contain trans-activating domains which are important in initiating transcription. Secondly, p50 and p52 are translated from precursor proteins p105 and p100 respectively. These precursor proteins are inhibitor of NF- $\kappa$ B (I $\kappa$ B) proteins characterized by the presence of ankyrin repeats at the C-terminus (Figure 1.8b). These motifs are removed upon partial proteasomal processing into p50 or p52 respectively. The glycine rich regions prevent complete degradation of the precursor protein. Apart from p105 and p100, other I $\kappa$ B proteins include I $\kappa$ B $\alpha$ , I $\kappa$ B $\beta$ , I $\kappa$ B $\epsilon$  and Bcl-3. The I $\kappa$ B proteins function by masking the nuclear localization signal (NLS) of NF- $\kappa$ B subunits and thus, retaining

**a**

**The NF- $\kappa$ B family**



**b**

**The I $\kappa$ B family**

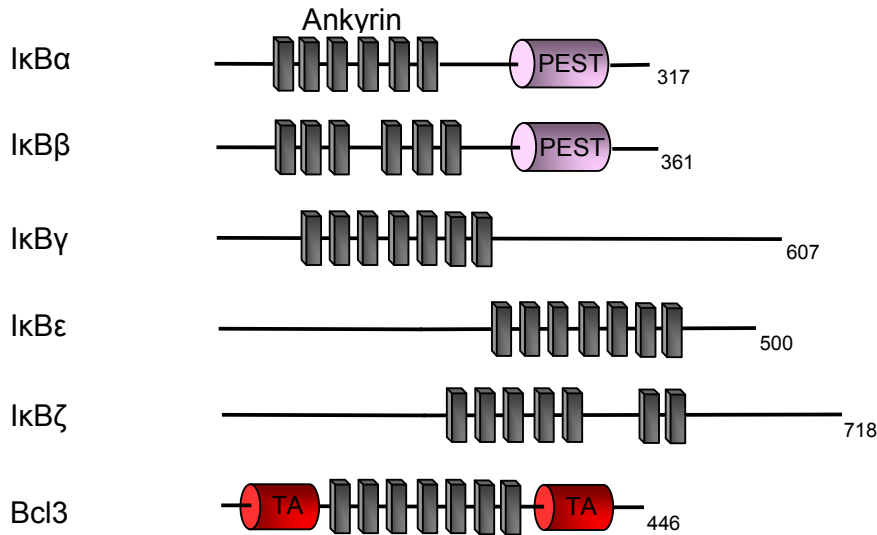


**Figure 1.8: NF- $\kappa$ B and I $\kappa$ B super-family of proteins.** (a) Illustration of domains present in NF- $\kappa$ B sub-units. LZ: leucine zipper domain, RH: Rel homology domain, TA: trans-activating domain, GRR: glycine rich region, DD: death domain, numbers indicate amino acid positions, grey arrows represent points where proteasomal processing terminates. (b) Illustration of domains present in I $\kappa$ B family of proteins. Grey boxes represent ankyrin domains, PEST: proline glutamate serine threonine, TA: trans-activating domains, numbers indicate amino acid positions. Adapted from Perkins 2007.

them in the cytoplasm. Bcl-3 is an exception amongst I $\kappa$ B proteins because it is nuclear localized and can function as a transcriptional co-activator (Ghosh and Hayden, 2008).

### **1.3.2 Activation of NF- $\kappa$ B pathways**

There are two main NF- $\kappa$ B pathways, namely, the canonical and alternative pathways (Figure 1.9). Transcriptional activity induced by canonical NF- $\kappa$ B signalling involves RelA-p50 dimers whereas the alternative pathway is dependent on RelB-p52 dimers. In total, there are more than 150 known extracellular stimuli that can activate these pathways leading to diverse outcomes and this epitomizes the role of NF- $\kappa$ B as a central mediator. Inflammatory stimuli such as tumour necrosis factor  $\alpha$  (TNF- $\alpha$ ), lipopolysaccharide (LPS) and interleukin-1 (IL-1) induce the activation of the canonical pathway. Stimuli across the respective receptors activate the I $\kappa$ B kinase (I $\kappa$ K) complex which consists of I $\kappa$ K $\alpha$ , I $\kappa$ K $\beta$  and I $\kappa$ K $\gamma$ . This stimulates phosphorylation of I $\kappa$ B $\alpha$  at two conserved serine residues which leads to its proteasomal degradation. Consequently, RelA-p50 dimers can translocate into the nucleus and are able to induce transcription.

Similarly in the alternative pathway, p100 preferentially binds and sequesters RelB in the cytoplasm. Proteasomal processing of p100 is triggered by activation of CD40, lymphotoxin- $\beta$  receptor (LT $\beta$ R), B-cell activating factor of the TNF family (BAFF) or receptor activator of NF- $\kappa$ B ligand (RANKL). Transduction of signals across these receptors sets off a signalling cascade involving NF- $\kappa$ B inducing kinase (NIK) and I $\kappa$ K $\alpha$  dimers, resulting in p100 phosphorylation and processing into p52. The loss of ankyrin domains from the C-terminus of p100 then allows translocation of RelB-p52 heterodimers into the nucleus (Baud and Karin, 2009, Perkins, 2007).

In addition to the various immune regulatory stimuli that activates the canonical and alternative NF- $\kappa$ B pathways, signalling via the epidermal growth factor receptor (EGFR) family members can also trigger the activation of NF- $\kappa$ B. This mode of activation is termed the atypical NF- $\kappa$ B pathway as it can trigger I $\kappa$ B $\alpha$  phosphorylation without invoking the usual I $\kappa$ K complexes. Instead, I $\kappa$ B $\alpha$  is phosphorylated by casein-kinase-II (CK2) (Sethi et al., 2007). Interestingly, CK2 can also induce the expression of I $\kappa$ K $\epsilon$  (Eddy et al., 2005), a kinase that is able to promote the transactivation potential of p52 through formation of a RelA-p52-I $\kappa$ K $\epsilon$  complex (Wietek et al., 2006). These studies highlight the complexity of interactions between

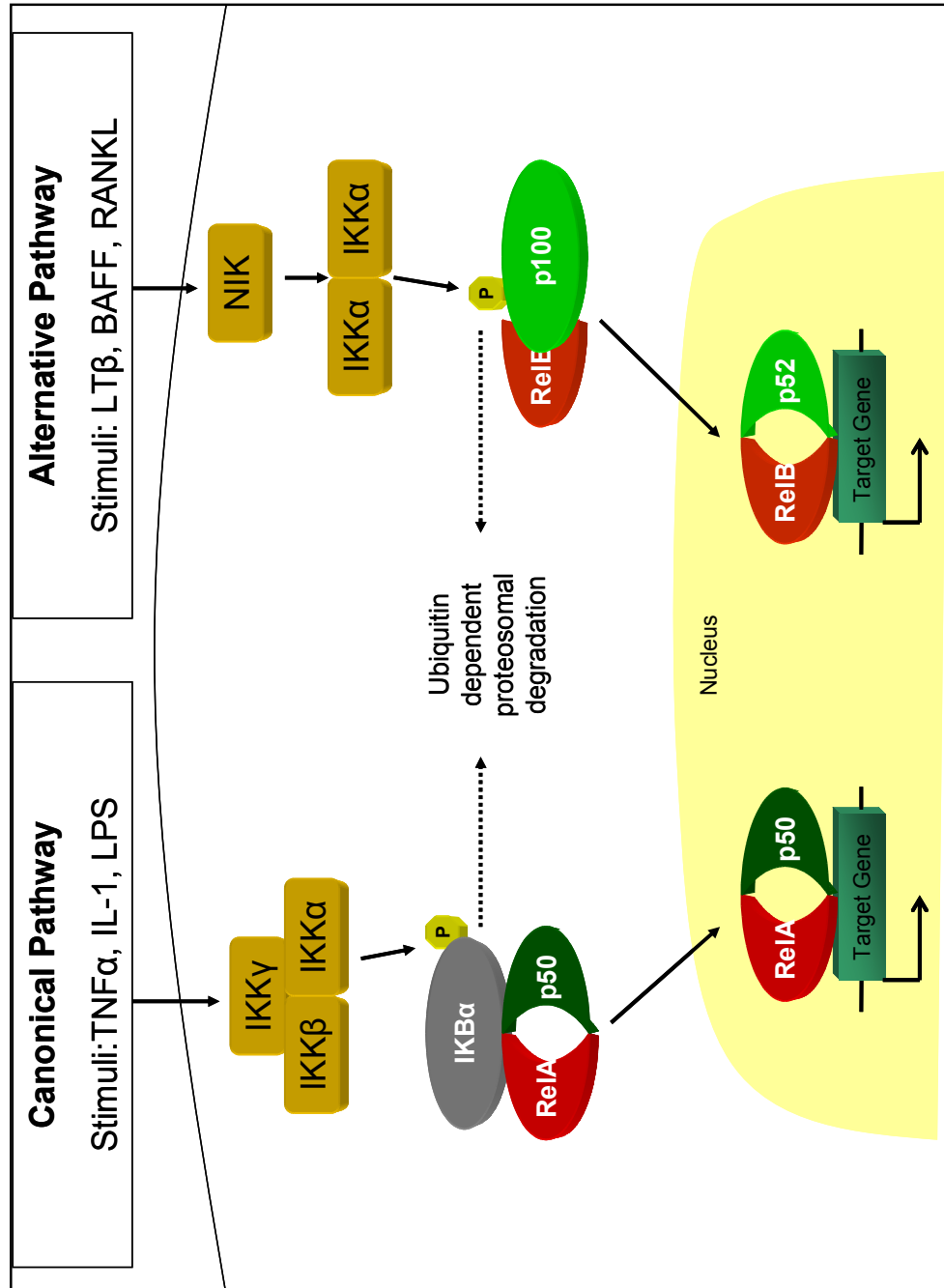


**Figure 1.9: Canonical and alternative NF- $\kappa$ B pathways.** Illustration of the activating stimuli, kinases and subunits involved in the canonical and alternative NF- $\kappa$ B pathways. Adapted from Cao & Karin 2003.

NF- $\kappa$ B subunits and hence, their involvement in physiology and pathology should not be limited to the canonical and alternative pathways.

### **1.3.3 Gene targets of NF- $\kappa$ B**

NF- $\kappa$ B transcription factors can either induce or repress gene targets by binding to specific DNA sequences termed  $\kappa$ B sites. In addition to the permutation of  $\kappa$ B sites, the binding of specific sub-units at these sites are dependent on the recruitment of co-activators or co-repressors. It is through the differential recruitment of NF- $\kappa$ B subunits by co-regulators that each sub-unit plays a distinct and non overlapping role (Hoffmann et al., 2003). Crosstalk between other transcription factors such as AP-1 and C/EBP $\beta$  provides an additional layer of complexity into NF- $\kappa$ B signalling. As a consequence, transcriptional output will be context dependent (Perkins and Gilmore, 2006).

In general, gene targets of NF- $\kappa$ B have a role in immune modulation, stress response, proliferation, survival and apoptosis. Among these are some genes which have a role in cancers such as Cyclin D1, Bcl-xL, Cox2, VEGF C and c-myc. Paradoxically, some tumour suppressor genes such as p53 and pro-apoptotic genes such as Fas are also regulated by NF- $\kappa$ B. This reiterates the need to regard NF- $\kappa$ B signalling based on the context of specific stimuli and cell type (Pahl, 1999, Perkins, 2007).

### **1.3.4 Modulation of NF- $\kappa$ B subunit activity**

As described, activation of the main NF- $\kappa$ B pathways converges upon I $\kappa$ K complexes where they then induce degradation of I $\kappa$ B proteins to allow translocation of NF- $\kappa$ B subunits into the nucleus. Additionally, NF- $\kappa$ B activity is also governed by direct post-translational modifications. Such modifications regulate the interaction of NF- $\kappa$ B subunits with either co-activators or co-repressors and this allows integration of stimuli from other signalling pathways (Perkins and Gilmore, 2006).

Despite the importance of post-translational modifications on the transcriptional output of NF- $\kappa$ B subunits, the true extent of these modifications is currently unknown. In the case of Rel A, examples of stimulatory phosphorylations which enhance its transcriptional activity include Ser-276 phosphorylation by protein kinase A (PKAc), Ser-311 by PKC $\zeta$  and Ser-468 by glycogen-synthase kinase-3 $\beta$

(Perkins and Gilmore, 2006). Moreover, acetylation of Rel A by p300 and CBP can enhance its transactivation potential (Chen and Greene, 2004). On the other hand, Rel A can also be subjected to inhibitory phosphorylation at Thr-505 by the checkpoint kinase CHK1, which inhibits its trans-activation and increases its association with histone deacetylase 1 (HDAC1) (Campbell et al., 2006, Rocha et al., 2005).

As for p52, it has been shown that this NF- $\kappa$ B subunit can regulate gene targets of the tumour suppressor p53. The co-operative regulation of these genes such as p21 and death receptor 5 (DR5) does not rely on the DNA binding properties of p52 (Schumm et al., 2006). In such cases, p52 functions by recruiting the co-activator p300/CBP or co-repressor HDAC1 to p53 promoter sites. This proves that the range of genes that can be regulated by NF- $\kappa$ B subunits is not restricted to those with  $\kappa$ B sites. Accordingly, phosphorylation of p52 has been shown to be important in determining the association of p52 with co-regulators. In a study addressing the regulation of the Skp2 gene by p52 and p53, phosphorylation of p52 at Ser-222 by GSK-3 $\beta$  was crucial in determining whether transcription takes place. Upon phosphorylation of p52 by GSK-3 $\beta$ , p52 homodimer/Bcl-3 trans-activating complexes were disrupted and this shifts the balance towards formation of p52/c-rel/HDAC1 complexes which are transcriptionally repressive. This demonstrates that Ser-222 phosphorylation of p52 induces the formation of transcriptionally repressive complexes under the conditions investigated (Barre and Perkins, 2010b).

### 1.3.5 Role of NF- $\kappa$ B in development

The function of NF- $\kappa$ B subunits during development have largely been dissected through genetically engineered knockout mouse models of individual or two subunits in combination (Gerondakis et al., 1999). An important anti-apoptotic role for NF- $\kappa$ B was identified from RelA<sup>-/-</sup> mice, where they die *in utero* due to extensive liver apoptosis (Beg et al., 1995). As for *Nfkb1*<sup>-/-</sup> mice which lack both p105 and p50, no histo-pathological effects have been reported (Grumont et al., 1998, Sha et al., 1995, Snapper et al., 1996). On the other hand, *Nfkb2*<sup>-/-</sup> mice which lack both p100 and p52 display defects in splenic micro-architecture and diminished peripheral lymph nodes (Caamano et al., 1998, Franzoso et al., 1998). However, when both *Nfkb1* and *Nfkb2* genes were ablated in combination, lymph nodes were absent altogether, suggesting overlapping and compensatory roles between p50 and p52 which were only evident when both genes were depleted (Lo et al., 2006). Even so,

respective NF- $\kappa$ B subunits have distinct functions in the development and function of immune cell populations, as revealed by knockouts of Relb, c-rel, Nfkb1 and Nfkb2 (Beinke and Ley, 2004, Gerondakis et al., 1999).

### ***1.3.6 NF- $\kappa$ B signalling during post-natal mammary gland development***

Expression of RelA and p50 have been shown in mammary epithelia of virgin, pregnant and involuting mice (Brantley et al., 2000). The levels of these subunits remain low until pregnancy where its activity peaks at D16 of gestation in mice and drops to undetectable levels during lactation. A second wave of NF- $\kappa$ B signaling is triggered after lactation ceases and peaks by day 3 of involution (Clarkson et al., 2000a).

A role for NF- $\kappa$ B during ductal morphogenesis is highlighted by a study where mammary epithelial cells (MECs) with the deletion of I $\kappa$ B $\alpha$  show that the lack of this repressor leads to increased ductal branching and intraductal hyperplasia (Brantley et al., 2001). This illustrates a positive regulatory role for NF- $\kappa$ B towards epithelial proliferation and branching at this developmental timepoint. The increase in the levels of NF- $\kappa$ B in mammary epithelia are coherent with the rate of lobuloalveolar development during pregnancy and again this illustrates a positive regulatory role for NF- $\kappa$ B in epithelial proliferation through the regulation of Cyclin D1 (Cao and Karin, 2003). In fact, knock in mice with a kinase inactive I $\kappa$ K $\alpha$  (I $\kappa$ K $\alpha$ <sup>AA/AA</sup>) and mice over-expressing a dominant I $\kappa$ B $\alpha$  super-repressor, both with defective NF- $\kappa$ B activation, showed defective lobuloalveolar development and lactational defects (Cao et al., 2001b). As lactation commences, levels of NF- $\kappa$ B and its activity decreases and this can be attributed to the activation of the prolactin receptor-JAK2-Stat5 pathway which is important for alveolar differentiation and milk production (Hennighausen and Robinson, 2001). Negative crosstalk between the two pathways exists and it is likely that NF- $\kappa$ B activity diminishes when Stat5 is functionally induced (Geymayer and Doppler, 2000, Luo and Yu-Lee, 2000). During involution, NF- $\kappa$ B plays an important role along with Stat3 to regulate the balance of apoptotic and inflammatory stimuli (Clarkson et al., 2004, Watson, 2006). The presence of nuclear RelA in a subpopulation of non-apoptotic cells during involution supports the notion that NF- $\kappa$ B has a role in survival of mammary epithelial cells (Clarkson et al., 2000b).

The dynamic and tightly regulated activity of NF- $\kappa$ B throughout postnatal mammary gland development emphasizes its importance in regulating proliferation and survival of MECs.

### ***1.3.7 Aberrant NF- $\kappa$ B activity in breast cancer***

The idea that aberrant NF- $\kappa$ B signaling may contribute to the aetiology and progression of breast cancers can be derived from observations where elevated levels of NF- $\kappa$ B subunits have been observed in breast cancer cell lines as well as primary human breast tumours (Dejardin et al., 1995, Sovak et al., 1997). In another study, constitutive levels and DNA binding of p52, Bcl3 and c-rel were much higher in human breast tumors relative to adjacent normal tissue (Cogswell et al., 2000). However, it is only in ER negative breast cancers that elevated NF- $\kappa$ B activity is widespread and this is due to the negative crosstalk that exists between the signaling pathways (Nakshatri et al., 1997). While this opposing relationship exists between ER and NF- $\kappa$ B signalling, a correlative linkage between EGFR family members and NF- $\kappa$ B signalling is evident (Biswas and Iglehart, 2006). This is not surprising as the EGFR family members can trigger NF- $\kappa$ B activation. In support of this, a study looking into 35 human breast cancer cell lines revealed that constitutive NF- $\kappa$ B activation was preferentially higher in the basal-like subtype cell lines where EGFR over-expression is common (Yamaguchi et al., 2009). Despite all these findings, it is not clear whether the activity of distinct NF- $\kappa$ B subunits have a role in defining the gene expression profiles of particular subtypes of breast cancer.

There have been many studies which have demonstrated a role for NF- $\kappa$ B in breast carcinogenesis. From mouse models, we know that over-expression of c-rel in the mammary gland leads to the development of tumours and similarly for p100/p52, hyperplastic glands develop (Connelly et al., 2007, Romieu-Morez et al., 2003). A role for the canonical NF- $\kappa$ B pathway in tumourigenesis has been coherently demonstrated via over-expression of the I $\kappa$ B $\alpha$  super repressor (SR), where inhibition of canonical NF- $\kappa$ B signaling delayed the tumour latency of Neu-oncogene (Liu et al., 2010, Pratt et al., 2009) and Polyoma middle T oncogene (PyVT) driven tumours respectively (Connelly et al., 2010). Moreover, these studies also demonstrated that NF- $\kappa$ B activity is important for the expansion of CaSCs (Liu et al., 2010, Pratt et al., 2009). It is not surprising that NF- $\kappa$ B activity contributes to the maintenance of CaSC

populations, since it induces EMT and promotes metastasis in a model of breast cancer (Huber et al., 2004b), both of which are traits associated with CaSCs.

During pregnancy, the expansion of normal mammary stem cells is dependent on the effects of progesterone but these mammary stem cells (MaSCs) lack expression of hormone receptors. However, these MaSCs express receptor activator of NF- $\kappa$ B (RANK) and it is through paracrine RANK ligand (RANKL) signalling by hormone receptor positive cells that mammary stem cells are stimulated to proliferate (Asselin-Labat et al., 2010). In the context of cancer, over-expression of RANK in MECs have been shown to promote progesterone-driven and carcinogen induced mammary tumours, and this effect can be mitigated through pharmacological inhibition of RANK. This is also true for Neu-oncogene driven tumours where tumourigenesis and formation of lung metastases can be decreased through RANK inhibition (Gonzalez-Suarez et al., 2010). Similarly, ablation of RANK in mammary epithelia resulted in delayed onset of tumours induced by synthetic progesterone analogues in combination with the carcinogen 7,12-dimethylbenz(a)anthracene (DMBA) (Schramek et al., 2010). The importance of this signalling axis in maintaining the self-renewal properties of CaSCs is further supported by kinase dead  $I\kappa K\alpha^{AA/AA}$  knockin mice. In these experiments the tumourigenicity of DMBA-induced and Neu-oncogene driven tumours were retarded and was associated with a reduction in tumour-initiating CaSCs (Cao et al., 2007).

The extent of RANKL-RANK- $I\kappa K\alpha$  signalling is not limited to regulating the proliferation and tumour-initiating properties of breast cancer cells. This signalling axis appears to play a role in breast cancer progression as well, since breast cancer cells stimulated with RANKL exhibit increased migration and metastatic abilities (Jones et al., 2006). Moreover, the metastatic spread of Neu-driven mammary tumours has been shown to be dependent on RANKL production by tumour-infiltrating regulatory T cells (Tan et al., 2011). Alternatively, RANK and RANKL expression can also be induced by hypoxia through hypoxia inducible factor 1alpha (HIF-1 $\alpha$ ) (Tang et al., 2011). Taken together, these studies demonstrate how the RANKL-RANK- $I\kappa K\alpha$  can be induced to promote metastases by various components of the tumour microenvironment. Overall, the RANKL-RANK- $I\kappa K\alpha$  axis appears to be important not only in tumour initiation and maintenance of CaSCs but also in promoting metastasis. Although this signalling axis lies upstream of the alternative

NF- $\kappa$ B pathway, there has not been direct evidence to show a role for p52 in these processes.

### 1.3.8 *The NFKB2 gene and its relevance to breast cancer*

The *NFKB2* gene which encodes for p52 and its I $\kappa$ B precursor p100 has also been implicated in breast cancer. In mouse models of breast cancer, high levels of p52 have been found in mammary gland tumours from MMTV-PyVT mice (Connelly et al., 2007). Increased RelB-p52 DNA binding was also detected in DMBA induced mammary tumours (Demicco et al., 2005).

In addition, the levels of RelB, which dimerizes with p52 in the alternative pathway, have been shown to be higher in ER negative breast cancer cell lines (Wang et al., 2007). Notably, RelB knockdown in these cells inhibited their invasive phenotype, illustrating an important role for RelB and possibly p52 mediated transcription in metastasis.

As of now, evidence for a role of p52 in tumour initiation and breast cancer progression remains inadequate. Although increased p52 levels and DNA binding have been observed in some of the studies, the transcriptional activity of p52 would be a better gauge of its aberrant role in cancer. This is because p52 dependent transcription can be regulated by other means such as the levels of trans-activating partners and its preference for forming active or repressive transcriptional complexes (Rocha et al., 2003). Furthermore, it has recently been demonstrated that post-translational modifications such as phosphorylation at serine-222 regulates the type of p52 complexes formed (Figure 1.10) (Barre and Perkins, 2010b). Such insights warrant the need for further investigations to fully understand p52's role in breast cancer and to evaluate its potential as a therapeutic target.

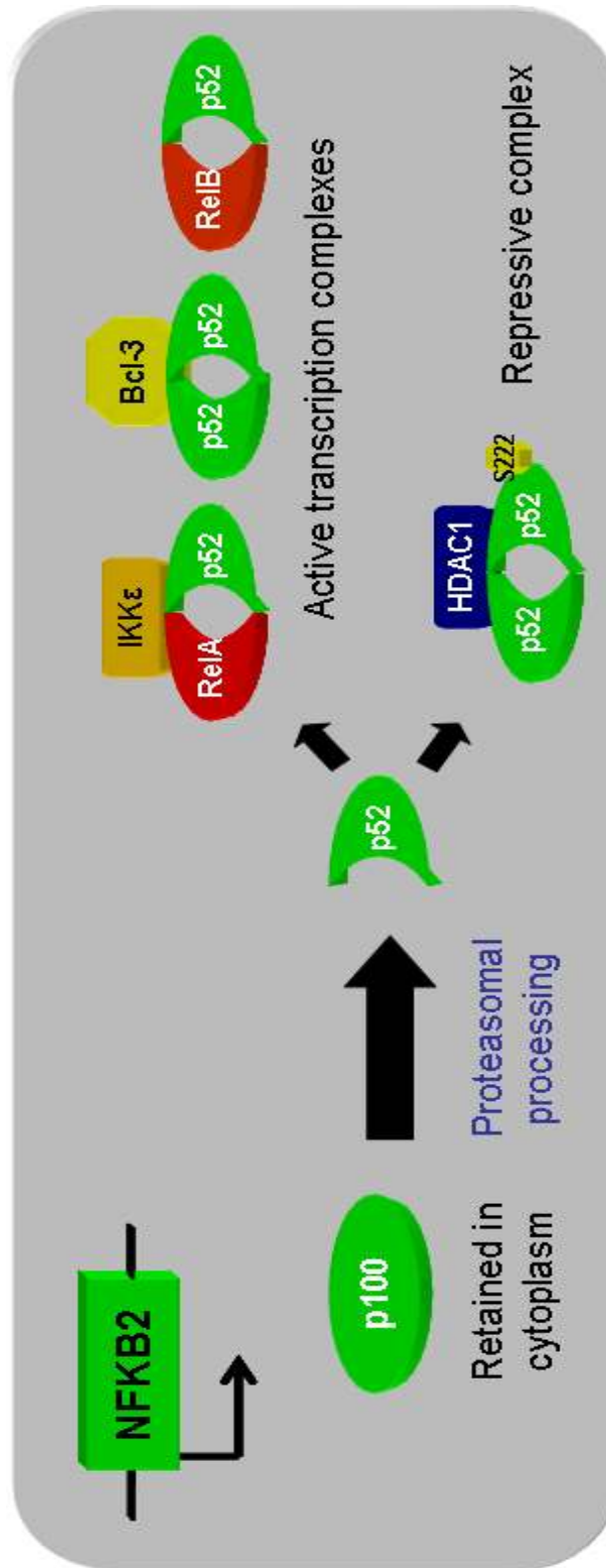


**Figure 1.10: The NFKB2 gene and its gene products p100/p52.** Illustration of the modulation of p100/p52 in transcription and the types of complexes formed by p52.

## 1.4 Aims & Objectives

During mammary gland involution, cell death is an important feature which allows its regression to a state that is similar to pre-pregnancy. However, the exact mechanisms responsible for cell death and whether caspases have a key role during involution is unclear. Hence, the aim of the initial study was:

- To address the effects of caspase inhibition during mammary gland involution.

Whilst it is well accepted that the ability to evade apoptosis is essential for tumourigenesis and metastasis, evidence for this has come from genetic studies involving regulators of apoptosis rather than the core caspase machinery itself. In addition, many of these apoptosis regulators have additional roles apart from inhibiting caspase activation. For that reason, experiments in this section were aimed:

- To substantiate the importance of evading apoptosis during breast cancer progression.

As described, evading apoptosis is an important feature of cancer cells and thus, disrupting a central regulator of apoptosis would be a sensible therapeutic strategy. The NF- $\kappa$ B pathway regulates a number of anti-apoptotic genes in mammary epithelial cells. Moreover, various genes pertinent to angiogenesis, proliferation and metastasis are regulated by NF- $\kappa$ B. It is known that the canonical pathway is important for tumourigenesis in ErbB2<sup>+</sup> breast cancers. In the case of the alternative NF- $\kappa$ B pathway, although increased levels of p52 have been observed, a role for p52 and its potential as a therapeutic target remains to be addressed. Accordingly, through genetic manipulations on breast cancer cell lines we aim:

- To determine the effects of silencing *Nfkb2* in breast cancer cells.
- To address the potential of diminishing p52 activity by promoting Ser-222 phosphorylation in breast cancer cells.

Based on the observed differential effects of silencing *Nfkb2* on different cell lines, we went on to address whether particular subtypes of breast cancer are more

dependent on p52 activity. Consequently in the final part of the study, the objective was:

- To identify possible correlations between p52 levels and breast cancer subtypes.

# **CHAPTER 2**

## Materials and Methods

## 2 Materials and methods

### 2.1 Animal experiments

Maintenance, breeding and scientific procedures involving animals were carried out according to the guidelines set by the U.K. Home Office Regulations (Animals [Scientific Procedures] Act 1986).

#### 2.1.1 Animals

P35 transgenic mice were generated by N. Omidvar in our lab. In these mice, the p35 transgene is under the control of a second generation tetracycline-regulatable promoter (Agha-Mohammadi et al., 2004). MMTV-rtTA and MMTV-Neu mice have been previously described (Guy et al., 1992, Gunther et al., 2002). These mice were acquired from Jax Mice and Services (Bar Harbor, Main, US). All mice were in-bred onto FvB genetic backgrounds for at least 6 generations to obtain appropriate transgenic animals for experiments.

Transgenic animals were fed with RM3 (E) expanded diet (Special Diets Service, Surrey, UK) and tap water *ad libitum*. Mice were housed in specific cages (maximum of 5/cage) according to designated colonies. Lights were kept constant at a 12 hour day/night cycle in breeding rooms. By about 4 weeks of age, mice were weaned and ear-marked for identification purposes.

For transplantation experiments, BalbC and NOD/SCID/BalbC mice of six to eight weeks of age were obtained from Charles River Laboratories (Wilmington, US). BalbC mice were housed in conventional cages and maintained in similar conditions as transgenic FvB mice. NOD/SCID/BalbC mice were housed in individually vented cages (Allentown Inc., New Jersey, US) and were fed with Teklad global 19% protein extruded rodent diet (Harlan Laboratories, Indianapolis, US) along with water *ad libitum*. These cages were housed in a room with 12 hour day/night cycles. To ensure sterile habitation, chow, water, saw dust and water bottles were autoclaved before use. Procedures involving NOD/SCID/BalbC mice were carried out in a sterilized laminar flow hood (Allentown Inc., New Jersey, US).

#### 2.1.2 Genotyping

To identify mice with desired transgenes, mice were genotyped by polymerase chain reaction (PCR) at 6-8 weeks of age. For this, DNA was obtained from tail or ear biopsies upon weaning at 4 weeks of age.

#### 2.1.2.1 DNA extraction

Ear or tail biopsies were collected in 1.5ml micro-centrifuge tubes and stored at -20°C until ready for extraction. DNA isolation was preceded by lysing tissues in 500ul of lysis buffer (100mM Tris-HCl; pH8.5 [Sigma], 5mM EDTA [Fisher Scientific, Loughborough, UK], 0.2% w/v sodium dodecyl sulphate [SDS; Sigma], 200mM NaCl [Fisher Scientific, Loughborough,UK]) and 5ul of 20mg/ml proteinase K (Roche, Welwyn Garden City, UK) overnight at 55°C. Lysed tissues were then mixed thoroughly and centrifuged for 10 minutes at a speed of 10,000rpm. The supernatant was then extracted and an equal volume (~500ul) of isopropanol (Fisher Scientific, Loughborough, UK) was added. The mix was left for 5 minutes to allow precipitation of DNA. Then, samples were centrifuged for 5 minutes to obtain a DNA pellet. After removal of isopropanol, 70% ethanol was added to the pellet without agitation to wash off any residual isopropanol. Consequently, the ethanol was discarded and the pellet was left to dry at 55°C before reconstitution in 100ul of nuclease free water at 55°C for an hour. The reconstituted DNA samples were then utilized in PCR reactions as depicted in Tables 2.1-2.3.

#### 2.1.2.2 Generic PCR protocol

DNA oligoneucleotides (Sigma-Genosys, Dorset, UK) for priming PCR reactions were designed using primer 3 software (<http://frodo.wi.mit.edu/primer3/>) or obtained from previously published sequences (Table 2.2). The sequences of primers used were validated by in silico PCR software to prevent any potential mis-priming (<http://genome.csdb.cn/cgi-bin/hgPcr>).

In general, PCR reactions were set up with 2ul of extracted DNA or with nuclease free water as negative controls. Reactions were carried out in 0.2ml 8-strip PCR tubes and 23ul of mastermix was added per reaction. The mastermix contains other reaction components as described in Table 2.3. Upon addition of mastermix to DNA samples, solutions were mixed by gentle pipetting. Then, reaction samples were spun briefly in a Technico Mini Centrifuge (Fisher Scientific, Loughborough, UK) before loaded into an iCycler PCR machine (BioRad, Hempstead, UK) according to respective cycling conditions (Table 2.1).

## 2.1.2.3 DNA gel electrophoresis

DNA gels were prepared by dissolving agarose tablets (Bioline, London, UK) in Tris-Acetic Acid-EDTA (TAE) buffer (Sigma, Dorset, UK) with addition of SafeView nucleic acid stain (NBS Biologicals, Huntingdon, UK) to a final concentration of 0.006% (v/v). All PCR products were resolved alongside a DNA marker, EasyLadder I (Bioline, London, UK), in 3% agarose gels ran in TAE buffer at 150V for 25 minutes. Separated DNA was then visualized under UV light with the aid of a GelDoc imager (BioRad, Hampstead, UK).

Reaction Step	<i>rtTA</i>			<i>p35</i>			<i>N2/NK</i>		
	No. Cycles	Temp (°C)	Time	No. Cycles	Temp (°C)	Time	No. Cycles	Temp (°C)	Time
<b>Initial Denaturation</b>	1	94	2 min	1	94	2 min	1	94	2 min
<b>Denature</b>	30	95	30 sec	15	95	30 sec	35	94	30 sec
<b>Anneal</b>		59	30sec		74*	30 sec		60	30 sec
<b>Extension</b>		72	40 sec		72	25 sec		72	1 min
<b>Denature</b>	-	-	-	26	95	30 sec	-	-	-
<b>Anneal</b>		-	-		58	30 sec		-	-
<b>Extension</b>		-	-		72	25 sec		-	-
<b>Final Extension</b>	1	72	5 min	1	72	4 min	1	72	5 min
<b>Hold</b>	1	4	∞	1	4	∞	1	4	∞

\*Decrease 2°C after every 2 cycles.

**Table 2.1:** Cycling conditions for PCR reactions.

Primer	Sequence	Product Size
MMTV-rtTA S	5'-ATC CGC ACC CTT GAT GAC TCC G -3'	349bp
MMTV-rtTA AS	5'-GGC TAT CAA CCA ACA CAC TGC CAC -3'	
P35 S	5'-GTG TAC GGT GGG AGG CCT AT -3'	320bp
P35 AS	5'-GAT CGC TGT AAT CGC GTT CT -3'	
MMTV-Neu S	5'-TTT CCT GCA GCA GCC TAC GC -3'	600bp
MMTV-Neu AS	5'-CGG AAC CCA CAT CAG GCC -3'	

**Table 2.2:** Sequence of primers used for genotyping.

PCR Reaction Component	<i>rtTA</i>	<i>P35</i>	<i>Neu</i>
Crude DNA	2µl	2µl	2µl
PCR-grade Water (Sigma)	13.75µl	14µl	15.5µl
Go Taq PCR Buffer (Promega)	5µl	5µl	5µl
Magnesium Chloride (25mM; Promega)	2µl	2µl	2.5µl
dNTPs (25mM; dATP, dCTP, dGTP, dTTP; Promega)	1µl	1µl	0.2µl
Forward Primer (Sigma Genosys, 10µM)	0.5µl	0.25µl	0.1µl
Reverse Primer (Sigma Genosys, 10µM)	0.5µl	0.25µl	0.1µl
Go Taq DNA Polymerase (Promega)	0.25µl	0.5µl	0.1µl
<b>Total Reaction Volume</b>	<b>25µl</b>	<b>25µl</b>	<b>25µl</b>

**Table 2.3:** Composition of PCR reactions.

### 2.1.3 Experimental procedures involving animals

#### 2.1.3.1 Doxycycline administration

For involution experiments, induction of p35 transgene in rtTA/p35 animals were achieved via doxycycline (Sigma, Dorset, UK) administration in drinking water at a concentration of 2mg/ml with 5% sucrose (Sigma, Dorset, UK) in opaque drinking bottles for 7 days prior to tissue harvest. Doxycycline was also administered at a concentration of 100ug in 100ul of saline, intra-peritoneally as indicated in experimental sections.

In primary tumour growth and metastasis experiments involving rtTA/p35/Neu transgenic mice, doxycycline was administered in drinking water (2mg/ml doxycycline; 5% sucrose) when tumours reached 5mm in diameter until tumours reached 20mm in diameter. Doxycycline solutions were changed twice a week along the course of treatment.

#### 2.1.3.2 Orthotopic cell transplants

Before transplantation, cells were prepared as single cell suspensions. This was done by washing the cells in serum free L-15 media (Invitrogen, Paisley, UK), then serum free Joklik's media before another wash in serum free L-15. Cells were then passed through a 40um cell strainer (BD Biosciences, Oxford, UK) and kept on ice until ready for transplantation.

For 4T1 and N202.1A cell transplants, Balb/C and NOD/SCID/Balb/C mice respectively which were between 8-12 weeks old were used. Before surgery, the mice were anaesthetized using a vaporizer to deliver 5% isoflurane (Abbot, Maidenhead, UK) with oxygen at a flow rate of 0.8 l/min and nitrous oxide at a flow rate of 0.4 l/min in an induction chamber. When the animal was anaesthetized, isoflurane was delivered at 2.5% through an anaesthetic mask. Consequently, a small patch of fur that is dorsal to the fourth abdominal mammary gland is removed and cleaned with surgical scrub. Then, a small superficial incision was made to expose the abdominal mammary gland and cells were injected directly into the mammary fat pad with a Hamilton or 29G needle syringe (BD Micro-Fine). The lymph nodes in the fourth abdominal gland were used to orientate the point of injections, where cells were transplanted dorsal to the lymph nodes. Wounds were then sealed with Vetbond Tissue Adhesive (3M). Animals were then allowed to recover in a temperature regulated chamber at 30<sup>0</sup>C for 15 minutes.

### 2.1.3.3 Tumour monitoring and measurementss

Endogenous tumours from mice carrying the Neu transgene or mice transplanted orthotopically with mammary cancer cells were inspected at least twice weekly for tumours via palpation. The growth kinetics of tumours were charted by measuring the diameter of tumours using digital calipers (Fisher Scientific, Loughborough, UK). The size of tumours were calculated as volume in mm<sup>3</sup> using the formula; Volume = (Length X Width<sup>2</sup>)/2.

## 2.2 Tissue sampling and processing

### 2.2.1 Removal and fixation of tissues

At appropriate experimental endpoints, animals were culled by cervical dislocation and subjected to necropsy.

#### 2.2.1.1 Mammary tissues for involution studies

Animals used for involution studies underwent forced involution at day 9 of lactation and tissues were harvested at either 48 or 72 hours after the removal of pups. The number of pups per experimental mouse during lactation was kept around 8-12 and this was to ensure coherent initiation of involution upon forced weaning. Before extraction of mammary tissues, the lymph nodes in the fourth abdominal glands were excised and discarded. The left abdominal gland was then removed and fixed in 4% formalin for histological analysis. For protein and RNA analysis, the remaining abdominal and inguinal glands were snap frozen and stored at -80°C.

#### 2.2.1.2 Tissues for tumour studies

Mice were allocated into either doxycycline positive (dox+) or negative (dox-) cohorts when tumours reached 5mm in diameter. Respective cohorts of mice were then maintained with or without water containing doxycycline until experimental endpoints, where tumours were about 3200mm<sup>3</sup>. Upon necropsy, the left abdominal mammary gland, liver, lung and a portion of tumour from experimental mice were fixed in 4% formalin for histological analysis. The remainder of tumour and normal mammary gland tissues was snap frozen and stored at -80°C until required for molecular analysis.

Tumour sections from BRCA2<sup>-/-</sup> p53<sup>-/-</sup> mice were a kind gift from Trevor Hay and Alan Clarke from Cardiff School of Biosciences. These mice have been described in (Hay et al., 2009).

### 2.2.2 Tissue processing and sectioning for histology

After fixing tissues in 4% formaldehyde for 4-8 hours, tissue processing and sectioning was carried out by the Histology Unit in Cardiff School of Biosciences.

#### 2.2.2.1 Dehydration of tissues

Paraffin emdedded sections were prepared by the School of Biosciences Histology Unit. With the aid of a Leica TP1050 automatic processor in the Histology Unit, tissues were dehydrated in a series of solvents for the designated amounts of time; 70% ethanol for 1 hour, 95% ethanol for 1 hour, 100% ethanol for 1.5 hours twice, 100% ethanol for 2 hours, xylene for 1 hour twice and paraffin for 2 hours twice. Following that, tissues were embedded in paraffin wax for sectioning into 5µm thick slices with the aid of a Leica RM2135 microtome cutter. Tissue sections were then immobilized onto poly-L-lysine (PLL) coated slides (Thermo Fisher, Loughborough, UK) and heated at 58°C for 24 hours. Slides were then stained with H&E or used for immuno-histochemistry (IHC).

## 2.3 Histological analysis of tissue sections

### 2.3.1 Dewaxing and rehydration

Paraffin was removed and tissues were rehydrated by incubating slides in a series of solvents for the designated amounts of time; 100% ethanol for 2 minutes twice, 95% ethanol for 2 minutes, 70% ethanol for 2 minutes and a rinse in distilled water.

### 2.3.2 Haematoxylin and eosin (H&E) staining

Slides were stained with H&E after dewaxing and rehydration. This was achieved by staining in Meyer's Haemalum (Thermo Fisher, Loughborough, UK) for 5 minutes, followed by a wash under running tap water for 5 minutes. Consequently, slides were counterstained in 1% aqueous Eosin (Thermo Fisher, Loughborough, UK) for 5 minutes before being washed with tap water for 15 seconds twice. Finally, slides were dehydrated, cleared and mounted as described in section 2.3.3.4.

### 2.3.3 Immuno-histochemistry (IHC)

In general, immuno-labelling of tissue sections was carried out according to the sections below and specific alterations for particular antigens are described in Table 2.4.

<b>Antigen</b>	1° Antibody source	Catalogue number	1° Antibody species	Antigen retrieval	Dilution ratio
<b>Cleaved Caspase-3</b>	Cell Signalling	9661	Rabbit	Pressure cooker	1:200
<b>Ki-67</b>	Vector Labs	VP-K452	Mouse	Boling water bath	1:20
<b>p100/p52</b>	Santa Cruz	Sc-7386	Mouse	Pressure cooker	1:200
<b>p63</b>	Abcam	Ab59561	Mouse	Pressure cooker	1:200
<b>ErbB2</b>	Cell Signalling	2242	Rabbit	Pressure cooker	1:200
<b>CK-14</b>	Lab Vision	LL002	Mouse	Pressure cooker	1:1
<b>Vimentin</b>	Santa Cruz	Sc-7557	Goat	Pressure cooker	1:100

**Table 2.4:** Details of antibodies and conditions used for immuno-histochemistry.

### 2.3.3.1 Antigen retrieval and prevention of endogenous staining

Epitope presentation and antigen retrieval was carried out either by heat alone or in a pressure cooker. In the case of heat mediated antigen retrieval, slides were boiled in citrate buffer at working concentration (Thermo Scientific, Loughborough, UK) for 20 minutes. The buffer was preheated to 99.9°C and placed in a coplin jar (Thermo Fisher, Loughborough, UK), which is placed in a waterbath to maintain the temperature.

For antigen retrieval using a pressure cooker, the chamber was filled with citrate buffer to a level that will ensure slides were fully immersed. The buffer was pre-heated to the point of boiling before slides were inserted into the chamber. Slides were then heated under pressure for 8 minutes. Consequently, slides that were treated with heat alone or with pressure cooker were left to cool at room temperature for at least 30 minutes. After a wash with distilled water for 5 minutes, tissue sections were treated with 3% hydrogen peroxide solution (Sigma, Dorset, UK) for 20 minutes. Then slides were washed in distilled water for 5 minutes twice followed by a 5 minute wash in PBS/T (Phosphate buffered saline plus 0.1% TWEEN-20 [Sigma, Dorset, UK]). To reduce non-specific antibody interactions, sections were blocked with a 5% serum solution from the host species of the secondary antibody (Dako, Ely, UK) made up in PBS/T for 20 minutes at room temperature.

### 2.3.3.2 Antibody incubation

Slides were then incubated with respective primary antibodies at working concentrations as described in Table 2.5. Antibodies were diluted in 5% BSA made up in PBS/T. Incubations were carried out in a humidified chamber at 4°C overnight before slides were washed three times in PBS/T. Consequently, biotinylated antibody (DAKO, Ely, UK) of the appropriate species was added onto slides at a dilution ratio of 1:200, made up in 5% BSA with PBS/T.

### 2.3.3.3 Amplification of signal and visualization of positivity by 3,3'-diaminobenzidine (DAB)

In order to amplify the signal for immuno-detection, an avidin-biotin complex (ABC) based kit, Vectastain ABC kit (Vector Labs, Peterborough, UK) was used. ABC reagent was prepared 30 minutes before usage by adding a drop of reagent A followed by a drop of reagent B in 5mls of PBS/T and the mixed reagents were

vortexed briefly. Upon completion of incubation with secondary antibody, slides were washed thrice for 5 minutes in PBS/T. Then, the ABC mix was applied onto slides and incubated at room temperature for 30 minutes. After that, slides were washed three times in PBS/T for 5 minutes. Signal visualization was achieved using a DAB+ kit (DAKO, Ely, UK), which was prepared by mixing a drop of chromogen with 1ml of substrate buffer. The resulting solution was then applied onto slides at room temperature for 5-10 minutes. Once, brown staining can be visualized, slides were washed for 5 minutes in PBS/T followed by two washes for 5 minutes in distilled water.

#### *2.3.3.4 Counter-staining, dehydration, clearing and mounting of slides*

Consequently, slides were counterstained with Meyer's Haematoxylin (Thermo Fisher, Loughborough, UK) for 45 seconds. Slides were then washed in running tap water. Dehydration of sections was achieved by immersing slides in a series of solvents; 70% ethanol for 30 seconds, 95% ethanol for 30 seconds, 100% ethanol for 30 seconds twice, xylene for 2 minutes twice. Finally, slides were mounted with DPX solution and appropriate sized cover slips.

#### *2.3.4 Terminal deoxy-nucleotidyl transferase dUTP nick end labeling (TUNEL)*

Slides were de-waxed and rehydrated as detailed in section 2.3.1. Then, slides were pre-treated with 20ug/ml proteinase K diluted in PBS by direct application onto slides for 15 minutes. Slides were then washed twice in distilled water for 2 minutes. After that, endogenous peroxidase activity was quenched by incubating slides with 3% hydrogen peroxide solution (Sigma, Dorset, UK) for 5 minutes at room temperature. Post-incubation, slides were washed twice with distilled water for 5 minutes.

TUNEL staining was carried out with the aid of Apoptag Peroxidase *in situ* apoptosis kit (Milipore, Watford, UK). The next step involved incubation of slides with 75ul/5cm<sup>2</sup> equilibration buffer which is provided with the kit for 10 seconds at room temperature. Consequently, sections were incubated with 55ul/5cm<sup>2</sup> working strength terminal deoxynucleotidyl transferase (TdT) made up in reaction buffer for 1 hour at 37°C. Upon incubation, slides were then immersed in working strength stop/wash buffer, agitated for 15 seconds and incubated for 10 minutes at room

temperature. During this time, the required amount of anti-dioxygenin conjugate was warmed up to room temperature. Then, slides were washed thrice in PBS for 1 minute. Following that, 65ul/5cm<sup>2</sup> of anti-dioxygenin conjugate was applied to slides and incubated in a humidified chamber for 30 minutes at room temperature. After that, slides were washed four times in PBS for 2 minutes each. Next, slides were developed by incubating with 75ul/5cm<sup>2</sup> of working strength peroxidase substrate for 3-6 minutes. Color development can be monitored under the microscope to gauge incubation times. Slides were then washed thrice for 1 minute in distilled water, followed by 5 minute incubation in distilled water at room temperature. Counter-staining, dehydration and mounting of slides were carried out according to section 2.3.3.4.

### 2.3.5 Visualization and quantification of stained sections

Tissue sections were visualized using an Olympus BX41 Light Microscope (Olympus, Essex, UK) and images were captured with a Colorview III camera (5 megapixel, Soft Imaging Systems) utilizing Analysis Software (Version 3.2, Build 831, Soft Imaging Systems).

#### 2.3.5.1 Quantification of luminal bodies during mammary gland involution

For quantification of luminal bodies, three random 10x magnification images were taken per mammary gland section and the number of luminal bodies counted. The mean between these different fields of view were then used to calculate the average number of luminal bodies between cohorts of transgenic animals. Cleaved caspase-3 negative luminal bodies were quantified as a percentage of total luminal bodies present per field of view.

#### 2.3.5.2 Quantification of cleaved caspase-3 and Ki67 positive cells in tumour samples

Similarly, quantification of cleaved caspase-3 or Ki-67 positive cells in tumours was done by taking three random 10x magnification images per section. The mean between these different fields of view were then used to calculate the average number of positively stained cells. In the case of lung metastases, the percentage of positively stained cells was calculated because metastatic nodules were of varying sizes within a field of view.

#### 2.3.5.3 Scoring and ranking of *BRCA2*<sup>-/-</sup> *p53*<sup>-/-</sup> (BAP) tumours

The degree of staining for p100/p52, ErbB2, p63, CK14 and vimentin for each tumour section was calculated based on a score. This score was derived from the product of two individual scores measuring percentage cover (P) and intensity (I) of staining for respective antigens. Scores for percentage cover were between 0-3, where 0 indicates no staining, 1 for tumour sections with upto 10% of cells stained, 2 for tumour sections with between 10-50% of cells stained and 3 for sections with more than 50% of cells stained. Scores for intensity were allocated as follows; 0 for no staining, 1 for low degree of staining, 2 for moderate degree of staining and 3 for high degree of staining. The product of both scores (IxP) would then give rise to an overall score which is between 0-9 for each tumour section. Tumours were then ranked based on the score for p100/p52 and the corresponding relationship with other antigens determined using Spearman's ranked correlation statistical test.

## **2.4 DNA sub-cloning and vectors**

### *2.4.1 Amplification of DNA constructs and general cloning procedures*

#### *2.4.1.1 Transformation of *E. coli* with DNA*

In general, competent *E. coli* cells (C2984; NEB, Herts, UK) were transformed with DNA constructs by heat shock protocol. With lentiviral vectors that contain long terminal repeat (LTR) sequences, Stbl-3 competent *E. coli* cells (Invitrogen, Paisley, UK) were used to prevent unwanted homologous recombination. Before transformation, about 50ng of circular DNA was added to bacterial cells and allowed to thaw at 4°C for 30 minutes. Then cells were immersed in a water bath set at 42°C for 45 seconds. Bacterial cells were then returned on ice for 2 minutes. Consequently, 250ul of SOC media (NEB, Herts, UK) were added to bacterial cells and incubated at 37°C for 1 hour. Then cells were spread and plated out onto ampicillin containing agar (Invivogen, San Diego, US) coated plates. Plates were incubated for 12-16 hours at 37°C. Resulting colonies were then picked and grown in 2mls of TB-Amp media (Invivogen, San Diego, US) for 8 hours with constant agitation. For maxi-prep cultures, 1ml of the resulting culture is removed and incubated with 200mls of TB-Amp media in a 500ml conical flask at 37°C for 12 hours with constant agitation. For DNA isolation, cells were then pelleted by centrifugation at 5000rpm for 10 minutes.

#### 2.4.1.2 Isolation of DNA from bacterial cells

DNA was isolated from pelleted bacterial growth cultures using QiaPrep MiniPrep Kit, Plasmid Maxi Kit or EndoFree Plasmid Maxi Kit (Qiagen, Sussex, UK) depending on the size of cultures and amount of DNA to be extracted. Isolation was carried out according to the manufacturer's instructions. In cases where plasmids were to be used for transfections, the EndoFree Plasmid Maxi Kit was used.

#### 2.4.1.3 Restriction digest and ligation reactions

All restriction enzymes were obtained from Promega (Southampton, UK) or NEB (Hertz, UK) and enzymatic reactions were carried out in 50ul reaction volumes (Table 2.5). In the case of double digests, the appropriate buffer recommended for optimal activity of both enzymes was used. Ligation reactions were carried out in 10ul reaction volumes and a vector to insert molar ratio of 1:3 was used.

<b>Restriction enzyme digests</b>	<b><i>Single digest</i></b>	<b><i>Double digest</i></b>
Plasmid DNA (1ug/ul)	1µl	1µl
PCR-grade Water (Sigma)	43µl	42µl
10X restriction enzyme buffer	5µl	5µl
Enzyme A	1µl	1µl
Enzyme B	-	1µl
<b>Total Reaction Volume</b>	<b>50µl</b>	<b>50µl</b>

**Table 2.5:** Reaction volumes and components for single or double restriction enzyme digests.

#### 2.4.2 Packaged *Nfkb2* shRNA lentiviral vectors

Packaged lentiviral vectors encoding shRNA against *Nfkb2* (NM\_019408) or non-target (NT) (SHC002V) control sequences were obtained from Sigma. The vector backbone contains a U6 promoter which drives shRNA expression and human phosphor-glycerate kinase (hPGK) eukaryotic promoter which drives expression of a puromycin resistance gene.

### 2.4.3 Sub-cloning of p52 constructs into lentiviral vectors

Plasmids containing wild-type (WT), S222A, S222D or DNA binding mutant (DBM) sequences of p52 within a pCMV-HA backbone were obtained from Professor Neil Perkins (Newcastle University). The respective HA-p52 and mutant sequences were excised by XbaI-PstI restriction enzyme (Promega, Southampton, UK) digestion, extracted after DNA gel electrophoresis, purified using DNA gel purification kit (Qiagen, Sussex, UK) and then ligated with XbaI-PstI digested P305 lentiviral plasmid. (Dr. Riccardo Brambilla, Cardiff University). After ligation of p52 inserts into p305 vector with T4 DNA Ligase (NEB), constructs were checked by XbaI-PstI or XbaI-EcoRV digestion (Figures 2.1a&b). Respective plasmids were then sent to the DNA Sequencing Core, Cardiff University to ensure the p52 constructs had the appropriate mutated base sequences (Figure 2.1c). The appropriate p52 sequences were located downstream of the hPGK promoter in the p305 vector. Primers used for sequencing are detailed in Table 2.6. The lentiviral construct was then kindly packaged by Dr. Riccardo Brambilla. The p305 plasmid also contains an IRES-GFP sequence 3' of the p52 insert site.

### 2.4.4 NF- $\kappa$ B Luciferase reporter plasmid

NF- $\kappa$ B luciferase assays were carried out using the 3x  $\kappa$ B luciferase reporter plasmid, which was a kind gift from Professor Ron Hay (University of St. Andrews). As controls for transfection efficiency, a pcDNA3.1 plasmid containing the LacZ sequence was used and this was obtained from Professor Trevor Dale (Cardiff University). Positive and negative controls used in luciferase assays were pGL3basic (Promega) and pGL3control (Promega) respectively.

## 2.5 Maintenance and culture of cells

### 2.5.1 Experimental cell lines

4T1 cells are a highly metastatic murine mammary cancer cell line (Aslakson and Miller, 1992) and were obtained from Dr. Robin Anderson (University of Melbourne). These cells were derived from a spontaneous tumour in a Balb/C mouse. N202.1A cells over-express the ErbB2 oncogene and were derived from a MMTV-Neu driven tumour from a mouse of FvB background (Nanni et al., 2000). These cells were a kind gift from Dr. Pier-Luigi Lollini (Sezione di Cancerologia, Italy). The Eph4 cell line is a spontaneously immortalized, non-transformed mammary epithelial

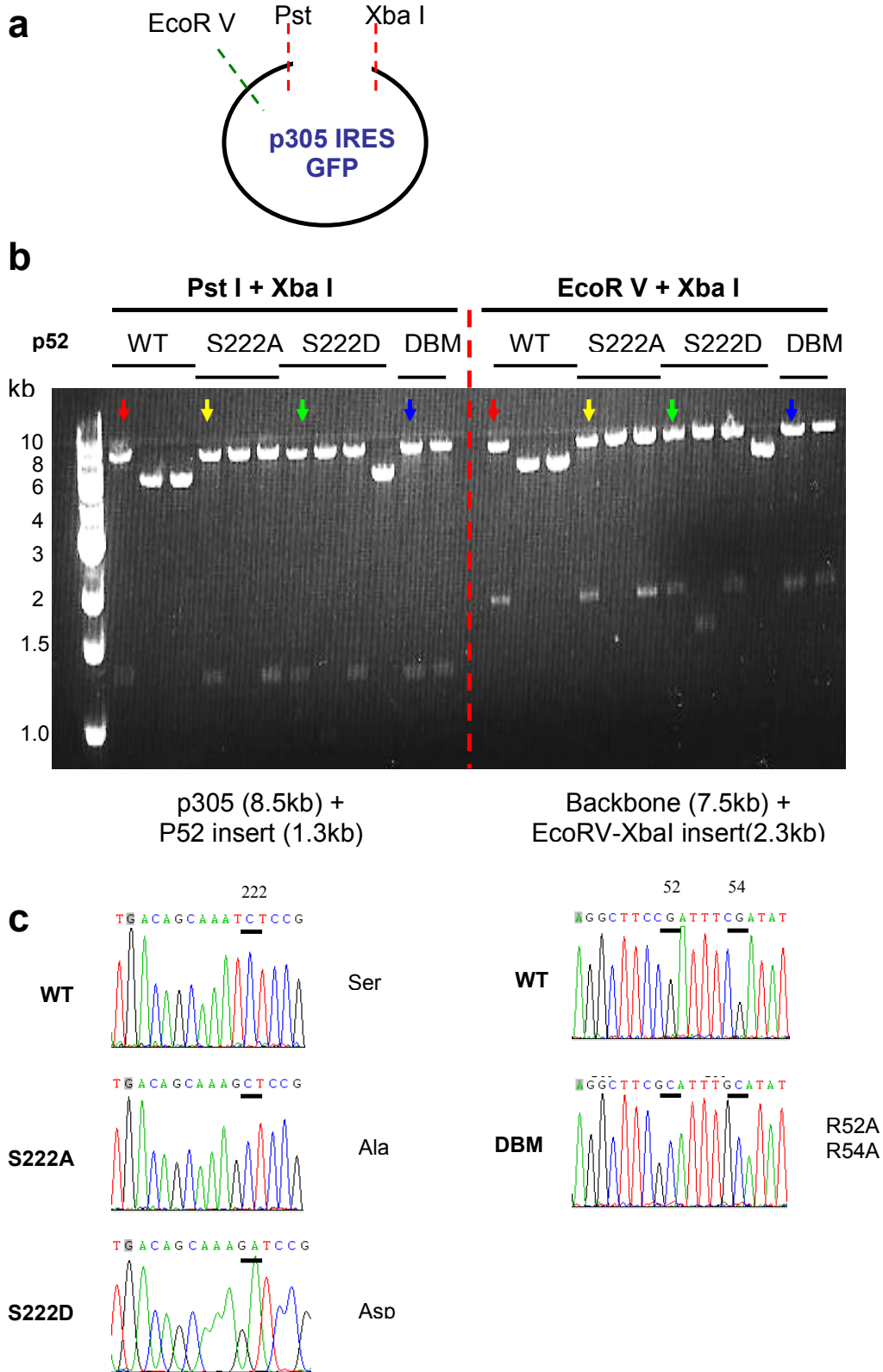


**Figure 2.1: (a)** Illustration of restriction enzyme sites within p305 plasmid. **(b)** DNA gel electrophoresis of p305:HA-p52 constructs digested with XbaI+PstI or XbaI +EcoRV respectively. Arrows indicate positive clones where DNA was then sent for sequencing. **(c)** Sequencing results showing p52 constructs with the appropriate mutated base sequences.

---

<b>Primer</b>	<b>Sequence</b>
<b>p52.1 Forward</b>	5'- ATG TAC CCA TAC GAT GTG C -3'
<b>p52.2 Forward</b>	5'- AAG GAC ATG ACT GCC CA -3'
<b>p52.3 Forward</b>	5'- AGG TTC GGT TCT ATG AGG A -3'
<b>p52 R1</b>	5'- TCT TTG GCC TCT TGC TC -3'
<b>p52 R2</b>	5'- CAC AAT GGA GGA GTT CAA -3'
<b>p305 hPGK F</b>	5'- CGA ATC ACC GAC CTC TC -3'

---

**Table 2.6:** List of primers used for sequencing p305:HA-p52 plasmids.

cell line (Fialka et al., 1996) and was obtained from Dr. Christine Watson (Cambridge University).

### 2.5.2 Maintenance of cell lines

For the 4T1 cell line, these cells were cultured in RPMI medium (Invitrogen, Paisley, UK) with 10% v/v fetal bovine serum (FBS; Sigma, Dorset, UK), 2mM L-glutamine (Invitrogen, Paisley, UK) and 50units/ml penicillin-streptomycin (Invitrogen, Paisley, UK). Eph4 and N202.1A cells were cultured in DMEM medium (Invitrogen, Paisley, UK) that is supplemented with 2mM L-glutamine and 50units/ml penicillin-streptomycin. FBS was supplemented into Eph4 and N202.1A cell media at 10% and 15% v/v respectively.

Cells were maintained in a sterile, humidified 37°C incubator and CO<sub>2</sub> levels were kept at 5%. All cell lines were routinely cultured in T25 tissue culture flasks (Nunc, Leics, UK). When cells reached a confluency of 80-90%, they were passaged on at a split ratio of 1:6-1:12 every two days or at appropriate times. Cell passaging was carried out by completely removing used medium, followed by a rinse with PBS. Then, 2mls of 0.05% Trypsin/EDTA (Invitrogen, Paisley, UK) was added per flask and left to incubate at 37°C for 5-10 minutes. After that, cells were checked under the microscope to ensure that all cells have detached, before being diluted with culture medium according to appropriate splitting ratios. All cell lines were not split for more than 30 recorded passages.

### 2.5.3 Long term cell storage

In order to have sufficient aliquots of cell lines that were of low passage number, cells were frozen and cryo-stored. For that, a confluent T75 flask (Nunc, Leics, UK) of respective cells were detached and resuspended in 10mls of culture medium in a 15ml tube. Then, the cells were pelleted by centrifuging at 1100rpm for 5 minutes. The pellet was then re-suspended in freezing medium (culture medium with 10% v/v dimethyl sulfoxide [DMSO; Sigma, Dorset, UK]) and aliquoted into 1ml cryo-tubes (Nunc, Leics, UK). The tubes were then placed in a container containing iso-propanol to facilitate freezing at -80°C overnight. After that, cell aliquots were transferred into liquid nitrogen storage.

When cells were retrieved from cryo-storage, they were quickly defrosted at 37°C in a waterbath, resuspended in 10mls of culture medium in a 15ml tube and

pelleted by centrifugation at 1100rpm for 5 minutes. The resulting pellet was then resuspended in 7mls of culture medium and cultured in T25 flasks.

#### 2.5.4 Cell counting

To aid the seeding of cells in assays, cells were counted using a haemocytometer counting chamber (Hawksley, Lancing, UK). For this, cells were detached with trypsin/EDTA as described in Section 2.5.2. Trypsinized cells were then pelleted by centrifugation at 1100rpm for 5 minutes and resuspended in the appropriate media. 10ul of cell suspension was loaded into the counting chamber and the number of cells in four 1mm<sup>2</sup> squares was quantified. The four counts were averaged and converted to the number of cells per ml of suspension by multiplying with  $1 \times 10^4$ .

#### 2.5.5 Lentiviral transduction of cell lines

Prior to transduction with lentivirus, 4T1 and Eph4 cell lines were seeded in 96-well plates at densities of 10,000 cells per well, whereas N202.1a cells were seeded at a density of 12,000 cells per well. One day post-seeding, media was removed from wells and replaced with 110µls of respective culture media containing hexadimethrine bromide (Sigma, Dorset, UK) at a final concentration of 8ug/ml. Plates were gently swirled and 2-15µl of respective lentiviral stock was added per well. Cells were incubated at 37°C with 5% CO<sub>2</sub> for 18-20 hours. After that, the medium in wells was replaced with 120µls of fresh culture media. Consequently, cells were either harvested for RNA/protein after 24 hours or passaged on to establish stably transduced cell lines.

##### 2.5.5.1 Generation of cell lines deficient of *Nfkb2*

In order to generate cell lines deficient of *Nfkb2* gene products, 4T1 cells were transduced with lentivirus encoding shRNA against the *Nfkb2* gene (Section 2.4.2). 4T1 cells were transduced with 5 shRNA sequences (Table 2.7) targeting the *Nfkb2* gene and cells were then cultured in 4ug/ml puromycin to select for stably transduced cells. Cells transduced with lentivirus encoding GFP (Sigma, Dorset, UK) were used as controls to show efficiency of transduction and selection at this concentration of puromycin (Figure 2.2a). The levels of knockdown achieved by different shRNA sequences were compared with cells transduced with non-target (NT) shRNA by qRT-PCR (Figure 2.2b). 4T1 cells transduced with sh43 and sh44 showed efficient

silencing of *Nfkb2* and the levels of p100/p52 knockdown in these cells were verified by Western blotting (Section 2.6).

For N202.1A and Eph4 cell lines, silencing of *Nfkb2* was achieved by transduction of respective cells with sh44 lentiviral constructs. Selection of stably transduced cells was achieved by culturing in 1 $\mu$ g/ml of puromycin for both cell lines.

shRNA	Sequence
<b>Mouse</b>	
<b>NF-<math>\kappa</math>B2</b>	
Sh43	CCGGCCTGTCTAATCGAAATCTTATCTCGAGATAAGATTTTCGATTAGACAGGTTTTT
Sh44	CCGGGCGAGGCTTCAGATTTTCGATACTCGAGTATCGAAATCTGAAGCCTCGCTTTTT
Sh45	CCGGCCTGCATGTAACCAAGAAGAAGACTCGAGTTCTTCTTGGTTACATGCAGGTTTTT
Sh46	CCGGCGTCATTTATCACGCTCAGTACTCGAGTACTGAGCGTGATAAATGACGTTTTT
Sh47	CCGGCGGACTCCAAACAGTTCACATCTCGAGATGTGAACTGTTGGAGTCCGTTTTT

**Table 2.7:** List of shRNA sequences targeting the *Nfkb2* gene.

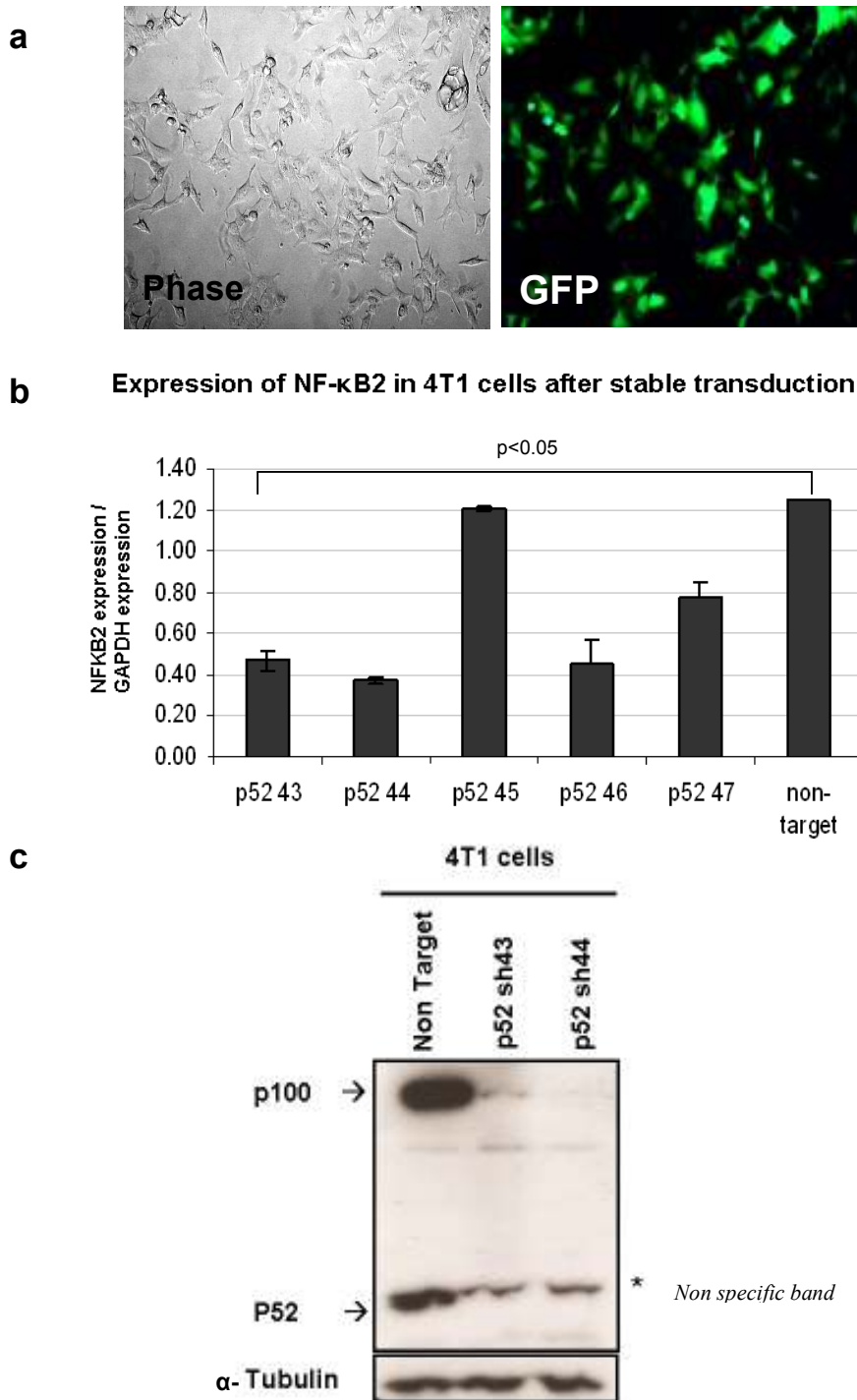


**Figure 2.2: Establishing stable 4T1 cell lines with *Nfkb2* knocked down.**

**(a)** Phase and GFP image of 4T1 cells transduced with GFP expression vectors and selected with 4 $\mu$ g/ml puromycin media. **(b)** QPCR analysis of *Nfkb2* transcript levels normalized against GAPDH expression for 4T1 cells transduced with lentiviral vectors. Data is presented as mean of duplicates and error bars represent SEM. Significant decreases were observed for p52 43 and p52 44 ( $p < 0.05$ , one-tailed t-test). **(c)** Western blot showing p100/p52 levels in 4T1 cells. Alpha-tubulin was probed as loading control. \* indicates non specific band.

#### 2.5.5.2 Generation of cell lines over-expressing p52

Stable 4T1 cells over-expressing either WT, S222A, S222D or DBM p52 were established by transduction with respective lentiviral constructs (Section 2.4.3). Cells successfully transduced also expressed green fluorescent protein (GFP) and were selected by fluorescence assisted cell sorting (FACS) using a FACS Aria cell sorter (BD Biosciences, Oxford, UK). Cell sorting was carried out with assistance from Dr. Kirsty Richardson from the Stem Cell Suite and Flow Cytometry Unit, Cardiff University.

### 2.5.6 *NF- $\kappa$ B luciferase reporter assays*

#### 2.5.6.1 Transfection of cells with reporter plasmids

For luciferase assays, cells were seeded into clear bottom black 96-well plates (Corning Inc., Lowell, US) in antibiotic free culture media. 4T1 and Eph4 cells were seeded at a density of 10,000 cells per well while N202.1A cells were seeded at a density of 12,000 cells per well.

After 24 hours, cells were transfected with 10ng of 3x  $\kappa$ B luciferase plasmid and 10ng of pcDNA3.1-LacZ plasmid per well. Empty pcDNA3.1 plasmid was also included to normalize the total weight of DNA transfected to 100ng. For positive and negative controls respectively, 10ng of pGL3control or pGL3basic were transfected in place of 3x  $\kappa$ B luciferase plasmid. Transfection of cells were carried out using Lipofectamine LTX (0.3ul/well) with PLUS reagent (0.1ul/well) (Invitrogen, Paisley, UK). The appropriate amounts of plasmids were diluted in Opti-MEM media (Invitrogen, Paisley, UK) and PLUS reagent was added to the plasmid mixture. This mixture was left at room temperature for 5 minutes. Then, appropriate amounts of Lipofectamine LTX reagent was added to the mixture and this was incubated at room temperature for 30 minutes. Consequently, the transfection mixture was added dropwise into wells and cells were incubated for 48 hours at 37°C with 5% CO<sub>2</sub>. If cells showed signs of toxicity, media was refreshed with respective culture media after 24 hours.

#### 2.5.6.2 Luciferase reaction assays

After 48 hours post-transfection with luciferase reporter plasmid, cells were lysed using 50ul/well of Glo-lysis buffer (Promega, Southampton, UK). The cells were left on a rocker for 20 minutes. Then, 20ul of lysate from each well is removed

and transferred into new clear bottom black wells for measuring LacZ activity (transfection efficiency control). Consequently, 30ul/well of Bright-Glo luciferase substrate (Promega, Southampton, UK) were added to wells with 30ul of lysate to measure luciferase activity. In the case of lacZ activity, 20ul/well of Beta-Glo substrate (Promega, Southampton, UK) were added to wells with 20ul of lysate. The luminescence produced from either reactions were then read using a Flurostar Optima plate reader (BMG Labtech, Bucks, UK). The resulting luciferase activity was then calculated as relative light units (R.L.U), where luciferase activity was normalized against lacZ activity.

### **2.5.7 Cell Titer Blue viability assays**

The viability of cells at experimental endpoints for particular assays were determined using Cell Titer Blue (Promega, Southampton, UK) reagent. This reagent allows the measurement of cellular metabolic activity using resazurin as an indicator dye. Viable cells which are metabolically active will have the ability to convert resazurin into resofurin, a highly fluorescent derivative. Hence, the viability of cells can be determined by measuring fluorescence levels after incubation with the substrate.

Before use, Cell Titer Blue reagent was thawed to room temperature. For assays carried out in 96-well plates, 20ul/well of Cell Titer Blue reagent was added and incubated at 37°C with 5% CO<sub>2</sub> for 1 hour. The resulting fluorescence was then measured by setting excitation/emission wavelengths to 560/590nm on a Flurostar Optima plate reader (BMG Labtech, Bucks, UK).

### **2.5.8 Trypan blue exclusion cell viability counts**

In order to estimate the number of cells present in a culture, cells were lifted from plates by 0.05% trypsin/EDTA incubation at 37°C for 5-10 minutes. The cells were then resuspended in a known volume of culture media. Trypan blue dye was then added to 10ul of cell suspension at a 1:1 ratio and this was loaded onto a haemocytometer cell counting chamber. Only viable cells which were not stained blue were counted and the number of cells in a ml of suspension can be calculated by the average number of cells per square multiplied by  $2 \times 10^4$ .

#### 2.5.8.1 Proliferation assay

For proliferation assays, 4T1, N202.1A and Eph4 cells were seeded at a density of 10,000 cells/well in 6-well plates (Nunc, Leics, UK). For each cell line, nine wells were seeded to represent triplicates of three timepoints. After 24 hours, cells from triplicate wells for the first time point were trypsinized and individually counted as described in Section 2.5.8. The same was done for each cell line at 48 hours and 72 hours post-seeding. The average cell counts for respective cell lines were then plotted on a log scale, normalized against the number of cells present at 24 hours.

#### 2.5.9 Colony formation assays

Colony forming assays were carried out by seeding 4T1 (500cells/well), N202.1A (1000cells/well) or Eph4 (500cells/well) cells in 6-well plates. Before plating, cells were checked under the microscope to ensure that cells have been dissociated into single cell suspensions. After incubation at 37°C with 5% CO<sub>2</sub> for 7 days, cells were fixed with methanol:acetone (1:1) for a few seconds, air dried and rinsed with water. Then cells were stained with Giemsa Stain (1:10 dilution in water, Sigma) for 1 minute and wells were then rinsed with water. The number of colonies with more than 50 cells was then quantified by inspecting under a microscope.

#### 2.5.10 Boyden chamber (Transwell) migration and invasion assays

The motility of mammary cancer cell lines was assessed by Boyden chamber trans-well migration assays. In this assay, cells were seeded in a chamber with porous membrane as solid support (cell culture insert) and this was placed into a well with normal culture media. Within this chamber, cells were seeded with limiting serum conditions and thus, cells were stimulated by a serum gradient to migrate across the membrane through the pores. For invasion assays, the upper side of the membrane in the chambers was coated with Matrigel basement membrane matrix.

4T1, N202.1A and Eph4 cells were suspended by trypsinization and prepared in respective culture media containing 0.1% FBS. 750ul of respective culture media with standard amounts of serum (10% for 4T1 and Eph4, 15% for N202.1A) were added into each 24-well cell culture insert companion plate (BD Biosciences, Oxford, UK). Cell culture inserts for motility or invasion assays respectively were then inserted into the wells containing standard culture media with the aid of a tweezer.

The inserts used had transparent polyethylene terephthalate (PET) membranes with 8µm pores (BD Biosciences, Oxford, UK). For invasion assays, BD BIOCoat™ Growth Factor Reduced Matrigel Invasion chambers (BD Biosciences, Oxford, UK) were used. 350ul of respective cell suspensions prepared in 0.1% FBS were then added into the chambers in 24-well plates. 4T1, N202.1A and Eph4 cells were seeded at a density of 25,000 cells/chamber. Cells were then incubated at 37°C with 5% CO<sub>2</sub> for 24 hours.

#### *2.5.10.1 Visualization of migrated cells*

After the incubation period, cells were fixed by replacing the media in the top and bottom sections of the chamber with 70% ice cold ethanol and left for at least an hour. Upon fixation, inserts were washed by dipping into a beaker with tap water. Then, the cells on the upper surface of the insert were removed mechanically using a moist cotton bud. This was followed by staining of inserts in Harris' Haematoxylin (Sigma, Dorset, UK) for 1 minute, a wash in tap water to remove excess stain and then staining in 0.5% eosin for 1 minute. Stained inserts were then washed in a beaker of tap water.

Stained membranes were then mounted onto microscope slides (R.A. Lamb, Loughborough, UK) with glycerol gelatin (Sigma, Dorset, UK). The glycerol gelatin solution was heated in a beaker of boiling water to ensure that it did not solidify. Membranes were excised from inserts using a sharp scalpel and transferred onto slides with a tweezer. Glycerol gelatin was then added onto the membrane and a coverslip was placed over with application of firm pressure. Slides were then air dried before counting.

#### *2.5.11 Anoikis and mammosphere formation assays*

##### *2.5.11.1 Anoikis assay*

To assess the survival of mammary cells under non-adherent conditions, cells were plated at a density of 10,000cells/well into 96-well ultra-low attachment plates (Corning Inc., Lowell, USA). As a control for the number of cells seeded, the same amount of cells was plated into a standard 96-well plate (Nunc, Leics, UK). After 24 hours, the viability of cells in both plates were determined with the Cell Titer Blue assay (Section 2.5.7). The viability of cells under anoikis conditions was then determined as a percentage of fluorescence produced by cells in ultra-low attachment

plates normalized against fluorescence produced by cells under normal culture conditions.

#### 2.5.11.2 Mammosphere assay

The mammosphere assay is a surrogate cancer stem cell (CaSC) assay which selects for CaSCs based on their ability to survive under non-adherent conditions and also their ability to self-renew and form spherical colonies. The spheres are enriched for stem/early progenitor cells and their self-renewal characteristics allow the formation of new colonies after disaggregation and re-seeding in consequent passages.

In this assay, cells were dissociated into single cell suspensions by mechanical agitation and re-suspended in mammosphere culture medium which consists of mammary epithelial basal media (MEBM; Lonza, Slough, UK) supplemented with B27 (Invitrogen, Paisley, UK), 5mg/ml insulin (Sigma), 20ng/ml Epidermal growth factor (EGF; Sigma, Paisley, UK), 1mg/ml hydrocortisone (Sigma) and 0.0008% v/v  $\beta$ -mercapthoethanol (Sigma, Paisley, UK). Cells were seeded at a density of 500cells/well in ultra-low attachment 96-well plates (Corning Inc., Lowell, USA) and incubated at 37°C with 5% CO<sub>2</sub> for 7 days. Then, the number of spheres formed per well were quantified and the percentage of mammosphere forming units (MFUs) were calculated as the number of spheres formed per cells seeded. The size of spheres formed was determined by capturing images of individual spheres through an Olympus BX41 Light Microscope (Olympus, Essex, UK) and Colorview III camera (Soft Imaging Systems). The diameter of spheres was then measured with ImageJ software.

Spheres could then be passaged on by enzymatic dissociation with 0.05% trypsin/EDTA and re-seeded at a similar density under mammosphere culture conditions. After a 7 day incubation period at 37°C with 5% CO<sub>2</sub>, the number and size of spheres in subsequent passages were determined as in the first passage.

#### 2.5.12 Treatment of cells with NF- $\kappa$ B inhibitor, BAY 11-7082

Dose response curves for mammary cancer cell lines were determined by treating respective cell lines with BAY 11-7082 (Cayman Chemical, San Diego US) with concentrations ranging from 0.05 $\mu$ M to 5 $\mu$ M diluted in respective media. BAY 11-7082 treated mammary cancer cells subjected to motility or mammosphere assays were maintained with 1 $\mu$ M BAY 11-7082 throughout the time period of the assay.

## 2.6 Protein analysis by immuno-blotting

### 2.6.1 Protein extraction from cells

For protein extraction, the medium from cells cultured in flasks were removed and cells were rinsed twice with ice cold PBS. Then, 5mls of PBS was added into the flask and cells were removed by scraping with a cell scraper (Nunc, Leics, UK). The solution of cells was then transferred into 15ml tubes and cells were pelleted by centrifugation at 1100rpm for 5 minutes. At this point, the cell pellet was either stored at -80°C or immediately used for extraction.

#### 2.6.1.1 Radio immuno-precipitation assay (RIPA) protein extracts

RIPA protein extracts were isolated by adding 100-300ul of RIPA buffer (150mM sodium chloride [Fisher Scientific, Loughborough, UK], 1% v/v Nonidet-P40 [Roche], 0.1% w/v sodium dodecyl sulphate [SDS, Sigma, Dorset, UK], 0.5% w/v sodium deoxycholate [Sigma], 50mM Tris pH8 [Sigma]) with the addition of complete mini protease inhibitor tablets (Roche, Welwyn Garden City, UK) and phosphatase inhibitors (10mM sodium fluoride [Fluka Biochemika], 1mM sodium orthovanadate [Sigma], 10mM sodium pyrophosphate [Sigma]) to cell pellets from section 2.6.1. Cell lysing was facilitated by passing the cell pellet with RIPA buffer through a 23G needle 10 times, before incubation on ice for 30 minutes. Cell debris was then pelleted by centrifuging the lysate at 10,000rpm for 15 minutes at 4°C. The supernatant was then removed and aliquoted into fresh tubes and snap frozen. Protein lysates were stored at -80°C until required.

#### 2.6.1.2 High salt nuclear and cytoplasmic protein extraction from cells

Cytoplasmic and nuclear protein from cells were fractionated from cell pellets as prepared in section 2.6.1. 400µl of NEBA+ buffer (filtered NEBA [10mM Hepes pH7.9, 10mM potassium chloride, 0.1mM EDTA pH8.0, 0.1mM EGTA pH8], 1mM 1,4 dithiothreitol [DTT, Fluka Biochemika], 50mM sodium chloride, 1mM sodium orthovanadate, 1mM sodium pyrophosphate and one complete mini protease inhibitor tablet) was then added and the cell pellet was re-suspended by pipetting. The mixture was then placed on ice for 15 minutes. Then, 25 µl of 10% v/v Nonidet-P40 [Roche] was added and the mixture was vortexed vigorously for 30 seconds. After that, nuclear fractions were separated by centrifuging the mixture at 10,000rpm for 30 seconds at 4°C. The cytoplasmic fraction which is contained within the supernatant is

then removed and aliquoted into 500µl tubes. Extraction of nuclear proteins were then achieved by adding 100ul of NEBC+ buffer (filtered NEBC [10% v/v glycerol, 20mM Hepes pH7.0, 0.4M sodium chloride, 1mM EDTA pH8.0, 1mM EGTA pH8.0], 1mM 1,4, dithiothreitol, 50mM sodium fluoride, 1mM sodium orthovanadate, 1mM sodium pyrophosphate and one complete mini protease inhibitor tablet), followed by vortexing the mixture for 5 seconds. This mixture was then incubated on ice for 30 minutes. To remove cell debris, the mixture was then centrifuged at 13,000rpm for 5 minutes at 4°C and the supernatant which contains the nuclear fraction is aliquoted into 500µl tubes. Nuclear and cytoplasmic cell extracts were stored at -80°C until ready for use.

### 2.6.2 *Determination of protein concentrations*

The concentrations of protein extracts were then determined with the aid of BCA protein assay kit (Pierce, Loughborough, UK) according to manufacturer's instructions. Respective protein samples were diluted 1:5 and 1:10 in RIPA buffer. In duplicates, 12.5µl of diluted sample was deposited into a 96-well round bottomed plate (Nunc, Leics, UK). The colorimetric assay reagent was prepared by adding BCA protein assay reagent A to reagent B at a ratio of 50:1 and 100µls of this mixture was added to each protein sample. The samples were then mixed thoroughly and left to incubate at 37°C for 30 minutes. The resulting colorimetric changes were then measured using a nanodrop spectrophotometer (ND-1000; Labtech International) at 562nm. A standard curve determined from bovine serum albumin of known concentrations was used to extrapolate the relative concentrations of protein extracts.

### 2.6.3 Analysis of proteins by Western blotting

#### 2.6.3.1 *Preparation of protein samples for loading onto gel*

Protein extracts with known protein concentrations were then diluted with RIPA buffer to a final volume of 10µl containing between 30-70µg of protein. Then 2.5µl of 5x Laemmli buffer (0.125M Tris-HCl pH6.8, 4% w/v SDS, 40% v/v glycerol, 0.1% w/v bromophenol blue [Sigma, Dorset, UK], 6% v/v beta-mercaptoethanol [Sigma, Dorset, UK] in distilled water) was added per protein sample. Prior to loading onto gels, samples were denatured by heating at 95°C for 5 minutes.

## 2.6.3.2 Casting of polyacrylamide gels

SDS-PAGE gels were set with the aid of Mini-Protean III (Biorad, Hempstead, UK) gel casting apparatus. The % of acrylamide used in resolving gels were dependent on the sizes of proteins to be probed. The mixture for resolving gels as described in Table 2.8 were poured into gel casts and allowed to set for 30 minutes. Then, the mixture for stacking gels (4% acrylamide, Table 2.8) was made up and poured on top of the resolving gel. Well combs with 10 or 15 wells were then inserted immediately into gel cast and the stacking gel was left to set for 30 minutes. Subsequently,, combs were removed and wells were rinsed with distilled water.

	8%	10%	12%	4%
<b>Reagent</b>	Resolving Gel	Resolving Gel	Resolving Gel	Stacking Gel
<b>Molecular weight of protein</b>	40-150kDa	25-100kDa	15-75kDa	-
<b>Distilled water</b>	4.7ml	4.1ml	3.4ml	6.1ml
<b>30% Acrylamide/Bis (Sigma)</b>	2.7ml	3.3ml	4.0ml	1.3ml
<b>1.5M Tris-Hcl, pH8.8</b>	2.5ml	2.5ml	2.5ml	-
<b>0.5M Tris-Hcl, pH6.8</b>	-	-	-	2.5ml
<b>10% w/v SDS</b>	100µl	100µl	100µl	100µl
<b>10% ammonium persulphate (Sigma)</b>	50µl	50µl	50µl	50µl
<b>TEMED (Sigma)</b>	5µl	5µl	5µl	5µl

**Table 2.8:** Composition of gels for SDS-PAGE.

#### 2.6.3.3 SDS-Polyacrylamide gel electrophoresis (SDS-PAGE)

Protein separation was carried out in Mini-Protean III (Bio-Rad, Hempstead, UK) electrophoresis tanks with 1x Tris-Glycine buffer (Table 2.9). Protein samples were loaded into appropriate gels along with protein molecular weight marker (PageRuler Plus, Fermentas, Loughborough, UK) and gels were run for 45-60 minutes at 150V.

#### 2.6.3.4 Transfer of proteins onto PVDF membranes

Before transfer, Immobilon-P polyvinylidene difluoride (PVDF, Milipore, Watfor, UK) membrane was cut to a size appropriate for gels and activated by soaking in methanol (Fisher Scientific, Loughborough, UK) for 10 seconds. The membrane was then rinsed with 1x Tris-Glycine transfer buffer (Table 2.9). Gels with separated proteins were then removed from glass plates and soaked in Tris-Glycine transfer buffer for 10 minutes. After that, the stacking gel was removed whilst the resolving gel was placed onto the activated membrane within a wet electroblotting system (BioRad, Hempstead, UK). The gel was rolled after each layer was added to ensure no air bubbles were present in between the surfaces. Proteins were transferred in 1x Tris-Glycine buffer (Table 2.9) with an ice block within the transfer apparatus to prevent over-heating. The transfer procedure was carried out for 1 hour with a constant current of 0.4mA.

#### 2.6.3.5 Immuno-probing of proteins on membranes

After proteins were immobilized onto PVDF membrane, it was blocked with milk blocking solution with agitation for 1 hour at room temperature. Subsequently, membranes were incubated with 5mls of appropriate primary antibody (Table 2.10) overnight at 4<sup>0</sup>C on a roller mixer (Stuart, Merton, UK). Post-incubation, membranes were washed thrice for 5 minutes in PBS/T before incubation in appropriate horseradish-peroxidase (HRP))-conjugated secondary antibody (Tables 2.10) at room temperature on a roller mixer for 1 hour. Then, membranes were washed thrice for 5 minutes in PBS/T before visualization of protein bands.

---

<b>Solution</b>	<b>Composition</b>
<b>10 x Electrophoresis Buffer</b>	30.3g Tris base (Sigma), 144.4g Glycine (Sigma), Upto 1L dH <sub>2</sub> O
<b>1 x Tris-Glycine SDS-PAGE Running Buffer (1L)</b>	890ml dH <sub>2</sub> O, 100ml 10 x Electrophoresis Buffer, 10ml 10% w/v SDS
<b>1 xTris-Glycine Transfer Buffer</b>	700ml dH <sub>2</sub> O, 100ml 10 x Electrophoresis Buffer, 200ml Methanol
<b>Milk Blocking Solution</b>	5% w/v non-fat milk powder (Marvel) in PBS/T
<b>Stripping Buffer</b>	62.5mM Tris-HCl (pH6.8), 2% w/v SDS, 100mM 2-beta-mercaptoethanol

---

**Table 2.9:** Buffers and respective compositions used for Western blot analysis.

<b>Antigen</b>	1° Antibody source	Catalogue number	1° Antibody species	Dilution ratio	Antigen size
<b>β-actin</b>	Abcam	Ab8227	Rabbit	1:5000	43kDa
<b>γ-tubulin</b>	Abcam	Ab6160	Rat	1:10000	50kDa
<b>p100/p52</b>	Santa Cruz	Sc-7386	Mouse	1:200	100/52 kDa
<b>ERα</b>	Santa Cruz	Sc-7207	Rabbit	1:200	68kDa
<b>ErbB2</b>	Cell Signaling	2242	Rabbit	1:200	185kDa
<b>p105/p50</b>	Santa Cruz	Sc-114	Rabbit	1:200	105/50 kDa
<b>p65</b>	Abcam	Ab7978-1	Rabbit	1:200	65kDa
<b>RelB</b>	Santa Cruz	Sc-226	Rabbit	1:200	70kDa
<b>c-rel</b>	Santa Cruz	Sc-71	Rabbit	1:200	78kDa
<b>IκBα</b>	Cell Signaling	9242	Rabbit	1:1000	39kDa
<b>Lamin A/C</b>	Cell Signaling	2032	Rabbit	1:1000	70kDa
<b>E-cadherin</b>	Upstate	07-697	Rabbit	1:500	106kDa
<b>Vimentin</b>	Santa Cruz	Sc-7557	Goat	1:100	57kDa

**Table 2.10:** Details of antibodies used for Western blotting analysis.

#### *2.6.3.6 Visualization of protein bands*

Immuno-labelled proteins were detected by chemiluminescence with ECL/ECL+ reagent kit (GE Healthcare, Bucks, UK) according to manufacturer's instructions. ECL solutions were made up and mixed before addition onto membranes (1.5mls per membrane). Membranes were incubated with ECL or ECL+ reagent in the dark for 1 minute or 5 minutes respectively. Subsequently, excess reagent was removed and the membrane was transferred into a light-proof cassette. Light sensitive films (Amersham Hyperfilm ECL; GE Healthcare, Bucks, UK) were then exposed to the membranes under safelight conditions for appropriate amounts of time to produce bands with fitting intensities. Films were developed using a Xograph Compact X4 automatic X-ray film processor.

#### *2.6.3.7 Stripping and re-probing of membranes*

Before probing of membranes with a subsequent antibody of interest, membranes were stripped in stripping buffer (Table 2.9) for 30 minutes at 55°C with agitation. Then, the membrane was rinsed thrice in distilled water for 5 minutes, followed by incubation for 30 minutes in PBS/T at room temperature. Membranes were then blocked in milk solution, probed with appropriate antibodies and visualized as described in Sections 2.6.3.5 and 2.6.3.6.

#### *2.6.3.8 Quantification of protein bands*

Where appropriate, protein bands were semi-quantified by measuring the intensity of bands on images of Western blots with ImageJ. The quantity of protein was determined by normalizing the intensity of a particular antigen against that of a loading control.

## **2.7 RNA analysis**

### *2.7.1 RNA isolation*

When working with RNA, all reagents and consumables used were RNase free. Bench surfaces and equipment were also treated with RNaseZAP (Ambion, Paisley, UK) to prevent contamination by RNases during isolation and purification processes.

### 2.7.1.1 RNA extraction from tissue samples

For tissue samples, RNA was extracted using Trizol (Invitrogen, Paisley, UK) reagent. Tissues were weighed (50mg) and cut on a petri dish resting on dry ice. Tissue slices were then placed into a spinLyse tube containing 1ml of Trizol reagent. Homogenization of tissue was achieved with the aid of a Precellys 24 machine, with the spinLyse settings set at 6500rpm for 45 seconds twice. Then, samples were centrifuged for 10 minutes at 8000x g at 4°C. Next, the supernatant was moved into a fresh micro centrifuge tube, before addition of 200ul of chloroform. Samples were then mixed vigorously for 30 seconds by hand and allowed to rest at room temperature for 3 minutes. The solvent fractions were then separated by centrifuging at 8000x g at 4°C for 15 minutes. Subsequently, the aqueous phase was extracted and transferred into a tube containing 400ul of isopropanol. The mixture was then shaken gently to precipitate the RNA and was then purified using RNeasy Mini Kit (Qiagen, Sussex, UK) according to the manufacturer's instructions. The quality and concentration of resulting isolates were then determined using a NanoDrop spectrophotometer (ND-1000, Labtech International).

### 2.7.1.2 RNA purification from cells

Isolation of RNA from cells was carried out by lysing cells in RLT buffer (RNeasy Mini Kit; Qiagen, Sussex, UK) prior to using the RNeasy Mini Kit (Qiagen, Sussex, UK) according to manufacturer's instructions. Similarly, the quality and concentration of isolated RNA was determined using a NanoDrop spectrophotometer.

### 2.7.2 Reverse transcriptase (RT) cDNA synthesis

Complementary DNA (cDNA) was synthesized from RNA samples using RevertAID Premium Reverse Transcriptase (Fermentas, Loughborough, UK). RNA samples were diluted to concentrations between 500-1000ng with RNase free water upto 12.5µl in volume for cDNA synthesis. Random primers and dNTPs which have been prepared as a mastermix (Table2.11) was then added to each sample (2µl) to make up a total volume of 14.5µl. Then, samples were mixed gently, briefly centrifuged and incubated at 65°C for 5 minutes, before being placed on ice. Consequently, a mastermix solution containing reverse transcriptase (Table2.11) was added (5.5µl) to each sample, making up a final reaction volume of 20µl. The reaction mix was then incubated at 25°C for 10 minutes, 50°C for 30 minutes and 85°C for 5

minutes before being cooled on ice. Negative controls lacking reverse-transcriptase were also prepared in parallel with similar reaction components. The synthesized cDNA was then used immediately or stored at  $-70^{\circ}\text{C}$  for future use.

<b>Master Mix 1 components</b>	<b>Volume per reaction</b>
dNTPs (10mM; dATP, dCTP, dGTP, dTTP, Promega)	1 $\mu\text{l}$
Random Primers (500ug/ml, Promega)	1 $\mu\text{l}$

<b>Master Mix 2 components</b>	<b>Volume per reaction</b>
5x RT Buffer (Fermentas)	4 $\mu\text{l}$
RNasin Plus (40u/ul, Promega)	0.5 $\mu\text{l}$
RevertAID Premium Reverse Transcriptase (200u/ul, fermentas)	1 $\mu\text{l}$

**Table 2.11** : Components of master mix for reverse transcriptase reactions.

### 2.7.3 Quantitative real-time polymerase chain reaction (qRT-PCR)

#### 2.7.3.1 Primer design

In order to distinguish PCR products of cDNA templates from that of genomic DNA sequences, primers were designed across exon boundaries with the aid of Primer 3 software available through <http://frodo.wi.mit.edu/primer3/>. The specificity of primers was then verified by in silico PCR software available through <http://genome.csdb.cn/cgi-bin/hgPcr>. Sequences for oligonucleotides used are detailed in Table 2.12 and all oligonucleotides were purchased from Sigma-Genosys.

### 2.7.3.2 qRT-PCR

Thermal cycling for qRT-PCR reactions was carried out with a Step One Plus Realtime PCR System (Applied Biosystems) with the aid of StepOne software (v2.1, Applied Biosystems). Three technical repeats were carried for each sample and a minimum of three biological replicated samples were examined. To control for differences in starting material, the amount of transcript was normalized against the level of a housekeeping gene (Cyclophilin B or GAPDH).

Respective control and cDNA samples (2.5µl) were loaded into separate wells of a 96-well qPCR plate (MicroAmp Fast Optical 0.1ml; Applied Biosystems, California, USA). A mastermix as detailed in Table 2.13 was then prepared and added into respective wells with cDNA template. SYBR Green reagent (Invitrogen) was used in the mastermix. The reaction mixture was then mixed by gentle pipetting before sealing plates with caps (MicroAmp Optical 8-capstrip; Applied Biosystems, California, USA). The reaction plate was then loaded into Step One Plus Realtime PCR machine. The cycling conditions used for all reactions consisted of; initial denaturation for 10 minutes at 95°C, followed by 45 cycles of 95°C for 15 seconds and 60°C for 1 minute. At the end of each cycle, readings were measured. Upon completion of cycles, the integrity of reaction products were examined by performing a melting curve cycle which consisted of; 95°C for 15 seconds, 60°C for 1 minute [with optics off], 60°C to 95°C at 0.2°C increments every 15 seconds [with optics on]. Data collection throughout cycling was automated by StepOne software.

### 2.7.3.3 QRT-PCR data analysis

$C_T$  values obtained from qRT-PCR experiments were calculated using the  $2^{-\Delta\Delta C_t}$  relative quantification method (Livak and Schmittgen, 2001). Briefly, the levels of transcript for a sample were normalized by calculating the difference between the  $C_T$  values of a target gene and that of a housekeeping gene, to give the value  $\Delta C_T$ . A relative value of the difference in transcript levels between two samples can then be calculated by determining the difference between the  $\Delta C_T$  of both samples, giving rise to the  $\Delta\Delta C_T$  value. Relative fold changes between samples were then calculated as  $2^{-\Delta\Delta C_t}$ .

<b>Primer</b>	<b>Sequence</b>	<b>Product Size</b>
<b>Cyclophilin B F</b>	5'- CCA TCG TGT CAT CAA GGA CTT CAT -3'	216bp
<b>Cyclophilin B R</b>	5'- TTG CCA TCC AGC CAG GAG GTC T -3'	
<b>GAPDH F</b>	5'- CAC AGT CAA GGC CGA GAA TG -3'	242bp
<b>GAPDH R</b>	5'- TCT CGT GTT CAC ACC CAT C -3'	
<b>P35 F</b>	5'- TGG ATT CCA CGA TAG CAT CA -3'	149bp
<b>P35 R</b>	5'- GAC CAA TTT GGG CAA ACA GT -3'	
<b>P52 F</b>	5'- GAT CTC CCG AAT GGA CAA GA -3'	99bp
<b>P52 R</b>	5'- AAC CGA ACC TCA ATG TCG TC -3'	
<b>SNAIL F</b>	5'- TGA GAA GCC ATT CTC CTG CT -3'	91bp
<b>SNAIL R</b>	5'- CTT CAC ATC CGA GTG GGT TT -3'	
<b>SLUG F</b>	5'- TCT GCA GAC CCA CTC TGA TG -3'	101bp
<b>SLUG R</b>	5'- AGC AGC CAG ACT CCT CAT GT -3'	
<b>Twist1 F</b>	5'- CAG GCC GGA GAC CTA GAT GTC AT -3'	158bp
<b>Twist1 R</b>	5'- TGC CCC ACG CCC TGA TTC TTG -3'	
<b>Twist2 F</b>	5'- CTT CTC CGT GTG GCG CAT -3'	133bp
<b>Twist2 R</b>	5'- CCG CAT CCA GTT CCG CAT -3'	
<b>ZEB2 F</b>	5'- CCG GGA GCT GTT TCT TCG -3'	120bp
<b>ZEB2 R</b>	5'- CGC AGG CTC GAT CTG TGA -3'	
<b>E cadherin F</b>	5'- CAG ATG ATG ATA CCC GGG ACA A -3'	136bp
<b>E cadherin R</b>	5'- GGA GCC ACA TCA TTT CGA GTC A -3'	
<b>N cadherin F</b>	5'- AGG ACC CTT TCC TCA AGA GC -3'	117bp
<b>N cadherin R</b>	5'- ATA ATG AAG ATG CCC GTT GG -3'	

**Table 2.12:** List of primers and respective sequences used for qRT-PCR reactions.

PCR Reaction Component	qRT-PCR
cDNA template	2.5µl
PCR-grade Water (Sigma)	12.65µl
Go Taq PCR Buffer (Promega)	5µl
Magnesium Chloride (25mM; Promega)	2.5µl
dNTPs (25mM; dATP, dCTP, dGTP, dTTP; Promega)	0.5µl
Forward Primer (Sigma Genosys, 10µM)	0.25µl
Reverse Primer (Sigma Genosys, 10µM)	0.25µl
Go Taq DNA Polymerase (Promega)	0.1µl
Sybr Green (Invitrogen)	1.25µl
<b>Total Reaction Volume</b>	<b>25µl</b>

**Table 2.13:** Reagents and components for qRT-PCR reactions.

## 2.8 Statistical analysis

### 2.8.1 Student's t-test

In order to determine statistical significance in differences between two data sets, two-tailed unpaired student's t-test was used. Calculations were done with Microsoft Excel software and  $p < 0.05$  was the threshold for significance.

### 2.8.2 Spearman's ranked correlation test

For comparison in IHC studies, the relationship between the degrees of staining for different antigens were determined by ranking tumours according to the staining scores (IxP), as described in Section 2.3.5.3. The difference between ranks for two antigens (D) was then calculated. In the case where tumours had the same ranking positions, they were assigned an averaged rank between tied tumours. The Spearman's rho coefficient can then be calculated based on the formula below (D=difference between ranks, N=number of tumour samples):

$$rho = 1 - \frac{6\sum D^2}{N(N^2-1)}$$

Rho values lie between the range of  $-1 < \rho < 1$ , where 1 indicates direct correlation, -1 indicates inverse correlation whereas 0 shows no correlation. The degree of correlation is portrayed by the rho value and a  $t$  value is calculated to determine whether a given rho value is statistically different from 0, using a Student's  $t$  distribution. Rho values were considered significantly different from 0 when  $p < 0.05$  for  $t$  values corresponding to  $(n-2)$  degrees of freedom.  $t$  values were calculated using the formula below:

$$t = r \sqrt{\frac{n-2}{1-r^2}}$$

### 2.8.3 Analysis of variance (ANOVA) test and Tukey's post-hoc analysis test

In order to determine whether the means between more than two independent groups were significantly different, ANOVA test was performed with the aid of SPSS software (Version 16.0, IBM). The means between at least two groups were considered significantly different when  $p$  values were less than 0.05. In the case where  $p < 0.05$  for ANOVA tests, Tukey's post hoc test was then carried out to determine the specific groups where statistically significant differences were observed. Again,  $p < 0.05$  was taken as the threshold for significance and Tukey's post-hoc test was carried out with the aid of SPSS software.

### 2.8.4 Analysis of co-variance (ANCOVA) test

ANCOVA test was used to determine whether growth curves for cell proliferation or *in vivo* tumour growth across varying time points were significantly different. Calculations were done with the general linear model (GLM) function for univariate analysis in SPSS software (Version 16.0, IBM) and  $p < 0.05$  was the threshold for significance.

## **CHAPTER 3**

Elucidating the effects of caspase inhibition during  
mammary tumour growth and metastasis.

### **3 Elucidating the effects of caspase inhibition during mammary tumour growth and metastasis**

#### **3.1 Introduction**

The ability to resist death stimuli has been recognized as a significant trait of cancer cells which can contribute to tumourigenesis (Hanahan and Weinberg, 2000b). Metastasis remains a major cause of death in breast cancer patients and there is evidence which suggests that the ability to evade apoptosis is important in this process. Although the role of apoptotic resistance in breast cancer metastasis has been addressed by previous studies (Bufalo et al., 1997, Martin et al., 2004), certain limitations exist with the experimental models used. In these studies, mammary cancer cells over-expressing anti-apoptotic proteins such as Bcl-2 or Bcl-XL respectively were shown to increase the metastatic potential of these cells when injected intravenously into immuno-compromised mice. However, a number of the initial steps of the metastatic cascade such as invasion and intravasation are omitted, along with the lack of immune surveillance due to xeno-transplantation. These issues were addressed in a study where mitogen-activated protein kinase kinase (MEK) transformed Eph4 cells were transplanted into the mammary glands of syngeneic mice. Indeed, increased spontaneous lung metastases were observed in cells that over-express Bcl-2 relative to parental cells (Pinkas et al., 2004). Nonetheless, anti-apoptotic proteins such as Bcl-2 have other roles in a cell which are distinct from its regulation of apoptosis (Furth et al., 1999) and the effects of these other signalling roles on metastases cannot be discounted.

For that reason, we set out to substantiate the importance of apoptotic resistance in primary tumour growth and metastasis of breast cancer using an inducible pan-caspase inhibitor (p35) mouse model that forms mammary tumours driven by the Neu oncogene. With this model, caspases, the core machinery of the apoptotic pathway can be inhibited by ectopic expression of p35 at designated time frames in endogenously formed tumours rather than transplanted cell lines.

## **3.2 Characterization of rtTA/p35 transgenic mice**

### **3.2.1 *Induction of p35 transcript levels in rtTA/p35 double transgenic mice is dependent on doxycycline administration***

In rtTA/p35 double transgenic mice, expression of the inducible transactivator, rtTA, is driven by the MMTV promoter whereas the p35 transgene is under the control of a tetracycline responsive element (TRE). Hence, p35 can be induced mainly in mammary epithelial cells when doxycycline (dox) is administered. Since the rtTA/p35 mouse model is novel, we set out initially to characterize the inducibility of p35 expression when these mice are administered with dox.

The levels of p35 transcript expression were determined by quantitative reverse transcriptase polymerase chain reaction (qRT-PCR). Only double transgenic mice which had been administered with doxycycline expressed significant levels of p35 mRNA relative to mice lacking dox or the p35 transgene (Figure 3.1). Accordingly, there was a dose dependent effect where mice subjected to 5 daily intraperitoneal (IP) injections of dox expressed p35 mRNA at about two orders of magnitude higher (~18000) relative to mice subjected to only 3 daily IP injections (~150). This difference is observed despite the fact that both these groups of mice received dox in their drinking water for a week, indicating that induction levels can be boosted more effectively when dox is administered via IP injections. On the other hand, both double transgenic mice that were not induced with dox and mice with only the rtTA transgene but induced with 5 IP injections, only showed background levels of p35 transcript. Thus, the expression of p35 in these mice is dependent on the administration of dox and due to the fact that there was a dose dependent induction, subsequent experiments were carried out with 5 daily IP injections before experimental endpoints.

### **3.2.2 *Caspase inhibition during mammary gland involution results in the accumulation of atypical luminal bodies***

During mammary gland involution, extensive cell death takes place and apoptosis has been implicated in this process (Chapman et al., 2000). In view of that, the functional characterization of rtTA/p35 double transgenic mice was carried out at this time point, in particular at 48 hours and 72 hours post-weaning. At both these time points, in DOX+ cohorts, where p35 induction is expected, the presence of

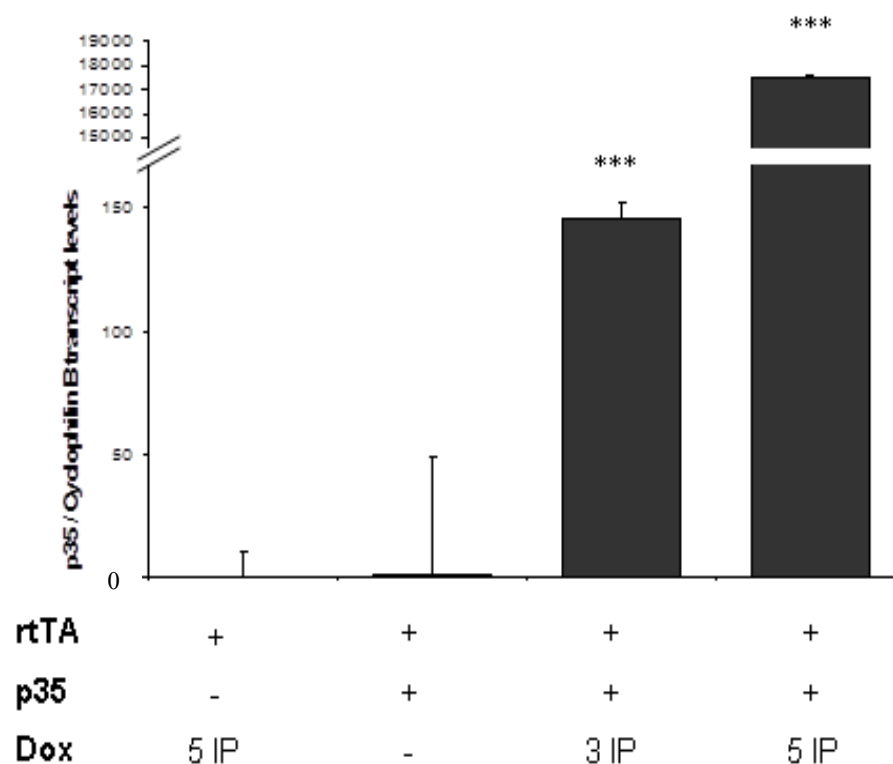


**Figure 3.1: Expression of p35 mRNA in rtTA/p35 mice is dependent on doxycycline administration.** Mice with respective transgenes (rtTA or rtTA/p35) were administered with indicated amounts of daily dox IPs prior to harvest. Mammary glands were harvested at 2-3 days post involution. Levels of p35 transcript were determined by qRT-PCR and normalized against cyclophilin B. Values were plotted as fold change relative to uninduced rtTA/p35 mice. Data points represent average of at least n=3 per group and error bars indicate standard error of the mean (SEM). \*\*\* indicates  $p < 0.001$ , where statistical significance relative to uninduced rtTA/p35 mice was determined by two-tailed t-test.

atypical luminal bodies can be observed (Figure 3.2a). In normal DOX- glands, almost all the luminal bodies observed have hypercondensed nuclei and compact cytosol compartments, whereas a proportion of luminal bodies in the DOX+ glands lacked nuclear condensation and had large vacuolar structures (Figure 3.2b). Furthermore, in DOX+ glands, a larger percentage of cleaved-caspase-3 (CC3) negative luminal bodies were present at 48 hours post weaning (Figures 3.3 a&b), as determined by immuno-histochemistry (12.4% in DOX +, 3.3% in DOX-). By 72 hours, there was no longer a difference in percentages of CC3 negative luminal bodies (Figure 3.3c), although there was a higher absolute number of these bodies in the DOX+ cohort. A majority of these CC3 negative bodies also exhibited atypical morphology suggesting that the morphological phenotypes observed were due to caspase inhibition. The fact that mammary epithelial cells (MECs) can detach and slough into the lumen without activation of the effector caspase-3 would also suggest that extensive caspase activation or apoptosis are not required for this process. It is also worth noting that none of the MECs within the alveolar structures stained positively for CC3 in either cohorts. This means that caspases are only activated upon detachment and cell sloughing at 48 and 72 hour involution time points.

In support of this, when these mammary glands were stained by terminal deoxynucleotidyl transferase dUTP nick end labeling (TUNEL), positively stained cells were observed in MECs within the alveolar structures of both cohorts (Figure 3.4). Since TUNEL staining is an indicator of programmed cell death, the presence of TUNEL positive cells but not CC3 positive cells within the alveolar structures would imply that a caspase-independent death program precedes caspase activation during involution.

### ***3.2.3 Inhibition of caspases by p35 does not delay the first phase of mammary gland involution***

To further assess whether caspases play an important role in the early stages of involution, we then appraised the gross morphology of mammary glands at 48 and 72 hours involution time points. In accordance with our previous observations that caspase-3 activation is not required for initiation of cell death and sloughing into the lumen, qualitative assessment of gross mammary gland architecture in both DOX+ and DOX- showed no differences (Figure 3.5). At 48 hours post weaning, there was

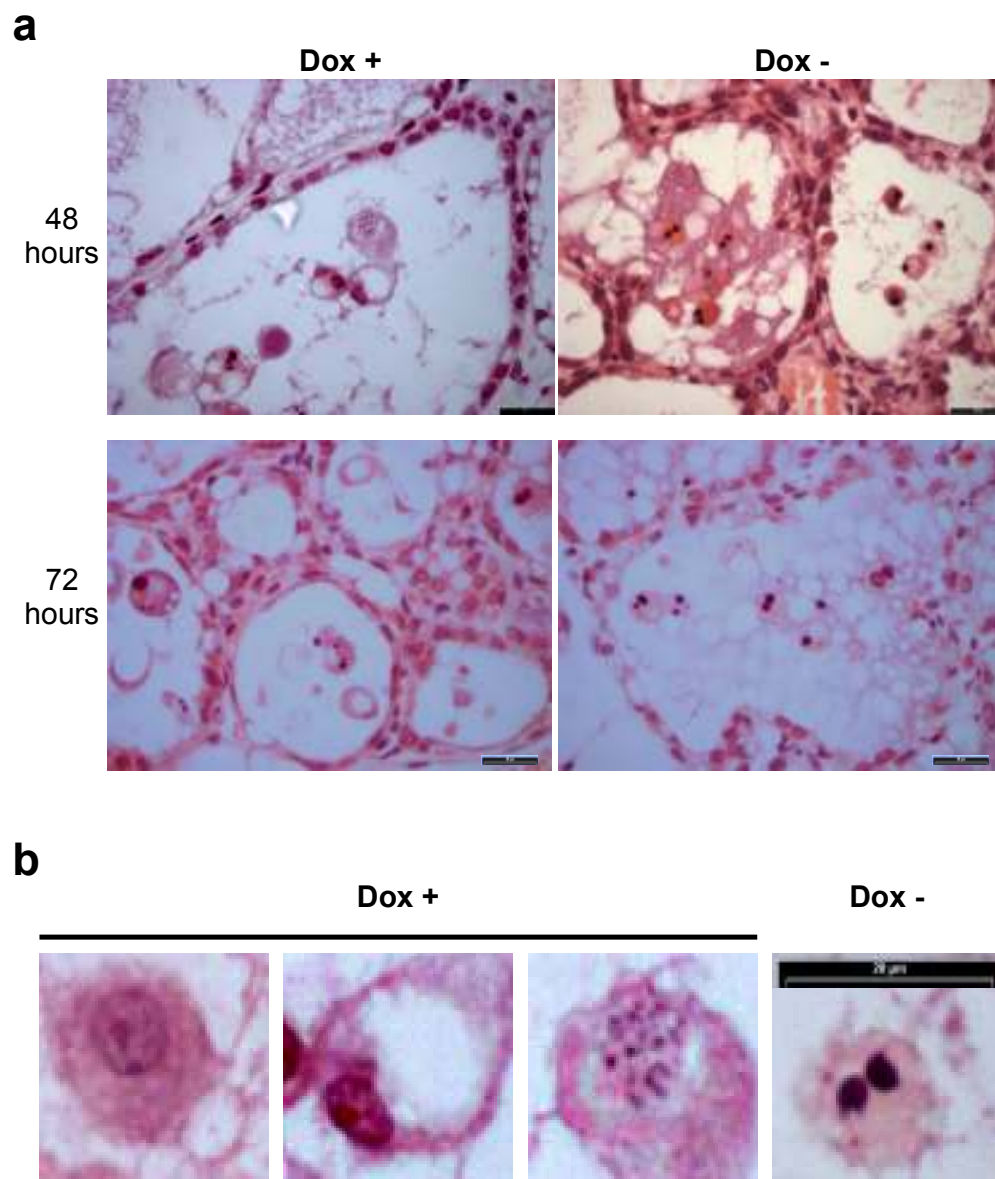


**Figure 3.2: Caspase inhibition during mammary gland involution leads to the formation of atypical luminal bodies. (a)** High power images of haematoxylin and eosin stained mammary gland sections from rtTA/p35 mice with or without dox at 48 hours and 72 hours involution time points. **(b)** Representative images of luminal bodies present in dox + and – cohorts. Scale bars represent 20µm.

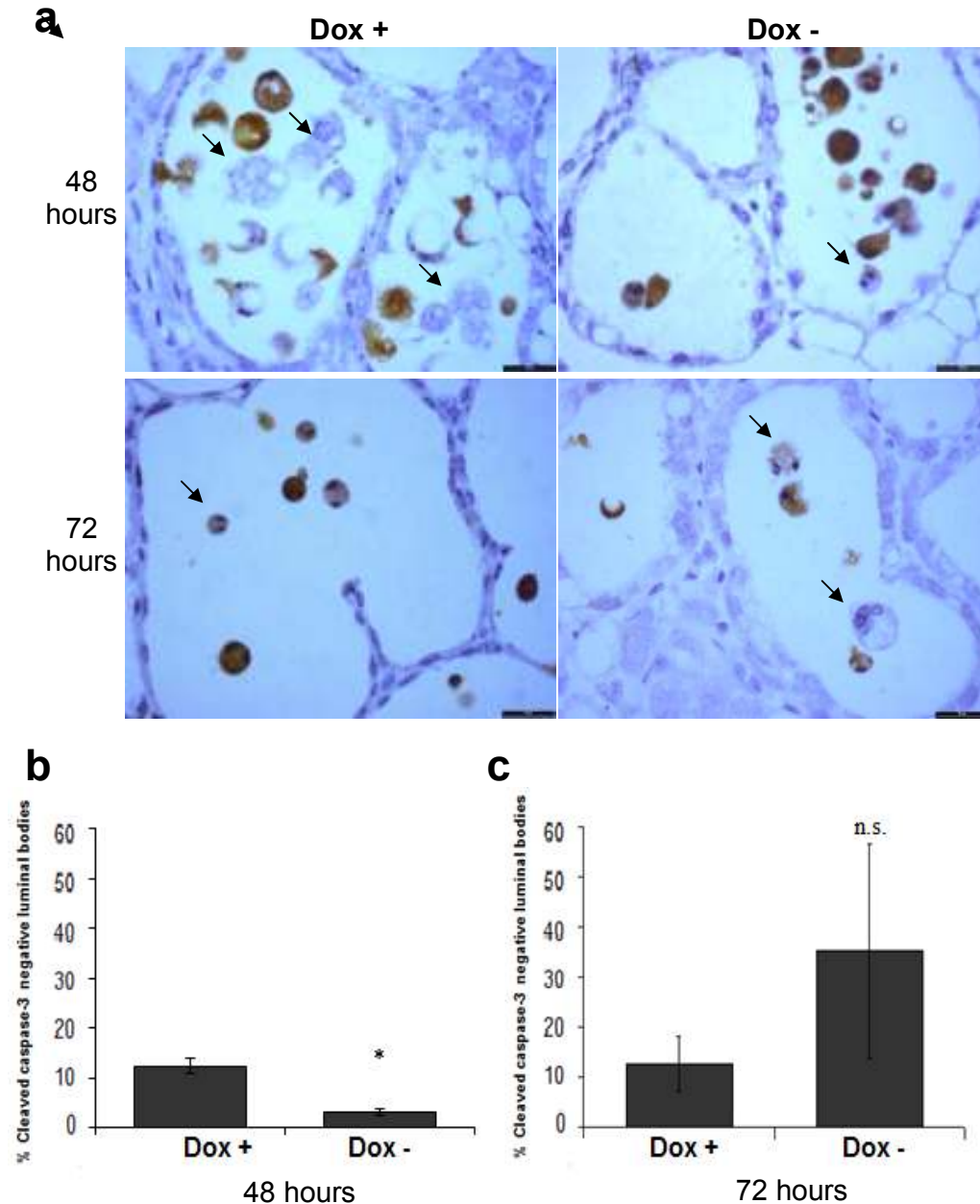


**Figure 3.3: Cleaved-caspase-3 staining of involuting mammary glands from rtTA/p35 mice. (a)** High power images of cleaved-caspase-3 stained mammary gland sections from rtTA/p35 mice with or without dox at 48 hours and 72 hours involution time points. Arrows indicate cleaved-caspase-3 negative atypical luminal bodies. Scale bars represent 20um. **(b)** Bar charts showing percentage of cleaved-caspase-3 negative luminal bodies present in dox + and - cohorts at 48 hours involution timepoint. **(c)** Bar charts showing percentage of cleaved-caspase-3 negative luminal bodies present in dox + and - cohorts at 72 hours involution timepoint. Data points represent means of at least n=3, error bars are standard errors of the mean. \* indicates p<0.05, n.s. indicates no statistical significance, where statistical significance was determined by two-tailed t-test.

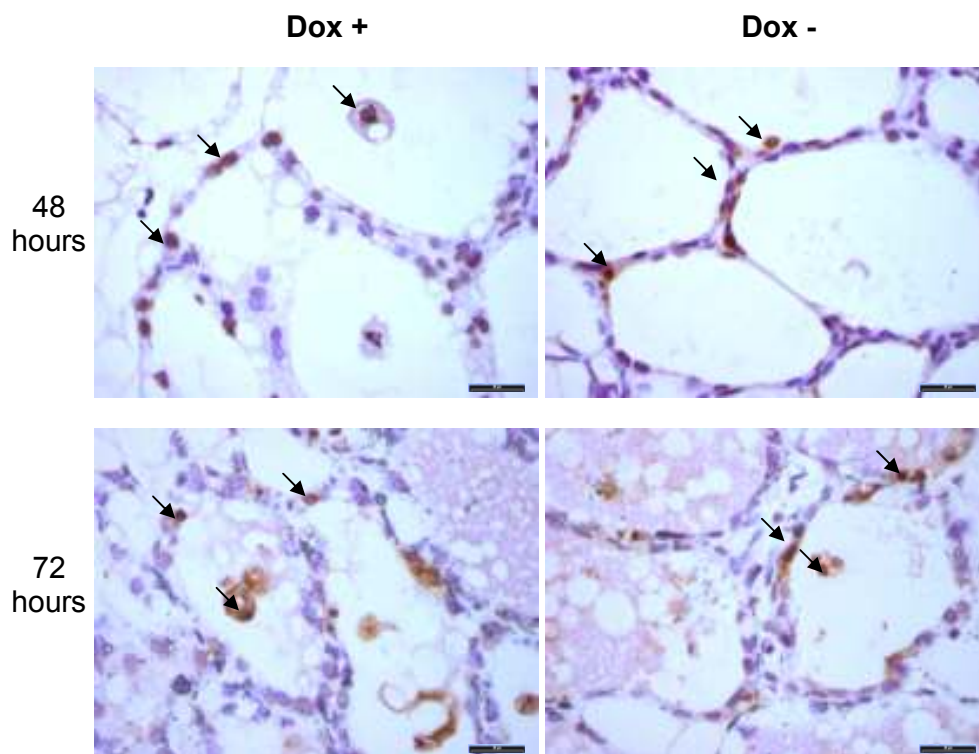


**Figure 3.4: TUNEL staining of involuting mammary glands from rtTA/p35 mice. (a)** High power images of TUNEL stained mammary gland sections from rtTA/p35 mice with or without dox at 48 hours and 72 hours involution time points. Arrows indicate representative examples of TUNEL + nuclei of cells within acinar structures. Scale bars represent 20 $\mu$ m.

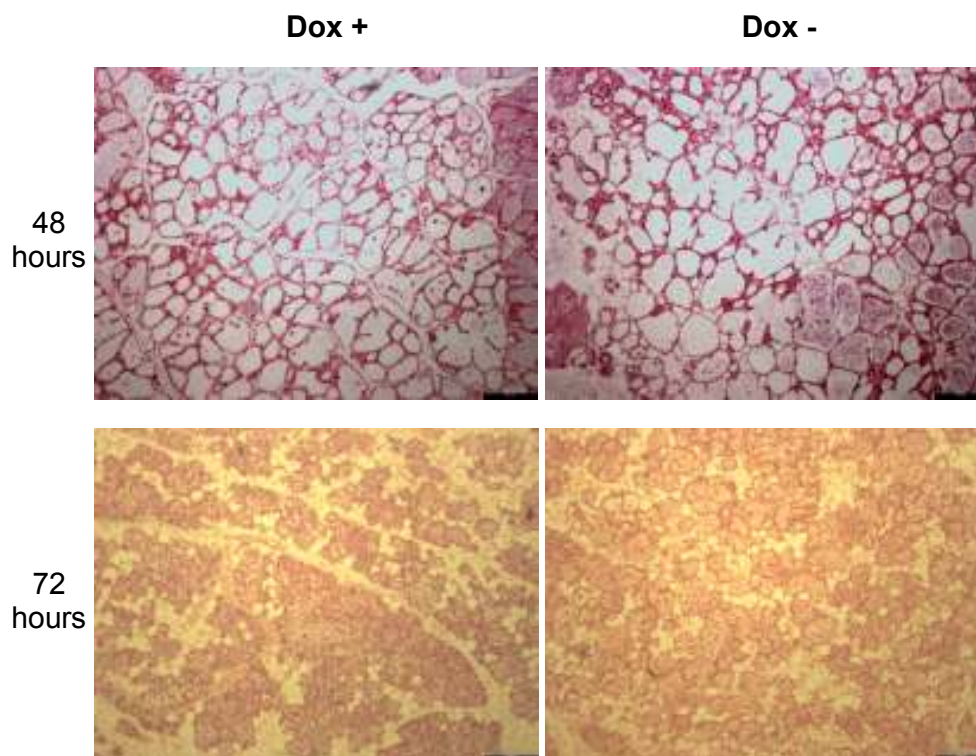


**Figure 3.5: Gross morphology of involuting mammary glands from rtTA/p35 mice. (a)** Low power images of haematoxylin and eosin stained mammary gland sections from rtTA/p35 mice with or without dox at 48 hours and 72 hours involution time points. Scale bars represent 200um.

still extensive coverage of alveolar structures in both cohorts. Similarly at 72 hours, no qualitative difference between the two cohorts was observed, as the rates at which adipocytes repopulated the gland were similar. This is in contrast to phenotypes of Stat3 knockout mice during involution, where evident delays in adipocyte repopulation can be observed (Chapman et al., 2000)].

When the number of luminal bodies per field of view for each cohort was quantified, no difference was observed at 48 hour time points (Figure 3.6a &b). This is in line with the gross morphology of glands from DOX+ and DOX- cohorts where no delay in involution was observed. However, at 72 hours, more luminal bodies were present in the DOX+ when compared to DOX- mammary glands. Although caspase inhibition does not affect the sloughing of cells into the lumen, this increase could be attributed to the delay in clearance of atypical luminal bodies when caspases are inactivated. Since luminal bodies are cleared through phagocytosis by professional and non-professional macrophages during involution, it is possible that caspase inhibition may prevent the exposure of 'eat me' signals such as phosphatidyl-serine, leading to the accumulation of luminal bodies by 72 hours.

Despite the lack of marked phenotypic changes during involution when caspases are inactivated, the presence of atypical luminal bodies which stain negative for CC3 provides evidence for the functionality of p35 induction in rtTA/p35 mice. Nonetheless, in DOX+ mice, the proportion of MECs which attain sufficient levels of p35 to be able to inhibit caspase activation remains to be addressed. Thus, it cannot be excluded that the lack of penetrance of p35 expression may be the reason for the indifferences pertaining to global mammary gland architecture.

### **3.3 Effects of caspase inhibition during primary tumour growth and breast cancer progression**

#### *3.3.1 Inhibition of caspases by p35 does not affect the growth rate of MMTV-Neu driven tumours*

By crossing rtTA/p35 double transgenic mice with MMTV-Neu mice, the effects of caspase inhibition in Neu oncogene driven tumours can be assessed in triple transgenic rtTA/p35/Neu progeny. In order to evaluate the effects of caspase inhibition on primary tumour growth and spontaneous metastasis formation, mice were segregated into DOX+ and DOX- cohorts when tumours grew to a size of 5mm

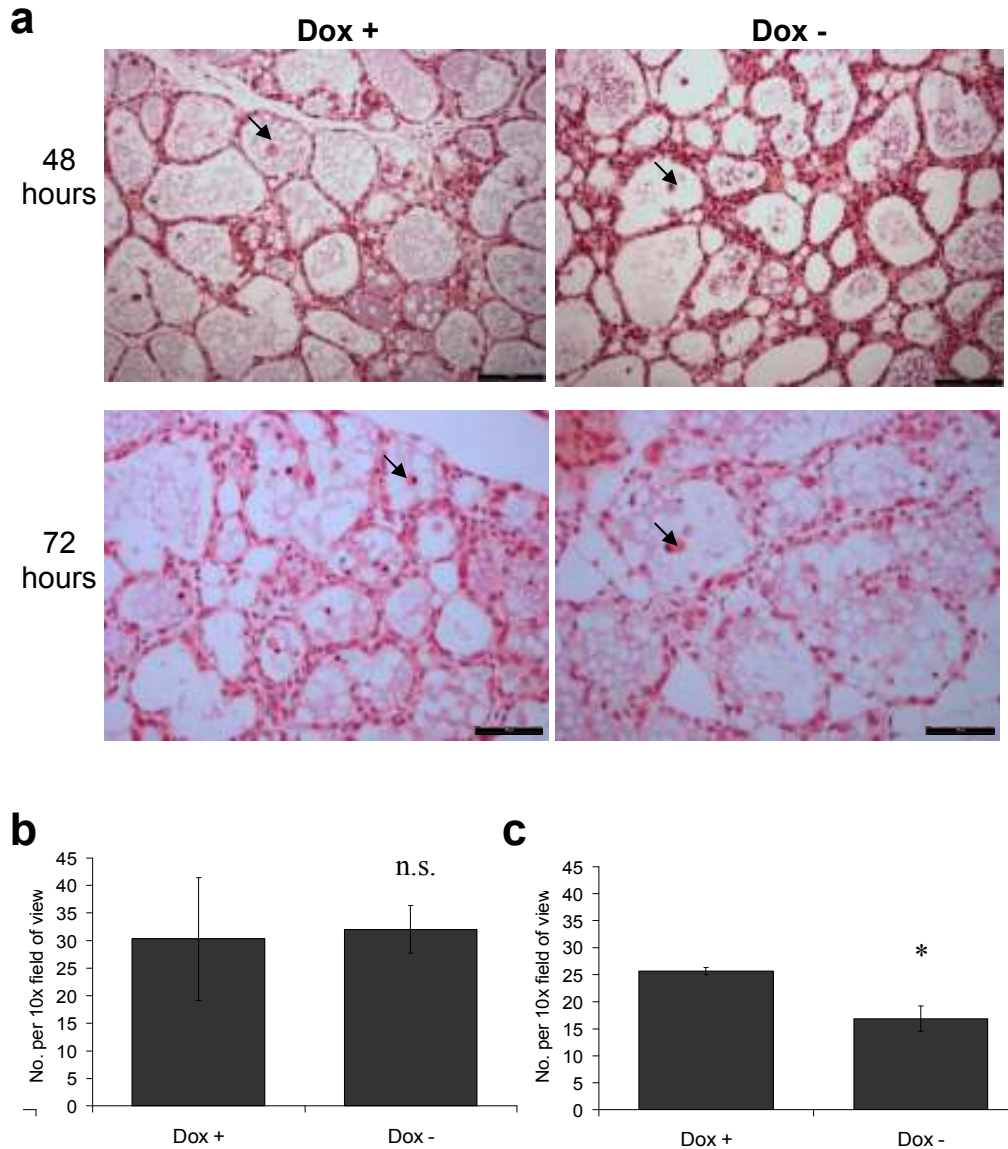


**Figure 3.6: Caspase inhibition during early phase mammary gland involution does not affect the number of luminal bodies.** (a) Representative images of haematoxylin and eosin stained mammary gland sections from rtTA/p35 mice with or without dox at 48 hours and 72 hours involution time points. Arrows indicate representative examples of luminal bodies. Scale bars represent 100µm. (b) Bar charts showing number of luminal bodies present in dox + and – cohorts at 48 hours involution time point. (c) Bar charts showing number of luminal bodies present in dox + and – cohorts at 72 hours involution time point. Data points represent means of at least n=3, error bars are standard errors of the mean. \* indicates  $p < 0.05$ , n.s. indicates no statistical significance, where statistical significance was determined by two-tailed t-test.

in diameter. This experimental design allows the effects of caspase inhibition on tumour initiation to be omitted (Figure 3.7a). In the period where tumours were between 5mm to 20mm in diameter, administration of dox did not affect primary tumour growth rate (Figure 3.7b). This correlates with the proportion of CC3 positive cells within tumours from both cohorts, as no difference was observed, showing that apoptotic rates within tumours were unchanged (Figures 3.8a & b).

### ***3.3.2 Inhibition of caspases in MMTV-Neu tumours increases their metastatic potential***

When rtTA/p35/Neu mice from DOX+ and DOX- cohorts reached the experimental endpoint (i.e. 20mm in diameter), they were sacrificed and their lungs and livers examined for metastases formation. Interestingly, all the mice administered with dox had lung metastases and one of the DOX+ mouse also had liver metastases. On the other hand, none of the DOX- mice had any liver or lung metastases (Table 3.1 & Figure 3.9). This illustrates that p35 expression which confers apoptotic resistance can enhance the metastatic potential of Neu oncogene driven tumours. To ascertain this observation, the number of animals per cohort will need to be increased. The proportion of CC3 positive cells in lung metastatic nodules from the DOX+ cohort were also compared to that of wild-type Neu lung metastases to assess whether caspase inhibition contributes to secondary tumour growth. However, no difference in the percentage of CC3 positive cells was observed (Figure 3.10), suggesting that once a metastatic colony is established at a secondary site, apoptotic resistance is less essential. Taken together with the data pertaining to primary tumour growth, our data would suggest the possibility that resistance to apoptosis is less crucial for sustaining primary tumour growth but is a key contributing factor to the formation of metastases.

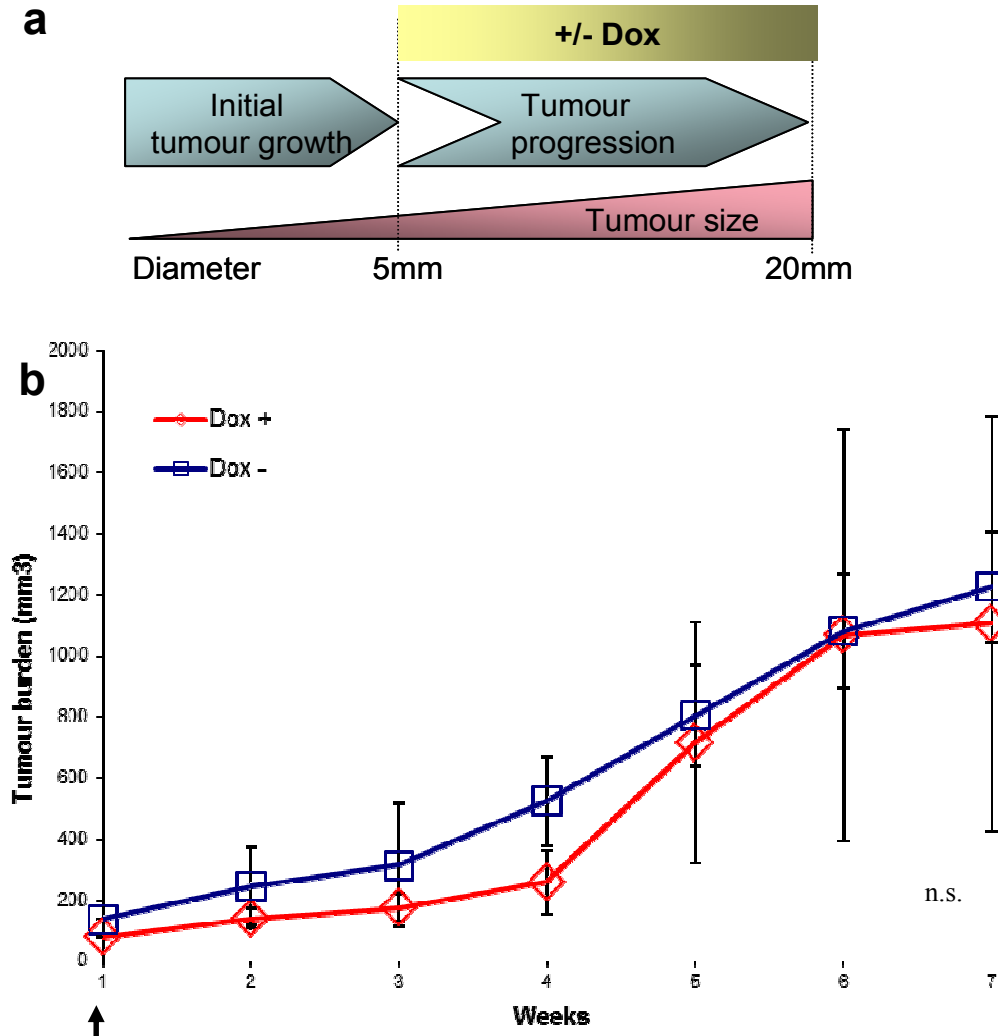


**Figure 3.7: Inhibition of caspases does not affect the growth rate of MMTV-Neu driven primary tumours.** (a) Schematic showing the experimental design for rtTA/p35/Neu mice. In the dox + cohort, p35 was induced when tumours were between 5-20mm in diameter. (b) Line graph showing the average growth rate of tumours from dox + and dox - cohorts of rtTA/p35/neu mice. Arrow indicates timepoint when dox was administered for the Dox+ cohort. Data points represent means of at least n=3 mice, error bars are standard errors of the mean. N.s. indicates not statistically significant, where statistical analysis was performed using ANCOVA test.

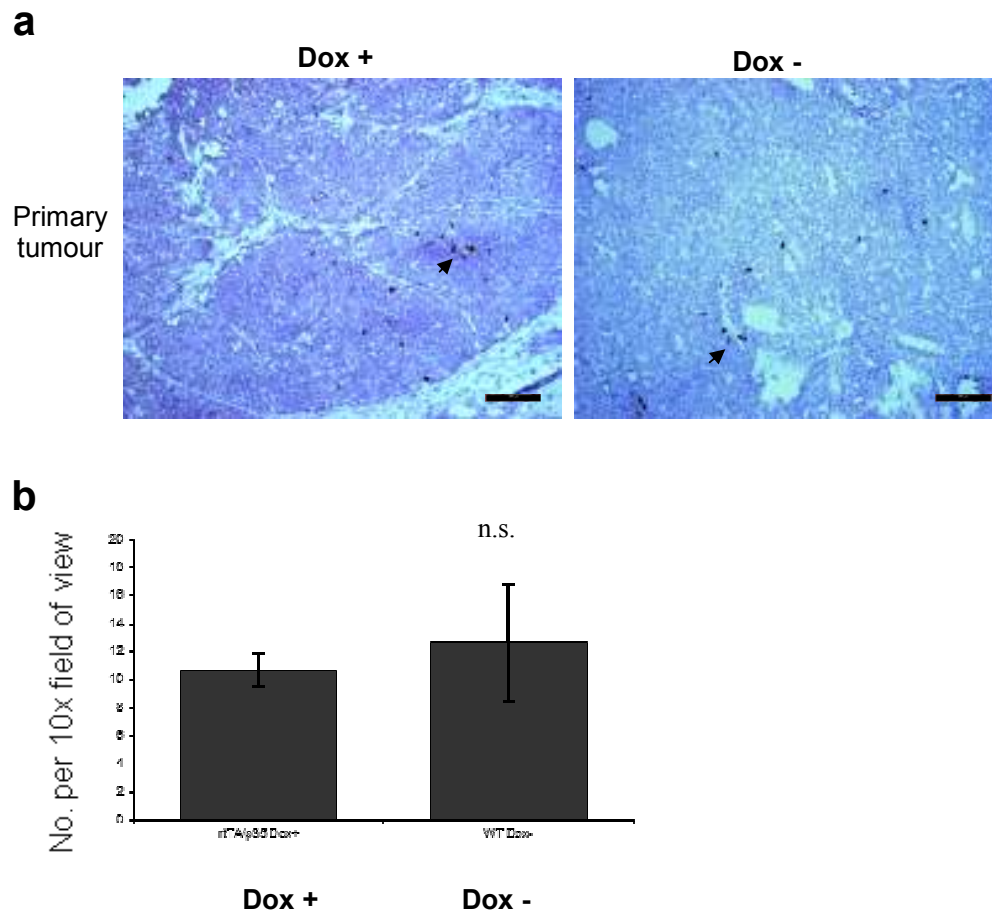


**Figure 3.8: Inhibition of caspases does not alter the proportion of cleaved-caspase-3 positive cells in MMTV-Neu driven primary tumours.**

**(a)** Low power images of cleaved-caspase-3 stained tumours from rtTA/p35/Neu mice with or without dox. Arrows indicate representative examples of cleaved-caspase-3 positive cells. Scale bars represent 200um.

**(b)** Bar charts showing number of cleaved-caspase-3 positive cells from dox + and dox - cohorts of rtTA/p35/Neu mice. Data points represent means of at least n=3, error bars are standard errors of the mean. n.s. indicates no statistical significance, where statistical significance was determined by two-tailed t-test.

Dox	Mice with liver metastases	Mice with lung metastases
+	1/3	3/3
-	0/3	0/3

**Table 3.1: Caspase inhibition increases the metastatic potential of MMTV-Neu driven tumours.** Table showing number of mice from rtTA/p35/Neu cohorts with or without dox and the respective number of mice with liver or lung metastases

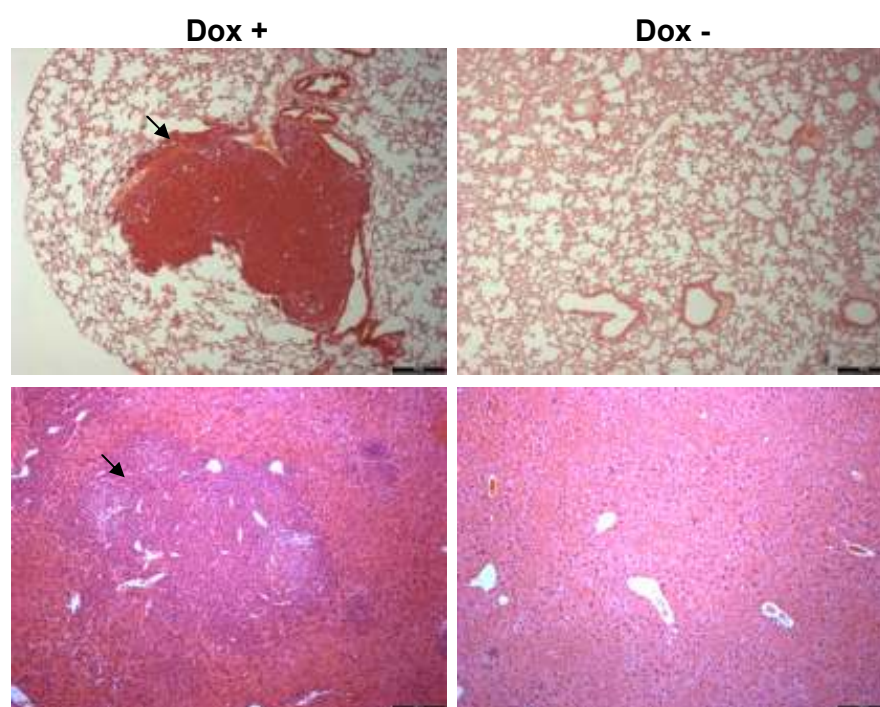


**Figure 3.9: Caspase inhibition increases the metastatic potential of MMTV-Neu driven tumours.** Representative images of haematoxylin and eosin stained lung and liver sections from rtTA/p35/Neu mice with or without dox. Arrows indicate metastatic nodules. Scale bars represent 200µm.

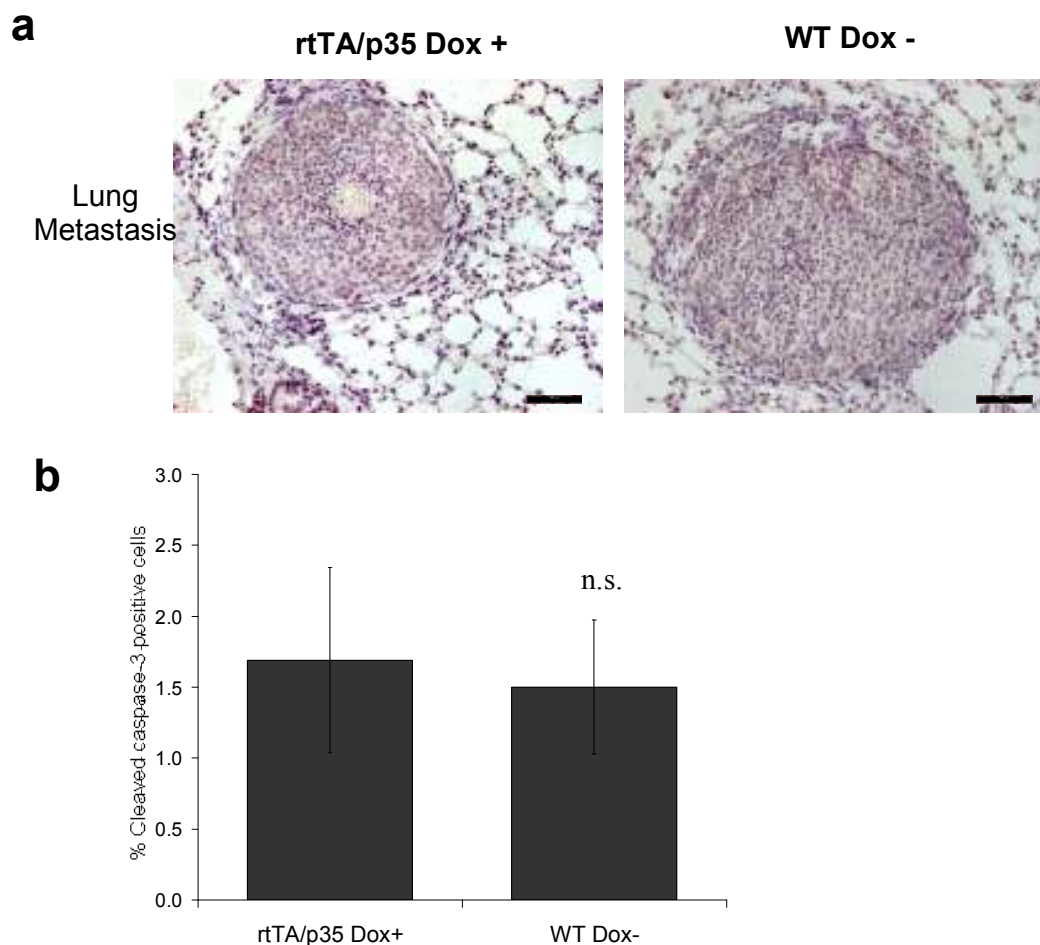


**Figure 3.10: Inhibition of caspases does not alter the proportion of cleaved-caspase-3 positive cells in lung metastases from MMTV-Neu driven primary tumours. (a)** Low power images of cleaved-caspase-3 stained lung metastases from rtTA/p35/Neu mice with dox or wild type Neu mice. Scale bars represent 100um. **(b)** Bar charts showing number of cleaved-caspase-3 positive cells from dox + rtTA/p35/Neu mice or wild-type Neu dox - mice. Data points represent means of at least n=3, error bars are standard errors of the mean. n.s. indicates no statistical significance, where statistical significance was determined by two-tailed t-test.

### **3.4 Discussion**

From the characterization of rtTA/p35 double transgenic mice, we have shown that expression of p35 transcript is dependent on administration of doxycycline. Functionally, p35 induction in the mammary glands of these mice during involution resulted in the formation of atypical luminal bodies which stain negative for cleaved-caspase-3 (Figures 3.2 & 3.3). However, we only observed a marginal increase in the proportion of cleaved-caspase-3 negative luminal bodies at 48 hours post weaning when p35 is induced. This may be due to p35 expression levels that are not sufficient to inhibit caspase activation in a majority of the cells. It would be useful to show the extent and levels of p35 expression in histological sections of the involuting glands to address this. There is also the possibility that caspase inhibition by p35 is only transiently effective, where caspases will eventually be activated in the cleaved-caspase-3 negative luminal bodies due to overriding stimuli. The transient nature of this population could explain the small proportion of cleaved-caspase-3 negative luminal bodies observed.

Nonetheless, from the small population of cleaved-caspase-3 negative luminal bodies, it appears that MEC sloughing into the lumen does not require caspase activation (Figure 3.3). Also, the presence of atypical luminal bodies when caspases are inhibited show that caspase activity after cell sloughing is important for the formation of luminal bodies with hyper-condensed nuclei and compact cytosol (Figure 3.2). As we observed an accumulation of luminal bodies at 72 hours post weaning in p35 expressing glands (Figure 3.6c), it would be interesting to investigate whether this would be exaggerated at later time points of involution or whether compensatory mechanisms will take place to remove the excess luminal bodies. This increase in luminal bodies when caspases are inhibited is not surprising because phosphatidyl-serine exposure is dependent on caspase activity (Martin et al., 1996). Consequently, caspase inhibition will prevent the exposure of such 'eat me' signals which are important for clearance by macrophages. It would be worthy to address whether this delay in clearance of luminal bodies can phenocopy MerTK or MFG-E8 knockout mice, where the absence of these receptors that recognize phosphatidyl-serine resulted in secondary necrosis, inflammation, fibrosis and defective development of mammary glands in subsequent pregnancies (Atabai et al., 2005, Hanayama and Nagata, 2005, Sandah et al., 2010).

From observations that DNA fragmentation (TUNEL +) is already prominent in MECs within the alveolar structures, and therefore precedes caspase activation in luminal bodies (Figures 3.3 & 3.4), it appears that caspase-independent cell death programs are initiated during involution prior to cell sloughing in the lumen. This would correlate with the absence of any delay in mammary gland remodeling when caspases are inhibited (Figure 3.5). However, we cannot exclude the possibility that p35 may be expressed at levels which are insufficient to inhibit apoptosis in a proportion of cells and thus, the overall involution of p35 expressing glands appears unaffected. Although a previous study of Stat3 knockout mice implicated a role for apoptosis during involution (Chapman et al., 2000), our data supports a more recent study where knockout of effector caspases in the mammary gland does not delay involution (Kreuzaler et al., 2011). This supports our observations that caspase activation is dispensable for the death of MECs during involution. Instead, it was shown in the study that a lysosomal mediated cell death program which is initiated by Stat3 through the regulation of cathepsins, drives the involution process. As lysosomal death pathways can crosstalk to apoptotic pathways (Stoka et al., 2001), it is not surprising that cleaved caspase-3 positive luminal bodies can be observed in involuting mammary glands (Figure 3.3). Taken together, this shows that the default physiological death pathway for MECs during involution is caspase-independent and not apoptosis as previously thought. In the context of diseases such as cancer, it is possible that aberrant cells may acquire the ability to circumvent this lysosomal mediated cell death pathway which is normally important for the homeostasis of the mammary gland through pregnancy cycles. Thus, the resistance of cancer cells to alternative forms of cell death should also be considered when designing therapeutics.

When p35 was expressed in established Neu-driven tumours, we found from a preliminary cohort of animals (n=3 for each arm) that caspase inhibition did not affect primary tumour growth but enhanced the formation of metastases (Figures 3.7-3.10). As p35 is induced only after tumours have reached a size of 5mm in diameter, the specific effects of caspase inhibition on tumour growth can be dissected from its co-operative effects with the Neu-oncogene on tumour initiation. Although, we did not address the effects of p35 expression on Neu-driven tumourigenesis, the model used can be easily employed for this purpose by changing the dox treatment regime. It is worth noting that our observations on the differential effects of p35 expression during primary tumour growth and metastasis formation mimics studies of those where Bcl-2

family members were over-expressed in breast cancer cells (Martin et al., 2004, Pinkas et al., 2004). This would imply that apoptotic stimuli at the primary site of these tumours are not sufficiently high enough such that caspase inhibition would confer a growth advantage. It could be possible that the homeostatic mechanisms limiting mammary tumour growth are non-caspase dependent, as with normal MECs during mammary gland involution (Figures 3.3& 3.4) (Kreuzaler et al., 2011).

Contrastingly, the formation of metastases can be enhanced by inhibition of apoptosis (Figure 3.4). This is not surprising as the metastatic cascade consists of many steps where apoptosis would be induced. Hence, with this model, we have managed to obtain preliminary evidence supporting the importance of apoptosis resistance in the formation of metastasis from endogenous mammary tumours. It remains an interesting prospect to identify the particular steps within the metastatic cascade where p35 confers a survival advantage. In order to address that, primary tumour cells could be harvested from rtTA/p35/Neu mice and subjected to *in vitro* assays which assess survival under anoikis conditions, motility and also tail vein transplantation assays. The expression of p35 can be regulated similarly *in vitro* through doxycycline treatment. Tail vein transplantation experiments would give insights into the effects of p35 expression during the latter stages of the metastatic cascade such as survival during circulation and at secondary sites. Intravital imaging techniques would need to be employed if the initial steps of invasion and intravasation were to be assessed *in vivo*. Another interesting aspect of the rtTA/p35/Neu mouse model is that p35 expression can be switched off upon removal of dox and this would be an important feature to address whether sustained apoptotic resistance is required for maintenance of metastatic nodules from endogenous tumours.

From these observations, it is plausible that therapeutics which reduce the apoptotic threshold in cancer cells might not affect primary tumour growth but still prove useful in preventing the formation of metastases. As mentioned, the resistance of breast cancer cells to alternative cell death mechanisms should also be considered as they may be important in promoting tumour growth.

### **3.5 Summary**

Through the characterization of rtTA/p35 mice, our data suggests that apoptosis is not essential for MEC death and cell sloughing during involution but caspase activation may be important for proper clearance of luminal bodies. In the context of mammary cancers, we have managed to provide preliminary evidence to reiterate the fact that caspase inhibition does not affect primary tumour growth but is a key factor in promoting the formation of metastases. The results substantiate the rationale for preventing the formation of breast cancer metastases by targeting pathways to re-sensitize breast cancer cells to apoptosis.

## **CHAPTER 4**

Elucidating the effects of silencing *Nfkb2* in  
mammary cancer cell lines.

## 4 Elucidating the effects of silencing *Nfkb2* in mammary cancer cell lines

### 4.1 Introduction

From the previous chapter (Section 3.3), our preliminary data supports the importance of apoptotic resistance in promoting breast cancer metastasis. Since metastasis is a major cause of cancer related deaths, it is important to develop therapeutics to prevent the spread of cancer cells to secondary sites. Consequently, a promising therapeutic strategy would involve targeting pathways that confer apoptotic resistance in breast cancer cells such that they would be re-sensitized to the milieu of death stimuli along the metastatic cascade.

For that reason, the NF- $\kappa$ B pathway is a prospective target as it regulates a range of anti-apoptotic genes (Clarkson and Watson, 1999) and have also been shown to negatively regulate lysosomal mediated cell death (Liu et al., 2003). Hence, it appears to be an important survival factor for MECs under physiological conditions and could represent a possible route by which aberrant cells are conferred with a survival advantage. In addition, a range of genes which have been implicated in promoting metastasis are also regulated by NF- $\kappa$ B (Pahl, 1999). The involvement of NF- $\kappa$ B signalling in maintaining CaSC properties (Cao et al., 2007) strengthens the rationale further as CaSCs are believed to be responsible for seeding new tumours.

The canonical NF- $\kappa$ B pathway has been shown to be important for tumorigenesis and CaSC properties especially in Neu/ErbB2 driven tumours (Liu et al., 2010, Pratt et al., 2009). The majority of studies focus on the canonical pathway in cancer, yet the alternative pathway is also known to play a key role in driving oncogenic pathways, [e.g. cyclin D1 (Rocha et al., 2003, Viatour et al., 2003)]. Less is known of the role of the alternative pathway in breast cancer tumourgenensis, yet aberrant levels of p52 pathway components have been described (Cogswell et al., 2000, Dejardin et al., 1995). A similarly important role for the RANKL-RANK-I $\kappa$ K $\alpha$  signalling axis has also been established (Cao et al., 2007, Gonzalez-Suarez et al., 2010, Schramek et al., 2010). Although this signalling axis can potentially drive the activation of the alternative pathway, there are many other functions ascribed to I $\kappa$ K $\alpha$ . Hence, it remains to be addressed whether the NF- $\kappa$ B subunit p52 has a role in one or more breast cancer subtypes, downstream of specific oncogenic pathways. Thus, we set out to define the involvement of p52 in regulating the properties of breast cancer cells through silencing of the *Nfkb2* gene and at the same time, assess the therapeutic

potential of such an intervention. Mouse mammary cancer cell lines were used in this study to allow the use of syngeneic transplantation mouse models. This circumvents the omission of certain components of the hosts' immune system which may have a role in promoting the tumourigenic properties of cancer cells studied.

## 4.2 Effects of silencing *Nfkb2* in mammary cancer cell lines

### 4.2.1 Silencing of *Nfkb2* leads to elevated basal NF- $\kappa$ B activity in *ErbB2*<sup>ve</sup> 4T1 and EPH4 cell lines but decreases the basal NF- $\kappa$ B activity of *ErbB2*<sup>+ve</sup> N202.1a cells

In order to assess the effects of *Nfkb2* silencing, three mammary cell lines were transduced with lentivirus encoding shRNA against *Nfkb2*. The 4T1 cell line is highly metastatic with ER<sup>+</sup> ErbB2<sup>-</sup> receptor status, the N202.1A cell line is derived from a MMTV-Neu driven tumour and has ER<sup>+</sup> ErbB2<sup>+</sup> receptor status whereas the Eph4 cell line is an immortalized non-tumourigenic cell line with ER<sup>+</sup> ErbB2<sup>-</sup> receptor status (Figure 4.1a). The levels of p100 protein were reduced to undetectable levels when shRNA against *Nfkb2* was expressed in all three cell lines, indicating effective silencing of the gene.

Initially, the effects of silencing *Nfkb2* on basal NF- $\kappa$ B transcriptional activity were assessed by luciferase reporter assays (Figure 4.1b). Interestingly, NF- $\kappa$ B activity was increased when p100/p52 is depleted in 4T1 and Eph4 cells, compared to respective cells that have been transduced with non-target (NT) shRNA. Conversely, the N202.1A cell line exhibited a decrease in basal NF- $\kappa$ B activity relative to NT control. It is also worth noting that the basal NF- $\kappa$ B activity for 4T1 NT and Eph4 NT cell lines were lower relative to N202.1A NT cells. This observation is in accordance with the fact that EGFR family members can drive the activation of NF- $\kappa$ B (Biswas and Iglehart, 2006), hence the higher NF- $\kappa$ B activity in N202.1A cells which are ErbB2<sup>+</sup>.

One explanation for the varying outcomes on NF- $\kappa$ B activity in different cell lines when *Nfkb2* is silenced could be the relative contribution of p100 and p52 to NF- $\kappa$ B signalling in different signalling backgrounds. Thus, it is possible that in 4T1 and Eph4 cells where the basal NF- $\kappa$ B activity is lower, loss of the inhibitory I $\kappa$ B protein, p100, is dominant over that of p52. This would eventually lead to an increase in NF- $\kappa$ B activity when p100/p52 is silenced. On the other hand, it is possible that p52

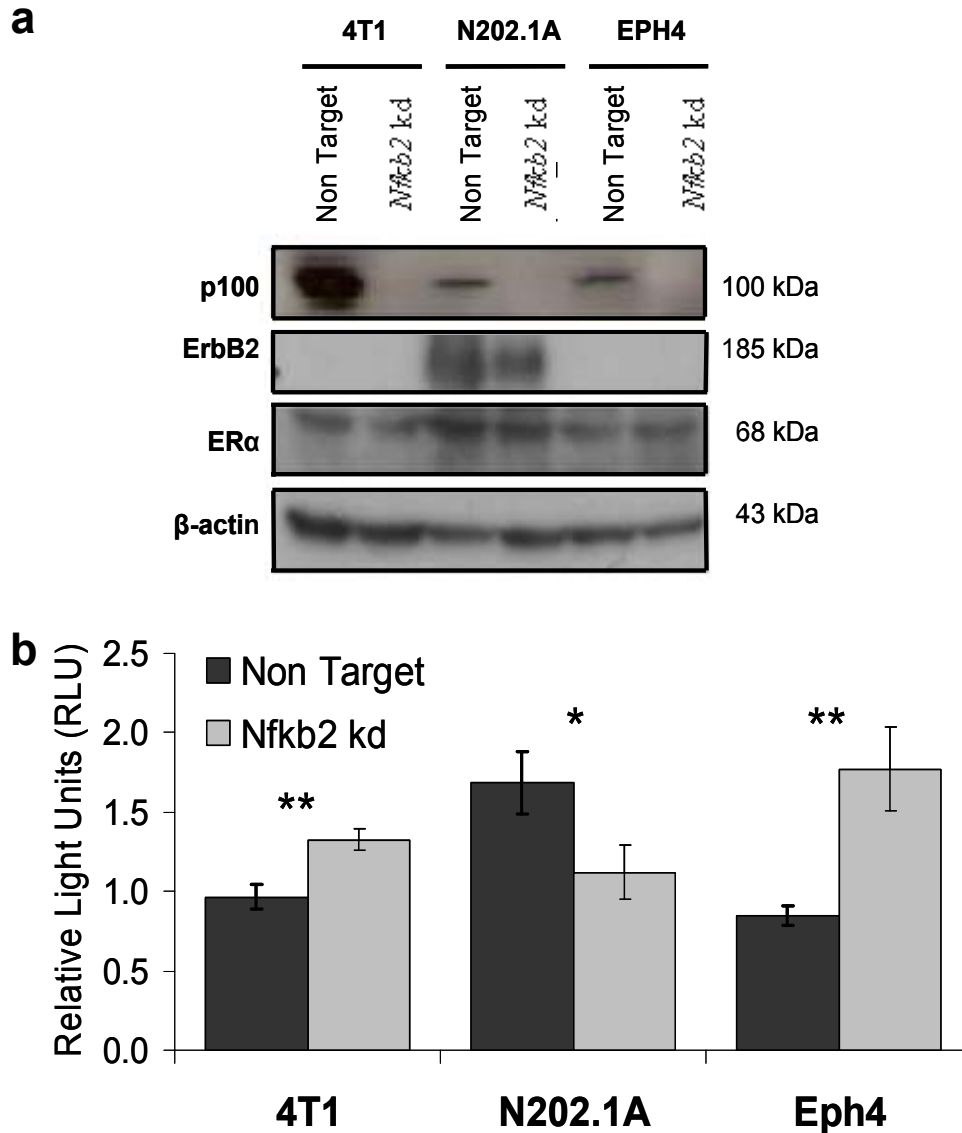


**Figure 4.1: Silencing of *Nfkb2* alters the basal NF- $\kappa$ B activity of mammary cell lines.** (a) Protein lysates from 4T1, N202.1A and EPH4 cell lines transduced with non target (NT) and shRNA against *Nfkb2* were harvested and separated by SDS-PAGE. Western blot shows levels of p100, ErbB2 and ER with  $\beta$ -actin as loading control in these cell lines. (b) 4T1, N202.1A and EPH4 cell lines transduced with non target (NT) and shRNA against *Nfkb2* were transfected with NF- $\kappa$ B luciferase reporter and pcDNA3.1:lacZ as transfection control. 48 hours after transfection, cell lysates were harvested and the ratio of luciferase to lacZ activity measured. Bar charts show basal NF- $\kappa$ B activity plotted as relative light units (RLU) in the respective cell lines. Data points represent average of at least  $n=6$  and error bars indicate standard error of the mean (SEM). \*\* indicates  $p<0.01$ , \* indicates  $p<0.05$ , where statistical significance relative to non target controls were determined by two-tailed t-test.

contributes to the higher basal NF- $\kappa$ B activity in N202.1A cells and thus, the effects of losing p52 outweigh that of losing p100, leading to an overall decrease in NF- $\kappa$ B activity upon *Nfkb2* silencing. Alternatively, the differential responses may be the result of more specific differences in the relative availability of canonical NF- $\kappa$ B components (eg. p50), heterodimer partners (eg. RelB) or co-factors (eg. p53, Bcl-3, HDAC1). Irrespective of the underlying mechanism for this difference however, it would be interesting to evaluate whether the changes in NF- $\kappa$ B activity correlate with respective cancer associated phenotypes.

#### **4.2.2 Loss of *Nfkb2* in 4T1 cells is associated with an increase in nuclear and cytoplasmic p50 levels**

Consequently, we also investigated the levels of NF- $\kappa$ B subunits and their nuclear localization in 4T1 cells. This was to determine whether the increase in basal NF- $\kappa$ B activity after *Nfkb2* silencing is associated with changes in the levels or localization of other NF- $\kappa$ B subunits. The first two rows (Figure 4.2) show complete depletion of p100/p52 protein in 4T1 cells when two different shRNAs (p52 shRNA 43&44) against *Nfkb2* were used. Interestingly, when p100/p52 is depleted, the levels of nuclear and cytoplasmic p105 were decreased. This was accompanied by increases in nuclear and cytoplasmic p50 in cells that express shRNA against *Nfkb2*. From these observations, it appears that more p105 is processed into p50, in order to compensate for the loss of p100/p52. Hence, it is possible that the increase in nuclear p50 levels is responsible for the increase in basal NF- $\kappa$ B activity of 4T1 cells when *Nfkb2* is silenced (Figure 4.1), since the levels of RelA, RelB and c-rel in the nucleus appear unperturbed. Although an increase in cytoplasmic c-rel is evident, it is unlikely that this would affect NF- $\kappa$ B transcription.

#### **4.2.3 Loss of *Nfkb2* sensitizes N202.1a cells to anoikis under non-adherent culture conditions in vitro**

We then went on to look at the survival of mammary cell lines under anoikis conditions upon *Nfkb2* knockdown because it represents the initial challenges faced by cancer cells in the metastatic cascade. In the 4T1 and EPH4 cell lines, no significant differences in the viability of these cells under anoikis conditions were observed when *Nfkb2* was silenced (Figure 4.3), despite increases in basal NF- $\kappa$ B

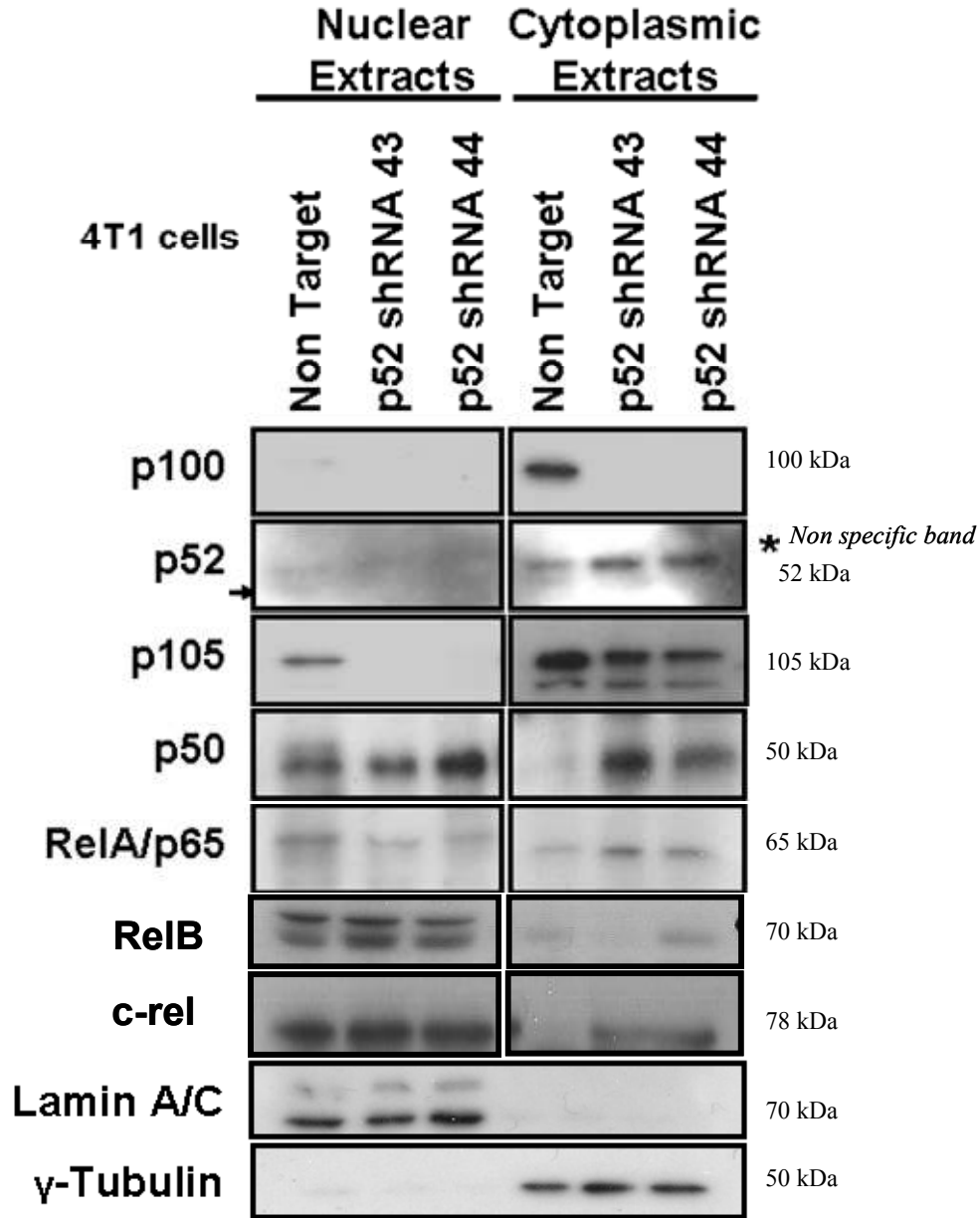


**Figure 4.2: Silencing of *Nfkb2* in 4T1 cells is associated with an increase in nuclear and cytoplasmic p50 levels.** Nuclear and cytoplasmic extracts from 4T1 cells transduced with non target (NT) and shRNA against *Nfkb2* (p52 shRNA 43&44) were harvested and separated by SDS-PAGE. Western blot shows levels of p100, p52, p105, p50, RelA, RelB and c-rel. Lamin A/C and  $\gamma$ -tubulin were used as loading controls for nuclear and cytoplasmic extracts respectively in these cell lines. \* indicates non specific band. Arrow indicates p52 band.

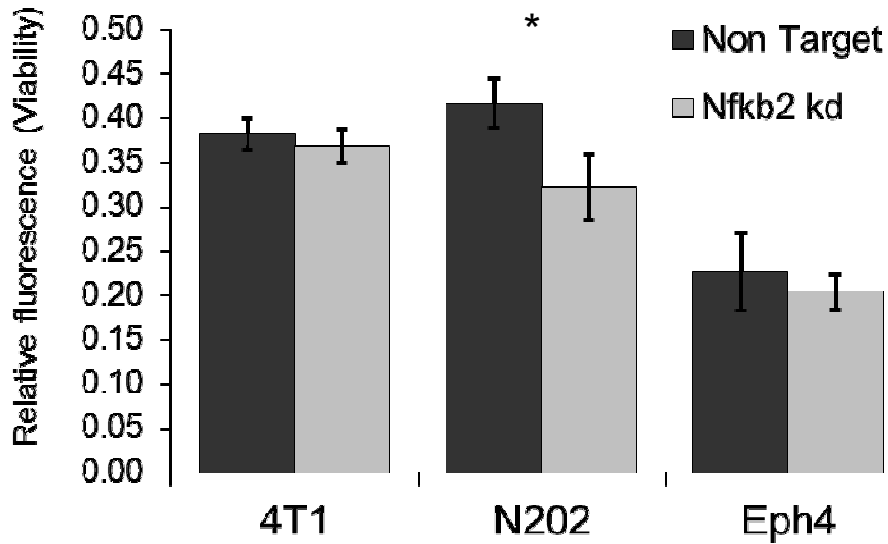


**Figure 4.3: Silencing of *Nfkb2* sensitizes N202.1A cells to anoikis *in vitro*.** 4T1, N202.1A and EPH4 cell lines transduced with non target (NT) and shRNA against *Nfkb2* were plated under non-adherent culture conditions and the viability of these cells were measured after 24 hours. Bar charts show viability of cells determined by *Cell Titer Blue* assay, plotted as relative fluorescence in the respective cell lines. Data points represent average of at least n=6 and error bars indicate standard error of the mean (SEM). \* indicates  $p < 0.05$ , where statistical significance relative to non target controls were determined by two-tailed t-test.

activity in both 4T1 *Nfkb2* kd and EPH4 *Nfkb2* kd cell lines (Figure 4.1). On the other hand, N202.1A cells displayed a marginal decrease (~10%) in cell viability upon depletion of p100/p52. This suggests that p100/p52 does contribute to the survival of N202.1A cells under non-adherent culture conditions.

#### ***4.2.4 Silencing of *Nfkb2* does not affect the proliferation of mouse mammary cancer cell lines***

As p52 has been shown to be able to regulate the expression of Cyclin D1 and proliferation (Cao et al., 2001a, Rocha et al., 2003), we then examined the effects of *Nfkb2* knockdown on the proliferative potential of mammary cell lines. Despite the association between p52 and proliferation in previous studies, we did not observe any effects on the growth rate of cells (Figure 4.4). In the case of the tumourigenic cell lines, 4T1 and N202.1A, the fact that no change in proliferation was observed would suggest that p100/p52 is not the main driving stimulus which promotes cell division in these cells. This is not surprising as many other oncogenes such as c-Myc could induce cell cycle progression. Similarly with EPH4 cells, the results would indicate that p100/p52 is not crucial in regulating the rate of cell division in these non-tumourigenic cells.

#### ***4.2.5 Silencing of *Nfkb2* does not affect the colony forming potential of mouse mammary cancer cell lines***

In order to assess whether the loss of p100/ p52 has any effects on the proportion of cells capable of extensive replication, we performed a colony forming assay on NT and *Nfkb2* kd cells of 4T1, N202.1A and EPH4 lineage respectively. No significant differences in the colony forming efficiency were observed between NT controls and *Nfkb2* kd cells for all three cell lines (figure 4.5). Hence, p100/p52 depletion does not affect the replicative potential of tumourigenic and non-tumourigenic mammary cell lines.

#### ***4.2.6 Silencing of *Nfkb2* increases the motility of 4T1 cells***

Another important feature for cancer cells to metastasize is the ability to be motile and invade into surrounding tissues. We addressed the role of p100/p52 in the regulation of these phenotypes *in vitro* through transwell migration assays. The loss of p100/p52 increased the motility of 4T1 cells but had no effect on N202.1A and EPH4

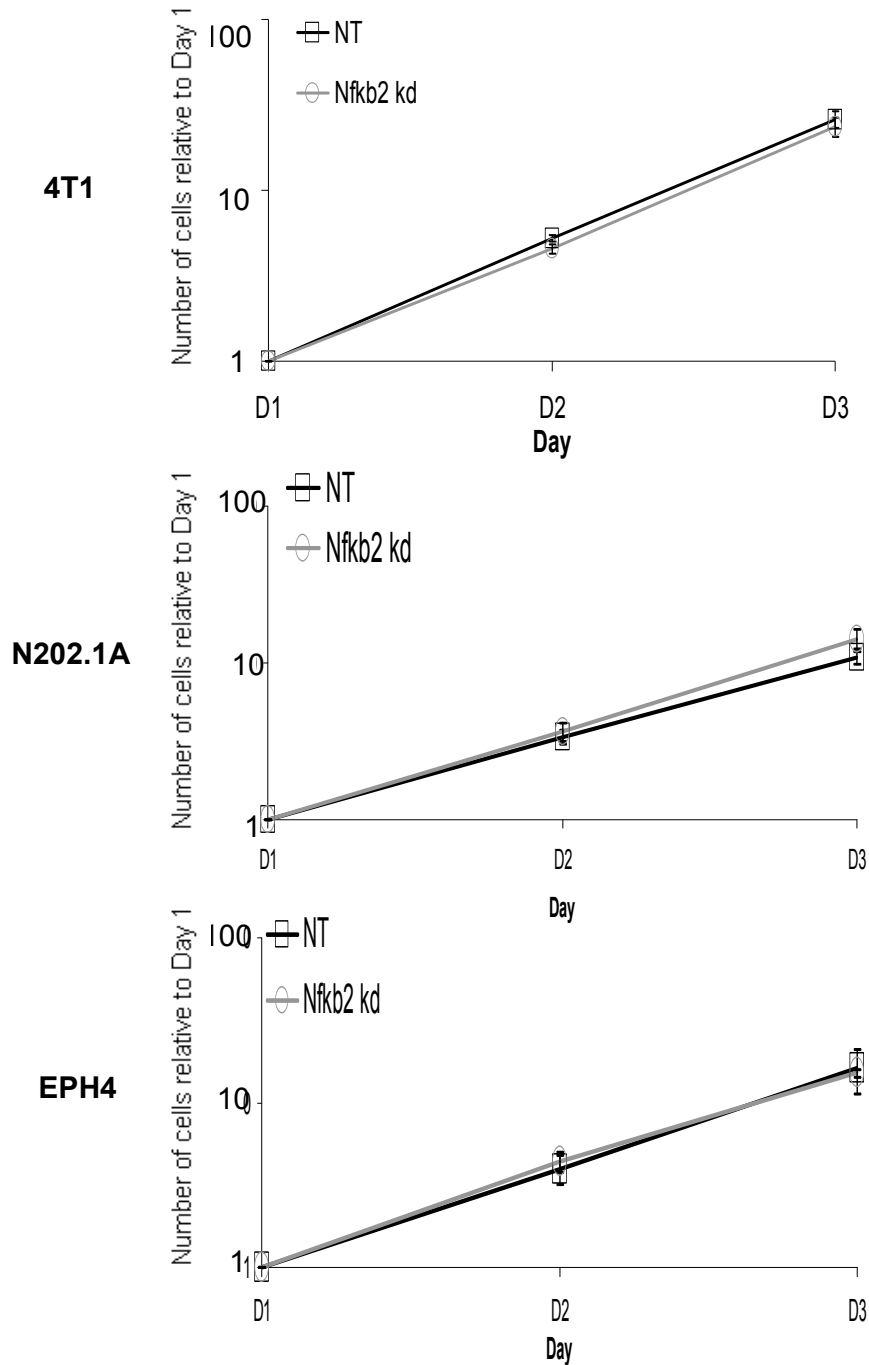


**Figure 4.4: Silencing of *Nfkb2* does not affect proliferation of 4T1, N202.1A and EPH4 cells.** 4T1, N202.1A and EPH4 cell lines transduced with non target (NT) and shRNA against *Nfkb2* were plated in 6-well plates. At respective timepoints, the number of cells in each well was counted with the aid of a haemo-cytometer. Line graphs showing cell counts relative to day 1 plotted on a log scale against time in days. Data points represent average of at least n=6 and error bars indicate standard error of the mean (SEM).

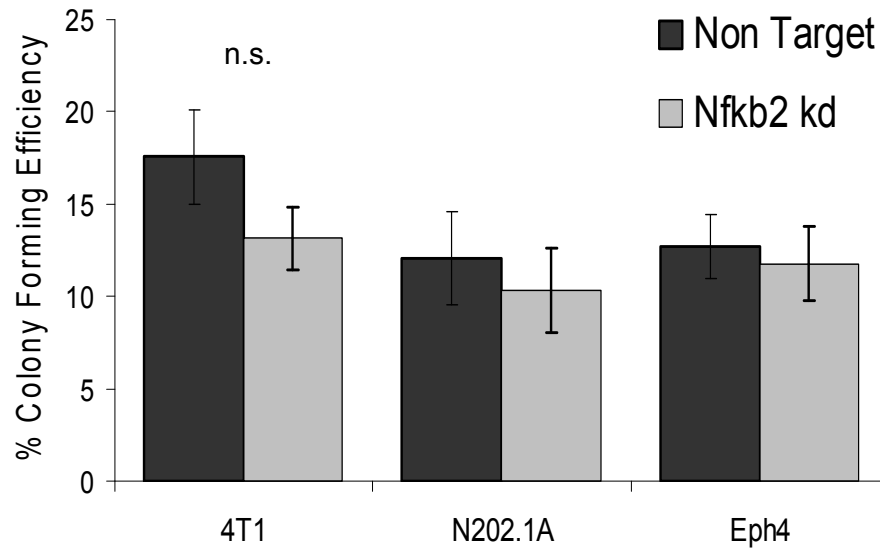


**Figure 4.5: Silencing of *Nfkb2* does not affect the colony forming potential of mammary cell lines.** 4T1, N202.1A and EPH4 cell lines transduced with non target (NT) and shRNA against *Nfkb2* were plated in 6-well plates at a density of 1000 cells per well. The number of colonies formed after 7 days were counted. Bar charts show the % colony forming efficiency, which is a percentage of the number of colonies formed per cells seeded. Data points represent average of at least  $n=6$  and error bars indicate standard error of the mean (SEM). N.S. indicates a non significant difference, where statistical significance relative to non target controls were determined by two-tailed t-test.

cells (Figure 4.6a). As the increase in motility in 4T1 cells correlates with an increase in basal NF- $\kappa$ B activity when *Nfkb2* is silenced (Figure 4.1), there is a possibility that NF- $\kappa$ B activity regulates the motility of these cells. Although an increase in basal-NF- $\kappa$ B activity was also observed in EPH4 cells, our results do not show a change in the motility of these cells upon *Nfkb2* knockdown. This would suggest that elevated NF- $\kappa$ B activity in a tumourigenic setting can promote motility, possibly in cooperation with other oncogenic stimulus but not in non-tumourigenic cells.

In addition, we also investigated the invasive ability of 4T1 and N202.1A cell lines through trans-well invasion assays. However, no significant differences were observed when *Nfkb2* was silenced in both cell lines (Figure 4.6b). Thus, perturbation of p100/p52 levels does not affect the invasive ability of 4T1 and N202.1A cells.

#### 4.2.7 Loss of *Nfkb2* leads to EMT in 4T1 cells

We went on to elucidate the possible mechanisms responsible for the increased motility in 4T1 cells (Figure 4.5a) upon *Nfkb2* silencing. Since we observed an increase in basal NF- $\kappa$ B activity in 4T1 *Nfkb2* kd cells (Figure 4.1) and NF- $\kappa$ B is known to be able to induce epithelial to mesenchymal transition (EMT) (Huber et al., 2004b), we wanted to determine whether EMT was induced in 4T1 *Nfkb2* kd cells. The levels of EMT-inducing transcription factors between 4T1 NT and 4T1 *Nfkb2* kd cells were compared by quantitative RT-PCR (Figure 4.7a) and we found a 1.6 fold increase in *Zeb2*. Accordingly, we observed a decrease in levels of E-cadherin and an increase in levels of N-cadherin relative to NT controls, which is characteristic of the EMT process. When we probed the levels of E-cadherin and vimentin proteins (Figure 4.7b), we observed diminished levels of E-cadherin which supports the quantitative RT-PCR data but no changes in the levels of vimentin was observed. It is possible that not all mesenchymal markers show increased expression upon EMT, since only N-cadherin expression was increased upon *Nfkb2* silencing.

#### 4.2.8 The motility of 4T1 cells is dependent on NF- $\kappa$ B activity

As we have now established an association between increased NF- $\kappa$ B activity, induction of EMT and increased motility in 4T1 cells when the *Nfkb2* gene is silenced, we then addressed whether the motile phenotypes observed were dependent on canonical NF- $\kappa$ B signalling. For that, we inhibited I $\kappa$ B $\alpha$  phosphorylation and its

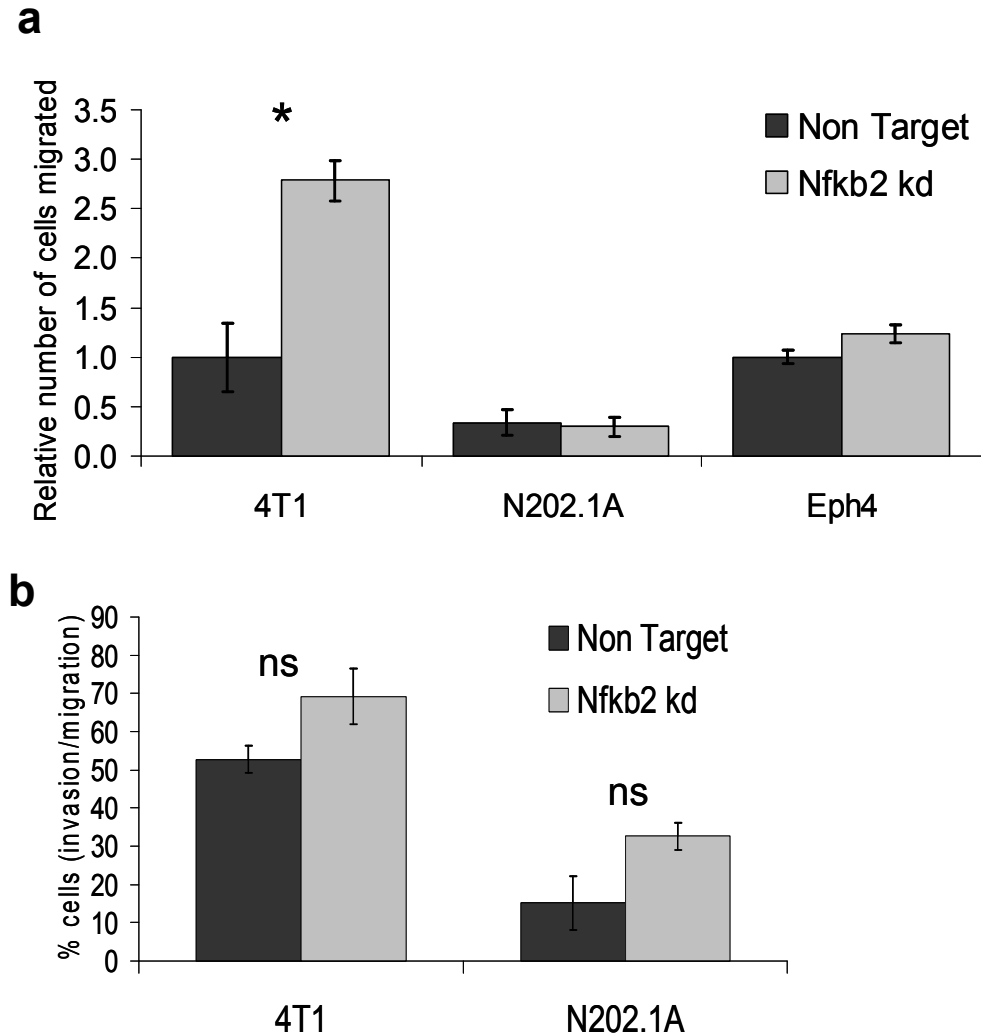


**Figure 4.6: Silencing of *Nfkb2* increases the motility of 4T1 cells. (a) Boyden motility assays.** 4T1, N202.1A and EPH4 cell lines transduced with non target (NT) and shRNA against *Nfkb2* were plated in Boyden trans-well migration chambers and migration was induced via a serum gradient. The cells that have migrated to the underside of the membrane were then stained and counted. Bar charts show the relative number of cells migrated (normalized to 4T1 NT). Data points represent average of at least n=6 and error bars indicate standard error of the mean (SEM). **(b) Boyden invasion assays.** 4T1 and N202.1A cell lines transduced with non target (NT) and shRNA against *Nfkb2* were plated in Boyden trans-well migration chambers coated with a layer of Matrigel and invasion was induced via a serum gradient. Bar charts show the percentage of cells invaded normalized against the number of cells migrated without Matrigel. \* indicates  $p < 0.05$ , n.s. indicates not significant, where statistical significance relative to non target controls were determined by two-tailed t-test.

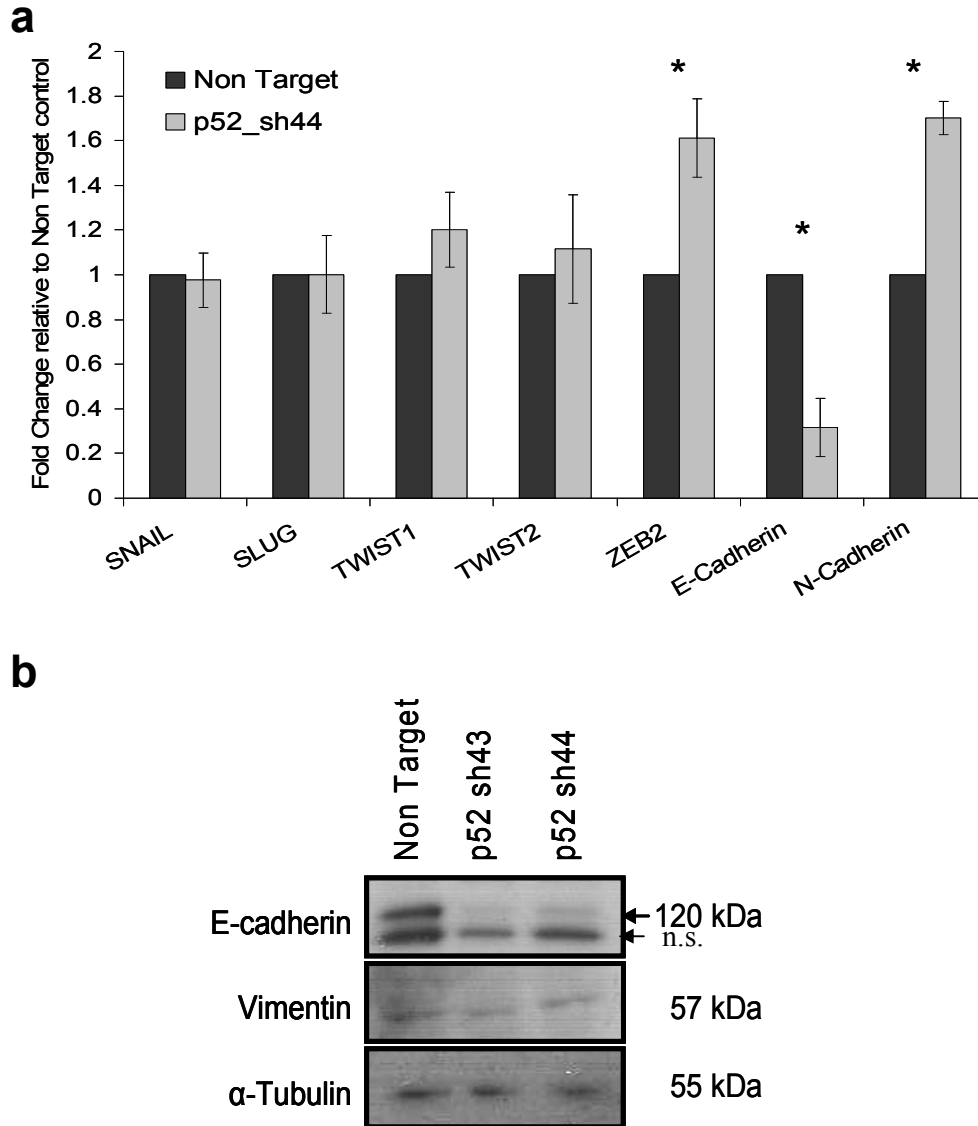


**Figure 4.7: Silencing of *Nfkb2* induces EMT in 4T1 cells.** (a) mRNA from 4T1 NT and 4T1 *Nfkb2* kd cells were harvested and purified. cDNA was synthesized from respective cell lines and the levels of EMT inducing transcription factors; Snail, Slug, Twist1, Twist2, Zeb2 and markers for EMT; E-cadherin and N-cadherin were quantified by qRT-PCR. Bar charts show the relative levels of transcripts normalized against NT controls using the  $\Delta\Delta CT$  method. Data points represent average of at least  $n=6$  and error bars indicate standard error of the mean (SEM). \* indicates  $p<0.05$ , where statistical significance relative to non target controls were determined by two-tailed t-test.

(b) Protein lysates from 4T1 NT and 4T1 cells transduced with shRNA against *Nfkb2* (p52 sh43& p52 sh44) were harvested and separated by SDS-PAGE. The levels of E-cadherin and vimentin in these cell lines were then quantified by immune-blotting.

degradation using a pharmacological inhibitor BAY 11-7082. In order to ensure that the viability of cells was not a contributing factor in subsequent assays, we assessed the effects of BAY 11-7082 at varying concentrations on the survival of 4T1 and N202.1A cells. We found that concentrations of up to 1 $\mu$ M did not affect the viabilities of both 4T1 and N202.1A cell lines that were transduced with NT or shRNA against *Nfkb2* (Figure 4.8a). At 5 $\mu$ M, although N202.1A cells were not severely affected, 4T1 cells were displaying decreased viabilities. Hence, the BAY 11-7082 inhibitor was utilized at 1 $\mu$ M for subsequent experiments. The efficacy of the inhibitor at this concentration range was also verified by monitoring levels of I $\kappa$ B $\alpha$  in 4T1 cells. When 4T1 cells were treated with TNF- $\alpha$ , the levels of I $\kappa$ B $\alpha$  was significantly reduced and in the presence of 0.1 $\mu$ M BAY 11-7082, this reduction can be decreased (Figure 4.8b).

In the case of 4T1 cells, transwell migration assays with the presence of BAY 11-7082 revealed that the inherent motility of 4T1 NT cells was largely dependent on NF- $\kappa$ B activity, where a 5-fold decrease in number of cells migrated was observed for BAY 11-7082 treated cells (Figure 4.8c). For 4T1 *Nfkb2* kd cells, the increased motility relative to NT controls was also dependent on NF- $\kappa$ B activity as the motility of these cells was diminished by BAY 11-7082, to a level that was similar to 4T1 NT cells in the presence of BAY 11-7082. This demonstrates that the increase in motility observed in 4T1 cells when *Nfkb2* is silenced is dependent on the increase in basal NF- $\kappa$ B activity in these cells and most likely occurs through the induction of EMT. Although we observed a similar trend for N202.1A cells, these changes were not significant (Figure 4.8d). This is likely due to the fact that the differences observed were within the magnitude of the error and could be addressed by optimization of experimental parameters.

#### **4.2.9 *The mammosphere forming potential of mammary cancer cell lines correlates with the changes in NF- $\kappa$ B activity after *Nfkb2* silencing***

According to the cancer stem cell hypothesis, only a sub-population of CaSCs have the ability to seed new tumours and form metastases. In order to determine whether p100/p52 has a role in governing the properties of CaSCs, we assessed the tumour initiating properties of mammary cancer cell lines by mammosphere assays. This *in vitro* surrogate assay allows the self-renewal potential of cancer cells to be

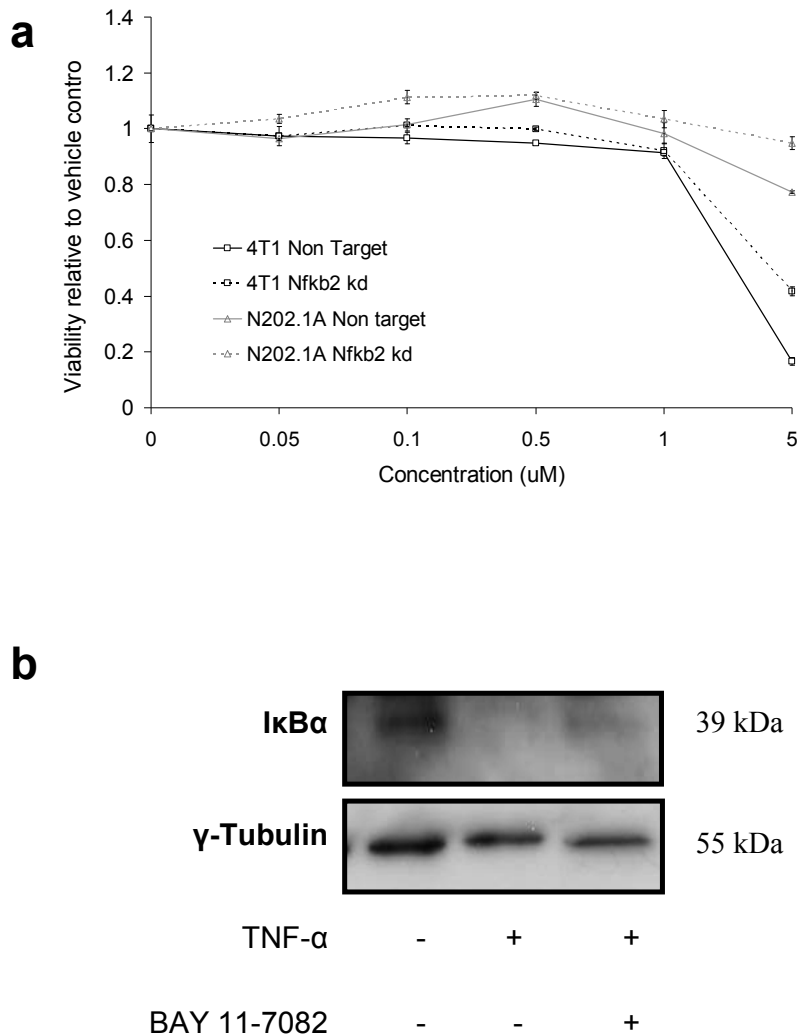


**Figure 4.8: The increase in motility in 4T1 cells upon *Nfkb2* silencing is dependent on NF- $\kappa$ B activity. (a)** 4T1 and N202.1A cells transduced with NT and shRNA against *Nfkb2* were treated with varying concentrations of BAY 11-7082 for 24 hours and the viability of these cells were then determined by *Cell Titer Blue* assay. Line graphs show dose response curves of 4T1 and N202.1A cell lines after BAY 11-7082 treatment. Data points represent average of at least  $n=6$  and error bars indicate standard error of the mean (SEM). **(b)** Protein lysates from 4T1 cells, 4T1 cells treated with 10ng/ml of TNF- $\alpha$  and 4T1 cells treated with 10ng/ml TNF- $\alpha$  + 0.1 $\mu$ M BAY 11-7082 were harvested and separated by SDS-PAGE. The levels of I $\kappa$ B $\alpha$  in these cell lines were then probed by immune-blotting.

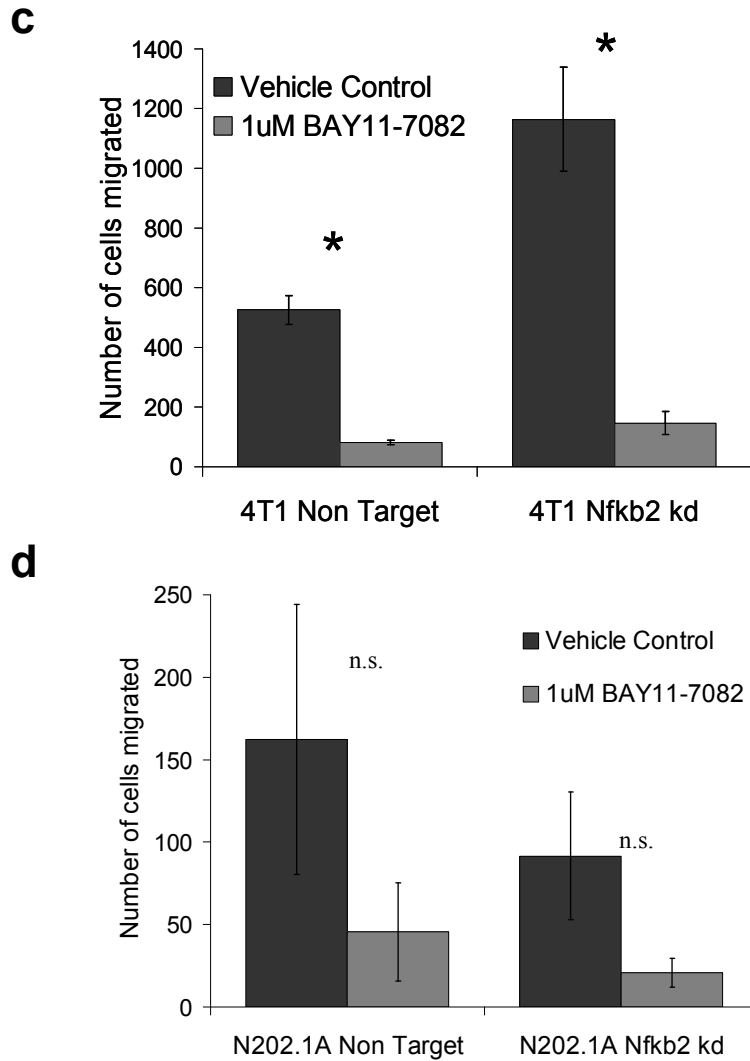


**Figure 4.8: (Continued) The increase in motility in 4T1 cells upon *Nfkb2* silencing is dependent on NF- $\kappa$ B activity.** (c) 4T1 NT and 4T1 Nfkb2 kd cells were plated in Boyden trans-well migration chambers in the presence or absence of 1uM BAY 11-7082 and migration was induced via a serum gradient. The cells that have migrated to the underside of the membrane were then stained and counted. Bar charts show the number of cells migrated. Data points represent average of at least  $n=6$  and error bars indicate standard error of the mean (SEM). (b) N202.1A NT and N202.1A Nfkb2 kd cells were plated in Boyden trans-well migration chambers in the presence or absence of 1uM BAY 11-7082 and migration was induced via a serum gradient. The number of cells that have migrated to the underside of the membrane was then stained and counted. Bar charts show the number of cells migrated. Data points represent average of at least  $n=6$  and error bars indicate standard error of the mean (SEM). \* indicates  $p<0.05$ , n.s. indicates not significant, where statistical significance relative to non target controls were determined by two-tailed t-test.

evaluated. In the first passage (P1), we did not observe any significant differences in the percentage of mammosphere forming units (MFUs) between NT and *Nfkb2* kd cell lines of 4T1, N202.1A and EPH4 lineage respectively (Figure 4.9a). However, in the second passage (P2), there was a two fold increase in % MFUs when *Nfkb2* was silenced in 4T1 cells (Figure 4.9b). Contrastingly for N202.1A cells, a significant decrease in % MFUs was observed when *Nfkb2* was silenced. Importantly, these changes in mammosphere forming ability of both 4T1 and N202.1A cells respectively when *Nfkb2* is silenced, implicates for the first time the involvement of p100/p52 in regulation of CaSC properties. The lack of correlation between P1 and P2 can be explained by the fact that in P1, the assay predominantly selects for cells which have the ability to survive anoikis without a strong selection pressure for self-renewing ability. When the spheres were dissociated and re-plated in P2, the self-renewal potential of CaSCs become more evident as cells without extensive replicative potential will no longer be able to form mammospheres. As for the normal EPH4 cell line, these cells have a low mammosphere forming efficiency and no difference was observed when p100/p52 is lost. Yet again, this would suggest that interfering with NF- $\kappa$ B activity through silencing of *Nfkb2* only affects tumourigenic cell lines. This could be due to a need for NF- $\kappa$ B co-operating in the context of other oncogenic signalling pathways.

The average sizes of spheres formed in these cell lines upon *Nfkb2* silencing exhibit a similar trend as that of their mammosphere forming potential (Figures 4.9 c&d). Since we do not observe a change in the rate of proliferation of all three cell lines when p100/p52 is depleted (Section 4.2.4), this would suggest that the differences in size of mammospheres can be attributed to the self-renewal ability of CaSCs. In other words, cells which can go through more cell divisions without entering senescence will form larger spheres. Taken together, the mammosphere forming efficiency and average sizes of spheres formed in 4T1 and N202.1A cells upon *Nfkb2* silencing correspond to the changes in basal NF- $\kappa$ B activity of the respective cell lines (Figure 4.1b), suggesting a dependence of these phenotypes on NF- $\kappa$ B activity.

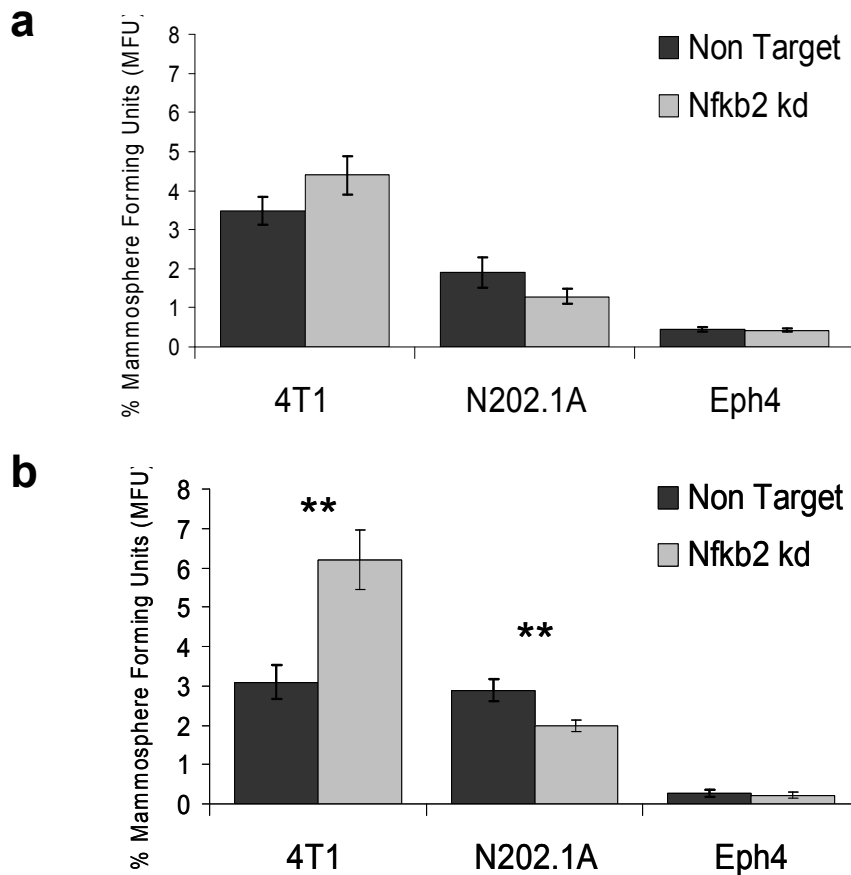


**Figure 4.9: Effects of silencing *Nfkb2* on mammosphere forming potential of mammary cell lines.** (a) 4T1, N202.1A and EPH4 cell lines transduced with non target (NT) and shRNA against *Nfkb2* were plated in non-adherent culture plates with mammosphere media and the number of spheres formed after 7 days were counted. Bar charts show % mammosphere forming units (MFUs) calculated as the number of spheres per cells seeded. (b) The spheres formed by respective cell lines in the first passage (P1) were dissociated and re-seeded at an equal density (P2) under non-adherent culture conditions in mammosphere media. Bar charts show % MFUs. Data points represent average of at least n=6 and error bars indicate standard error of the mean (SEM). \*\* indicates p<0.01, n.s. indicates not significant, where statistical significance relative to non target controls were determined by two-tailed t-test.

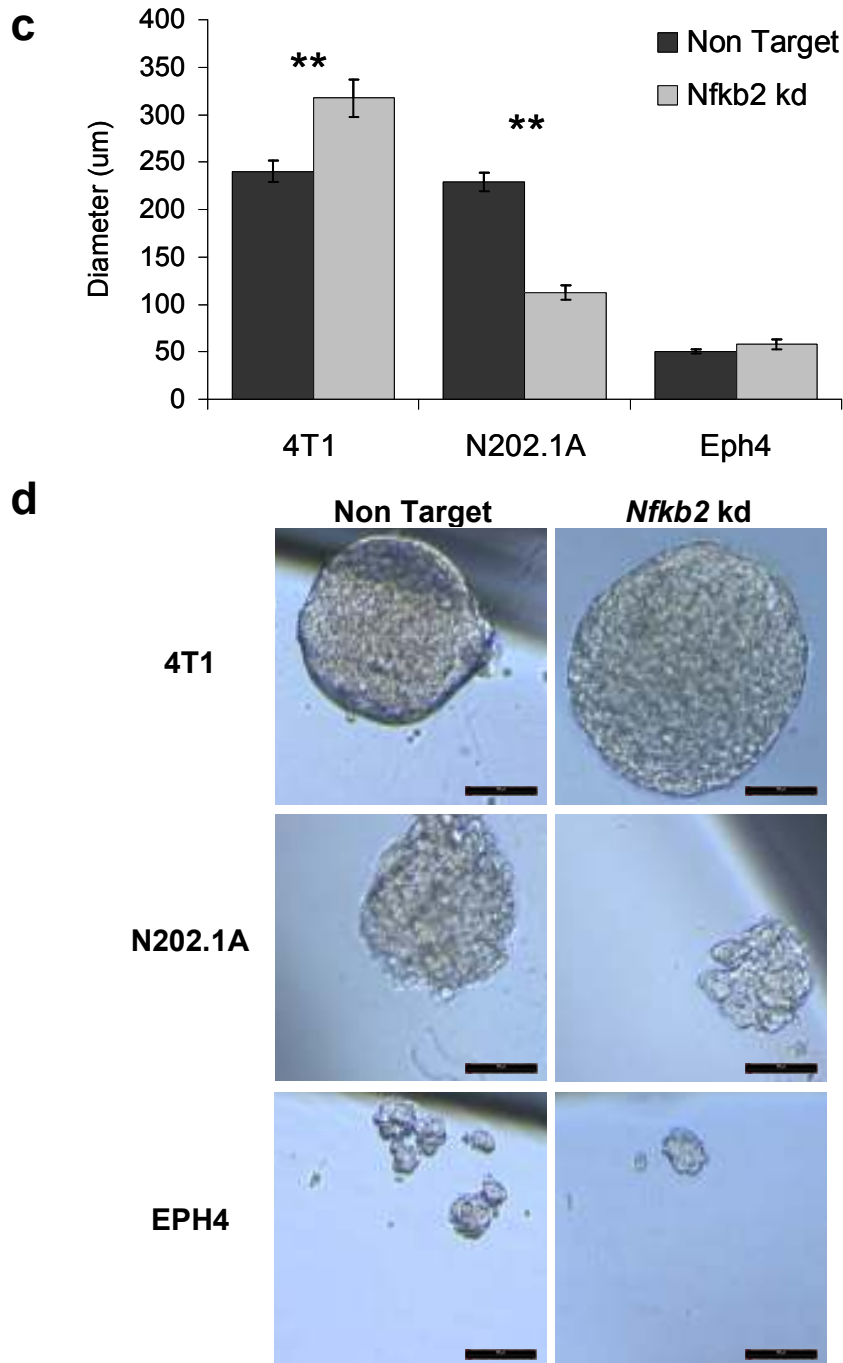


**Figure 4.9: (continued) Effects of silencing *Nfkb2* on mammosphere forming potential of mammary cell lines. (c)** 4T1, N202.1A and EPH4 cell lines transduced with non target (NT) and shRNA against *Nfkb2* were plated in non-adherent culture plates with mammosphere media and the sizes of spheres formed after 7 days were measured using ImageJ. Bar charts show diameter of mammospheres in um. Data points represent average of at least n=10 and error bars indicate standard error of the mean (SEM). \*\* indicates  $p < 0.01$ , where statistical significance relative to non target controls were determined by two-tailed t-test. **(d)** Representative images of the size of spheres formed by 4T1, N202.1A and EPH4 mammospheres transduced with NT and shRNA against *Nfkb2* kd. Scale bar represents 100um.

#### **4.2.10 The mammosphere forming potential of mammary cancer cell lines are dependent on NF- $\kappa$ B activity**

Accordingly, we then went on to determine whether NF- $\kappa$ B activity is a requirement for maintaining self-renewal properties in mammary cancer cells. In P1 experiments, inhibition of NF- $\kappa$ B by BAY 11-7082 resulted in significant decreases in mammosphere forming potentials for 4T1 NT and *Nfkb2* kd cells (Figure 4.10a). In P2, the mammosphere forming potential of 4T1 cells were completely abolished in the presence of BAY 11-7082 (Figure 4.10b). Similarly for N202.1A cells, the numbers of MFUs were decreased in P1 (Figure 4.10c) and almost completely depleted in P2 in the presence of BAY 11-7082 (Figure 4.10d). These experiments show that the mammosphere forming potential of tumorigenic 4T1 and N202.1A cells were dependent on NF- $\kappa$ B activity.

#### **4.2.11 Over-expression of p52 rescues the decrease in mammosphere forming potential of N202.1a cells but not the increase in motility and mammosphere forming potential of 4T1 cells after *Nfkb2* silencing**

Although silencing the *Nfkb2* gene in mammary cancer cell lines have shown some interesting changes with regards to the motility (Section 4.2.6) and mammosphere forming potential (Section 4.2.9) of 4T1 and N202.1A cells, we were not able to distinguish the specific effects of losing p100 or p52 respectively. This distinction is important as both these gene products of *Nfkb2* play opposing roles in the NF- $\kappa$ B pathway. For that reason, we went on to elucidate whether over-expression of the p52 subunit can rescue the phenotypes observed. In 4T1 cells, the increased motility upon *Nfkb2* knockdown was not changed despite p52 being re-expressed in the *Nfkb2* kd cell line (figure 4.11a). This would indicate that the increase in motility is due to the loss of p100 and not p52. However, over-expression of p52 in the *Nfkb2* kd cell line did not increase the motility of these cells further. This could be due to the cells reaching an upper limit of their migration capacity. In the case of the mammosphere forming potential of 4T1 cells, the increase in MFUs which results from *Nfkb2* knockdown is not rescued when p52 is over-expressed (Figure 4.11b), implicating the loss of p100 as a possible cointributing factor in this observation. This would agree with the increased basal NF- $\kappa$ B activity observed in 4T1 *Nfkb2* kd cells relative to NT controls (Section 4.2.1), since p100 is an I $\kappa$ B $\alpha$  protein with negative regulatory functions in this pathway.

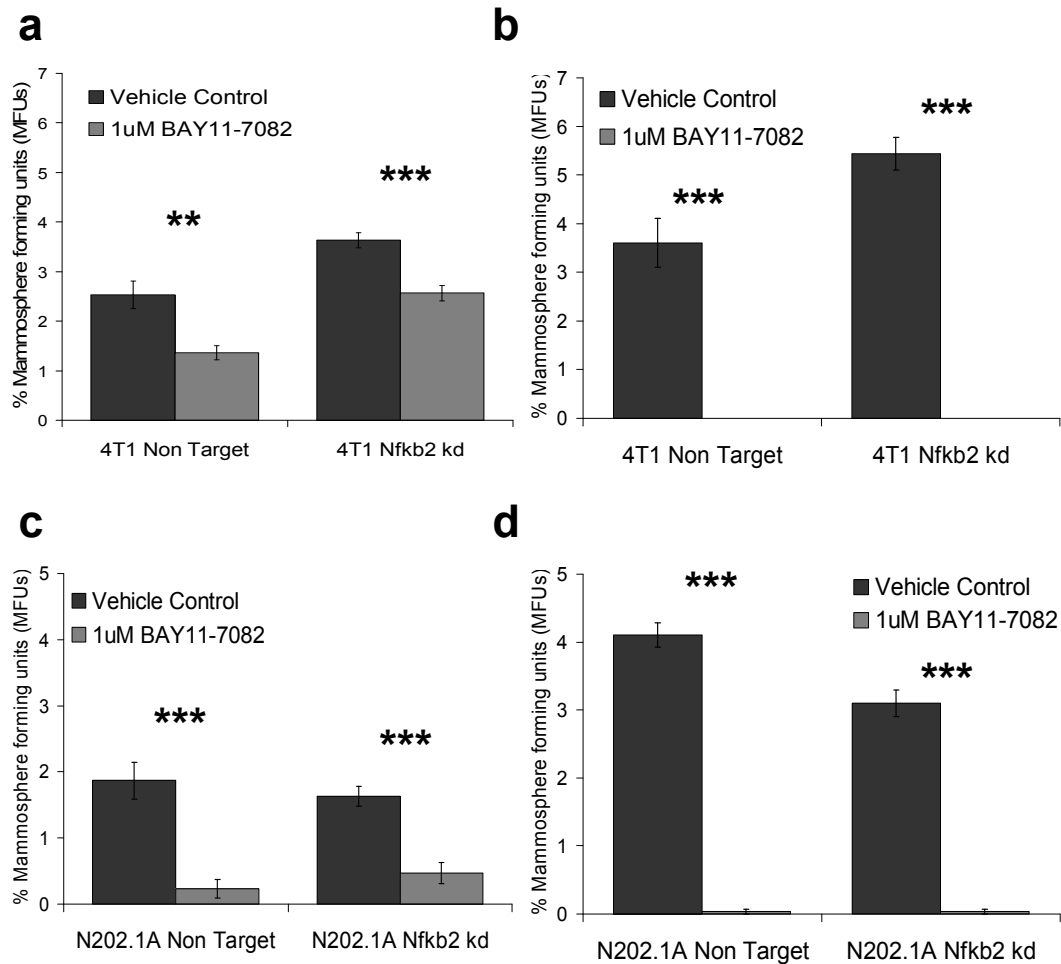


**Figure 4.10: The mammosphere forming potential of 4T1 and N202.1A cells are dependent on NF- $\kappa$ B activity.** (a) 4T1 cell lines transduced with non target (NT) and shRNA against *Nfkb2* were plated in non-adherent culture plates with mammosphere media and the number of spheres formed in the presence or absence of BAY 11-7082 after 7 days were counted. (b) The spheres formed by respective 4T1 cell lines in the first passage (P1) were dissociated and re-seeded at an equal density (P2) under non-adherent culture conditions in mammosphere media. (c) N202.1A cell lines transduced with non target (NT) and shRNA against *Nfkb2* were plated in non-adherent culture plates with mammosphere media and the number of spheres formed in the presence or absence of BAY 11-7082 after 7 days were counted. (d) The spheres formed by respective N202.1A cell lines in the first passage (P1) were dissociated and re-seeded at an equal density (P2) under non-adherent culture conditions in mammosphere media. Bar charts show % MFUs. Data points represent average of at least n=6 and error bars indicate standard error of the mean (SEM). \*\*\* indicates  $p < 0.001$ , \*\* indicates  $p < 0.01$ , where statistical significance relative to non target controls were determined by two-tailed t-test.

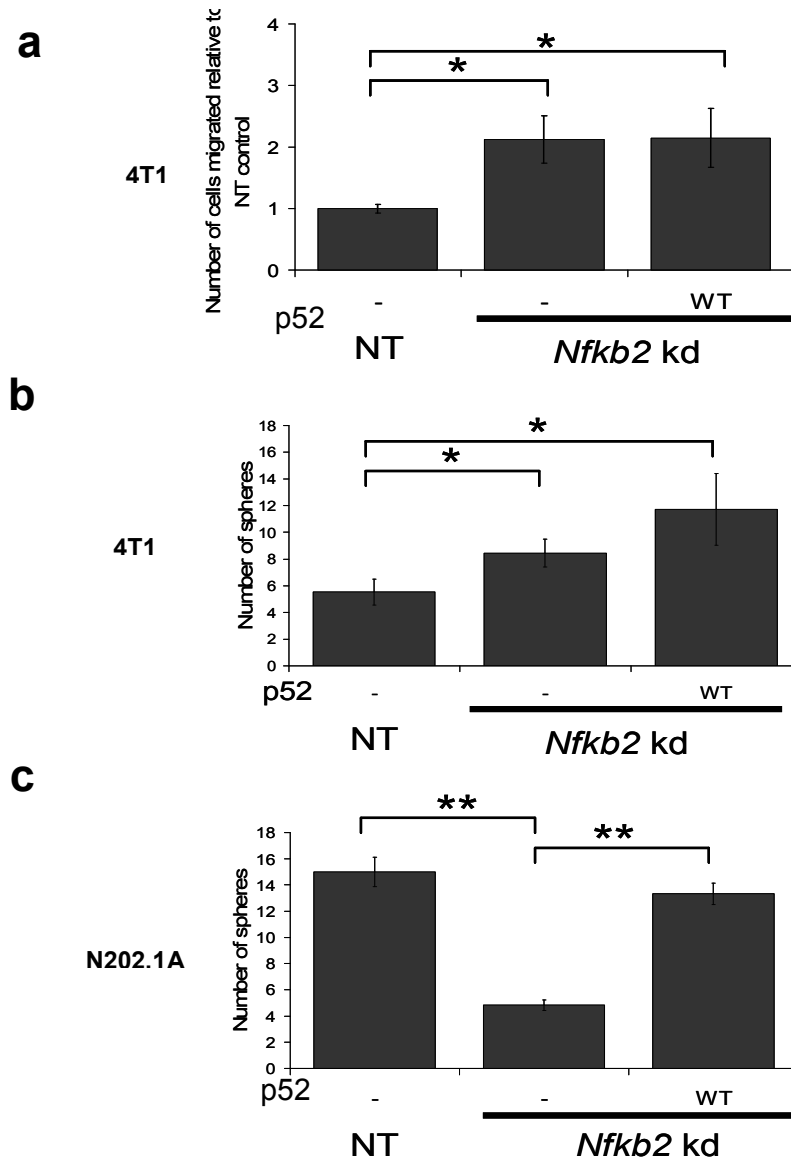


**Figure 4.11: Rescue experiments by over-expression of p52.** (a) 4T1 cells transduced with non target (NT) shRNA, shRNA against *Nfkb2* and shRNA against *Nfkb2* with p52 over-expression were plated in Boyden trans-well migration chambers and migration was induced by a serum gradient. The number of cells which have migrated to the underside of the membrane were then stained and counted. Bar charts show number of cells migrated normalized against NT control. (b) 4T1 cells transduced with non target (NT) shRNA, shRNA against *Nfkb2* and shRNA against *Nfkb2* with p52 over-expression were plated in non-adherent culture plates with mammosphere media and the number of spheres formed after 7 days in passage 2 was counted. Bar charts show the number of spheres formed. (c) N202.1A cells transduced with non target (NT) shRNA, shRNA against *Nfkb2* and shRNA against *Nfkb2* with p52 over-expression were plated in non-adherent culture plates with mammosphere media and the number of spheres formed after 7 days in passage 2 were counted. Bar charts show the number of spheres formed. Data points represent average of at least n=6 and error bars indicate standard error of the mean (SEM). \* indicates  $p < 0.05$ , where statistical significance relative to non target controls were determined by two-tailed t-test.

For N202.1A cells, silencing of *Nfkb2* resulted in decreased basal NF- $\kappa$ B activity (Section 4.2.1) which is accompanied by decreased survival under anoikis conditions (Section 4.2.3) and mammosphere forming potential (Section 4.2.9). To address whether the decrease in MFUs upon silencing of *Nfkb2* was mediated by p52, over-expression of p52 in N202.1A cells depleted of p100/p52 rescued the decrease in mammosphere forming potential to a level that is comparable with NT controls (Figure 4.11c). Hence, this demonstrates for the first time in mammary cancer cells, a role for the p52 subunit in regulation of CaSC properties. These experiments could be complemented by non-processable p100 over-expression (Maruyama et al., 2010) to elucidate the specific phenotypes which are dependent on the I $\kappa$ B $\alpha$  protein. From the current results, it appears that the differential effects observed between 4T1 and N202.1A cell lines could be due to the p100 and p52 subunits having more dominant effects respectively in each of the cell lines.

#### 4.2.12 Loss of *Nfkb2* enhances 4T1 tumour growth *in vivo*

From previous *in vitro* experiments, 4T1 cells exhibited more aggressive phenotypes when p100/p52 was depleted. Thus, we wanted to address whether these features would be recapitulated *in vivo*. When 4T1 NT and *Nfkb2* kd cells were transplanted orthotopically into syngeneic hosts, we found that 4T1 *Nfkb2* kd cells had enhanced growth kinetics (Figure 4.12a). Significant differences in the size of tumours between NT and *Nfkb2* kd cohorts were evident by day-13 post-transplant and this difference was further amplified by day-27 post-transplant. When the histology of respective tumours were examined, no difference in the morphology of cells between the different cohorts can be observed (Figure 4.12b). Nonetheless, immuno-staining for p100/p52 illustrated that these proteins were not detectable in *Nfkb2* kd tumours, proving that *Nfkb2* silencing is maintained within these cells for weeks *in vivo*.

Although 4T1 *Nfkb2* kd tumours were growing relatively faster than 4T1 NT tumours, we did not observe any differences in neither the proliferation nor the number of apoptotic cells between the two cohorts, as shown by Ki67 and cleaved caspase-3 immuno-staining respectively (Figures 4.13 a-c). Analysis of the gradients of respective graphs also suggests no difference in the rate of change in size at selected time intervals (Figure 4.12a). Similarly *in vitro*, we did not observe a difference in proliferation rates of 4T1 cells when *Nfkb2* is knocked down (Section

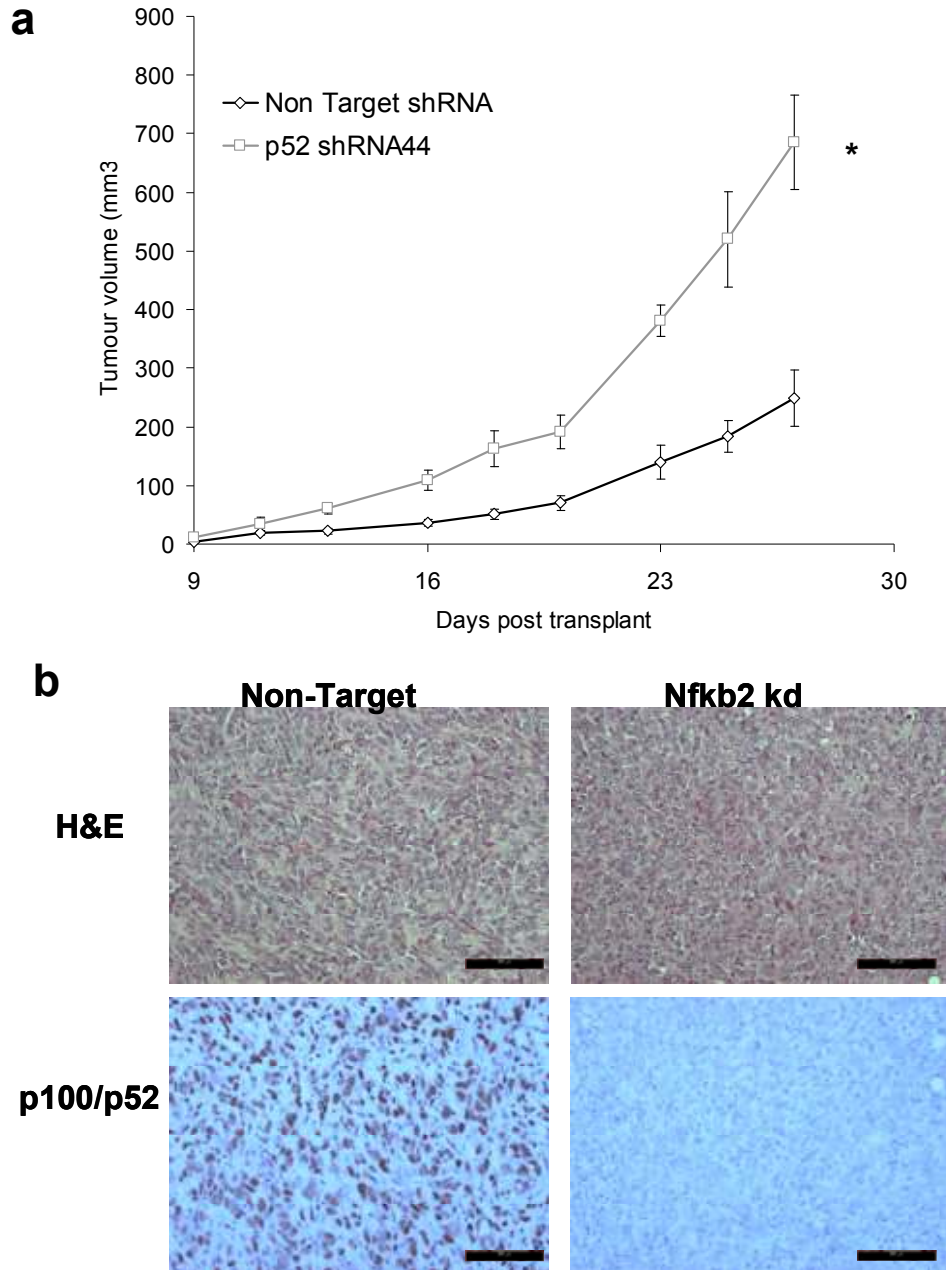


**Figure 4.12: Loss of *Nfkb2* enhances 4T1 tumour growth *in vivo*.** (a) 10,000 4T1 Non Target or *Nfkb2* kd cells were transplanted into the right mammary fat pads of Balb/C mice respectively. The resulting tumours were measured and the growth kinetics plotted as line graphs. Data points represent averages from  $n=5$  animals per cohort and error bars represent standard error of the mean. \* indicates  $p<0.05$ , where statistical significance between growth curves was determined by ANCOVA test;  $F=8.370$ ,  $p=0.018$ . (b) Representative images from 4T1 NT and *Nfkb2* kd tumours stained with haematoxylin and eosin or immuno-labelled with antibody against p100/p52. Scale bar represents 100 $\mu$ m.

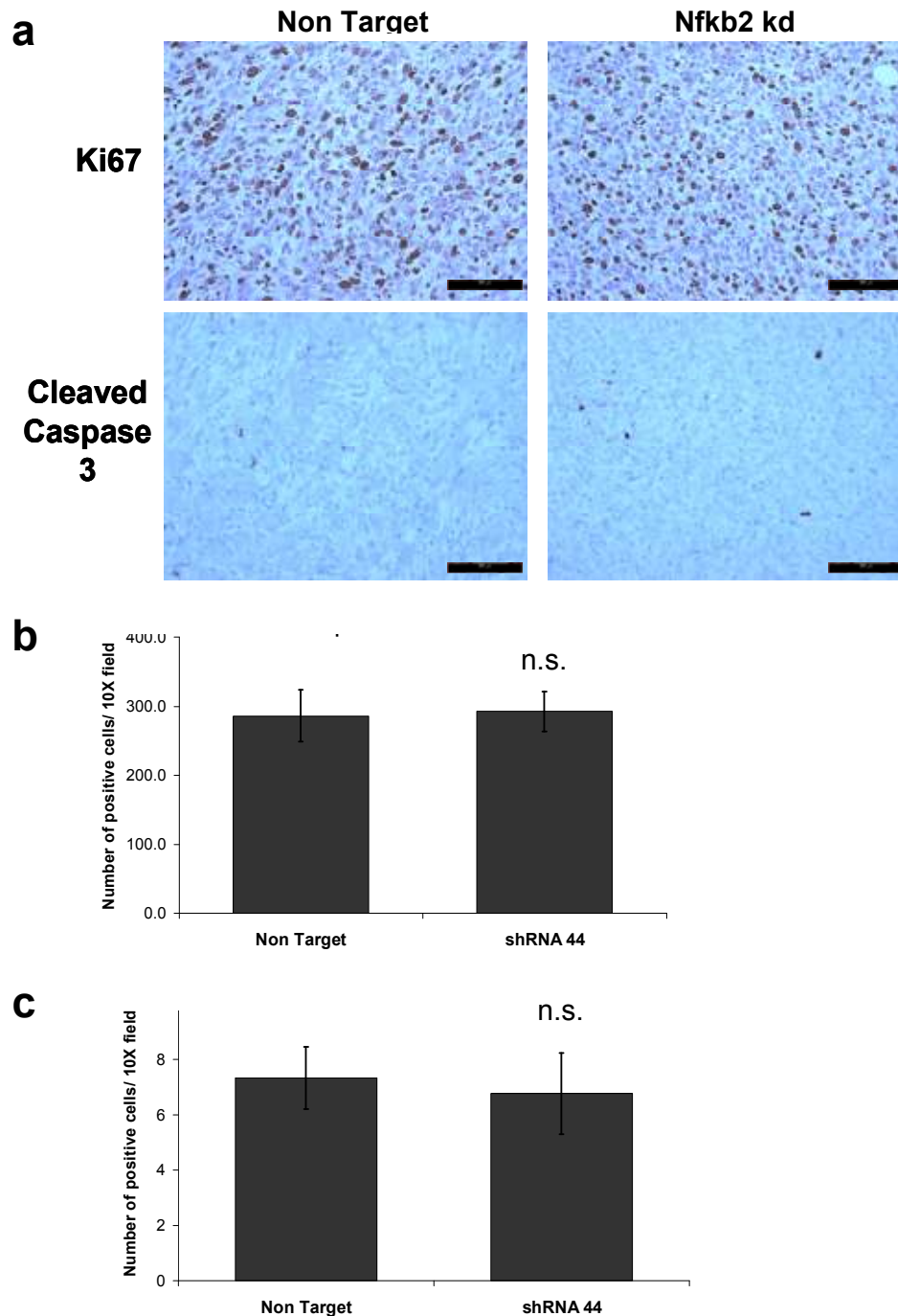


**Figure 4.13: The increased 4T1 tumour growth *in vivo* is not associated with a change in the proliferation to apoptosis ratio.** (a) Representative images from 4T1 NT and *Nfkb2* kd tumours immuno-labelled with antibodies against Ki67 and cleaved caspase-3 respectively. Scale bar represents 100 $\mu$ m. (b) Bar charts showing number of Ki67 positive nuclei per 10x field of view. (c) Bar charts showing number of cleaved caspase-3 positive cells per 10x field of view. Data represent averages from n=5 per cohort and error bars indicate standard error of the mean. n.s. indicates not significant where statistical significance was determined by a two-tailed t-test.

4.2.4) but an increase in mammosphere forming ability is evident (Section 4.2.9). Thus, it is possible that the difference in tumour size between NT and *Nfkb2* kd cohorts was due to increased numbers of tumour initiating cells within the 4T1 *Nfkb2* kd population. This would allow the *Nfkb2* kd tumours to expand from a larger population of replication competent cells, providing a head start in terms of growth kinetics, albeit maintaining a similar proliferation rate as 4T1 NT cells. It would be interesting to address whether this is the case by limiting dilution experiments.

Upon necropsy at designated experimental endpoints, we also had a look at the lungs of mice transplanted with 4T1 NT or *Nfkb2* kd cells for metastases formation. Quantification of the area with lung metastases between the two cohorts did not reveal any significant differences (Figures 4.14 a&b). The fact that experimental endpoints were based on size of tumours (i.e.  $\sim 700\text{mm}^3$ ) would mean that there is less time for metastases formation in animals transplanted with 4T1 *Nfkb2* kd cells because these tumours exhibit faster growth kinetics. Hence, we were not able to directly conclude whether silencing of *Nfkb2* had any effects on metastatic formation.

#### 4.2.13 Loss of *Nfkb2* diminishes N202.1A tumour growth *in vivo*

As we observed decreased survival under anoikis conditions and mammosphere forming potential for N202.1A cells after *Nfkb2* silencing, we then wanted to address whether p100/p52 depletion in these cell lines would retard tumour growth *in vivo*. For that, we transplanted these cells orthotopically into immunocompromised NOD/SCID mice. Interestingly, the tumour size of tumours from N202.1A cells lacking *Nfkb2* were diminished (Figure 4.15) and this is in contrast to the effects of silencing *Nfkb2* in 4T1 cells (Section 4.2.12). Again, analysis of the gradients of respective graphs also suggests no difference in the rate of change in size at selected time intervals (Figure 4.15). Although the contrasting effects due to *Nfkb2* silencing on tumour growth correlates with the contrasting effects seen for both these cell lines in *in vitro* experiments, we cannot rule out the possibility that the immune-components of transplanted mice were responsible for the differences seen. That is, 4T1 cells were transplanted into syngeneic hosts whereas N202.1A cells were transplanted into NOD/SCID mice which are deficient in natural killer cells and lack both B and T cells. This could be addressed with syngeneic transplants of N202.1A cells. Nonetheless, the retardation of N202.1A tumour growth *in vivo* demonstrates the potential of targeting p52 in breast cancer cells.

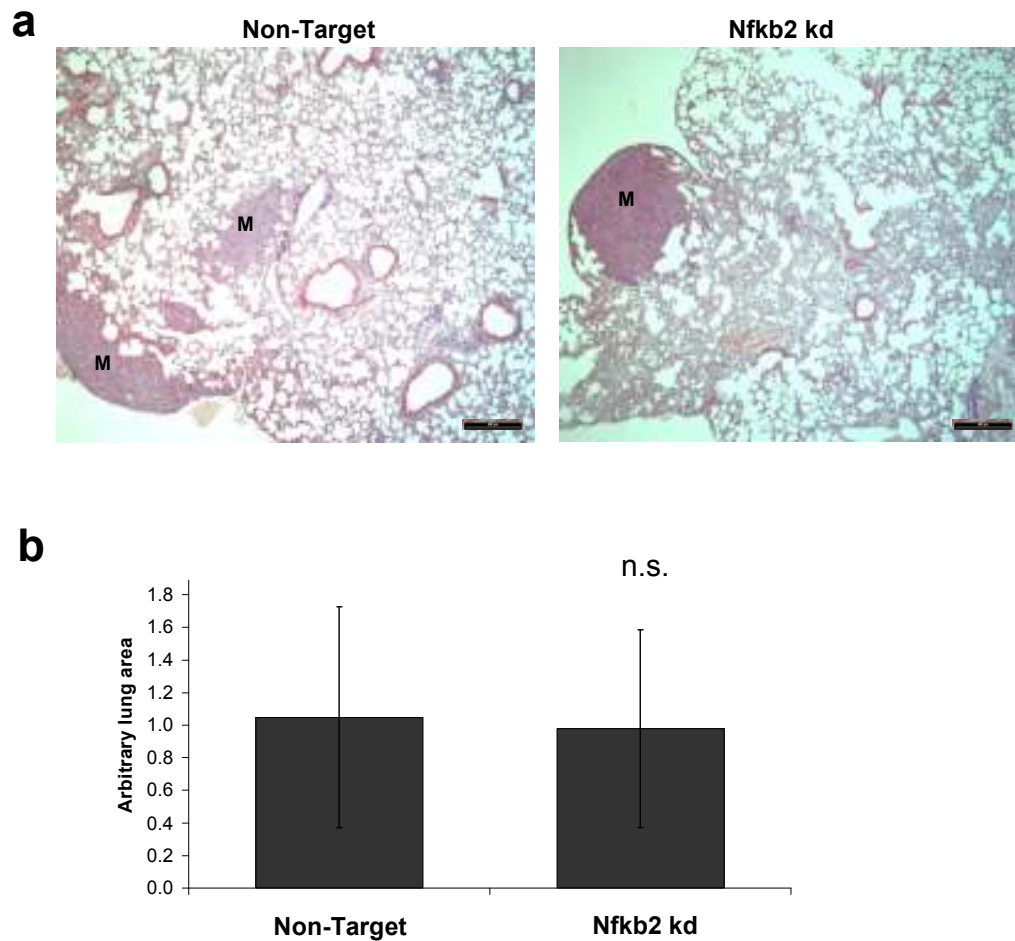


**Figure 4.14: Metastatic burden of mice transplanted with 4T1 NT and *Nfkb2* kd cells.** (a) Representative images from lungs of mice transplanted orthotopically with 4T1 NT and *Nfkb2* kd cells. M indicates metastatic nodules. Scale bar represents 200 $\mu$ m. (b) Bar charts showing average area of lung metastases from mice transplanted orthotopically with 4T1 NT and 4T1 *Nfkb2* kd cells. Data represent averages from n=5 per cohort and error bars indicate standard error of the mean. n.s. indicates not significant where statistical significance was determined by a two-tailed t-test.

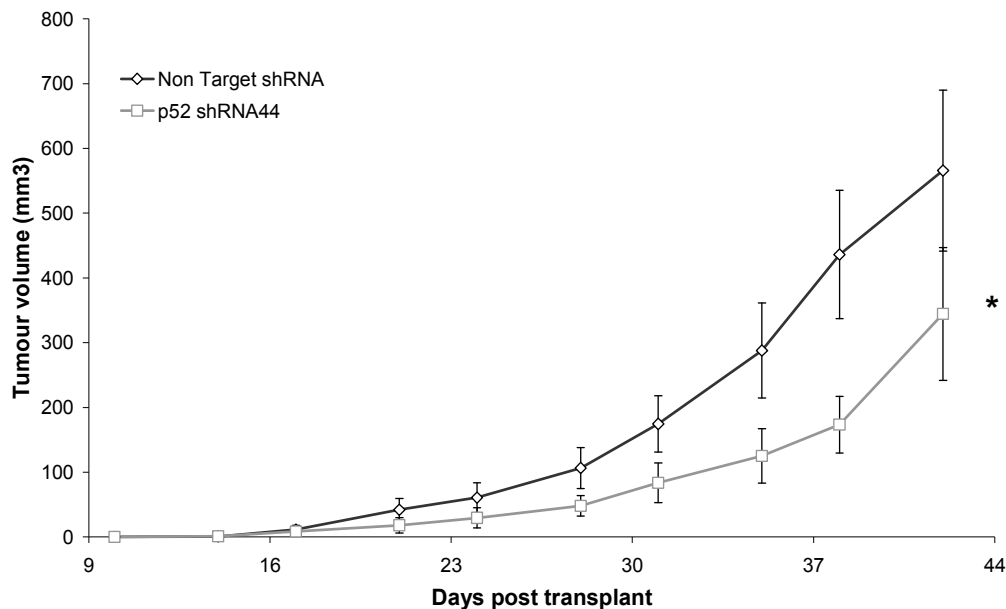


**Figure 4.15: Loss of *Nfkb2* diminishes N202.1A tumour growth *in vivo*.** (a) 50,000 N202.1A Non Target or *Nfkb2* kd cells were transplanted into the right mammary fat pads of NOD/SCID mice respectively. The resulting tumours were measured and the growth kinetics plotted as line graphs. Data points represent averages from  $n=5$  animals per cohort and error bars represent standard error of the mean. \* indicates  $p<0.05$ , where statistical significance between growth curves was determined by ANCOVA test;  $F=7.754$ ,  $p=0.021$ .

### 4.3 Discussion

From our experiments on 4T1, N202.1A and EPH4 cell lines, it appears that the effects of silencing *Nfkb2* are context dependent. In the non-tumourigenic EPH4 cell line, despite elevations in basal NF- $\kappa$ B activity after *Nfkb2* knockdown, there were no changes in the ability to survive under anoikis conditions, proliferation, colony forming potential, motility or mammosphere forming potential. These observations would suggest that in normal mammary epithelial cells, negative regulatory mechanisms exist to counter-act the increase in basal NF- $\kappa$ B activity. In fact, it has been shown in breast cancer cell lines that oncogenic stimulus such as Src can induce epigenetic changes which results in maintenance of a positive feedback loop involving NF- $\kappa$ B and inflammatory pathways (Illiopoulus et al., 2009). Thus, it is likely that in non-transformed Eph4 cells, such epigenetic changes have not been established and this prevents the acquisition of malignant traits in these cells.

On the other hand, in 4T1 cells, the increase in basal NF- $\kappa$ B activity after *Nfkb2* knockdown resulted in more aggressive cancer phenotypes. This increase in basal NF- $\kappa$ B activity correlated with increased nuclear and cytoplasmic p50 levels. It is also possible that the loss of p100 contributes to elevations in NF- $\kappa$ B activity in this cell line because it can sequester other NF- $\kappa$ B subunits such as p50 in the cytoplasm. To address this, a non-processable mutant form of p100 (Maruyama et al., 2010) can be over-expressed in 4T1 cells and the corresponding NF- $\kappa$ B activity measured. Due to its non-processable nature, any contribution from p52 can be eliminated. In addition over-expression of wild-type (WT) p100 would demonstrate whether both p100 and p52 are required to rescue the increase in NF- $\kappa$ B activity, since p100 can be processed into p52. Additional knockdown of p50 in cells lacking *Nfkb2* could also indicate whether compensatory activity by p50 is responsible for the increased malignancy in 4T1 cells lacking *Nfkb2*.

As a result of increased NF- $\kappa$ B activity in 4T1 cells after p100/p52 depletion, we observed changes in markers which were indicative of EMT. Consequently, this correlates with increased motility and mammosphere forming potential, both attributes associated with the EMT process. We showed that both these changes were dependent on NF- $\kappa$ B activity (Section 4.2.8&4.2.10) and cannot be rescued by over-expression of p52, again suggesting that the phenotypes observed could be due to loss of p100. We cannot rule out the possibility that increased compensatory activity by other NF- $\kappa$ B subunits such as p50 were responsible for the phenotypes observed.

However, it would be interesting to indentify and distinguish whether knockdown of p50 or overexpression of p100 can rescue the phenotypes observed. Tumour growth *in vivo* was also accelerated upon *Nfkb2* silencing and this increase is likely due to the increase in tumour initiating cells, since no difference in proliferation and apoptosis were observed in these tumours. Although we did not detect any difference in metastatic burden between mice with transplanted tumours from 4T1 NT and *Nfkb2* kd cells, this could be due to unequal lengths of time for metastatic formation. Tail vein transplant experiments can be carried out to eliminate the differences in tumour growth kinetics between the two cell lines. Nonetheless, the enhanced motility in 4T1 *Nfkb2* kd cells that was observed *in vitro* might become less apparent in such an assay because the initial steps of metastasis are omitted. Even so, it will be interesting to investigate whether the increased tumour initiating potential in 4T1 *Nfkb2* kd cells will lead to increased metastatic burden upon tail vein transplantation. Overall, our data demonstrates that *Nfkb2* silencing leads to acquisition of more aggressive phenotypes in 4T1 cells and suggests that p100 may have important suppressive roles with regards to disease progression. Accordingly, activation of the alternative NF- $\kappa$ B pathway may affect breast cancer progression not only by increased p52 mediated transcription but also by inducing the loss of p100. Hence, targeting p52 at the gene level will not be an appropriate therapeutic strategy because the loss of p100 could lead to detrimental effects in certain breast cancer subtypes.

Contrastingly, targeting *Nfkb2* by gene silencing resulted in some therapeutically beneficial effects in N202.1A cells. These cells exhibited decreased NF- $\kappa$ B activity which then resulted in diminished anoikis resistance, mammosphere forming potential and tumour growth *in vivo*. The decreased mammosphere forming ability upon *Nfkb2* silencing could be rescued by over-expression of p52 and through these experiments, we have demonstrated for the first time a role for p52 in regulating self-renewal properties of CaSCs. This is in line with findings that the RANKL-RANK-I $\kappa$ B $\alpha$  signalling axis is important for maintenance of stem cell functions in normal mammary stem cells, mammary cancers and metastasis (Asselin-Labat et al., 2010, Gonzalez-Suarez et al., 2010, Liu et al., 2010, Tan et al., 2011). Thus, it is likely that RANKL signalling promotes CaSC properties at least in part through activation of the alternative NF- $\kappa$ B pathway. To further address the importance of alternative NF- $\kappa$ B pathway activation downstream of RANKL signalling in regulating CaSC properties, the differential effects on breast cancer cell lines expressing WT or

the unprocessable mutant form of p100 respectively upon RANKL stimulation can be assessed. It is also important to histologically characterize the N202.1A transplanted tumours in order to understand the mechanisms behind diminished tumour growth upon *Nfkb2* silencing in these cells. The metastatic burden especially in the lungs of these mice will also need to be quantified to reveal whether *Nfkb2* knockdown reduces N202.1a metastasis formation.

Despite the clear differential effects of *Nfkb2* silencing between various cell lines studied, the mechanisms responsible for these context dependent effects are not clear. It is plausible that N202.1A cells which over-express the EGFR family member, ErbB2, have increased activation of NF- $\kappa$ B and this makes them more dependent on NF- $\kappa$ B activity for their tumourigenic properties. As for 4T1 cells, lower basal NF- $\kappa$ B activity could mean less p100 processing into p52 and consequently, the loss of p100 will be more pronounced than that of p52 when *Nfkb2* is silenced. To address whether the differential effects are dependent on ErbB2 mediated signalling, *Nfkb2* can be silenced in N202.1E cells, a sub-line related to N202.1A cells which has reverted to low levels of ErbB2 expression. Perhaps in a cell lineage similar to that of N202.1A but with lower NF- $\kappa$ B activity, *Nfkb2* silencing may lead to more malignant phenotypes. An unbiased analysis involving global gene expression analysis might also reveal the various co-operating pathways required to bring about the differential effects due to *Nfkb2* silencing in the cell lines studied.

Compensatory mechanisms between NF- $\kappa$ B subunits have been detailed in various studies involving knockout mice (Moellering et al., 2009). From our observations, this also occurred in 4T1 cells, where increased p50 was observed after *Nfkb2* silencing. It would be worth determining whether such compensation has taken place in N202.1A cells as well. This highlights some of the potential problems when targeting the NF- $\kappa$ B pathway through manipulation of subunit levels. From experiments involving pharmacological inhibition of the canonical NF- $\kappa$ B pathway (Sections 4.2.8 & 4.2.10), we showed that inhibition of canonical NF- $\kappa$ B signalling alone in both 4T1 and N202.1A cell lines could effectively diminish motility and mammosphere forming potential. This would indicate that targeting the canonical NF- $\kappa$ B pathway independently might suffice to achieve a therapeutic outcome in these cell lines. However, it remains to be addressed whether certain subtypes of breast cancers are more dependent on the canonical or the alternative NF- $\kappa$ B pathways. This is possible as NF- $\kappa$ B subunits have certain non-overlapping functions and they can

regulate subsets of unique genes respectively. Hence, targeting p52 mediated transcription may be more relevant to particular subtypes of breast cancer than others.

Even so, in N202.1A cells, we have demonstrated decreased tumour initiating potential and growth *in vivo* after *Nfkb2* silencing and this illustrates the prospects of targeting p52 mediated transcription in breast cancers. Importantly, the effects of p52 depletion are context dependent, as demonstrated by the outcomes in 4T1 and N202.1A cell lines. Hence, it will be crucial to identify the subtype of breast cancers which are dependent on p52 and most likely to benefit from its targeting.

#### **4.4 Summary**

In this chapter, we have shown that the effects of silencing *Nfkb2* in mammary cancer cells are context dependent (Figure 4.16). Although the exact mechanisms behind the differential effects have not been elucidated, it is likely due to p100 or p52 having more dominant roles respectively in varying cell lines. We have also demonstrated a role for p52 in maintenance of CaSC properties and this strengthens its prospects as a therapeutic target. However, targeting p52 at the gene level could be detrimental as the loss of p100 or compensatory mechanisms by other NF- $\kappa$ B subunits may exacerbate the malignant phenotypes of breast cancer cells. Hence, other therapeutic strategies for targeting p52 will need to be addressed and particular subtypes of breast cancer which depend on p52 mediated activity identified.

Phenotype	EPH4	4T1	N202.1A
Basal Nf- $\kappa$ B activity	↑	↑	↓
Proliferation	↔	↔	↔
Colony formation	↔	↔	↔
EMT	n/a	↑	n/a
Motility	↔	↑	↔
Anoikis resistance	↔	↔	↓
Mammosphere formation	↔	↑	↓
Tumour growth <i>in vivo</i>	n/a	↑	↓

**Figure 4.16: Summary of changes due to silencing of *Nfkb2* in Eph4, 4T1 and N202.1A cells.** Red arrows show an increase after silencing relative to non-target controls, green arrows show a decrease after silencing and blue arrows indicate no significant changes after silencing. N/a indicates not addressed.

## **CHAPTER 5**

Elucidating the effects of Ser-222 phosphorylation  
of p52 on the phenotypes of mammary cancer cells

## **5 Elucidating the effects of Ser-222 phosphorylation of p52 on the phenotypes of mammary cancer cells**

### **5.1 Introduction**

The findings from Chapter 4 showed that depletion of p100/p52 can be therapeutically beneficial in N202.1A cells but such an intervention resulted in increased malignancy in 4T1 cells. As the increased malignancy in 4T1 cells was likely due to the loss of the inhibitory functions of p100 and/or compensatory activity by p50, prospective strategies for diminishing p52 activity, downstream of p100/p52 processing, ought to circumvent the loss of p100 and not depend on altering the levels of p52 in a cell. This would prevent exacerbation of disease progression in cases where misdiagnosis may occur, or where tumour phenotype may change during treatment.

For these reasons, our next approach was to address whether altering the trans-activating ability of p52 by manipulating its post-translational modifications could result in therapeutically beneficial outcomes. As it has been shown that phosphorylation of p52 at serine-222 (S222) can regulate the preference for p52 to form transcriptionally active or repressive complexes (Barre and Perkins, 2010a), we wanted to address whether such changes could alter the oncogenic phenotypes of mammary cancer cells. In the study by Barre and Perkins, S222 phosphorylation promoted p52 complex formation with histone deacetylase 1 (HDAC1) and such complexes repressed transcription. Conversely, the lack of S222 phosphorylation promoted p52 homodimers and complex formation with B-cell lymphoma 3 (Bcl-3) which can drive transcription. Thus, we wanted to investigate whether promoting Ser-222 phosphorylation of p52 would diminish NF- $\kappa$ B activity and consequently the malignant phenotypes of mammary cancer cells. Another plausible outcome for this targeting strategy is that both classical and alternative NF- $\kappa$ B gene targets with  $\kappa$ B promoter sites that are recognizable by p52 can be repressed. This would abrogate the concerns pertaining to compensatory activity and at the same time, broaden the effective scope of such a therapeutic to breast cancers that depend on NF- $\kappa$ B activity in general, rather than just the alternative pathway itself. If therapeutic outcomes were observed through such manipulations, the results from the following experiments would substantiate targeting of upstream regulators of Ser222 phosphorylation of p52.

## 5.2 Over-expression of phospho-mimetic p52 mutant in 4T1 cells

### 5.2.1 Effects of over-expressing phospho-mimetic p52 mutant on basal NF- $\kappa$ B activity

4T1 cells that were transduced with non-target (NT) or shRNA against *Nfkb2* were subsequently infected with lentivirus encoding either wild-type (WT), S222A, S222D or DNA binding mutant (DBM) versions of p52 respectively. The S222A and S222D mutations in p52 represented phospho-deficient and phospho-mimetic states of serine-222 of p52 respectively. The expression levels of respective p52 constructs in 4T1 cells were demonstrated by Western blotting (Figure 5.1a). All sub-lines expressed haemagglutinin (HA) tagged p52 to a significant degree. It is also worth noting that over-expression of WT, S222A and S222D p52 in 4T1 *Nfkb2* kd cells resulted in re-expression of p100 at minute levels. This is not surprising as p52 can drive the transcription of the *Nfkb2* gene as a negative feedback mechanism. Both NT and *Nfkb2* kd cells were evaluated because NT cells which express p100 may mask the effects of p52 over-expression through its I $\kappa$ B $\alpha$  functions.

When the basal NF- $\kappa$ B activities of 4T1 cells over-expressing respective p52 were examined by luciferase reporter assays, no significant differences were observed between 4T1 NT sub-groups. In the case of 4T1 *Nfkb2* kd cells, the changes in basal NF- $\kappa$ B when various p52 were over-expressed were also not significantly different (Figure 5.1b). As these results represent p52 transcriptional activity from a promoter with three consensus  $\kappa$ B sequences, it is possible that p52 dependent transcription in these cells may require other enhancer elements or presence of cooperative binding partners which are not permissive with the use of these luciferase reporter constructs. Thus, we were not able to ascertain whether over-expression of varying p52 constructs had any effect on the levels of its gene targets in these 4T1 sub-lines.

### 5.2.2 Effects of over-expressing phospho-mimetic p52 mutants on the sensitivity of 4T1 cells to anoikis

Despite the lack of change in basal NF- $\kappa$ B activity as determined by luciferase assays (Figure 5.1b), we went on to phenotypically assess the effects of over-expressing various p52 constructs in 4T1 cells. In 4T1 NT cells, over-expression of WT p52 increased the survival of these cells relative to parental or cells over-

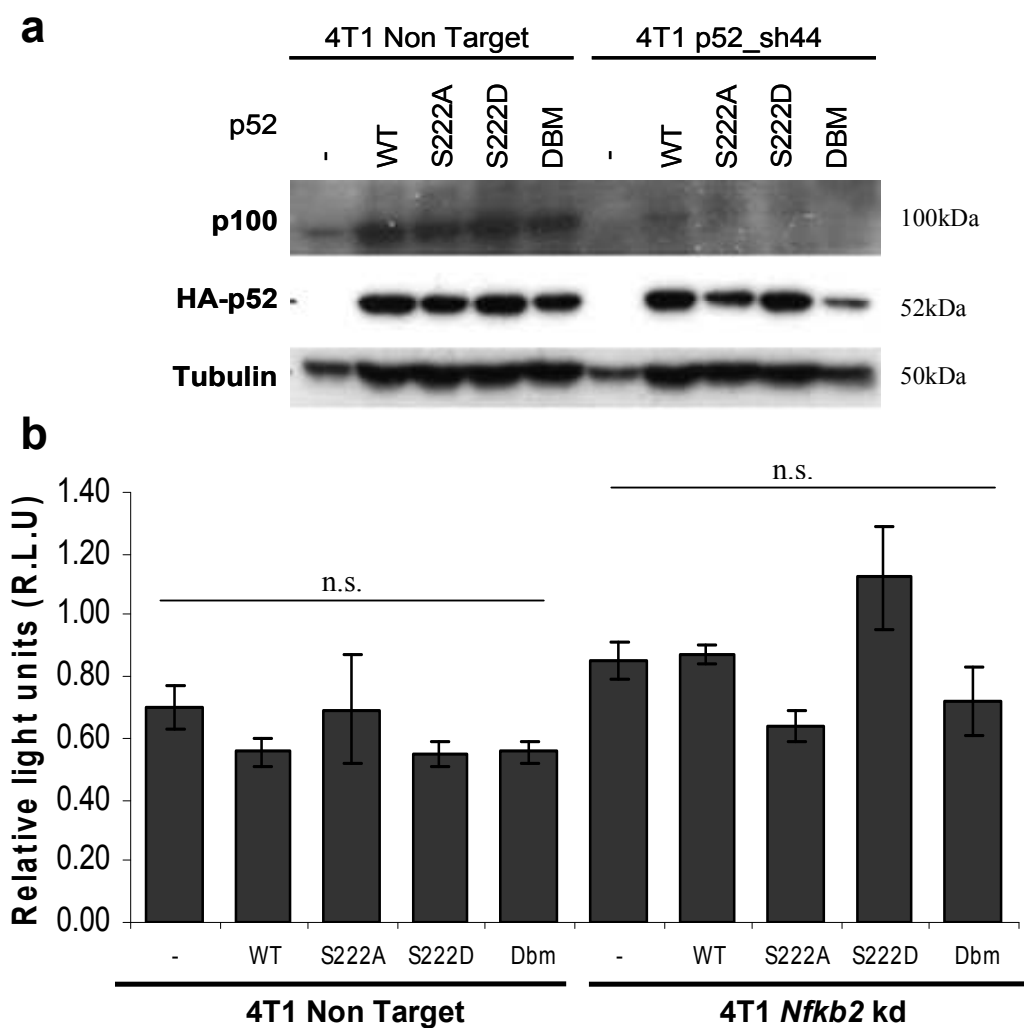


**Figure 5.1: Effects of over-expressing p52 and corresponding mutants on the basal NF- $\kappa$ B activity of 4T1 cells.** (a) 4T1 NT or Nfkb2 kd cells respectively were transduced with lentivirus encoding WT, S222A, S222D or DBM versions of p52. Selection of p52 over-expressing cells were carried out by FACS sorting of green fluorescent protein (GFP) positive cells, since transduced cells co-expressed GFP. The levels of p100 and HA-p52 were then evaluated through Western blotting of respective cell lysates. (b) 4T1 NT or Nfkb2 kd cells over-expressing either WT, S222A, S222D or DBM p52 were transfected with NF- $\kappa$ B luciferase reporter and pcDNA3.1:lacZ as transfection control. 48 hours after transfection, cell lysates were harvested and the ratio of luciferase to lacZ activity measured. Bar charts show basal NF- $\kappa$ B activity plotted as relative light units (RLU) in the respective cell lines. Data points represent average of at least  $n=3$  and error bars indicate standard error of the mean (SEM). One-way ANOVA test was used to determine statistical significance; Non-target cells,  $F(4,7)=0.861$ ,  $p=0.531$ ; Nfkb2 kd cells,  $F(4,7)=3.398$ ,  $p=0.076$ . N.s. indicates not statistically significant.

expressing S222A, S222D or DBM p52 (Figure 5.2). The lack of change when S222A or S222D p52 was over-expressed would suggest that both p52/c-rel/HDAC1 hetero- and p52/p52/Bcl3 homo-dimers are required to increase the survival of 4T1 NT cells under anoikis conditions. Similarly for 4T1 *Nfkb2* kd cells, over-expression of WT p52 led to increased survival under anoikis conditions relative to parental or cells over-expressing DBM p52. Although loss of p52 did not result in decreased survival (NT parental against *Nfkb2* kd parental), over-expression of WT p52 could enhance the ability of 4T1 cells to survive under non-adherent conditions. This would imply that the inherent ability of 4T1 cells to resist anoikis is not dependent on p52 but this ability can be enhanced by p52 over-expression. As no change was observed in luciferase reporter assays when WT p52 was over-expressed (Section 5.2.1), we cannot rule out the fact that this increase in anoikis resistance is independent of the transcriptional activity of p52. However, it is possible that the luciferase reporter assay reflects transcription from the canonical NF- $\kappa$ B pathway with preference over that of transcription that is mediated by p52. Hence, the changes observed in this assay were a result of specific p52 transcriptional activity that is not conveyed by the luciferase reporter assays.

### ***5.2.3 Effects of over-expressing phospho-mimetic p52 mutant on the proliferative, colony forming potential and mammosphere forming potential of 4T1 cells***

In order to further assess whether promoting S222 phosphorylation has any therapeutic effects on 4T1 cells, respective cell lines over-expressing either WT, S222A, S222D or DBM p52 were investigated in proliferation (Figure 5.3a), colony forming (Figure 5.3b) and mammosphere assays (Figure 5.4a&b). However no significant differences were observed between 4T1 NT cells over-expressing respective p52 variants or 4T1 kd cells over-expressing the different forms of p52 in all these assays. These results corroborate the lack of changes observed for basal NF- $\kappa$ B activity (Figure 5.1b) and indicate that the regulation of these phenotypes in 4T1 cells cannot be perturbed by p52 over-expression, irrespective of S222 phosphorylation status.

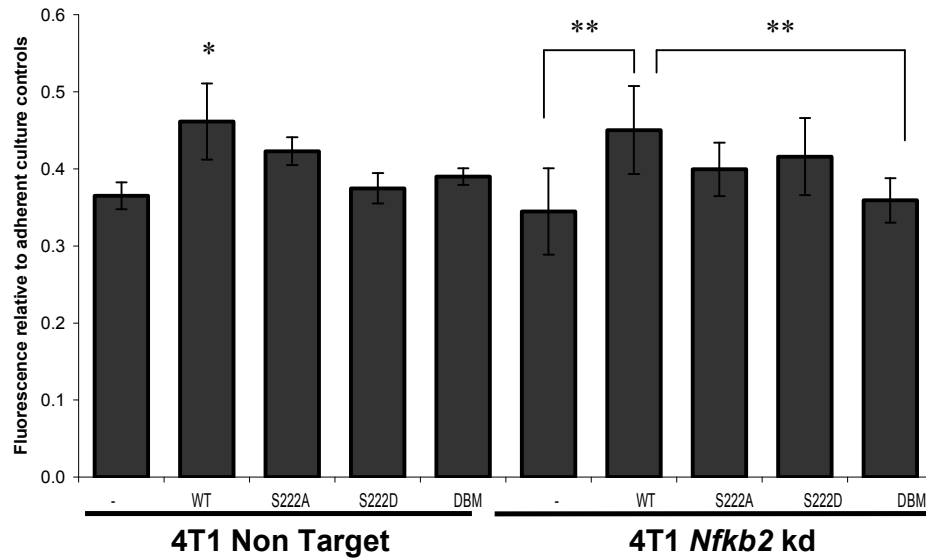


**Figure 5.2: Effects of over-expressing p52 and corresponding mutants on the ability of 4T1 cells to survive under anoikis conditions.** 4T1 NT or *Nfkb2* kd cells over-expressing WT, S222A, S222D or DBM p52 respectively were plated under non-adherent culture conditions and the viability of these cells were measured after 24 hours. Bar charts show viability of cells determined by *Cell Titer Blue* assay, plotted as relative fluorescence in the respective cell lines. Data points represent average of at least n=6 and error bars indicate standard error of the mean (SEM). Statistical significance was determined by one-way ANOVA test and in cases where significance were observed, a post-hoc Tukey's test was carried out between individual groups. For 4T1 NT cells; one-way ANOVA  $F(4,10)=4.22$ ,  $p=0.03$ ; for *Nfkb2* kd cells, one-way ANOVA  $F(4,10)=10.509$ ,  $p=0.001$ . For post-hoc Tukey's test, \* indicates  $p<0.05$ , \*\* indicates  $p<0.01$ .

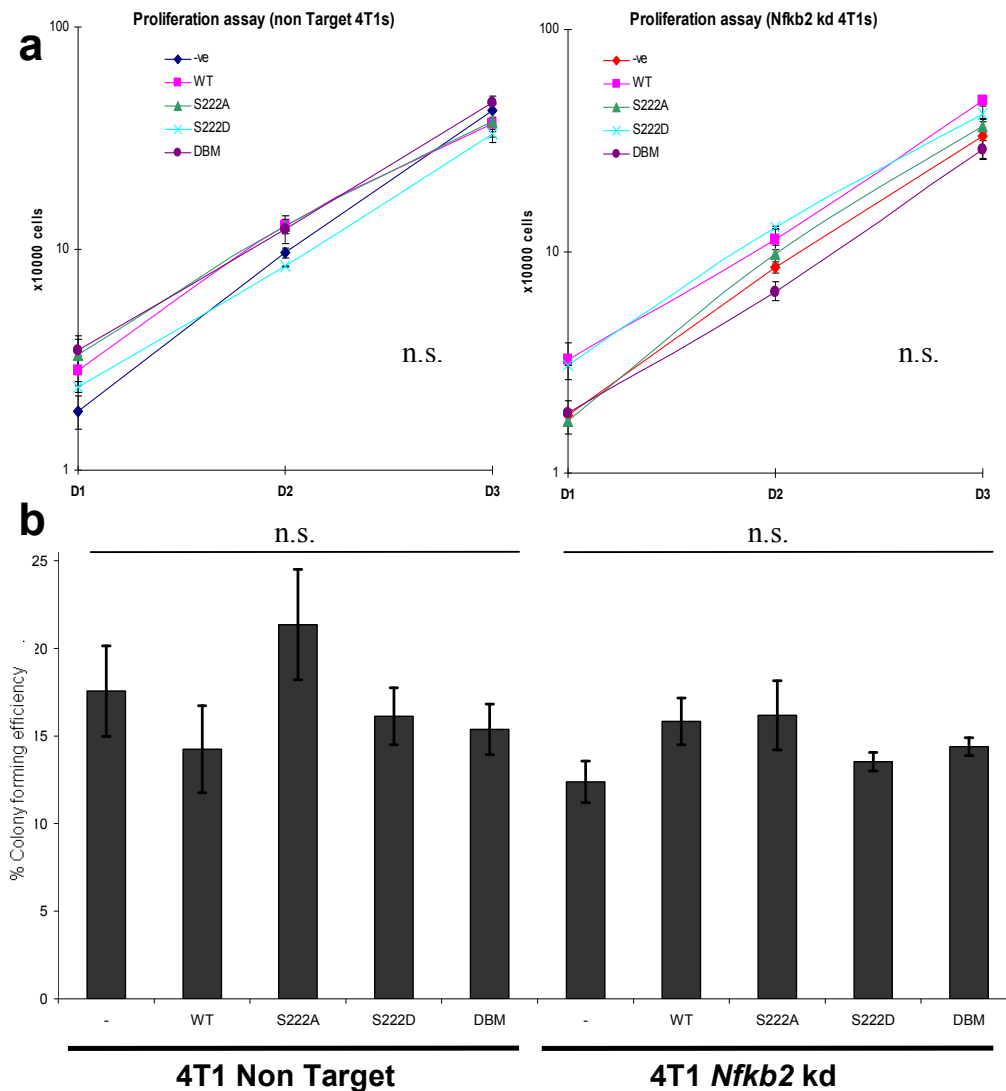


**Figure 5.3: Effects of over-expressing p52 and corresponding mutants on the proliferative and colony forming potential of 4T1 cells.** (a) 4T1 NT and *Nfkb2* kd cells over-expressing WT, S222A, S222D or DBM p52 were plated in 6-well plates. At respective timepoints, the number of cells in each well was counted with the aid of a haemo-cytometer. Line graphs show cell counts relative to day 1 plotted on a log scale against time in days. Data points represent average of at least  $n=6$  and error bars indicate standard error of the mean (SEM). Statistical significance was determined by ANCOVA test; for Non-target cells,  $F(4,8)=0.861$ ,  $p=0.526$ ; for *Nfkb2* kd cells,  $F(4,8)=2.658$ ,  $p=0.112$ . (b) 4T1 NT and *Nfkb2* kd cells over-expressing WT, S222A, S222D or DBM p52 were plated in 6-well plates at a density of 1000 cells per well. The number of colonies formed after 7 days were counted. Bar charts show the % colony forming efficiency, which is a percentage of the number of colonies formed per cells seeded. Data points represent average of at least  $n=6$  and error bars indicate standard error of the mean (SEM). Statistical significance was determined by one-way ANOVA test; for Non-target cells,  $F(4,37)=1.479$ ,  $p=0.228$ ; for *Nfkb2* kd cells,  $F(4,34)=1.392$ ,  $p=0.257$ . N.s. indicates not statistically significant.

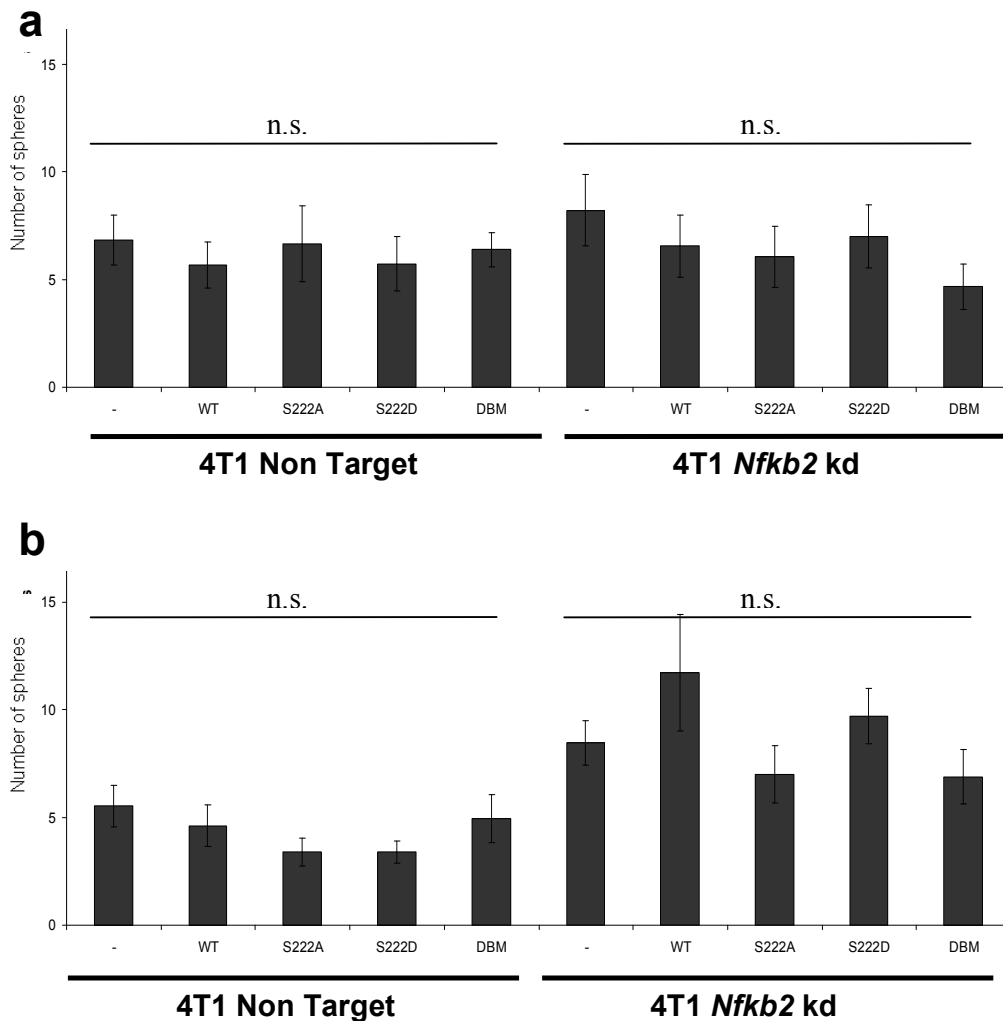


**Figure 5.4: Effects of over-expressing p52 and corresponding mutants on the mammosphere forming potential of 4T1 cells. (a)** 4T1 NT and *Nfkb2* kd cells over-expressing WT, S222A, S222D or DBM p52 were plated in non-adherent culture plates with mammosphere media and the number of spheres formed after 7 days were counted. Bar charts show the number of spheres formed per well. Statistical significance was determined by one-way ANOVA test; for 4T1 NT cells,  $F(4,85)=0.228$ ,  $p=0.922$ ; for *Nfkb2* kd cells,  $F(4,85)=0.841$ ,  $p=0.503$ . **(b)** The spheres formed by respective cell lines in the first passage (P1) were dissociated and re-seeded at an equal density (P2) under non-adherent culture conditions in mammosphere media. Bar charts show number of spheres formed per well. Data points represent average of at least  $n=6$  and error bars indicate standard error of the mean (SEM). Statistical significance was determined by one-way ANOVA test; for 4T1 NT cells,  $F(4,84)=1.74$ ,  $p=0.149$ ; for *Nfkb2* kd cells,  $F(4,85)=2.312$ ,  $p=0.064$ . N.s. indicates not statistically significant.

#### 5.2.4 Effects of over-expressing phospho-mimetic p52 mutant on the motility of 4T1 cells

We also investigated the motility of 4T1 NT and *Nfkb2* Kd cells upon over-expression of respective p52 variants. In both cell lines, we found increases of about 3-fold in motility, relative to respective parental cell lines when the S222A form of p52 was over-expressed (Figure 5.5). This is in contrast to the S222D mutant where over-expression of this form of p52 did not affect motility. This suggests that the activity of p52 homodimer complexes, possibly in cooperation with Bcl-3 was responsible for increasing motility in 4T1 cells. Although WT p52 did not result in similar increases as the S222A mutant, this can be explained by the fact that negative regulatory mechanisms may exist in 4T1 cells which promote the phosphorylation of WT p52, resulting in a similar outcome as over-expressing the phospho-mimetic S222D mutant. The use of phospho-specific antibodies to determine whether increased levels of Ser-222 phosphorylated p52 are detected upon over-expression of WT p52 would be needed to verify this. Thus, it appears that the inherent motility of 4T1 cells cannot be diminished by promoting repressive p52 heterodimers but can be further exacerbated by promoting p52 homodimers.

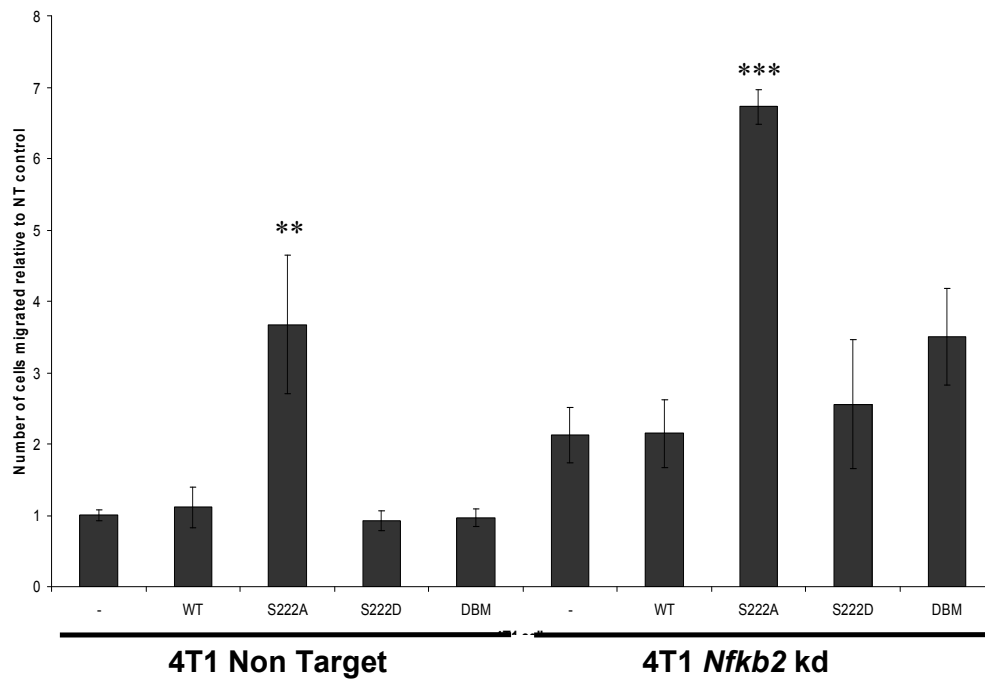


**Figure 5.5: Effects of over-expressing p52 and corresponding mutants on the motility of 4T1 cells.** 4T1 NT and *Nfkb2* kd cells over-expressing WT, S222A, S222D or DBM p52 were plated in Boyden trans-well migration chambers and migration was induced via a serum gradient. The cells that have migrated to the underside of the membrane were then stained and counted. Bar charts show the relative number of cells migrated (normalized to 4T1 NT -). Data points represent average of at least n=6 and error bars indicate standard error of the mean (SEM). Statistical significance was determined by one-way ANOVA test; for 4T1 NT cells,  $F(4,25)=6.777$ ,  $p=0.001$ ; for *Nfkb2* kd cells,  $F(4,24)=12.444$ ,  $p<0.001$ . Post-hoc Tukey's test was then performed to determine the level of significance between individual groups. For post-hoc Tukey's test, \*\* indicates  $p<0.01$ , \*\*\* indicates  $p<0.001$ .

### 5.3 Discussion

In this chapter, we were evaluating the potential therapeutic outcomes of promoting p52 repressive complexes in 4T1 cells through over-expression of the phospho-mimetic S222D mutant. 4T1 cells were chosen as the experimental model because in the previous chapter (Sections 4.2.8 & 4.2.10), the motility and mammosphere forming potential of these cells were significantly diminished when BAY 11-7082 was administered. This indicates that the motility and mammosphere forming potential of these cells were dependent on canonical NF- $\kappa$ B signalling. As we were interested to know whether promoting p52 repressive complexes would also reduce transcription from the canonical pathway due to repression of  $\kappa$ B promoter sites in general, the 4T1 cell line seemed appropriate for this purpose.

However, we found that over-expression of WT, S222A or S222D forms of p52 did not affect basal NF- $\kappa$ B activity in 4T1 NT or *Nfkb2* kd cells, as determined by luciferase assays (Section 5.2.1). Since the  $\kappa$ B sequences on the reporter plasmid can also be recognized by other NF- $\kappa$ B subunits (e.g. RelA-p50), it is likely that competition may exist between the different populations of subunits. In fact, preferential recruitment of particular NF- $\kappa$ B dimers to these promoter sites cannot be discounted because some dimers may exert dominant binding over others. The differential preference for binding of NF- $\kappa$ B subunits can be achieved through interactions with binding partners (Basak et al., 2008), recruited through enhancer sequences which were not present in the reporter plasmid used. In addition, distinct NF- $\kappa$ B dimers bind different  $\kappa$ B sequences with varying preference, and thus the use of a set of consensus  $\kappa$ B sequences in the reporter plasmid may lead to biased recruitment of NF- $\kappa$ B dimers. Accordingly, p52 homo- or heterodimers may still affect the regulation of certain gene targets despite the lack of change seen in luciferase assays.

No significant changes were observed in proliferation, colony forming and mammosphere forming assays when respective p52 variants were over-expressed in 4T1 NT or *Nfkb2* kd cells (Section 5.2.3) and this correlates with the lack of difference in basal NF- $\kappa$ B activities (Section 5.2.1). Our results would imply that the genes responsible for maintaining these phenotypes in 4T1s cannot be perturbed by over-expression of p52, let alone promoting formation of repressive p52 complexes. This could be due to the genes not being targets regulated by p52.

In the case of anoikis and motility assays however, changes in levels of p52 did affect these particular phenotypes in 4T1 cells. Over-expression of WT p52 increased anoikis resistance in 4T1 NT and *Nfkb2* kd cells relative to respective parental cell lines (Section 5.2.2). However, there was no significant effect of over-expressing S222A or S222D mutants on anoikis resistance, suggesting that both phosphorylated and non-phosphorylated forms of p52 were required to increase anoikis resistance. Whilst this shows the potential involvement of p52 mediated transcription in increasing survival of 4T1 cells under anoikis conditions, over-expression of S222D p52 did not result in a therapeutically beneficial effect.

Similarly in motility assays, only over-expression of the S222A form of p52 increased motility of 4T1 NT and *Nfkb2* kd cells relative to respective parental cell lines (Section 5.2.4). This indicates the involvement of p52 homodimer complexes in promoting the motility of these cells. It is possible that these increases in motility involve and are possibly dependent on p52 homodimer complexes with Bcl-3. This would correlate with data where Bcl-3 was shown to be important for promoting metastasis in MMTV-Neu driven tumours and important for motility of EGFR+ or ErbB2+ breast cancer cell lines (Wakefield & Clarkson, unpublished data). In order to verify this, it would be interesting to investigate whether silencing of Bcl-3 may rescue the increases due to p52 S222A over-expression in 4T1 cells. It would also be interesting to investigate whether the cell lines which depend on Bcl-3 for their metastatic phenotypes can be affected by over-expression of S222D p52. From over-expression of respective p52 mutants thus far, we have illustrated changes in phenotypes of mammary cancer cells which are governed by different phosphorylation states of p52. These experiments also show that p52 may exacerbate disease progression but only when present in aberrant levels with/without certain post-translational modifications. Hence, the levels of serine-222 phosphorylated and unphosphorylated p52 in breast cancers rather than just absolute levels of p52 may need to be accounted for if its transcriptional activity is to be gauged.

In all of the assays examined, we did not observe any therapeutically beneficial effects when the S222D form of p52 is over-expressed in 4T1 cells. This may be due to the fact that the repressive complexes do not exert a dominant negative effect, allowing recruitment of other NF- $\kappa$ B subunits at promoter sites to occur unperturbed. Another possible explanation for the lack of change in phenotype is the requirement for additional proteins or modifications to form repressive complexes.

Although S222 phosphorylation promotes p52 heterodimers, it is possible that the recruitment of additional proteins such as HDAC1 is dependent on additional requirements. Thus, further understanding of the regulatory mechanisms governing the formation of such repressive complexes may be needed to achieve the proposed therapeutic outcomes in mammary cancer cells. A plausible starting point may be to identify the genes repressed by Ser222 phosphorylated p52 by high-throughput chromatin immuno-precipitation (ChIP on chip). By doing so, the DNA regions repressed by p52 in a particular context will be known and with that DNA sequence, reverse ChIP can be performed to identify the proteins involved in the complex. Consequently, it may also be possible to identify the post-translational modifications present on the proteins involved in the complex by mass spectrometry. Such knowledge may aid the feasibility of our proposed strategy to promote repressive complexes in breast cancer cells. Since silencing of *Nfkb2* had significant effects on the mammosphere forming potential (Section 4.2.9) and tumour growth (Section 4.2.13) of N202.1A cells, it would be interesting to address the effects of over-expressing the respective p52 isoforms in these cells.

Another limitation associated with over-expressing varying p52 constructs is that the levels of expression may not recapitulate the normal levels found in the cells examined. This may skew the formation of complexes formed especially if p52 exists in abundance within the nucleus. Alternatively, the phospho-mimetic and phospho-deficient p52 mutations can be incorporated into genomic copies of the *Nfkb2* gene, through utilization of genome editing tools such as zinc finger nucleases. This will allow the expression of particular mutants at levels closer to normal in the cells investigated.

#### **5.4 Summary**

We set out to induce formation of repressive p52 complexes through over-expression of the S222D mutant form of p52 in 4T1 cells but did not observe any therapeutic effects in the assays examined. However, we did find that over-expression of WT p52 increased the survival of 4T1 cells under anoikis conditions whereas over-expression of the S222A form of p52 increased motility in 4T1 cells. These results demonstrate that specific functions of p52 are regulated by Ser-222 phosphorylation. Further understanding of the mechanisms regulating the formation of p52 repressive complexes may be required to achieve therapeutic outcomes in breast cancer cells.

## **CHAPTER 6**

Identifying a correlation between levels of nuclear  
p52 and subtypes of breast cancer

## 6 Identifying a correlation between levels of nuclear p52 and subtypes of breast cancer

### 6.1 Introduction

As we have shown through silencing of the *Nfkb2* gene (Chapter 4), only a subset of breast cancers may respond positively to therapeutic interventions which disrupt p52 mediated transcription. Hence, it would be crucial to identify cases in which such therapies may benefit the most.

For that reason, we set out to examine a small cohort of tumours generated from BRCA2<sup>-/-</sup> p53<sup>-/-</sup> mice (Hay et al., 2009) and determine whether any correlations exist between levels of nuclear p52 and markers relevant to breast cancer subtypes or disease progression. Tumours from BRCA2<sup>-/-</sup> p53<sup>-/-</sup> mice were used in this study because these tumours lacked DNA damage repair mechanisms and represent models of genomic instability. Accordingly, the resulting tumours may be driven by different oncogenic pathways and this could provide a wide range of tumour subtypes to be examined.

Since elevations in NF-κB activity in general have been associated with ErbB2 over-expressing (Biswas and Iglehart, 2006) and basal-like subtypes of breast cancer (Yamaguchi et al., 2009), the ErbB2 and p63 antigens were selected as markers for the respective subtypes to be examined. The basal phenotype in breast cancers have been shown to be associated with p63 (Ribeiro-Silva et al., 2005) and thus it was used as a putative marker for basal-like breast cancers. In addition, vimentin, a mesenchymal marker was also included in the panel of antigens to be examined because the NF-κB pathway is a known regulator of the EMT process (Huber et al., 2004a).

In brief, the aim of the experiments in this chapter was to identify via immunohistochemistry, the possible correlations between levels of nuclear p52 and ErbB2, p63 or vimentin across a panel of BRCA2<sup>-/-</sup> p53<sup>-/-</sup> tumours. This could provide some insights into the subtypes of breast cancer which are dependent on p52 mediated activity.

## **6.2 Identifying possible correlations between the levels of nuclear p52 and ErbB2, vimentin or p63 in BRCA2<sup>-/-</sup> p53<sup>-/-</sup> tumours by immuno-histochemistry**

### *6.2.1 Nuclear p52 levels correlate with p63 expression in a cohort of BRCA2<sup>-/-</sup> p53<sup>-/-</sup> tumours*

A total of 20 BRCA2<sup>-/-</sup> p53<sup>-/-</sup> tumours were examined in this study and we started off by scoring the levels of nuclear p52 in these tumours. The scores for staining of a particular antigen (IxP scores) were derived from the intensities of staining (I) and the percentage cover of staining across a tumour section (P), as described in Section 2.3.5.3 in Chapter 2. Consequently, the respective tumours were ranked from highest to lowest IxP scores for nuclear p52 (Figure 6.1a). The degree of staining for p63 (Figure 6.1b), ErbB2 (Figure 6.1c) and vimentin (Figure 6.1d) for each of the ranked tumours were also determined by IxP scores.

The relationship between levels of nuclear p52 and respective antigens (Table 6.1) were then determined by Spearman's ranked correlation test. Interestingly, nuclear p52 levels correlated with p63 staining (Spearman's  $R=0.5203$ ,  $p<0.05$ ) and this suggests that increased p52 activity may be associated with basal like breast cancers. However, there was no correlation between the levels of nuclear p52 with ErbB2 or vimentin.

## **6.3 Discussion**

From the immuno-histological analysis of nuclear p52 levels in a panel of twenty BRCA2<sup>-/-</sup> p53<sup>-/-</sup> tumours, we found a positive correlation between nuclear p52 levels and p63. Although this suggests a possible correlation between increased nuclear p52 and basal-like breast cancers, not all basal-like breast cancers express p63 (Livasy et al., 2006). Thus, this positive correlation may only hold true in a subset of basal-like breast cancers which express p63. This may explain the discrepancy between our findings and data from a previous study where only 9 out of 64 triple negative (ER<sup>-</sup>, ErbB2<sup>-</sup>, PR<sup>-</sup>) human breast tumours expressed nuclear p52 (Lerma et al., 2007b).

Further analysis will be required to identify the varying forms of p63 (i.e. TAp63 and  $\Delta$ Np63) which are present in the tumours examined because the antibody

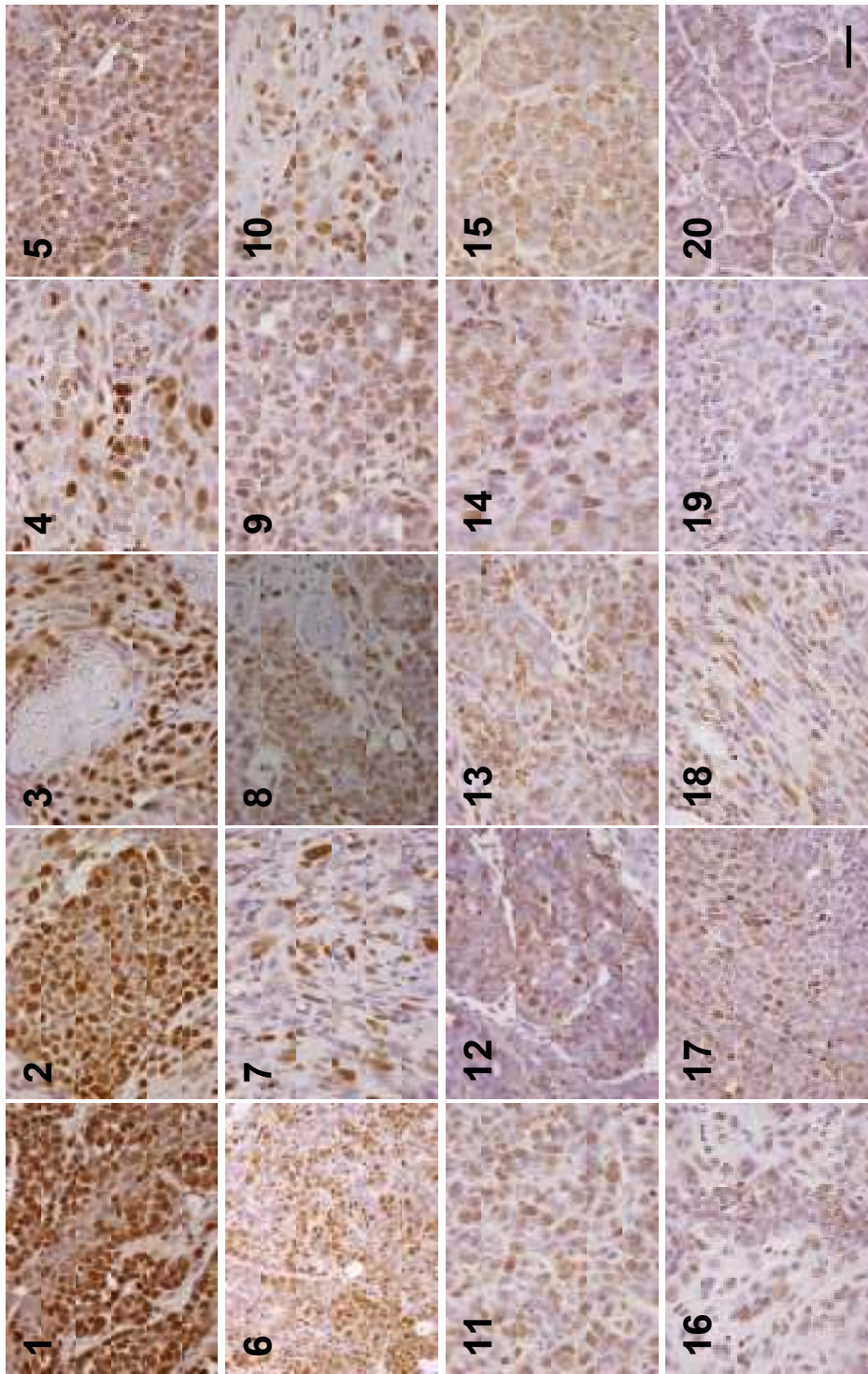


**Figure 6.1:** (a) BRCA2<sup>-/-</sup> p53<sup>-/-</sup> tumours were stained immuno-histochemically with antibodies against p52 and the levels of nuclear p52 staining in respective tumours were determined by IxP scores. Tumours were then ranked from 1-20 based on IxP scores for nuclear p52 (highest to lowest staining). Scale bar represents 20µm and the numbers inset show ranking of tumours.

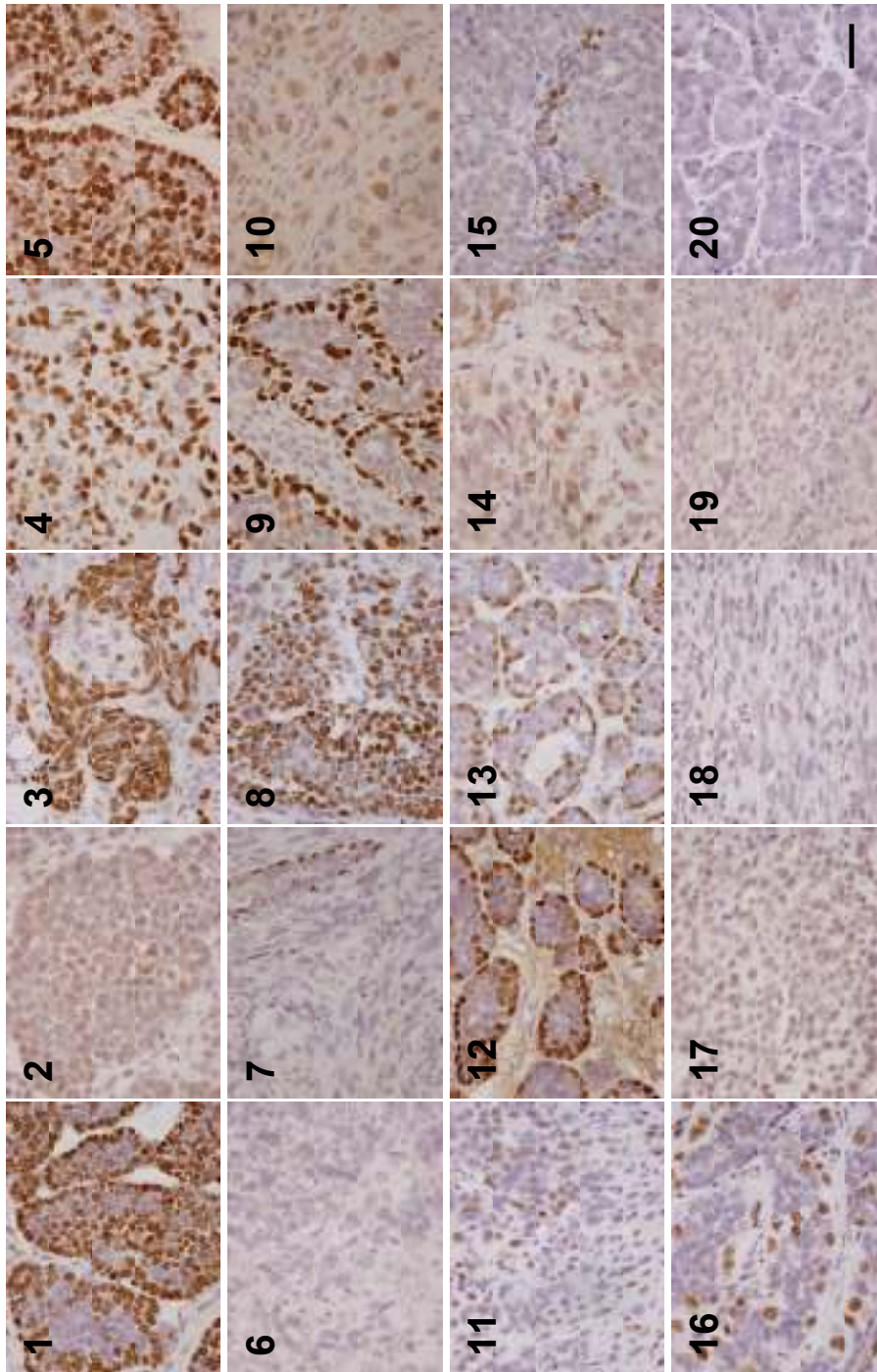


**Figure 6.1: (b)** BRCA2<sup>-/-</sup> p53<sup>-/-</sup> tumours were stained immunohistochemically with antibodies against p63 and the levels of p63 staining in respective tumours were determined by IxP scores. Ranking of tumours were based on IxP scores for nuclear p52 (highest to lowest staining). Scale bar represents 20µm and the numbers inset show ranking of tumours based on nuclear p52 IxP scores.

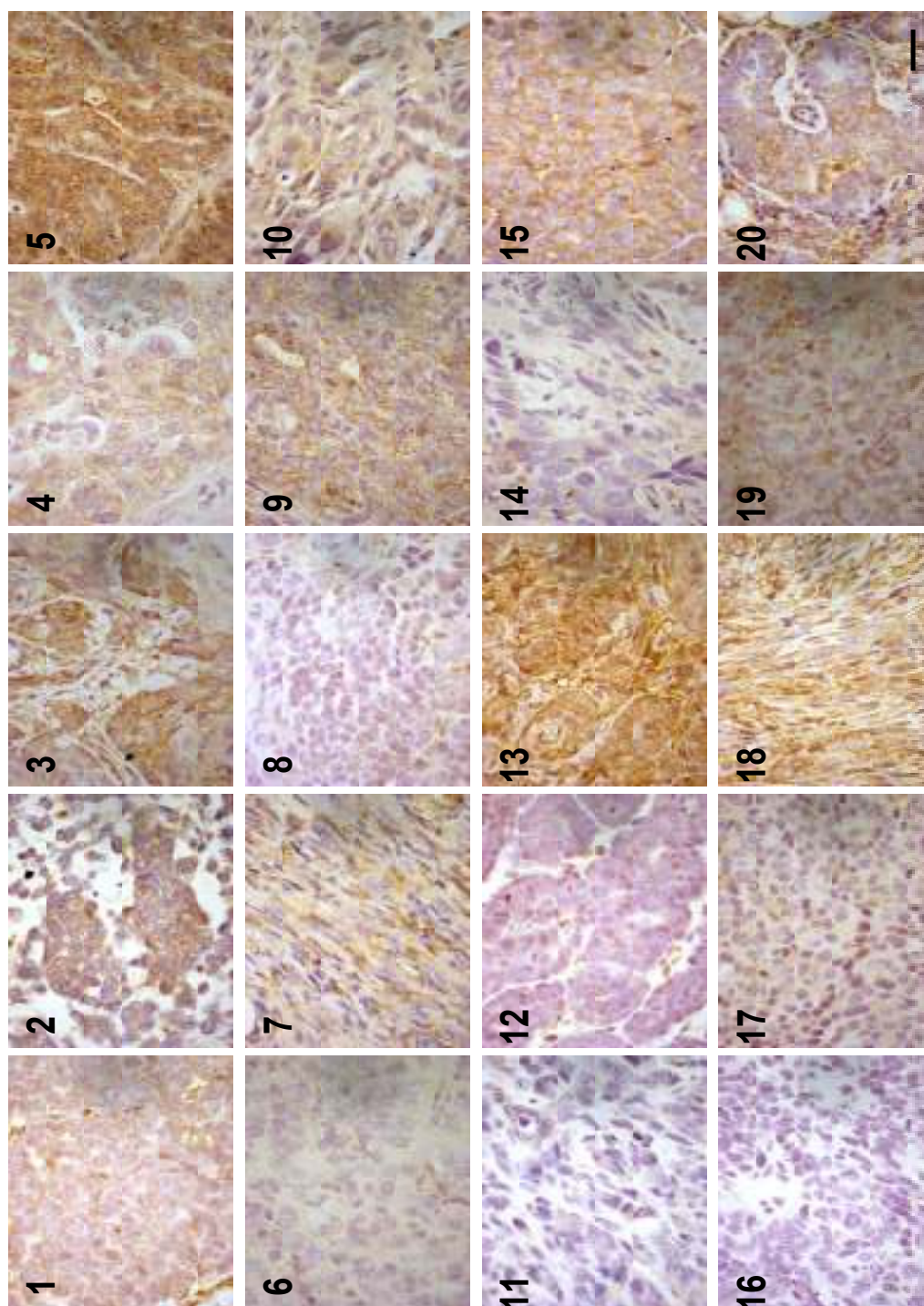


**Figure 6.1:** (c) BRCA2<sup>-/-</sup> p53<sup>-/-</sup> tumours were stained immuno-histochemically with antibodies against ErbB2 and the levels of ErbB2 staining in respective tumours were determined by IxP scores. Ranking of tumours were based on IxP scores for nuclear p52 (highest to lowest staining). Scale bar represents 20µm and the numbers inset show ranking of tumours based on nuclear p52 IxP scores.

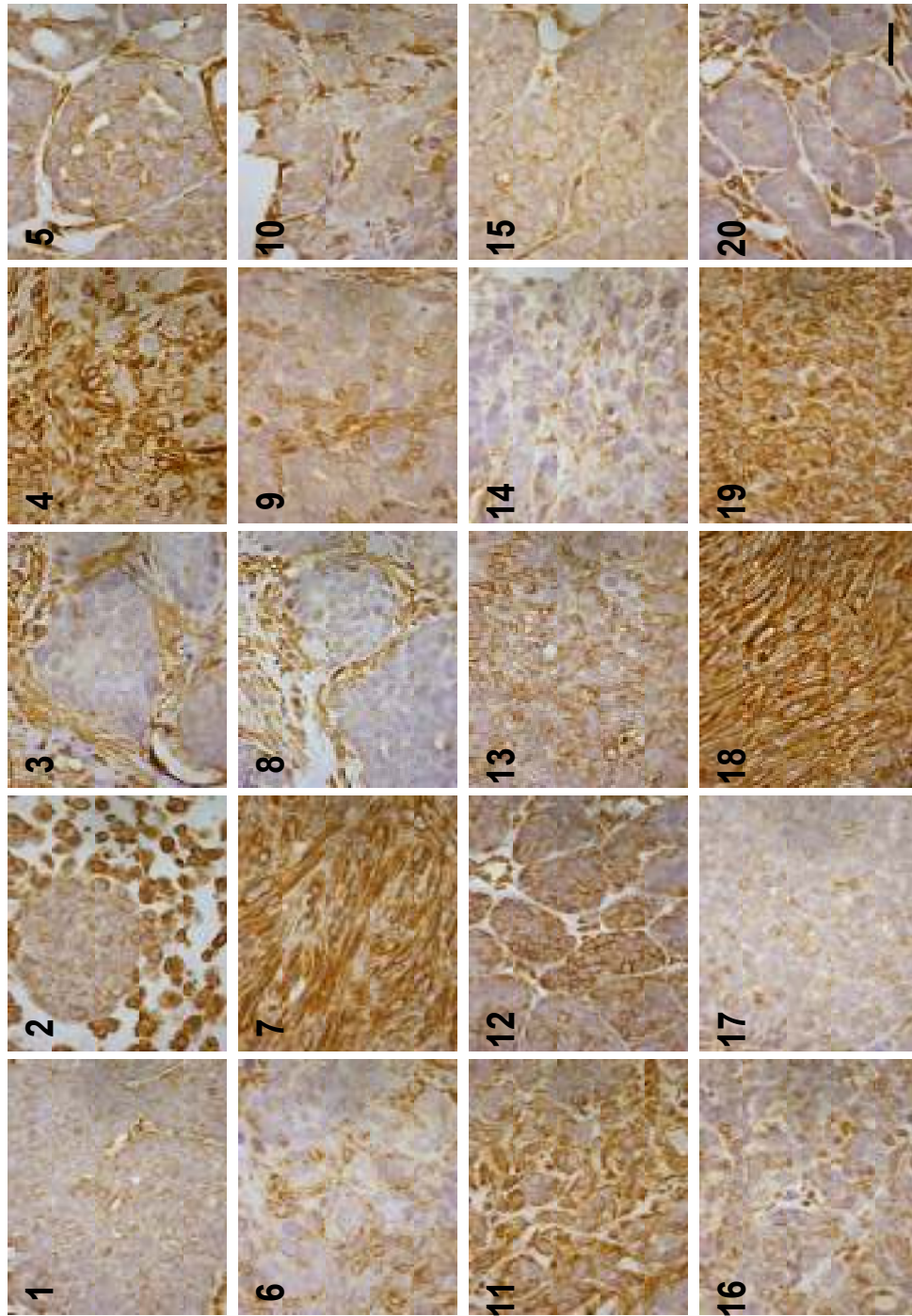


**Figure 6.1:** (d) BRCA2<sup>-/-</sup> p53<sup>-/-</sup> tumours were stained immunohistochemically with antibodies against vimentin and the levels of vimentin staining in respective tumours were determined by IxP scores. Ranking of tumours based on IxP scores for nuclear p52 (highest to lowest staining). Scale bar represents 20µm and the numbers inset show ranking of tumours based on nuclear p52 IxP scores.

Tumour ID	Ranking by p52 staining	p52 (IxP)	p63 (IxP)	ErbB2 (IxP)	Vimentin (IxP)
BAP 2231 R3	1	9	9	0	2
VEG 347 L3	2	9	2	1	6
BAP 2213 R4	3	6	6	2	0
VEG 272 R3	4	6	6	1	9
VEG 347 R4	5	6	9	6	2
VEG 312 R5	6	6	0	0	2
VEG 411 L5	7	6	0	1	9
BAP 2231 L3	8	4	6	0	0
VEG 532 R3	9	4	3	4	2
VEG 272 L4	10	4	2	0	1
VEG 475 L2	11	4	1	0	6
BAP 2212 R2	12	3	3	0	6
BAP 2148 R3	13	3	2	3	4
VEG 417 R3	14	3	2	0	1
BAP 2268 R4	15	3	1	3	2
VEG 550 L1	16	2	2	0	2
VEG 532 L1	17	2	1	0	1
BAP 2231 L5	18	2	0	3	9
BAP 2164 R3	19	2	0	1	9
BAP 2198 R2	20	2	0	2	0

**Table 6.1: Table of scores for respective antigens in BRCA2<sup>-/-</sup> p53<sup>-/-</sup> tumours.** Tumours were stained immuno-histochemically and the intensity X percentage cover (IxP) scores were determined for respective antigens. Tumours were then ranked by the degree of nuclear p52 staining. Statistical significance for the relationship between nuclear p52 staining and p63, ErbB2 or vimentin was then determined by Spearman's ranked correlation test. For p63, R=0.5203, p<0.05; for ErbB2, R=0.0688, n.s.; for vimentin, R=0.1078, n.s. N.s indicates not statistically significant.

used does not discriminate between its different splice variants. This is important as the varying forms of p63 have different transcriptional activities (Trink et al., 2007). Crosstalk between p63 and NF- $\kappa$ B pathways exists, where both transcription factors can directly affect the expression levels of the other (Sen et al., 2011) and form complexes to cooperatively regulate the expression of genes (Yang et al., 2011). This would suggest that the correlation observed in our studies (Table 6.1) may be due to mechanistic interactions between p52 and p63. However, the involvement of specific p63 subunits and phosphorylation status of p52 would need to be identified to achieve a better understanding of the relationship between the two transcription factors.

The BRCA2<sup>-/-</sup> p53<sup>-/-</sup> tumours that were investigated in this study consisted of tumours with a large degree of inter-tumour heterogeneity. This is illustrated by the histologies of respective tumours (Figure 6.1) where staining patterns for p63, ErbB2 and vimentin varied extensively between tumours. This inter-tumour heterogeneity was ideal as it allowed comparisons between different tumour subtypes to be made. However, the cohort used in this study is relatively small and it would be necessary to extend our findings in a larger set of samples. The fact that all these tumours were deficient in BRCA2 and p53 may also lead to a bias in the subtypes of tumours formed. Hence, it would be ideal if the aims of this chapter can be addressed in a larger set of human breast cancer tissue samples. Moreover, the availability of gene-expression profiling data from certain breast cancer tissue banks would enable the differences in p52 levels to be mapped directly to the subtypes of breast cancer based on their gene expression profiles (Perou et al., 2000, Sorlie et al., 2001). This is much more advantageous than using a restricted number of markers if correlations between specific tumour subtypes were to be addressed.

Based on the findings in Chapter 5 and that of Barre & Perkins (Barre and Perkins, 2010a), phosphorylation of p52 at Ser-222 governs the type of complexes formed by p52, which in turn regulates whether p52 is transcriptionally active or repressive. Hence, it would be more appropriate if the phosphorylation status of p52 is accounted for when determining any correlations with breast cancer subtypes. This could be achieved with phospho-specific antibodies for p52, where the ratio of phosphorylated p52 to that of total p52 can be matched to a particular breast cancer subtype. For that reason, although our results indicate a correlation between nuclear p52 levels and p63 (Table 6.1), it does not necessarily represent increased p52 activity in these tumours.

## **6.4 Summary**

In this chapter, we have managed to identify a positive correlation between levels of nuclear p52 and p63 in a cohort of BRCA2<sup>-/-</sup> p53<sup>-/-</sup> tumours. This suggests that p52 could play a role in basal-like breast cancers but this needs to be addressed in a larger cohort of samples which are better characterized in terms of tumour subtypes. The identification of p52 activity in respective tumours with phospho-specific antibodies would also be essential if more specific correlations were to be made.

# **CHAPTER 7**

## General Discussion

## **7 General Discussion**

### **7.1 Apoptosis and mammary gland involution**

The notion that apoptosis is crucial in driving the involution process of the mammary gland had been long withstanding (Chapman et al., 2000). However, it has been demonstrated that cell death is initiated via a lysosomal-mediated pathway during the early phase of involution (Kreuzaler et al., 2011) and can proceed without the activation of caspases. This is supported by studies from rtTA/p35 mice during early involution (Sections 3.2.2 and 3.2.3). We observed sloughing of MECs into the lumen of alveoli without activation of caspase-3 when p35 is induced (Figure 3.3) and the numbers of luminal bodies in mammary glands of mice with or without p35 expression were indifferent (Figure 3.5). However, we were not able to address whether caspase inhibition had any effects on mammary gland architecture as a whole because we were not able to determine the distribution and levels of p35 protein expression in these glands. By knowing the extent of p35 expression in the general population of MECs, the effects of caspase inhibition on the second phase of involution and also clearance of luminal bodies by phagocytes could be addressed.

### **7.2 Regulators of apoptosis as therapeutic targets in the prevention of breast cancer metastasis**

Resistance to apoptosis is an important feature for cancer cells to disseminate to secondary sites (Mehlen and Puisieux, 2006). This association has been demonstrated with the use of transplantation models of breast cancer (Bufalo et al., 1997, Martin et al., 2004, Pinkas et al., 2004) but there is still a lack of adequate models which fully recapitulate the entire metastatic process, as reviewed by Mehlen and Puisieux. With the use of the rtTA/p35/Neu mouse model, inducible expression of the pan-caspase inhibitor, p35, has allowed us to demonstrate the importance of apoptotic resistance in promoting the formation of metastases from an endogenous tumour (Section 3.3.2). Thus, the requirement for apoptotic resistance throughout the entire metastatic cascade in whole was addressed. Although this would strongly advocate the targeting of apoptosis regulators to curb metastasis, there was no effect of inhibiting caspases on primary tumour growth (Section 3.3.1) and this correlates with previous findings (Martin et al., 2004, Pinkas et al., 2004). As such, it is possible that resistance to alternative forms of cell death may be more important in promoting

the growth of mammary tumours examined. This would be in line with the sensitivity of normal MECs to lysosomal mediated cell death during the first phase of involution (Kreuzaler et al., 2011). In order to address this, the activation of cathepsins (initiators of lysosomal mediated cell death) in mammary tumours can be investigated and the effects of cathepsin inhibitors on primary tumour growth examined.

Importantly, the rtTA/p35/Neu mouse model could also be used to address the importance of apoptosis resistance once a tumour has been established at a secondary site. Removal of doxycycline would halt transgene expression and metastases can be monitored longitudinally by *in vivo* imaging techniques such as magnetic resonance imaging. This would provide clinically important insights as to whether a decrease in apoptotic resistance can result in the regression of metastases or just serve as a strategy for adjuvant therapies to prevent relapse of disease.

One of the main inefficiencies of the metastatic process is due to the induction of anoikis upon loss of cell contact with the extracellular matrix (ECM) (Simpson et al., 2008). Cells which manage to overcome anoikis usually exhibit an increased apoptotic threshold via up-regulation of anti-apoptotic factors such as c-FLIP or by sustaining the activation of ECM dependent survival pathways mediated by integrins (Sakamoto and Kyprianou, 2010). Accordingly, targeting of anti-apoptotic factors to reduce the apoptotic threshold could potentially induce cell death in detached cells and prevent the dissemination of cancer cells to secondary sites. The limitation of transplantation and xenograft models has not allowed this to be experimented *in vivo*. In order to specifically address the importance of anoikis resistance during the initial stages of metastasis with the rtTA/p35/Neu mouse model, intra-vital imaging techniques (Kedrin et al., 2008) would need to be employed. By monitoring the changes in proportion of cells which survive cell detachment and intravasation upon caspase inhibition, the importance of anoikis resistance can be fundamentally addressed. Such knowledge could guide and provide a rationale for developing therapeutics which impede this initial stage of metastasis.

### **7.3 The NF- $\kappa$ B p52 subunit and its potential as a therapeutic target in breast cancer metastasis**

With the aim of sensitizing breast cancer cells to apoptotic stimuli, the NF- $\kappa$ B pathway which regulates the transcription of not only a range of anti-apoptotic genes (Clarkson and Watson, 1999), but also genes which can promote metastatic traits such

as motility and EMT (Huber et al., 2004a) lies at a crucial nodal point for therapeutic intervention. Moreover, the induction of EMT itself has been shown to increase the anoikis resistance of breast cancer cells (Kumar et al., 2011).

Hence, emphasis was placed on addressing whether the NF- $\kappa$ B p52 subunit contributed to the malignancy of breast cancer cells and if suppressing its transcriptional activity would result in therapeutically beneficial outcomes. Interestingly, silencing of the *Nfkb2* gene which encodes both p100 and p52 lead to opposing outcomes in 4T1 and N202.1A mammary cancer cell lines. In 4T1 cells, loss of *Nfkb2* lead to increased basal NF- $\kappa$ B activity (Section 4.2.1), induction of EMT (Section 4.2.7), increased motility (Section 4.2.6), mammosphere forming ability (Section 4.2.9) and accelerated tumour growth *in vivo* (Section 4.2.12). As over-expression of p52 in 4T1 *Nfkb2* kd cells did not rescue the motility and mammosphere forming phenotypes of these cells (Section 4.2.11), it is likely that loss of p100 or compensatory p50 activity is responsible for the increased malignancy upon loss of *Nfkb2*. This can be demonstrated by rescue experiments involving over-expression of p100 (unprocessable and WT forms) and knockdown of p50 respectively in 4T1 *Nfkb2* kd cells. On the other hand, in N202.1A cells, knockdown of *Nfkb2* resulted in decreases in basal NF- $\kappa$ B activity (Section 4.2.1) and correspondingly, decreased survival under anoikis conditions (Section 4.2.3), mammosphere forming potential (Section 4.2.11) and tumour growth rate *in vivo* was observed (Section 4.2.13). The decreased mammosphere forming ability in N202.1A cells could be rescued by over-expression of p52 (Section 4.2.11), indicating that it is the loss of p52 and not p100 that is responsible for the decreased tumour initiating potential *in vitro* and *in vivo*. It would also be crucial to examine whether the phenotypes due to *Nfkb2* silencing in these two cell lines are corroborated by tail vein and serial dilution transplantation experiments. This would provide a better indication of the metastatic and tumour initiating potentials of the respective cell lines *in vivo*.

The notable contrast when *Nfkb2* is silenced in 4T1 and N202.1A cells calls for further investigation into the mechanisms governing the differences observed. Since receptor status (i.e. ErbB2, ER, PR) is a conventional method of sub-typing breast tumours and the 4T1 and N202.1A cell lines differ in ErbB2 expression status, it is worth exploring the contribution of ErbB2 signalling on the effects of *Nfkb2* silencing. This is mainly because signalling via EGFR family receptors can activate the NF- $\kappa$ B pathway (Biswas and Iglehart, 2006) and this would determine the basal

NF- $\kappa$ B activity in these cells. The effects of silencing the *Nfkb2* gene in other ErbB2/EGFR<sup>+</sup> and ErbB2/EGFR<sup>-</sup> cell lines would indicate if active signalling by ErbB2/EGFR dictates the outcomes observed. Alternatively, the gene expression profiles of the range of breast cancer cell lines studied could be explored to determine if certain gene clusters regulate the differential outcomes of *Nfkb2* knockdown. This will be of great importance in the identification of breast cancer subtypes which are most likely to benefit from therapies against p52. In parallel, the positive correlation between p52 and p63 (Section 6.2.1) needs to be explored, preferably in clinical samples with gene expression profile data. This will determine whether p52 activity is elevated in basal-like breast cancers or perhaps a unique sub-group of breast cancers which express p63.

In the process of evaluating the therapeutic potential of p52, we have implicated its importance in the regulation of phenotypes pertinent to metastasis formation such as anoikis resistance (Sections 4.2.3 & 5.2.2) and tumour initiating potential (Section 4.2.9). In addition, the motility of cancer cells can also be increased when S222A p52 is over-expressed (Section 5.2.4). Altogether, these findings indicate that aberrant p52 activity can contribute to the metastatic traits of particular cancer cells and thus, diminishing its activity may stand as an effective strategy to curb disease progression contextually. Activation of the RANKL-RANK-I $\kappa$ B $\alpha$  signalling axis which lies upstream of p52 has also been shown to confer breast cancer cells with such metastatic traits (Jones et al. 2006; Cao et al. 2007; Gonzalez-Suarez et al. 2010; Schramek et al. 2010) and this would suggest that p52 contributes, at least in part to the malignancy associated with RANKL-RANK-I $\kappa$ B $\alpha$  signalling. It would be interesting to address the effects of RANKL stimulation on breast cancer cells after genetically manipulating the p100 and p52 subunits respectively (e.g. via silencing of *Nfkb2*, over-expression of unprocessable p100), to directly demonstrate the importance of p52 downstream of RANKL signalling.

Although the canonical NF- $\kappa$ B pathway has been shown to be important for the tumorigenicity of ErbB2 positive breast cancers in particular (Liu et al., 2010, Pratt et al., 2009), simultaneous targeting of p52 should be considered in these tumours. This is mainly because compensatory activity by the alternative pathway may lead to therapeutic resistance, especially since our results demonstrated a role for p52 in malignancy.

## 7.4 Strategies for targeting p52

In this thesis, we have addressed two possible strategies to diminish the transcriptional activity of p52. We evaluated the effects of silencing the *Nfkb2* gene in Chapter 4 and over-expressing S222D p52 in Chapter 5. Although *Nfkb2* knockdown had therapeutically beneficial effects in N202.1A cells, it exacerbated the malignancy of 4T1 cells. As such, there would be risks associated with targeting p52 via shRNA in the clinic, making it an inappropriate strategy. In the case of over-expressing the S222D form of p52, this did not result in any therapeutic effects. This may be due to the lack of other requirements for the formation of transcriptionally repressive p52 complexes. Further investigations into whether p52 repressive complexes are formed and recruited to appropriate promoter sites in cells over-expressing S222D p52 would be required to fully understand the reasons for the lack of change. In addition, a better understanding of other factors which facilitate the formation of p52 repressive complexes may be required.

The therapeutic strategies evaluated in our studies were based on genetic interventions relevant to p52. The specific nature of such interventions was crucial as we were also interested in identifying a role for p52 in breast cancer cells. However, pharmacological targeting of p52 need not be restricted to gene-based therapies and other possible strategies for diminishing p52 activity should be considered. At the present time, there are no commercially available drugs which target p52, but based on our findings of the role of p52 in the malignancy of certain breast cancer subtypes, the development of such agents is warranted. One of the possible strategies would be to directly inhibit the DNA binding activity of p52 via specifically interacting peptides and such approaches have been proven to be effective in the inhibition of other transcription factors such as Notch (Moellering et al., 2009). Alternatively, targeting of modifying enzymes of p52 remains a prospective possibility to inhibit its transcriptional activity. Although targeting p52 may not result in ‘magic bullet’ type therapies, the addition of such a therapeutic agent to the arsenal of drugs that are available for breast cancer patients represents a step closer towards personalized medicine. It is possible that in the future, the subtypes of breast cancer will be scrutinized further; resulting in more distinct subgroups and the availability of more distinct drugs may be required.

## **Bibliography**

- ADAMS, J. & WATT, F. 1993. Regulation of development and differentiation by the extracellular matrix. *Development*, 117, 1183-1198.
- AGHA-MOHAMMADI, S., O'MALLEY, M., ETEMAD, A., WANG, Z., XIAO, X. & LOTZE, M. 2004. Second-generation tetracycline-regulatable promoter: repositioned tet operator elements optimize transactivator synergy while short minimal promoter offers tight basal leakiness. *J. Gene Med.*, 6, 817-828.
- AL-HAJJ, M., WICHA, M. S., BENITO-HERNANDEZ, A., MORRISON, S. J. & CLARKE, M. F. 2003. Prospective identification of tumorigenic breast cancer cells. *PNAS*, 100, 3983-3988.
- ALISON, M. 2001. *The Cancer Handbook*, London, Nature Publishing Group.
- ALLRED, D. & MEDINA, D. 2008. The relevance of mouse models to understanding the development and progression of human breast cancer. *Journal of Mammary Gland Biology and Neoplasia*, 13, 279-288.
- ASHKENAZI, A. & DIXIT, V. 1998. Death receptors: Signaling and modulation. *Science*, 281, 1305-1308.
- ASLAKSON, C. J. & MILLER, F. R. 1992. Selective events in the metastatic process defined by analysis of the sequential dissemination of subpopulations of a mouse mammary tumor. *Cancer Res.*, 52, 1399-1405.
- ASSELIN-LABAT, M.-L., VAILLANT, F., SHERIDAN, J. M., PAL, B., WU, D., SIMPSON, E. R., YASUDA, H., SMYTH, G. K., MARTIN, T. J., LINDEMAN, G. J. & VISVADER, J. E. 2010. Control of mammary stem cell function by steroid hormone signalling. *Nature*, 465, 798-803.
- ATABAI, K., FERNANDEZ, R., HUANG, X., UEKI, I., KLINE, A., LI, Y., SADATMANSOORI, S., SMITH-STEINHART, C., ZHU, W., PYTELA, R., WERB, Z. & SHEPPARD, D. 2005. Mfge8 is critical for mammary gland remodeling during involution. *Mol. Biol. Cell*, 16, 5528-5537.
- AUBELE, M., MATTIS, A., ZITZELSBERGER, H., WALCH, A., KREMER, M., HUTZLER, P., HOFER, H. & WERNER, M. 1999. Intratumoral heterogeneity in breast carcinoma revealed by laser-microdissection and comparative genomic hybridization. *Cancer Genet. Cytogenet.*, 110, 94-102.
- BARRE, B. & PERKINS, N. 2010a. The Skp2 promoter integrates signaling through the NF-kappaB, p53, and Akt/GSK3beta pathways to regulate autophagy and apoptosis. *Mol. Cell.*, 38, 524-538.
- BARRE, B. & PERKINS, N. 2010b. The Skp2 promoter integrates signalling through the NF-kappaB, p53, and Akt/GSK3beta pathways to regulate autophagy and apoptosis. *Molecular cell*, 38, 524-548.
- BASAK, S., SHIH, V. & HOFFMANN, A. 2008. Generation and Activation of Multiple Dimeric Transcription Factors within the NF- B Signaling System. *Molecular and Cellular Biology*, 28, 3139-3150.
- BAUD, V. & KARIN, M. 2009. Is NF-kB a good target for cancer therapy? Hopes and pitfalls. *Nature Reviews Drug Discovery*, 8, 33-40.
- BAUM, B., SETTLEMAN, J. & QUINLAN, M. P. 2008. Transitions between epithelial and mesenchymal states in development and disease. *Semin. Cell Dev. Biol.*, 19, 294-308.
- BEG, A. A., SHA, W. C., BRONSON, R. T., GHOSH, S. & BALTIMORE, D. 1995. Embryonic lethality and liver degeneration in mice lacking the RelA component of NF-kB. *Nature*, 376, 167-170.
- BEIDLER, D. R., TEWARI, M., FRIESEN, P. D., POIRIER, G. & DIXIT, V. M. 1995. The baculovirus p35 protein inhibits Fas- and tumor necrosis factor-induced apoptosis. *J. Biol. Chem.*, 270, 16526-16528.
- BEINKE, S. & LEY, S. 2004. Functions of NF-kB1 and NF-kB2 in immune cell biology. *Biochem. J.*, 382, 393-409.

- BISWAS, D. K. & IGLEHART, J. D. 2006. Linkage between EGFR family receptors and nuclear factor kappaB (NF-kappaB) signaling in breast cancer. *J. Cell Physiol.*, 209, 645-652.
- BOMBONATI, A. & SGROI, D. C. 2011. The molecular pathology of breast cancer progression. *J Pathol*, 223, 307-317.
- BONADONNA, G., HORTOBAGYI, G. & VALAGUSSA, P. 2006. Textbook of Breast Cancer: A clinical guide to therapy
- BRANTLEY, D., CHEN, C. L., MURAOKA, R., BUSHDID, P. B., BRADBERRY, J. L. & KITTRELL, F. 2001. Nuclear-kB (NF-kB) regulates proliferation and branching in mouse mammary epithelium. *Mol. Biol. Cell*, 12, 1445-1455.
- BRANTLEY, D., YULL, F., MURAOKA, R., HICKS, D., COOK, C. & KERR, L. 2000. Dynamic expression and activity of NF- $\kappa$ B during post-natal mammary gland morphogenesis. *Mechanisms of Development*, 97, 149-155.
- BUFALO, D., BIROCCIO, A., LEONETTI, C. & ZUPI, G. 1997. Bcl-2 overexpression enhances the metastatic potential of a human breast cancer line. *FASEB J.*, 11, 947-953.
- CAAMANO, J. H., RIZZO, C. A., DURHAM, S. K., BARTON, D. S., RAVENTOZ-SUAREZ, C., SNAPPER, C. M. & BRAVO, R. 1998. Nuclear factor (NF)-kB2 (p100/p52) is required for normal splenic microarchitecture and B cell-mediated immune responses. *J. Exp. Med.*, 187, 185-196.
- CAMPBELL, K. J., WITTY, J. M., ROCHA, S. & PERKINS, N. 2006. Cisplatin mimics ARF tumour suppressor regulation of RelA (p65) nuclear factor-kB transactivation. *Cancer Research*, 66, 929-935.
- CANCER., C. G. O. H. F. I. B. 1996. Breast cancer and hormonal contraceptives: collaborative reanalysis of individual data on 53297 with breast cancer and 100239 women without breast cancer from 54 epidemiological studies. *Lancet*, 347, 1713-1727.
- CANCER., C. G. O. H. F. I. B. 1997. Breast cancer and hormone replacement therapy: collaborative reanalysis of data from 51 epidemiological studies of 52705 women with breast cancer and 108411 women without breast cancer. *Lancet*, 350, 1047-1059.
- CAO, Y. 2005. Opinion: Emerging mechanisms of tumour lymphangiogenesis and lymphatic metastasis. *Nature Reviews Cancer*, 5, 735-743.
- CAO, Y., BONIZZI, G., SEAGROVES, T. N., GRETEN, F. R., JOHNSON, R. & SCHMIDT, E. V. 2001a. IKK $\alpha$  provides an essential link between RANK signaling and cyclin D1 expression during mammary gland development. *Cell*, 107, 763-775.
- CAO, Y., BONIZZI, G., SEAGROVES, T. N., GRETEN, F. R., JOHNSON, R. & SCHMIDT, E. V. 2001b. IKK $\alpha$  provides an essential link between RANK signaling and cyclin D1 expression during mammary gland development. *Cell*, 107, 763-775.
- CAO, Y. & KARIN, M. 2003. NF-KB in mammary gland development and breast cancer. *Journal of Mammary Gland Biology and Neoplasia*, 8, 215-223.
- CAO, Y., LUO, J. & KARIN, M. 2007. I B kinase kinase activity is required for self-renewal of ErbB2/Her2-transformed mammary tumor-initiating cells. *PNAS*, 104, 15852-57.
- CAREY, L. 2010. Through a glass darkly: Advances in understanding breast cancer biology, 2000-2010. *Clinical Breast Cancer*, 10, 188-195.
- CHAPMAN, R. S., LOURENCO, P., TONNER, E., FLINT, D., SELBERT, S., TAKEDA, K., AKIRA, S., CLARKE, A. R. & WATSON, C. J. 2000. The role of Stat3 in apoptosis and mammary gland involution. Conditional deletion of Stat3. *Adv. Exp. Med. Biol.*, 480, 129-138.

- CHAPMAN, R. S., LOURENCO, P. C., TONNER, E., FLINT, D. J., SELBERT, S., TAKEDA, K., AKIRA, S., CLARKE, A. R. & WATSON, C. 1999. Suppression of epithelial apoptosis and delayed mammary gland involution in mice with a conditional knockout of Stat3. *Genes Dev.*, 13, 2604-2616.
- CHARAFE-JAUFFRET, E., GINESTIER, C., IOVINO, F., WICINSKI, J., CERVERA, N., FINETTI, P., HUR, M. H., DIEBEL, M. E., MONVILLE, F., DUTCHER, J., BROWN, M., VIENS, P., XERRI, L., BERTUCCI, F., STASSI, G., DONTU, G., BIRNBAUM, D. & WICHA, M. S. 2009. Breast cancer cell lines contain functional cancer stem cells with metastatic capacity and distinct molecular signature. *Cancer Res.*, 69, 1302-1313.
- CHEN, L. F. & GREENE, W. C. 2004. Shaping the nuclear action of NF- $\kappa$ B. *Nature Rev. Mol. Cell Biol.*, 5, 392-401.
- CHRISTIANSEN, J. J. & RAJASEKARAN, A. K. 2006. Reassessing epithelial to mesenchymal transition as a prerequisite for carcinoma invasion and metastasis. *Cancer Res.*, 66, 8319-8326.
- CLARKSON, R., HEELEY, J., CHAPMAN, R., AILLET, F., HAY, R., WYLLIE, A. & WATSON, C. 2000a. NF- $\kappa$ B Inhibits Apoptosis in Murine Mammary Epithelia. *The Journal of Biological Chemistry*, 275, 12737-12742.
- CLARKSON, R., WAYLAND, M., LEE, J., FREEMAN, T. & WATSON, C. 2004. Gene expression profiling of mammary gland development reveals putative roles for death receptors and immune mediators in post-lactational regression. *Breast Cancer Research*, 6, 92-109.
- CLARKSON, R. W., HEELEY, J. L., CHAPMAN, R., AILLET, F., HAY, R. T., WYLLIE, A. & WATSON, C. J. 2000b. NF- $\kappa$ B inhibits apoptosis in murine mammary epithelia. *J. Biol. Chem.*, 275, 12737-12742.
- CLARKSON, R. W. E. & WATSON, C. J. 1999. NF- $\kappa$ B and apoptosis in mammary epithelial cells. *J. Mammary Gland Biol. Neoplasia*, 4, 165-175.
- CLEM, R. J., FECHHEIMER, M. & MILLER, L. K. 1991. Prevention of apoptosis by a baculovirus gene during infection of insect cells. *Science*, 254, 1388-1390.
- COGSWELL, P., GUTTRIDGE, D., FUNKHOUSER, W. & BALDWIN, A. J. 2000. Selective activation of NF- $\kappa$ B subunits in human breast cancer: potential roles for NF- $\kappa$ B2/p52 and for Bcl-3. *Oncogene*, 19, 1123-31.
- CONNELLY, L., BARHAM, W., ONISHKO, H. M., SHERRILL, T., CHODOSH, L. A., BLACKWELL, T. & YULL, F. E. 2010. Inhibition of NF- $\kappa$ B activity in mammary epithelium increases tumor latency and decreases tumor burden. *Oncogene*, 2010, 1-11.
- CONNELLY, L., ROBINSON-BENION, C., CHONT, M., SAINT-JEAN, L., LI, H., POLOSUKHIN, V., BLACKWELL, T. & YULL, F. 2007. A Transgenic Model Reveals Important Roles for the NF- $\kappa$ B Alternative Pathway (p100/p52) in Mammary Development and Links to Tumorigenesis. *Journal of Biological Chemistry*, 282, 10028-10035.
- COUTURIER, J., VINCENT-SALOMON, A., MATHIEU, M. C., VALENT, A. & BERNHEIM, A. 2008. Diagnosis of HER2 gene amplification in breast carcinoma. *Pathol. Biol.*, 56, 375-379.
- DEBNATH, J., MILLS, K. R., COLLINS, N. L., REGINATO, M. J., MUTHUSWAMY, S. K. & BRUGGE, J. S. 2002. The role of apoptosis in creating and maintaining luminal space within normal and oncogene-expressing mammary acini. *Cell*, 111, 29-40.
- DEGTEREV, A., BOYCE, M. & YUAN, J. 2003. A decade of caspases. *Oncogene*, 22, 8543-67.

- DEJARDIN, E., BONIZZI, G., BELLAHCENE, A., CASTRONOVO, V., MERVILLE, M. & V, B. 1995. Highly-expressed p100/p52 (NFkB2) sequesters other NF-kappa B-related proteins in the cytoplasm of human breast cancer cells. *Oncogene*, 11, 1835-1841.
- DEMICCO, E., KAVANAGH, K., ROMIEU-MOUREZ, R., WANG, X., SHIN, S., LANDESMANBOLLAG, E., SELDIN, D. & SONENSHEIN, G. 2005. RelB/p52 NF- B Complexes Rescue an Early Delay in Mammary Gland Development in Transgenic Mice with Targeted Superrepressor I B- Expression and Promote Carcinogenesis of the Mammary Gland. *Molecular and Cellular Biology*, 25, 10136-10147.
- DIEHN, M., CHO, R. W., LOBO, N. A., KALISKY, T., DORIE, M. J., KULP, A. N., QIAN, D., LAM, J. S., AILLES, L. E., WONG, M., JOSHUA, B., KAPLAN, M. J., WAPNIR, I., DIRBAS, F. M., SOMLO, G., GARBEROGLIO, C., PAZ, B., SHEN, J., LAU, S. K., QUAKE, S. R., BROWN, J. M., WEISMANN, I. L. & CLARKE, M. F. 2009. Association of reactive oxygen species levels and radioresistance in cancer stem cells. *Nature*, 458, 780-783.
- DYKXHOORN, D. M., WU, Y., XIE, H., YU, F., LAL, A., PETROCCA, F., MARTINVALET, D., SONG, E., LIM, B. & LIEBERMAN, J. 2009. miR-200 enhances mouse breast cancer cell colonization to form distant metastases. *PLoS One.*, 4, e7181.
- EASTON, D. F. 1999. How many more breast cancer predisposition genes are there? *Breast Cancer Res.*
- EDDY, S., GUO, S., DEMICCO, G., ROMIEU-MOUREZ, R., LANDESMANBOLLAG, E., SELDIN, D. & SONENSHEIN, G. 2005. Inducible IKB Kinase/IKB Kinase E Expression Is Induced by CK2 and Promotes Aberrant Nuclear Factor-KB Activation in Breast Cancer Cells. *Cancer Research*, 65, 11375-11383.
- FATA, J. E., WERB, Z. & BISSELL, M. J. 2004. Regulation of mammary gland branching morphogenesis by the extracellular matrix and its remodeling enzymes. *Breast Cancer Res.*, 6, 1-11.
- FERLAY, J., PARKIN, D. & STELIAROVA-FOUCHER, E. 2010. GLOBOCAN 2008, Cancer Incidence and Mortality Worldwide. *IARC CancerBase*, 10.
- FIALKA, I., SCHWARZ, H., REICHMANN, E., OFT, M., BUSSLINGER, M. & BEUG, H. 1996. The estrogen-dependent c-JunER protein causes a reversible loss of mammary epithelial cell polarity involving a destabilization of adherens junctions. *Journal of Cell Biology*, 132, 1115-1132.
- FORD, D., EASTON, D. F. & STRATTON, M. 1998. Genetic heterogeneity and penetrance analysis of the BRCA1 and BRCA2 genes in breast cancer families. *Am. J. Hum. Genet.*, 62, 334-345.
- FRANZOSO, G., CARLSON, L., POLJAK, L., SHORES, E. W., EPSTEIN, S., LEONARDI, A., GRINBERG, A., TRAN, T., SCHARTON-KERSTEN, T. & ANVER, M. 1998. Mice deficient in nuclear factor (NF)-kB2/p52 present with defects in humoral responses, germinal center reactions and splenic microarchitecture. *J. Exp. Med.*, 187.
- FRIEDENREICH, C. M., THUNE, I. & BRINTON, L. A. 1998. Epidemiologic issues related to the association between physical activity and breast cancer. *Cancer*, 83, 600-610.
- FUJII, H., MARSH, C., CAIRNS, P., SIDRANSKY, D. & GABRIELSON, E. 1996. Genetic divergence in the clonal evolution of breast cancer. *Cancer Res.*, 56, 1493-1497.

- FURTH, J. & KAHN, M. 1937. The transmission of leukemia of mice with a single cell. *Am. J. Cancer*, 31, 276-282.
- FURTH, P. A., BAR-PELED, U., LI, M., LEWIS, A., LAUCIRICA, R., JAGER, R., WEIHER, H. & RUSSELL, R. G. 1999. Loss of anti-mitotic effects of Bcl-2 with retention of anti-apoptotic activity during tumor progression in a mouse model. *Oncogene*, 18, 6589-6596.
- GEIGER, T. & PEEPER, D. 2009. Metastasis mechanisms. *Biochimica et Biophysica Acta*, 1796, 293-308.
- GERONDAKIS, S., GROSSMANN, M., NAKAMURA, Y., POHL, T. & GRUMONT, R. 1999. Genetic approaches in mice to understand Rel/NF-kB and I $\kappa$ B functions: Transgenics and knockouts. *Oncogene*, 18, 6888-6895.
- GEYMAYER, S. & DOPPLER, W. 2000. Activation of NF-kB p50/p65 is regulated in the developing mammary gland and inhibits STAT5-mediated beta-casein gene expression. *FASEB J.*, 14, 1159-1170.
- GHOSH, S. & HAYDEN, M. 2008. New regulators of NF-KB in inflammation. *Nature Reviews Immunology*, 8, 837-848.
- GLOCKNER, S., BUURMAN, H., KLEEBERGER, W., LEHMANN, U. & KREIPE, H. 2002. Marked intratumoral heterogeneity of c-myc and CyclinD1 but not of c-erbB2 amplification in breast cancer. *Lab. Invest.*, 82, 1419-1426.
- GONZALEZ-SUAREZ, E., JACOB, A. P., JONES, J., MILLER, R., ROUDIER-MEYER, M. P., ERWERT, R., PINKAS, J., BRANSTETTER, D. & DOUGALL, W. C. 2010. RANK ligand mediates progesterin-induced mammary epithelial proliferation and carcinogenesis. *Nature*, 468, 103-107.
- GOSSEN, M. & BUJARD, H. 1992. Tight control of gene expression in mammalian cells by tetracycline-responsive promoters. *PNAS*, 89, 5547-5551.
- GREEN, K. A. & STREULI, C. H. 2004. Apoptosis regulation in the mammary gland. *Cell. Mol. Life Sci.*, 61, 1867-1883.
- GRUMONT, R., ROURKE, I. J., O'REILLY, L. A., STRASSER, A., MIYAKE, K., SHA, W. C. & GERONDAKIS, S. 1998. B lymphocytes differentially use the Rel and nuclear factor kB1 (NF-kB1) transcription factors to regulate cell cycle progression and apoptosis in quiescent and mitogen activated cells. *J. Exp. Med.*, 187, 663-674.
- GUNTHER, E. J., BELKA, G. K., WERTHEIM, B. W., WANG, J., HARTMAN, J. L., BOXER, R. B. & CHODOSH, L. A. 2002. A novel doxycycline-inducible system for the transgenic analysis of mammary gland biology. *FASEB J.*, 16, 283-292.
- GUY, C. T., WEBSTER, M. A., SCHALLER, M., PARSONS, T. J., CARDIFF, R. D. & MULLER, W. J. 1992. Expression of the neu protooncogene in the mammary epithelium of transgenic mice induces metastatic disease. *PNAS USA*, 89, 10578-10582.
- HANAHAAN, D. & WEINBERG, R. 2000a. The Hallmarks of Cancer. *Cell*, 100, 57-70.
- HANAHAAN, D. & WEINBERG, R. 2000b. The hallmarks of cancer. *Cell*, 100, 57-70.
- HANAYAMA, R. & NAGATA, S. 2005. Impaired involution of mammary glands in the absence of milk fat globule EGF factor 8. *PNAS*, 102, 16886-16891.
- HARRISON, H., FARNIE, G., HOWELL, S. J., ROCK, R. E., STYLIANOU, S., BRENNAN, K. R., BUNDRED, N. J. & CLARKE, R. B. 2010. Regulation of breast cancer stem cell activity by signaling through the Notch4 receptor. *Cancer Res.*, 70, 709-718.
- HAY, B. A., WOLFF, T. & RUBIN, G. M. 1994. Expression of baculovirus p35 prevents cell death in *Drosophila*. *Development*, 120, 2121-2129.

- HAY, T., MATTHEWS, J. R., PIETZKA, L., LAU, A., CRANSTON, A., NYGREN, A. O., DOUGLAS-JONES, A., SMITH, G. C., MARTIN, N. M., O'CONNOR, M. & CLARKE, A. R. 2009. Poly(ADP-ribose) polymerase-1 inhibitor treatment regresses autochthonous Brca2/p53-mutant mammary tumors in vivo and delays tumor relapse in combination with carboplatin. *Cancer Res.*, 69, 3850-3855.
- HENNIGHAUSEN, L. & ROBINSON, G. W. 2001. Signaling pathways in mammary gland development. *2001*, 1, 467-475.
- HENS, J. & WYSOLMERSKI, J. 2005. Molecular mechanisms involved in the formation of the embryonic mammary gland. *Breast Cancer Research*, 7, 220-224.
- HISCOX, S., DAVIES, E. & BARRETT-LEE, P. 2009. Aromatase inhibitors in breast cancer. *Maturitas*, 63, 275-279.
- HOFFMANN, A., LEUNG, T. H. & BALTIMORE, D. 2003. Genetic analysis of NF- $\kappa$ B/Rel transcription factors defines functional specificities. *EMBO J.*, 22, 5530-5539.
- HOVEY, R., TROTT, J. & VONDERHAAR, B. 2002. Establishing a framework for the functional mammary gland: from endocrinology to morphology. *Journal of Mammary Gland Biology and Neoplasia*, 7, 17-38.
- HOWARD, B. & GUSTERSON, B. 2000. Human breast development. *Journal of Mammary Gland Biology and Neoplasia*, 5, 119-137.
- HUBER, M. A., AZOITEI, N., BAUMANN, B., GRUNERT, S., SOMMER, A., PEHAMBERGER, H., KRAUT, N., BEUG, H. & WIRTH, T. 2004a. NF- $\kappa$ B is essential for epithelial-mesenchymal transition and metastasis in a model of breast cancer progression. *J. Clinical Investigation*, 114, 569-581.
- HUBER, M. A., AZOITEI, N., BAUMANN, B., GRUNERT, S., SOMMER, A., PEHAMBERGER, H., KRAUT, N., BEUG, H. & WIRTH, T. 2004b. NF- $\kappa$ B is essential for epithelial-mesenchymal transition and metastasis in a model of breast cancer progression. *J. Clin. Invest.*, 114, 569-581.
- HUGO, H., ACKLAND, M. L., BLICK, T., LAWRENCE, M. G., CLEMENTS, J. A., WILLIAMS, E. D. & THOMPSON, E. W. 2007. Epithelial-mesenchymal and mesenchymal-epithelial transitions in carcinoma progression. *J. Cell Physiol.*, 213, 374-383.
- HUMPHREYS, R. C., KRAJEWSKA, M., KRNACIK, S., JAEGER, R., WEIHER, H., KRAJEWSKI, S., REED, J. C. & ROSEN, J. M. 1996. Apoptosis in the terminal endbud of the murine mammary gland: a mechanism of ductal morphogenesis. *Development*, 122, 4013-4022.
- HUNTER, D. J., SPIEGELMAN, D. & ADAMI, H.-O. 1996. Cohort studies of fat intake and the risk of breast cancer- a pooled analysis. *N. Engl. J. Med.*, 334, 356-361.
- ILLIOPOULUS, D., HIRSCH, H. A. & STRUHL, K. 2009. An epigenetic switch involving NF- $\kappa$ B, Lin28, Let-7 MicroRNA and IL6 links inflammation to cell transformation. *Cell*, 139, 693-706.
- JONES, D. H., NAKASHIMA, T., SANCHEZ, O. H., KOZIERADZKI, I., KOMAROVA, S. V., SAROSI, I., MORONY, S., RUBIN, E., SARAO, R., HOJILLA, C. V., KOMNENOVIC, V., KONG, Y.-Y., SCHREIBER, M., DIXON, S. J., SIMS, S. M., KHOKHA, R., WADA, T. & PENNINGER, J. M. 2006. Regulation of cancer cell migration and bone metastasis by RANKL. *Nature*, 440, 692-696.
- JORDAN, V. 2007. Tamoxifen: Catalyst for the change to targeted therapy. *European Journal of Cancer*, 44, 30-38.

- KEDRIN, D., GLIGORIJEVIC, B., WYCKOFF, J., VERKHUSHA, V. V., CONDEELIS, J., SEGALL, J. E. & VAN RHEENEN, J. 2008. Intravital imaging of metastatic behavior through a mammary imaging window. *Nature Methods*, 5, 1019-1021.
- KELSEY, J. L., GAMMON, M. D. & JOHN, E. M. 1993. Reproductive factors and breast cancer. *Epidemiol. Rev.*, 15, 36-47.
- KERR, J. F., WYLLIE, A. H. & CURRIE, A. R. 1972. Apoptosis: a basic biological phenomenon with wide ranging implications in tissue kinetics. *Br. J. Cancer*, 26, 239-257.
- KEY, T. J., VERKASALO, P. K. & BANKS, E. 2001. Epidemiology of breast cancer. *The Lancet Oncology*, 2, 133-140.
- KIM, S., IIZUKA, K., AGUILA, H. L., WEISSMAN, I. L. & YOKOYAMA, W. M. 2000. *In vivo* natural killer cell activities revealed by natural killer cell-deficient mice. *PNAS*, 97, 2731-2736.
- KON, S. & COWIE, A. 1961. *Milk: the mammary gland and its secretion*, New York, Academic Press.
- KORKAYA, H., PAULSON, A., CHARAFE-JAUFFRET, E., GINESTIER, C., M., B., DUTCHER, J., CLOUTHIER, S. G. & WICHA, M. S. 2009. Regulation of mammary stem/progenitor cells by PTEN/Akt/beta-catenin signaling. *PLoS Biol.*, 7, e1000121.
- KOUROS-MEHR, H. & WERB, Z. 2006. Candidate regulators of mammary branching morphogenesis identified by genome-wide transcript analysis. *Dev. Dyn.*, 235, 3404-3412.
- KREUZALER, P. A., STANISZEWSKA, A. D., LI, W., OMIDVAR, N., KEDJOUAR, B., TURKSON, J., POLI, V., FLAVELL, R. A., CLARKSON, R. W. & WATSON, C. J. 2011. Stat3 controls lysosomal-mediated cell death in vivo. *Nature Cell Biology*, 13, 303-309.
- KRITIKOU, E. A., SHARKEY, A., ABELL, K., CAME, P. J., ANDERSON, E., CLARKSON, R. & WATSON, C. 2003. A dual, non-redundant, role for LIF as a regulator of development and Stat3-mediated cell death in mammary gland. *Development*, 130, 3459-3468.
- KUMAR, S., PARK, S. H., CIEPLY, B., SCHUPP, J., KILLIAM, E., ZHANG, F., RIMM, D. L. & FRISCH, S. M. 2011. A pathway for the control of anoikis sensitivity by E-cadherin and epithelial-to-mesenchymal transition. *Mol. Cell Biol.*, 19, 4036-4051.
- LAPIDOT, T., SIRARD, C., VORMOOR, J., MURDOCH, B., HOANG, T., CACERES-CORTES, J., MINDEN, M., PATERSON, B., CALIGIURI, M. A. & DICK, J. E. 1994. A cell initiating human acute myeloid leukaemia after transplantation into SCID mice. *Nature*, 367, 645-648.
- LAYDE, P. M., WEBSTER, L. A. & BAUGHMAN, A. L. 1989. The independent associations of parity, age at first full term pregnancy and duration of breast feeding with the risk of breast cancer. *J. Clin. Epidemiol.*, 42, 963-973.
- LERMA, E., PEIRO, G., RAMON, T., FERNANDEZ, S., MARTINEZ, D., PONS, C., MUNOZ, F., SABATE, J., ALONSO, C., OJEDA, B., PRAT, J. & BARNADAS, A. 2007a. Immunohistochemical heterogeneity of breast carcinomas negative for estrogen receptors, progesterone receptors and Her2/neu (basal-like breast carcinomas). *Modern Pathology*, 20, 1200-1207.
- LERMA, E., PEIRO, G., RAMON, T., FERNANDEZ, S., MARTINEZ, D., PONS, C., MUNOZ, F., SABATE, J., ALONSO, C., OJEDA, B., PRAT, J. & BARNADAS, A. 2007b. Immunohistochemical heterogeneity of breast carcinomas negative for estrogen receptors, progesterone receptors and Her2/neu. *Modern Pathology*, 20, 1200-1207.

- LI, X., LEWIS, M. T., HUANG, J., GUTIERREZ, C., OSBORNE, C. K., WU, M. F., HILSENBECK, S. G., PAVLICK, A., ZHANG, X., CHAMNESS, G. C., WONG, H., ROSEN, J. & CHANG, J. C. 2008. Intrinsic resistance of tumorigenic breast cancer cells to chemotherapy. *J. Natl. Cancer Inst.*, 100, 672-679.
- LIPWORTH, L., BAILEY, L. R. & TRICHOPOULOS, D. 2000. History of breast feeding in relation to breast cancer risk: a review of the epidemiologic literature. *J. Natl. Cancer Inst.*, 92, 302-312.
- LIU, M., SAKAMAKI, T., CASIMIRO, M. C., WILLMARTH, N. E., QUONG, A. A., JU, X., OJEIFO, J., JIAO, X., YEOW, W. S., KATIYAR, S., SHIRLEY, L. A., JOYCE, D., LISANTI, M. P., ALBANESE, C. & PESTELL, R. G. 2010. The canonical NF-kappaB pathway governs mammary tumorigenesis in transgenic mice and tumor stem cell expansion. *Cancer Research*, 70, 10464-10473.
- LIU, N., RAJA, S. M., ZAZZERONI, F., METKAR, S. S., SHAH, R., ZHANG, M., WANG, Y., BROMME, D., RUSSIN, W. A., LEE, J. C., PETER, M. E., FROELICH, C. J., FRANZOSO, G. & ASHTON-RICKARDT, P. G. 2003. NF-kB protects from the lysosomal pathway of cell death. *EMBO J.*, 22, 5313-5322.
- LIU, S., DONTU, G., MANTLE, I. D., PATEL, S., AHN, N. S., JACKSON, K. W., SURI, P. & WICHA, M. S. 2006. Hedgehog signaling and Bmi-1 regulate self-renewal of normal and malignant human mammary stem cells. *Cancer Res.*, 66, 6063-6071.
- LIVAK, K. J. & SCHMITTGEN, T. D. 2001. Analysis of relative gene expression data using real-time quantitative PCR and the 2-delta-deltaCT method. *Methods*, 25, 402-408.
- LIVASY, C., KARACA, G., NANDA, R., TRETIAKOVA, M., OLOPADE, O., MOORE, D. & PEROU, C. 2006. Phenotypic evaluation of the basal-like subtype of invasive breast carcinoma. *Modern Pathology*, 19, 264-271.
- LO, J. C., BASAK, S., JAMES, E. S., QUIAMBO, R. S., KINSELLA, M. C. & ALEGRE, M. L. 2006. Coordination between NF-kappaB family members p50 and p52 is essential for mediating LTbetaT signals in the development and organization of secondary lymphoid tissues. *Blood*, 107, 1048-1055.
- LUO, G. & YU-LEE, L. 2000. Stat5b inhibits NF-kB mediated signaling. *Mol. Endocrinol.*, 14, 114-123.
- MAGNUSSON, C. M., BARON, J. & CORREIA, N. 1999. Breast cancer risk following long term oestrogen and oestrogen progestin replacement therapy. *Int. J. Cancer*, 81, 339-344.
- MAILLEUX, A. A., OVERHOLTZER, M., SCHMELZLE, T., BOUILLET, P., STRASSER, A. & BRUGGE, J. S. 2007. BIM regulates apoptosis during mammary ductal morphogenesis, and its absence reveals alternative cell death mechanisms. *Developmental Cell*, 12, 221-234.
- MANI, S. A., GUO, W., LIAO, M. J., EATON, E. N., AYYANAN, A., ZHOU, A. Y., BROOKS, M., REINHARD, F., ZHANG, C. C., SHIPITSIN, M., CAMPBELL, L. L., POLYAK, K., BRISKEN, C., YANG, J. & WEINBERG, R. 2008. The epithelial-mesenchymal transition generates cells with properties of stem cells. *Cell*, 133, 704-715.
- MARTIN, S. J., FINUCANE, D. M., AMARANTE-MENDES, G. P., O'BRIEN, G. A. & GREEN, D. R. 1996. Phosphatidylserine externalization during CD95-induced apoptosis of cells and cytoplasts requires ICE/CED-3 protease activity. *Journal of Biological Chemistry*, 271, 28753-28756.

- MARTIN, S. S. & LEDER, P. 2001. Human MCF10A mammary epithelial cells undergo apoptosis following actin depolymerization that is independent of attachment and rescued by Bcl-2. *Mol. Cell. Biol.*, 21, 6529-6536.
- MARTIN, S. S., RIDGEWAY, A. G., PINKAS, J., LU, Y., REGINATO, M. J., KOH, E. Y., MICHELMAN, M., DALEY, G. Q., BRUGGE, J. S. & LEDER, P. 2004. A cytoskeleton-based functional genetic screen identifies Bcl-xL as an enhancer of metastasis, but not primary tumor growth. *Oncogene*, 23, 4641-4645.
- MARUYAMA, T., FUKUSHIMA, H., NAKAO, K., SHIN, M., YASUDA, H., WEIH, F., DOI, T., AOKI, K., ALLES, N., OHYA, K., HOSOKAWA, R. & JIMI, E. 2010. Processing of the NF-kappa B2 precursor p100 to p52 is critical for RANKL-induced osteoclast differentiation. *J. Bone Miner. Res.*, 25, 1058-1067.
- MAY, C. D., SPHYRIS, N., EVANS, K. W., WERDEN, S. J., GUO, W. & MANI, S. A. 2011. Epithelial-mesenchymal transition and cancer stem cells: a dangerously dynamic duo in breast cancer progression. *Breast Cancer Res.*, 13, 202-211.
- MCDERMOTT, S. P. & WICHA, M. S. 2010. Targeting breast cancer stem cells. *Molecular Oncology*, 4, 404-419.
- MEHLEN, P. & PUISIEUX, A. 2006. Metastasis: a question of life or death. *Nature Reviews Cancer*, 6, 449-458.
- MEIER, P., FINCH, A. & EVAN, G. 2000. Apoptosis in development. *Nature*, 407, 796-801.
- MEYER, M. J., FLEMING, J. M., ALI, M. A., PESESKY, M., GINSBURG, E. & VONDERHAAR, B. K. 2009. Dynamic regulation of CD24 and the invasive, CD44<sup>pos</sup>CD24<sup>neg</sup> phenotype in breast cancer cell lines. *Breast Cancer Res.*, 11, R82.
- MILLER, D. K. 1997. The role of the caspase family of cysteine proteases in apoptosis. *Semin Immunol.*, 9, 35-49.
- MOELLERING, R. E., CORNEJO, M., DAVIS, T. N., DEL BIANCO, C., ASTER, J. C., BLACKLOW, S. C., KUNG, A. L., GILLILAND, D. G., VERDINE, G. L. & BRADNER, J. E. 2009. Direct inhibition of the NOTCH transcription factor complex. *Nature Cell Biology*, 462, 182-188.
- MONKS, J. & HENSON, P. M. 2009. Differentiation of the mammary epithelial cell during involution: Implications for breast cancer. *Journal of Mammary Gland Biology and Neoplasia*, 14, 159-170.
- MOREL, A. P., LIEVRE, M., THOMAS, C., HINKAL, G., ANSIEAU, S. & PUISIEUX, A. 2008. Generation of breast cancer stem cells through epithelial-mesenchymal transition. *PLoS One.*, 3, e2888.
- MULLER, A., HOMEY, B., SOTO, H., CATRON, N., BUCHANAN, M., MCCLANAHAN, T., MURPHY, E., YUAN, W., WAGNER, S., BARRERA, J., MOHAR, A., VERASTEGUI, E. & ZLOTNIK, A. 2001. Involvement of chemokine receptors in breast cancer metastasis. *Nature Reviews Cancer*, 410, 50-56.
- MURRAY, C. J. L. & LOPE, A. D. 1997. Mortality by cause for eight regions of the world: Global burden of disease study. *Lancet*, 349, 1269-1276.
- NAKSHATRI, H., BHAT-NAKSHATRI, P., MARTIN, D. A., GOULET JR, R. A. & SLEDGE JR, G. W. 1997. Constitutive activation of NF-kB during progression of breast cancer to hormone-independent growth. *Molecular and Cellular Biology*, 17, 3629-3639.
- NANNI, P., PUPA, S. M., NICOLETTI, G., GIOVANNI, C. D., LANDUZZI, L., ROSSI, I., ASTOLFI, A., RICCI, C., DE VECCHI, R., INVERNIZZI, A. M.,

- DI CARLO, E., MUSIANI, P., FORNI, G., MENARD, S. & LOLLINI, P.-L. 2000. p185neu protein is required for tumor and anchorage-independent growth, not for cell proliferation of transgenic mammary carcinoma. *Int. J. Cancer*, 87, 186-194.
- NELSON, C. M., VANDUIJN, M. M., INMAN, J. L., FLETCHER, D. A. & BISSELL, M. J. 2006. Tissue geometry determines sites of mammary branching morphogenesis in organotypic cultures. *Science*, 314, 298-300.
- NGUYEN, A. V. & POLLARD, J. 2000. Transforming growth factor beta3 induces cell death during the first stage of mammary gland involution. *Development*, 127, 3107-3118.
- NORMANNO, N., MORABITO, A., DE LUCA, A., PICCIRILLO, C., GALLO, M., MAIELLO, M. & PERRONE, F. 2009. Target-based therapies in breast cancer: current status and future perspectives. *Endocrine-Related Cancer*, 16, 675-702.
- NORTHERN IRELAND CANCER REGISTRY 2010. Cancer Incidence and Mortality.
- NOWELL, P. C. 1976. The clonal evolution of tumor cell populations. *Science*, 194, 23-28.
- OAKES, S., ROGERS, R., NAYLOR, M. & ORMANDY, C. 2008. Prolactin regulation of mammary gland development. *Journal of Mammary Gland Biology and Neoplasia*, 13, 13-28.
- OFFICE FOR NATIONAL STATISTICS 2010. Cancer Statistics registrations: Registrations of cancer diagnosed in 2007, England.
- PAGET, S. 1889. The distribution of secondary growths in cancer of the breast. *Lancet Oncology*, 1, 571-573.
- PAHL, H. 1999. Activators and target genes of Rel/NF-kB transcription factors. *Oncogene*, 18, 6853-6866.
- PECORINO, L. 2008. *Molecular Biology of Cancer*, New York, Oxford University Press.
- PERKINS, N. 2007. Integrating cell-signalling pathways with NF-kB and IKK function. *Nature Reviews Molecular Cell Biology*, 8, 49-62.
- PERKINS, N. & GILMORE, T. D. 2006. Good cop, bad cop: the different faces of NF-kB. *Cell Death Differ.*, 13, 759-772.
- PEROU, C., SORLIE, T., EISEN, M., VAN DE RIJN, M., JEFFREY, S., REES, C., POLLACK, J., ROSS, D., JOHNSEN, H., AKSLEN, L., FLUGE, O., PERGAMENSCHIKOV, A., WILLIAMS, C., ZHU, S., LONNING, P., BORRESEN-DALE, A., BROWN, P. & BOTSTEIN, D. 2000. Molecular portraits of human breast tumours. *Nature*, 406, 747-752.
- PETO, J., COLLINS, N. & BARFOOT, R. 1999. The prevalence of BRCA1 and BRCA2 mutations amongst early onset breast cancer cases in the UK. *J. Natl. Cancer Inst.*, 91, 943-949.
- PINKAS, J., MARTIN, S. S. & LEDER, P. 2004. Bcl-2 mediated cell survival promotes metastasis of Eph4  $\beta$ MEKDD mammary epithelial cells. *Mol. Cancer Res.*, 10, 551-556.
- POLYAK, K. & WEINBERG, R. 2009. Transitions between epithelial and mesenchymal states: acquisition of malignant and stem cell traits. *Nature Reviews Cancer*, 9, 265-273.
- PRATT, M., TIBBO, E., ROBERTSON, S., JANSSON, D., HURST, K., PEREZ-IRATXETA, C., LAU, R. & NIU, M. 2009. The canonical NF-kB pathway is required for formation of luminal mammary neoplasias and is activated in the mammary progenitor population. *Oncogene*, 8, 2710-2722.

- PRINDULL, G. 1995. Apoptosis in the embryo and tumorigenesis. *Eur. J. Cancer*, 31a, 116-123.
- RACHET, B., MARINGE, C., NUR, U., QUARESMA, M., SHAH, A., WOODS, L., ELLIS, L., WALTERS, S., FORMAN, D., STEWARD, J. & COLEMAN, M. 2009. Population-based cancer survival trends in England and Wales up to 2007: an assessment of the NHS cancer plan for England. *Lancet Oncology*, 10, 351-369.
- RAY, P., TANG, W., WANG, P., HOMER, R., KUHN, C., FLAVELL, R. A. & ELIAS, J. A. 1997. Regulated overexpression of interleukin 11 in the lung. Use to dissociate development-dependent and -independent phenotypes. *J. Clin. Invest.*, 100, 2501-2511.
- RIBEIRO-SILVA, A., RAMALHO, L. N., GARCIA, S. B., BRANDAO, D. F., CHAHUD, F. & ZUCOLOTO, S. 2005. p63 correlates with both BRCA1 and cytokeratin 5 in invasive breast carcinomas: further evidence for the pathogenesis of the basal phenotype of breast cancer. *Histopathology*, 47, 458-466.
- RICHERT, M., SCHWERTFEGER, K., RYDER, J. & ANDERSON, S. 2000. An Atlas of Mouse Mammary Gland Development. *Journal of Mammary Gland Biology and Neoplasia*, 5, 227-241.
- ROCHA, S., GARRETT, M. D., CAMPBELL, K. J., SCHUMM, K. & PERKINS, N. 2005. Regulation of NF- $\kappa$ B and p53 through activation of ATR and Chk1 by the ARF tumour suppressor. *EMBO J.*, 24, 1157-1169.
- ROCHA, S., MARTIN, A., MEEK, D. & PERKINS, N. 2003. p53 Represses Cyclin D1 Transcription through Down Regulation of Bcl-3 and Inducing Increased Association of the p52 NF- $\kappa$ B Subunit with Histone Deacetylase 1. *Molecular and Cellular Biology*, 23, 4713-4727.
- ROMIEU-MOREZ, R., KIM, D., SHIN, S., DEMICCO, E., LANDESMANBOLLAG, E., SELDIN, D., CARDIFF, R. & SONENSHEIN, G. 2003. Mouse mammary tumour virus c-rel transgenic mice develop mammary tumours. *Molecular Cell Biology*, 23, 5738.
- SAKAMOTO, S. & KYPRIANOU, N. 2010. Targeting anoikis resistance in prostate cancer metastasis. *Mol. Aspects Med.*, 31, 205-214.
- SANDAH, M., HUNTER, D. M., STRUNK, K. E., EARP, H. S. & COOK, R. S. 2010. Epithelial cell-directed efferocytosis in the post-partum mammary gland is necessary for tissue homeostasis and future lactation. *BMC Developmental Biology*, 10.
- SANSONE, P., STORCI, G., TAVOLARI, S., GUARNIERI, T., GIOVANNINI, C., TAFFURELLI, M., CECCARELLI, C., SANTINI, D., PATERINI, P., MARCU, K. B., CHIECO, P. & BONAFE, M. 2007. IL-6 triggers malignant features in mammospheres from human ductal breast carcinoma and normal mammary gland. *J. Clin. Invest.*, 117, 3988-4002.
- SAVILL, J. & FADOK, V. 2000. Corpse clearance defines the meaning of cell death. *Nature*, 407, 784-788.
- SCHERE-LEVY, C., BUGGIANO, V., QUAGLINO, A., GATTELLI, A., CIRIO, M. C., PIAZZON, I., VANZULLI, S. & KORDON, E. C. 2003. Leukemia inhibitory factor induces apoptosis of the mammary epithelial cells and participates in mouse mammary gland involution. *Exp. Cell. Res.*, 282, 35-47.
- SCHRAMEK, D., LEIBBRANDT, A., SIGL, V., KENNER, L., POSPISILIK, J. A., LEE, H. J., HANADA, R., JOSHI, P. A., ALIPRANTIS, A., GLIMCHER, L., PASPARAKIS, M., KHOKHA, R., ORMANDY, C. J., WIDSCHWENDTER, M., SCHETT, G. & PENNINGER, J. M. 2010. Osteoclast differentiation

- factor RANKL controls development of progestin-driven mammary cancer. *Nature*, 468, 98-102.
- SCHUMM, K., ROCHA, S., CAAMANO, J. & PERKINS, N. 2006. Regulation of p53 tumour suppressor target gene expression by the p52 NF- $\kappa$ B subunit. *The EMBO Journal*, 25, 4820-4832.
- SEN, T., SEN, N., HUANG, Y., SINHA, D., LUO, Z. G., RATOVITSKI, E. A. & SIDRANSKY, D. 2011. Tumor protein p63/nuclear factor  $\kappa$ B feedback loop in regulation of cell death. *J. Biol. Chem.*, 286, 43204-43213.
- SETHI, G., AHN, K., CHATURVEDI, M. & AGGARWAL, B. 2007. Epidermal growth factor (EGF) activates nuclear factor- $\kappa$ B through I  $\kappa$ B  $\alpha$  kinase-independent but EGF receptor-kinase dependent tyrosine 42 phosphorylation of I  $\kappa$ B  $\alpha$ . *Oncogene*, 26, 7324-7332.
- SHA, W. C., LIOU, H. C., TUOMANEN, E. I. & BALTIMORE, D. 1995. Targeted disruption of the p50 subunit of NF- $\kappa$ B leads to multifocal defects in immune responses. *Cell* 80, 321-330.
- SHI, Y. 2002. Mechanisms of caspase activation and inhibition during apoptosis. *Mol. Cell*, 9, 459-70.
- SILBERSTEIN, G. 2001. Postnatal mammary gland morphogenesis. *Microscopy research and technique*, 52, 155-162.
- SIMPSON, C. D., ANYIWE, K. & SCHIMMER, A. D. 2008. Anoikis resistance and tumor metastasis. *Cancer Letters*, 272, 177-185.
- SMITH-WARNER, S. A., SPIEGELMAN, D. & YAUN, S. S. 1998. Alcohol and breast cancer in women: a pooled analysis of cohort studies. *JAMA*, 279, 535-540.
- SNAPPER, C., ZELAZOWSKI, P., ROSAS, F. R., KEHRY, M. R., TIAN, M., BALTIMORE, D. & SHA, W. C. 1996. B cells from p50/NF- $\kappa$ B knockout mice have selective defects in proliferation, differentiation, germ-line CH transcription and Ig class switching. *J. Immunol.*, 156, 183-191.
- SORLIE, T., PEROU, C., TIBSHIRANI, R., AAS, T., GEISLER, S., JOHNSEN, H., HASTIE, T., EISEN, M., VAN DE RIJN, M., JEFFREY, S., THORSEN, T., QUIST, H., MATESE, J., BROWN, P., BOTSTEIN, D., LONNING, P. & BORRESEN-DALE, A. 2001. Gene expression patterns of breast carcinomas distinguish tumor subclasses with clinical implications. *PNAS*, 98, 10869-10874.
- SOVAK, M. A., BELLAS, R. E., KIM, D., ZANIESKI, G. J., ROGERS, A. E., TRAISH, A. M. & SONENSHEIN, G. 1997. Aberrant nuclear factor- $\kappa$ B/Rel expression and the pathogenesis of breast cancer. *J. Clin. Invest.*, 100, 2952-2960.
- STEIN, T., MORRIS, J. S., DAVIES, C. R., WEBER-HALL, S. J., DUFFY, M. A., HEATH, V. J., BELL, A. K., FERRIER, R. K., SANDILANDS, G. P. & GUSTERSON, B. A. 2004. Involution of the mouse mammary gland is associated with an immune cascade and an acute-phase response, involving LBP, CD14 and STAT3. *Breast Cancer Research*, 6, R75-91.
- STOKA, V., TURK, B., SCHENDEL, S. L., KIM, T. H., CIRMAN, T., SNIPAS, S. J., ELLERBY, L. M., BREDESEN, D., FREEZE, H., ABRAHAMSON, M., BROMME, D., KRAJEWSKI, S., REED, J. C., YIN, X. M., TURK, B. & SALVESSEN, G. S. 2001. Lysosomal protease pathways to apoptosis. Cleavage of bid, not pro-caspases, is the most likely route. *J. Biol. Chem.*, 276, 3149-3157.
- STREULI, C. H. & GILMORE, A. P. 1999. Adhesion-mediated signaling in the regulation of mammary epithelial cell survival. *J. Mammary Gland. Biol. Neoplasia*, 4, 183-191.

- SUGIMOTO, A., FRIESEN, P. D. & ROTHMAN, J. H. 1994. Baculovirus p35 prevents developmentally programmed cell death and rescues a ced-9 mutant in the nematode *Caenorhabditis elegans*. *EMBO J.*, 13, 2023-2028.
- TAN, W., ZHANG, W., STRASNER, A., GRIVENNIKOV, S., CHENG, J. Q., HOFFMAN, R. M. & KARIN, M. 2011. Tumour-infiltrating regulatory T cells stimulate mammary cancer metastasis through RANKL-RANK signalling. *Nature*, 470, 548-553.
- TANG, Z.-N., ZHANG, F., TANG, P., QI, X.-W. & JIANG, J. 2011. Hypoxia induces RANK and RANKL expression by activating HIF-1alpha in breast cancer cells. *Biochemical and Biophysical Research Communications*, 408, 411-416.
- TIFFEN, P. G., OMIDVAR, N., MARQUEZ-ALMUINA, N., CROSTON, D., WATSON, C. & CLARKSON, R. 2008. A dual role for oncostatin M signaling in the differentiation and death of mammary epithelial cells in vivo. *Mol. Endocrinol.*, 22, 2677-2688.
- TRINK, B., OSADA, M., RATOVITSKI, E. & SIDRANSKY, D. 2007. p63 transcriptional regulation of epithelial integrity and cancer. *Cell Cycle*, 6, 240-245.
- TURNER, N., TUTT, A. & ASHWORTH, A. 2004. Hallmarks of 'BRCAness' in sporadic cancers. *Nature Reviews Cancer*, 4, 814-819.
- VARGO-GOGOLA, T. & ROSEN, J. 2007. Modelling breast cancer: one size does not fit all. *Nature Reviews Cancer*, 7, 659-672.
- VAUX, D. L., CORY, S. & ADAMS, J. 1988. Bcl-2 gene promotes haemopoietic cell survival and cooperates with c-myc to immortalize pre-B cells. *Nature*, 335, 440-442.
- VAUX, D. L. & STRASSER, A. 1996. The molecular biology of apoptosis. *PNAS*, 93, 2239-2244.
- VIATOUR, P., BENTIREN-ALJ, M., CHARIOT, A., DEREGOWSKI, V., DE LEVAL, L., MERVILLE, M. & BOURS, V. 2003. NF-kappa B2/p100 induces Bcl-2 expression. *Leukemia*, 17, 1349-1356.
- WANG, X., BELGUISE, K., KERSUAL, N., KIRSCH, K., MINEVA, N., GALTIER, F., CHALBOS, D. & SONENSHEIN, G. 2007. Oestrogen signalling inhibits invasive phenotype by repressing RelB and its target BCL2. *Nature Cell Biology*, 9, 470-478.
- WATSON, C. 2006. Involution: apoptosis and tissue remodelling that convert the mammary gland from milk factory to quiescent organ. *Breast Cancer Research*, 8, 203-207.
- WEISS, L., ELKIN, G. & BARBERA-GUILLEM, E. 1993. The differential resistance of B16 wild-type and F10 cells to mechanical trauma *in vitro*. *Invasion metastasis*, 13, 92-101.
- WELSH CANCER INTELLIGENCE AND SURVEILLANCE UNIT 2010. Cancer Incidence in Wales.
- WIETEK, C., CLEAVER, C., LUDBROOK, V., WILDE, J., WHITE, J., BELL, D., LEE, M., DICKSON, M., RAY, K. & O'NEILL, L. 2006. I B Kinase Interacts with p52 and Promotes Transactivation via p65. *Journal of Biological Chemistry*, 281, 34973-34981.
- WONG, C. W., LEE, A., SHIENTAG, L., YU, J., DONG, Y., KAO, G., AL-MEHDI, A. B., BERNHARD, E. J. & MUSCHEL, R. J. 2001. Apoptosis: an early event metastatic inefficiency. *Cancer Res.*, 61, 333-338.
- WYCKOFF, J. B., JONES, J. G., CONDEELIS, J. S. & SEGALL, J. E. 2000. A critical step in metastasis: *in vivo* analysis of intravasation at the primary tumour. *Cancer Res.*, 60, 2504-2511.

- YAMAGUCHI, N., ITO, T., AZUMA, S., ITO, E., HONMA, R., YANAGISAWA, Y., NISHIKAWA, A., KAWAMURA, M., IMAI, J., WATANABE, S., SEMBA, K. & INOUE, J. 2009. Constitutive activation of nuclear factor-kB is preferentially involved in the proliferation of basal-like subtype breast cancer cell lines. *Cancer Sci.*
- YANG, J. & WEINBERG, R. 2008. Epithelial-mesenchymal transition: at the crossroads of development and tumor metastasis. *Dev. Cell*, 14, 818-829.
- YANG, X., LU, H., YAN, B., ROMANO, R. A., BIAN, Y., FRIEDMAN, J., DUGGAL, P., ALLEN, C., CHUANG, R., EHSANIAN, R., SI, H., SINHA, S., VAN WAES, C. & CHEN, Z. 2011. DeltaNp63 verssatilely regulates a broad NF-kB gene program and promotes squamous epithelial proliferation, migration and inflammation. *Cancer Res.*, 71, 3688-3700.
- ZHENG, T., ZHU, Z., WANG, Z., HOMER, R. J., MA, B., RIESE JR., R. J., CHAPMAN JR., H. A., SHAPIRO, S. D. & ELIAS, J. A. 2000. Inducible targeting of IL-13 to the adult lung causes matrix metalloproteinase and cathepsin-dependent emphysema. *J. Clin. Invest.*, 106, 1081-1093.